Properties of the Vacuum in Models for QCD: Holography vs. Resummed Field Theory. A Comparative Study.

Dissertation

zur Erlangung des Grades eines
Doktors der Naturwissenschaften

der Fakultät für Physik
der Ludwig-Maximillians-Universität zu München

vorgelegt von
Andrey V. Zayakin
aus Yakutsk

Oktober 2010

1. Gutachter: Priv. Doz.Dr. J. Erdmenger, LMU München

2. Gutachter: Prof. Dr. Christian Römelsberger, LMU München

Tag der mündlichen Prüfung: 17.01.2011

To the political prisoners in present-day Russia

Contents

Introduction

0.1 Motivation . . . 5
0.1.1 The Problem of the Strong Coupling . . . 5
0.1.2 AdS/CFT Correspondence . . . 7
0.1.3 Structure of this Work . . . 10
0.2 Perturbative and Non-Perturbative Approaches to QCD: a Short Review . 12
0.2.1 Condensates and Hadron Physics . . . 12
0.2.2 Gluon Condensate and Holography . . . 17
0.2.3 Chiral Condensate and Holography . . . 32
0.2.4 Condensates and Field Theory Resummations . . . 32

I Holography **33**

1 Chiral Magnetic Effect in Soft-Wall AdS/QCD **34**
1.1 Introduction . . . 34
1.2 The Soft-Wall Model . . . 35
1.2.1 Gauge Part of the Action . . . 35
1.2.2 On-shell Action and Symmetry Currents . . . 38
1.2.3 The Divergence of the Vector Current . . . 39
1.2.4 The Bardeen Counterterm . . . 40
1.3 Scalars and Pseudoscalars . . . 41
1.3.1 Kinetic Term and Potential . . . 41
1.3.2 Chern-Simons Action with Scalars . . . 42
1.4 Summary . . . 45

2 Low-Energy Theorems in Holography **47**
2.1 Introduction . . . 47
2.2 Normalization of Operators . . . 48

2.3 Low-Energy Theorems . . . 56
2.3.1 Dilatation Ward Identities in a Self-Dual Background . . . 56
2.3.2 Decoupling Theorem in Backgrounds with Gluon Condensate . . . 61
2.4 Quarkonium Transport in Self-Dual Background . . . 64
2.4.1 Self-Dual Background at Zero Temperature . . . 64
2.4.2 Self-Dual Background at Finite Temperature . . . 65
2.5 Discussion . . . 68
2.6 Appendix: Equations of Motion . . . 68

3 Chiral Condensate Scaling in a Magnetic Field 71
3.1 Motivation . . . 72
3.1.1 Chiral Condensate in Field Theory . . . 72
3.1.2 Limitations of Traditional Approaches . . . 73
3.1.3 Chiral Symmetry Breaking and Holography . . . 73
3.2 D7 Brane with a Maxwell Field in a Deformed AdS Background . . . 75
3.3 Condensate . . . 76
3.4 Summary . . . 79

4 Vacuum Magnetization in Strong Fields 80
4.1 Notion of Vacuum and Condensate Magnetization . . . 80
4.2 Vacuum Magnetization from Holography . . . 85
4.3 Discussion . . . 89

II Resummed Field Theory 91

5 A Novel Resummation of Wilson Loops 92
5.1 Overview . . . 92
5.2 ESSZ Equation . . . 93
5.3 Dyson–Schwinger Equations . . . 97
5.4 Solving ESSZ Equation . . . 101
5.5 Summary . . . 104

6 Dyson–Schwinger Equations, Non-Local Condensates and Effective Actions 108
6.1 Overview . . . 108
6.2 Dyson–Schwinger Equations . . . 110
6.2.1 Formulation of DSE with Quarks . . . 110

6.3 Non-local Condensate . . . 113
6.3.1 Dependence on Mass of the Condensate Shape . . . 113
6.3.2 Local Quark Condensate and Quark Virtuality Dependence on Mass 114
6.3.3 Condensate Response to an External Field . . . 116
6.4 Effective Action due to Condensates . . . 119
6.5 Discussion . . . 122
6.6 A Recently Proposed Experiment . . . 123
6.7 The $\gamma\gamma$ Scattering in Holography . . . 126
6.8 Phantom QCD Effects . . . 128
6.9 Abuse of Condensates . . . 131
6.10 Instead of a Conclusion: What does QCD Contribute? . . . 132

7 Comparison: Resummations vs. Holography 133
7.1 Main Results . . . 133
7.2 Comments on Compared Values . . . 135
7.2.1 Decoupling . . . 135
7.2.2 Wilson Line and Quark-Quark Potential . . . 136
7.2.3 Linear Condensate Scaling . . . 137
7.2.4 Magnetization . . . 137
7.3 Conclusion . . . 137
7.4 Developments of Holographic Models . . . 138
Acknowledgements . . . 140

Zusammenfassung

Diese Doktorarbeit betrachtet zwei Methoden der Untersuchung des Vakuums – Holographie und die resummierte Feldtheorie. Im UV-Bereich spielen die nichtperturbative QCD-Effekte nur eine untergeordnete Rolle, und die Dynamik der Theorie kann exakt durch die Störungstheorie vorhergesagt. Im Gegensatz dazu, ist die IR Physik (z.B. Spektren und Zerfälle leichter Mesonen) sehr empfindlich auf die nichtperturbativen Eigenschaften der Theorie. Die Beispiele nichtperturbativer Parameter der QCD sind das Gluon-Kondensat und das Quark-Kondensat. Kondensate gehen in viele niederenergetische Beobachtungsgrössen ein, und sind daher direkt auf Experimente verbunden. Andererseits, erreicht die Leistung der jetzt geplanten moderner Hochleistungslaser-Einrichtungen (z.B. das ELI-Projekt) bereits nahezu die Grenze der Quark-Skala.

Deshalb ist die Dynamik der Kondensate von besonderer Wichtigkeit; jedoch ist wenig über den Erzeugungsmechanismus jedes der Kondensate bekannt, und unterschiedliche Hypothesen darüber werden gehandelt. Deswegen kann hier ein Modell-bildender Ansatz nützlich sein. In dieser Dissertation vergleiche ich zwei Klassen verschiedener Modelle für die Dynamik von Kondensaten. Die erste Klasse enthält die sogenannten holographischen Modelle der QCD. Basierend auf der Maldacena-Vermutung wird hier versucht, die Eigenschaften von QCD-Korrelationsfunktionen aus dem Verhalten von klassischen Lösungen der Feldgleichungen in einer mehr-dimensionalen Theorie zu berechnen. Der Vorteil holographischer Modelle besteht darin, dass sie eine stark-gekoppelte vierdimensionale Eichfeldtheorie als dualen Partner einer schwach-gekoppelten (und dadurch lösbaren) String/Supergravitations-Theorie liefern können. Die Schwierigkeit dieser Modelle ist ihre Relevanz für die tatsächliche QCD. Keines der derzeit gehandelten Modelle wird als “vollständig” dual zur tatsächlichen QCD angesehen. Mögliche Defizite der Dualität sind die Anwesenheit zusätzlicher Teilchen im Spektrum, die verbleibenden Supersymmetrien, falsche Wiedergabe der Spektren von Mesonen und Baryonen etc. Dennoch stimmt der Holographische Ansatz in vielen Bereichen hervorragend mit experimentellen Daten überein. Diese Erfolge beziehen sich auf die Vorhersage eines sehr kleinen Verhältnisses von Viskosität zu Entropie Verhaltens und die Vorhersage von Mesonen-Spectra auf eine Genauigkeit von bis zu 5% in einigen Modellen. Andererseits sind die Resummierungsmethoden in der Feldtheorie bislang sind noch nicht verworfen worden; im Gegenteil es existiert eine ganze “Resummierungsindustrie” für die QCD-Korellatoren durch Integralgleichungen, vor allem die Dyson–Schwinger-Gleichungen.

Beide Methodenklassen haben einen Zugang zu den Kondensaten. So wird eine umfasende Untersuchung von Kondensaten ermöglicht, in der meine Berechnungen in resummierter Feldtheorie und Holographie miteinander verglichen werden, sowie mit Resultaten

aus Gitter-Rechnungen und Experimenten. Ich beweise, dass die Niederenergie-Theoreme der QCD in holographischen Modellen mit einem Gluon-Kondensat in nicht-trivialer Weise ihre Gültigkeit behalten. Ich zeige, dass das sogenannte "Decoupling relation" der QCD in holographischen Modellen mit chiralen und Gluon-Kondensaten gültig bleibt, wohingegen diese Relation im Dyson–Schwinger Ansatz versagt. Im Gegensatz dazu stimmen meine Ergebnisse zum chiralen magnetischen Effekt bei holographischer Behandlung nicht mit den Vorhersagen bei der schwachen Kopplung überein; dort ist der chirale magnetische Effekt (d.h. die Erzeugung elektrisches Stromes in einem Magnetfeld) dreimal geringer als in der schwach gekoppelten QCD. Für das chirale Kondensat ergibt sich eine quadratische Abhängigkeit in einem magnetischen Feld sowohl bei Behandlung im Dyson–Schwinger-Ansatz als auch bei holographischer Behandlung. Dabei wissen wir, dass im exakten chiralen Limes das Kondensat linear sein sollte. Deshalb fehlt beiden Klassen von Modellen das korrekte Verhalten des Kondensats im chiralen Limes. Ich finde auch, dass die Magnetisierung des QCD Vakuums nicht mit Gitter-Daten zur Magnetisierung des chiralen Kondensates übereinstimmt. Man findet eine merkwürdige nicht-monotone Abhängigkeit vom Magnetfeld mit einer Spitze bei einem charakteristischen Wert des Feldes. Ich vermute hier, die Spitze mit der kürzlich vorgeschlagenen Hypothese einer elektromagnetischen Supraleitung des QCD Vakuums in Verbindung stehen könnte. Schließlich vergleiche ich das Quark-Quark-Potenzial aus der Holographischen Modellen und aus Gitter-Rechnungen, und mit dem Potenzial, das ich aus einer Kombination von Dyson-Schwinger und Erickson–Semenoff–Szabo–Zarembo Resummierungen berechne. Abgesehen vom perturbativen Coulomb-Potenzial, finde ich Confinement in der resummierten Theorie, jedoch ist dies auf eine sehr kurze Reichweite begrenzt und erlaubt uns nicht tief ins IR vorzudringen. Dies wird als ein Hinweis auf eine sehr begrenzte Anwendbarkeit von Resummationen im tiefen IR interpretiert; im Gegensatz dazu, liefert die Holographie stabile und realistische Ergebnisse.

Wenn resummierte nichtlokale Kondensate mit bekannten nicht-lokalen phänomenologischen Werten verglichen werden, stellt sich die Abschätzung der Nichtlokalität leichter Quarks als um viele Größenordnungen falsch heraus, was wiederum auf die Unfähigkeit der Dyson–Schwinger-Gleichungen zur korrekten Beschreibung der Physik im IR hinweist. Wenn man diese Eigenschaften der Kondensate zusammengefaßt, muß ich schlußfolgern, dass die Holographie, im Gegensatz zu Dyson–Schwinger Gleichungen, als Methode der Wahl für die Behandlung der QCD-Physik betrachtet werden sollte. Man könnte hoffen, dass in wenigen Jahren zumindest die elektrischen Felder der Quark-Skala zugänglich sein werden und einige der Vorhersagen dieser Dissertation experimentell überprüft werden können.

Abstract

This Thesis is dedicated to a comparison of the two means of studying the electromagnetic properties of the QCD vacuum – holography and resummed field theory. In the UV range the non-pertubative QCD effects play an insignificant role and the dynamics of the theory is exactly predicted by the perturbation theory. On the contrary, the IR physics (e.g. light meson spectra and decays) is very sensitive to the non-perturbative features of the theory. Archetypal examples of a non-perturbative parameter in QCD are gluon condensate and quark condensate. Condensates enter into many low-energy observables and thus are directly experiment-related. On the other hand, the power of modern experimental laser-physics facilities being planned (e.g. the ELI project) is already almost reaching the boundary of quark scales (though not hadron scales yet).

Thus the dynamics of the condensates is of special importance. Yet little is known about the generation mechanism of either of the condensates and various hypotheses are on the market. Therefore, a model-building approach might be useful here. In this Thesis I compare two classes of distinct models for the dynamics of the condensates. The first class consists of the so-called holographic models of QCD. Based upon the Maldacena conjecture, it tries to establish the properties of QCD correlation functions from the behavior of classical solutions of field equations in a higher-dimensional theory. The advantage of the holographic models is that they render a strongly-coupled four-dimensional gauge theory as a dual of some weakly-coupled string/supergravity. This is actually the reason of the immense popularity of holographic models nowadays. The problem of these models is their relevance to actual QCD. None of the models currently on the market is supposed to be "exactly" dual to real-life QCD. The possible shortcomings of duality are the presence of extra particles in the spectrum, remaining supersymmetries, wrong reproduction of the meson and baryon spectra etc. Yet in many aspects the holographic approach has been found to be in an excellent agreement with data. These successes are the prediction of the very small viscosity-to-entropy ratio and the predictions of meson spectra up to 5% accuracy in several models.

On the other hand, the resummation methods in field theory have not been discarded so far. There exists a whole industry of resummation for the correlators in QCD, by means of integral equations, Dyson–Schwinger equations first of all. Non-local observables, such as Wilson loops, are also subjects to resummations, as proposed by Erickson and Zarembo. The success of resummation methods was marked by the agreement of lattice calculations of Green functions with Dyson–Schwinger results.

Both classes of methods have access to condensates. Thus a comprehensive study of condensates becomes possible, in which I compare my calculations in holography and

resummed field theory with each other, as well as with lattice results, field theory and experiment. I prove that the low-energy theorems of QCD keep their validity in holographic models with a gluon condensate in a non-trivial way. I also show that the so-called decoupling relation holds in holography models with chiral and gluon condensates, whereas this relation fails in the Dyson–Schwinger approach. On the contrary, my results on the chiral magnetic effect in holography disagree with the weak-field prediction; the chiral magnetic effect (that is, the electric current generation in a magnetic field) is three times less than the current in the weakly-coupled QCD. The chiral condensate behavior is found to be quadratic in external field both in the Dyson–Schwinger approach and in holography, yet we know that in the exact limit the condensate must be linear, thus both classes of models are concluded to be deficient for establishing the correct condensate behaviour in the chiral limit. The magnetization of the QCD vacuum does not agree with the lattice data on chiral condensate magnetization; it is found to have a peculiar non-monotonous dependence on the magnetic field, with a peak at some point, which cannot be explained so far. I speculate here that the peak might be related to the recently proposed electromagnetic superconductivity in QCD vacuum. Finally, I compare the quark-quark potential obtained from the holographic models and the potential obtained from the lattice to the potential I calculate via a combination of Dyson–Schwinger and Ericson–Semenoff–Szabo–Zarembo resummations. Apart from the perturbative Coulomb potential, I find confinement in the resummed theory; yet it is limited by a very short range and does not really allow us to go deeply in the infrared. This is interpreted as a signal of a very limited applicability of resummations to the deep infrared; on the contrary, holography yields robust and realistic results. When resummed non-local condensates are compared to known phenomenological values of non-locality, the estimate for non-locality of light quarks is wrong by several orders of magnitude, which again signalizes an inability of Dyson–Schwinger equations to describe correct physics in the infrared.

Summing up these features of condensates, I must conclude that holography must be considered as a method to be used for IR physics *par excellence*, rather than Dyson–Schwinger equations. One could hope that in a few years at least the quark-scale electric fields will be feasible and some of the predictions of this work could be actually tested.

Introduction

0.1 Motivation

0.1.1 The Problem of the Strong Coupling

Non-perturbative quantum chromodynamics (QCD) has been a challenge for a number of decades. A variety of methods to handle it have been developed trying to overcome the two most notorious problems: strong coupling and colour confinement. Of special interest has always been the non-perturbative behaviour of QCD in external electromagnetic fields. This is motivated by the various heavy-ion collision [1] and laser physics [2] experiments already available, where fields close to the critical electron Schwinger field can be reached in the near future.

The attempts of going beyond the naive perturbative approach to the said problems have always been related to some resummation of a part of the perturbative series. Examples of successful resummations are for example those by Erickson, Semenoff, Szabo and Zarembo [3] performed for the Wilson loop and predicting properly strong-coupling behaviour. Another example of an efficient resummation in field theory is the viscosity calculation of quark-gluon plasma by Yaffe and Jeon [4].

Yet no resummation can account for the very specific property of QCD which is the non-triviality of vacuum. Speaking figuratively, we can think of the QCD vacuum as filled with complicated "under-the-barrier" combinations of fields, and therefore, building perturbation theory upon the perturbative vacuum and then resumming may not necessarily bring the correct answer, even if the resummation is full. Thus "instanton physics" was born [5], its method being decomposition around non-trivial vacuum solutions of QCD equations. This method is the key e.g. to "statistical CP-violating" effects like Kharzeev's chiral magnetic effect [6], claimed to have been observed at RHIC by the STAR collaboration.

The instanton physics, despite the richness of its effects, is unfortunately not a model-free construction, since the behaviour and properties of the instanton liquid are largely

prescribed *ad hoc*. Thus alternative ways must be sought for a true non-perturbative approach to QCD.

A possibility for such an approach could be generalizations of the AdS/CFT correspondence. The latter was conjectured by Maldacena in 1997 [7], see also Witten's paper [8]. For a review of Maldacena's conjecture in general, see [9, 10]. A comprehensive modern treatment of the AdS/CFT corespondence can be found in the recent book [11]. The statement of the conjecture is that a strongly-coupled gauge theory on a four-dimensional spacetime is dual in a very well-defined sense to a weakly-coupled gravity theory on a ten-dimensional space (more specifically, a five-dimensional space of constant negative curvature times a five-dimensional sphere). Although the initial version of the conjecture dealt with a supersymmetric theory, it is possible by choosing a suitable geometry on the gravity side to break extra symmetries. The choice of geometry is, however, not at all arbitrary, since the metric must be a solution of the Einstein equation. This makes the predictions of holography robust and model independent.

The famous viscosity-to-entropy ratio prediction from duality and its confirmation in a series of experiments has made holography one of the most prominent candidates to explain the true non-perturbative physics. The low viscosity prediction is illustrated in Fig. (1), taken from [1]. Another tremendous success of AdS/CFT was prediction of strong jet

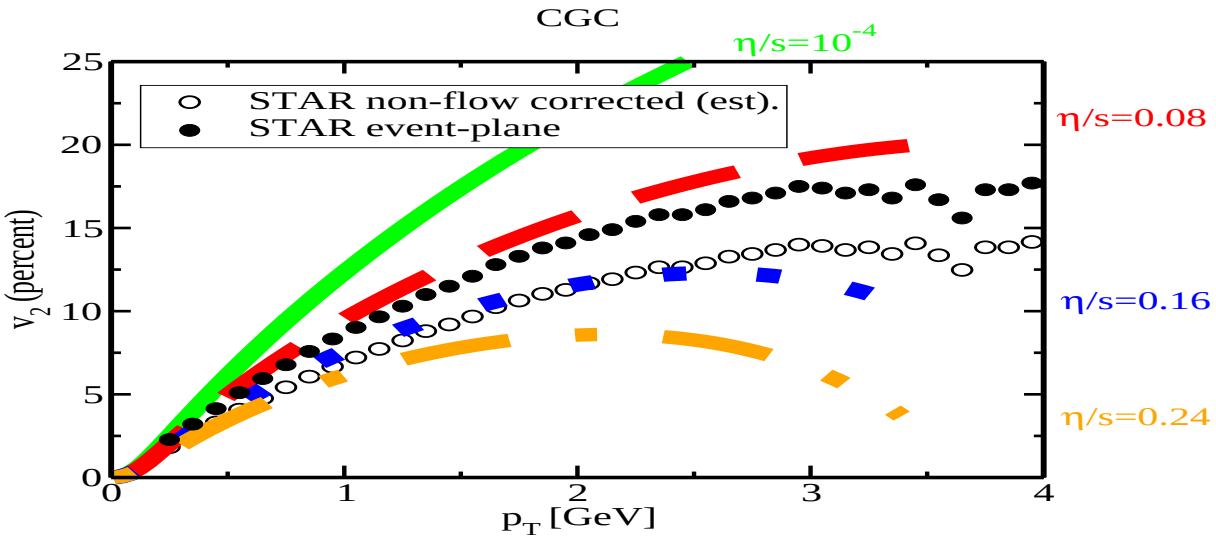

Figure 1: From the 2008 paper by Luzum and Romatschke [1]. Elliptic flow coefficient v_2 for different viscosities, comparison of theory predictions and STAR collaboration experimental measurements.

quenching [12], illustrated in Fig. (2), which means that the quark-gluon plasma is very

strongly coupled.

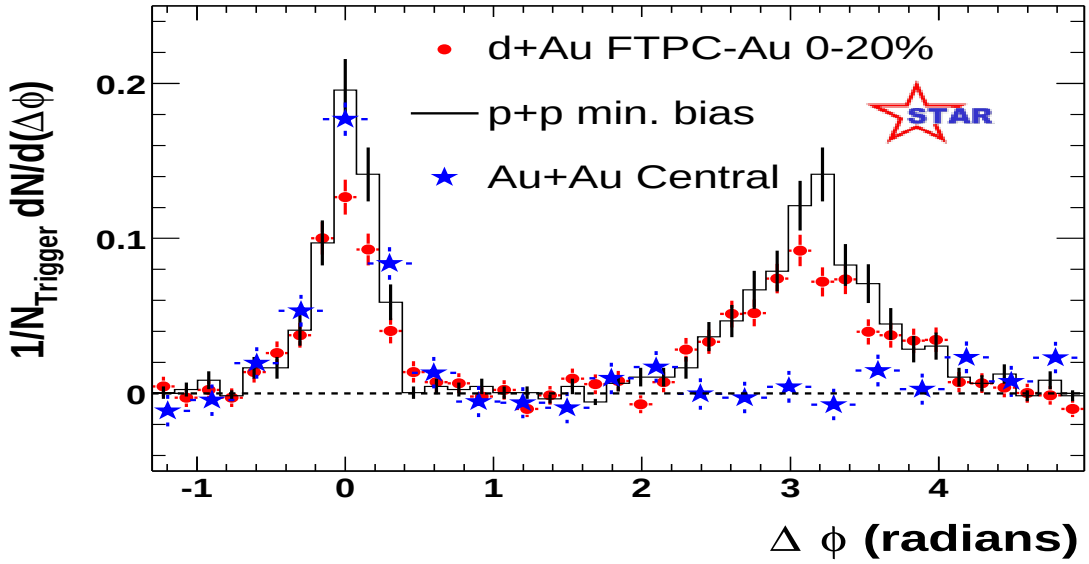

Figure 2: From the STAR collaboration paper [12]. Jet quenching for Au-Au collisions.

0.1.2 AdS/CFT Correspondence

The AdS/CFT or Maldacena conjecture, referred also to as holography, states the equivalence (also referred to as duality) between the following theories: the type IIB superstring theory on $AdS_5 \times S^5$ spacetime, and the $\mathcal{N} = 4$ supersymmetric Yang–Mills gauge theory in 4 dimensions with the gauge group $SU(N_c)$. The superstring theory (or its supergravity limit) is known as bulk theory, gauge theory in 4d is known as boundary theory. Here both AdS_5 and S^5 have the same radius R, the string coupling is g_s, Yang–Mills coupling is g_{YM}, Yang-Mills is in its superconformal phase. The following identifications of the parameters must be done in order to relate bulk to boundary: coupling constants are related as

$$4\pi g_s = g_{YM}^2, \tag{1}$$

and the radius of AdS is related to string tension α' and coupling:

$$R^4 = 4\pi g_s N_c \alpha'^2. \tag{2}$$

Equivalence supposes a precise map between the states (and fields) on the superstring side and the local gauge invariant operators on the gauge theory side. Each field Φ_J in supergravity has its counterpart O_J – an operator in gauge theory. The AdS/CFT

conjecture is the equivalence of partition functions of $Z_{SYM}[J]$ bulk and $Z_{string}[\Phi_{\partial AdS}]$ boundary theories

$$Z_{SYM}[J] = Z_{string}[\Phi] \tag{3}$$

under the following condition: $Z_{SYM}[J]$ is calculated in the presence of four-dimensional sources $J(x)$ on the boundary $z = 0$, and $Z_{string}[\Phi]$ is calculated with the following boundary conditions upon bulk fields Φ:

$$\Phi_J(x, z) z^{\delta}\big|_{z\to 0} \to J(x), \tag{4}$$

where δ is related to the dimension of field Φ. Some examples of this operator-field correspondence:

- The dilaton field ϕ in supergravity is dual to the gauge field strength operator $\mathrm{tr}\, G^2$ in gauge theory.
- The graviton field $h_{\mu\nu}$ is dual to the energy-momentum current $T_{\mu\nu}$ in gauge theory.

The geometry of $AdS_5 \times S^5$ is shown schematically in Fig. (3). It is designed in such a

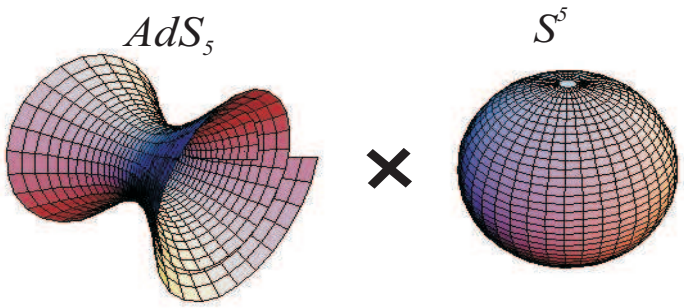

Figure 3: A cartoon of $AdS_5 \times S^5$

way that its group of motion would coincide with the internal and Lorentzian symmetry of the field theory. We illustrate how these symmetries are related with the dynamics of the bulk theory in Fig. (4). As shown there, the geometry is sourced by pack of N_c copies $D3$ branes, $N_c \gg 1$, all placed into the same place in a ten-dimensional spacetime. The branes being heavy act as a source term for the (super)gravity equations of motion. When solved, they yield the $AdS_5 \times S^5$ metric with equal radii of the sphere and the AdS part which is illustrated in the figure below: it is flat at $y \to \infty$, and looks like a "throat" at $y \to 0$. The "throat" geometry is shown in Fig. (5).

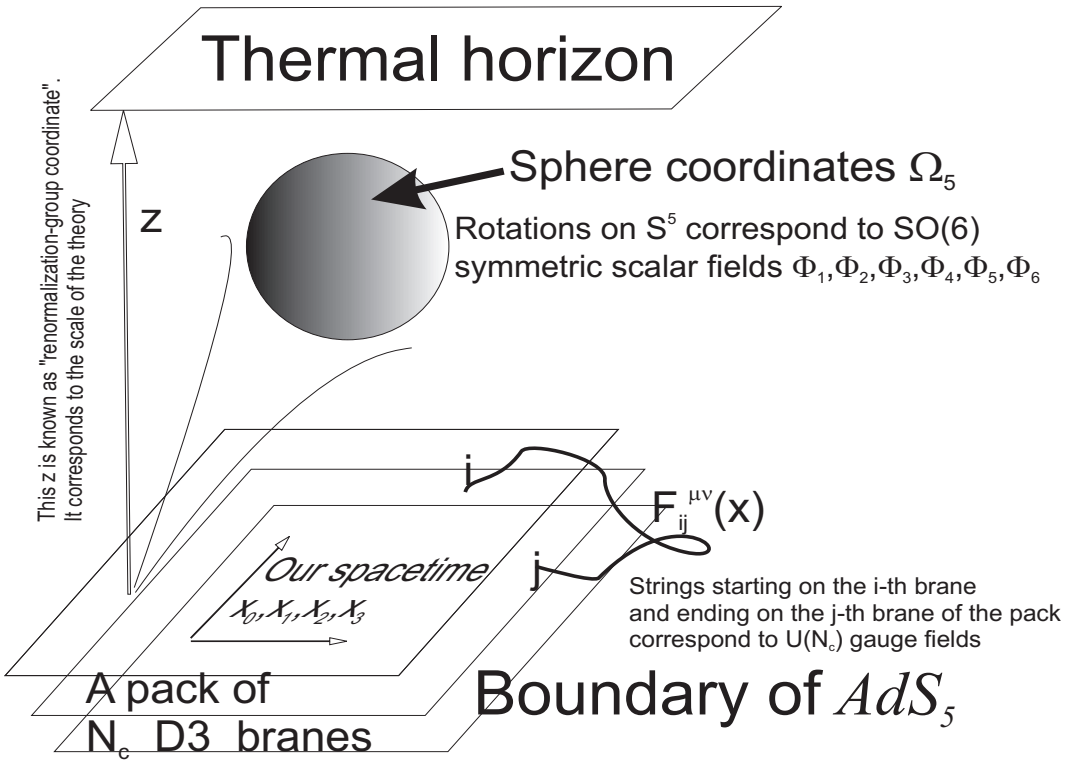

Figure 4: Cartoon of holography physics

AdS/CFT provides a general framework for our thinking. If we want however to make some specific predictions for a non-supersymmetric theory with fundamental matter fields, we must specify some hadronic scale and enter some additional construction elements responsible for fermionic degrees of freedom.

"Top-down" presumes a formulation of the theory, wherein all elements of the action (the ten-dimensional supergravity part of the action, the Dirac–Born–Infeld contributions from additional objects) are string-theory motivated and geometrically well-defined. An illustration of how one makes e.g. a quark degree of freedom geometrically defined is shown in Fig. (6). The "throat" geometry is shown in Fig. (5). The Dirac–Born–Infeld action actually describes fluctuations of the brane surface, which physically are similar to meson fields in chiral theory. Thus only those fields are allowed which have a clear geometric interpretation in terms of fluctuations of some objects. A "bottom-up" model [13] is built, on the contrary, *ad hoc*, the bulk action is formulated in 5 dimensions; the field content of the theory is chosen also *ad hoc*, dependent on which operators we want to study on gauge theory side, so that as many QCD results are fitted as possible.

The first successful and widely accepted top-down recipe of adding flavour to AdS/CFT

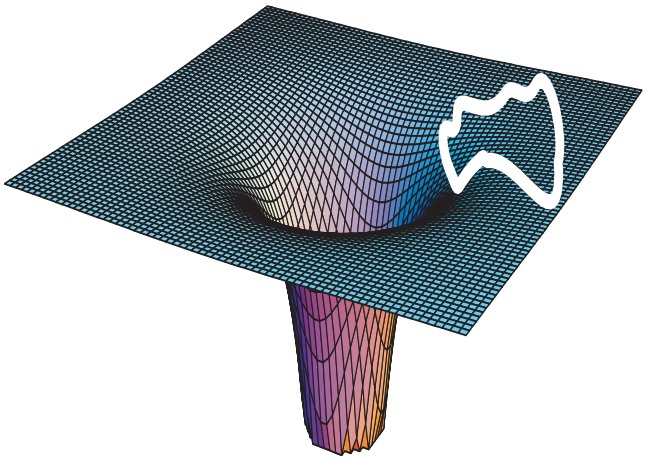

Figure 5: AdS throat, with a cartoon of a closed string in it.

was suggested by Karch and Katz in 2002 [14] by embedding some extra $D7$ branes into the geometry. Later the idea was developed by Sakai and Sugimoto in their $D4-D8-\overline{D8}$ model. The Karch–Katz model breaks the symmetry from $\mathcal{N}=4$ to $\mathcal{N}=2$, which is still far away from the real world. One must implement supersymmetry breaking and conformal symmetry breaking to get closer to physical reality. For imitating QCD, chiral symmetry must also be broken, both spontaneously (strongly) and explicitly (weakly). This was performed in [15], where a Constable–Myers deformed non-supersymmetric background was used instead of pure AdS space. This has allowed to break chiral symmetry, and eventually to obtain a realistic meson spectrum. Further successes of this model are listed in Section 0.2.2. In the holographic part of this work, I extend and develop the ideas of studying the Karch–Katz model in deformed backgrounds with scale.

0.1.3 Structure of this Work

In my work I explore the possible approaches to the non-perturbative QCD in external fields and compare them. In Chapter 1 I study an instantonic effect in the external fields – the chiral magnetic effect – at strong coupling. The result is remarkable, since the current at strong coupling is obtained to be 1/3 of the current at weak coupling. In Chapter 2 by studying quark and gluon one- and two-point correlators, I establish the well-known decoupling relation and prove that dilatation Ward identities hold non-trivially. The scalar condensate within the same model is studied in Chapter 3. Unlike the chiral perturbation theory, my holographic calculation predicts a quadratic, not linear, growth of the condensate. This fact surprisingly allows me to discover an underlying field

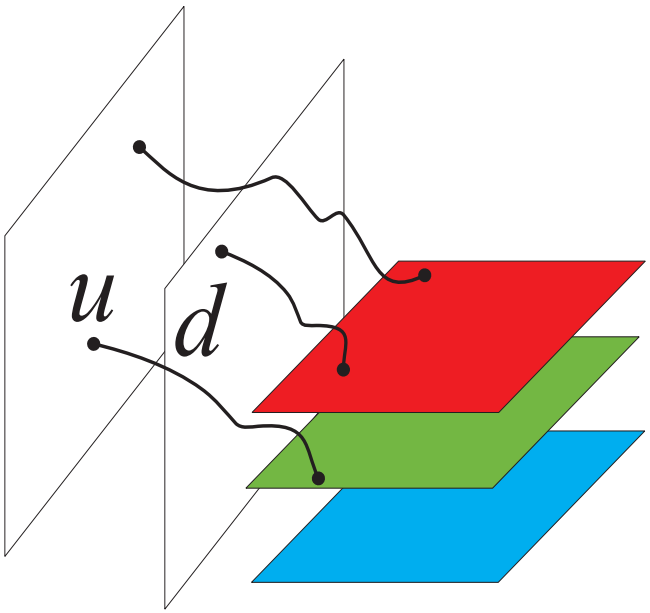

Figure 6: Flavour branes u, d are added to "colour" branes (shown in red, green, blue respectively); quark degrees of freedom are represented by strings, running between them, as shown in the Figure.

theory structure, which makes it feasible also in chiral perturbation theory to restore the quadratic dependence at the large N_c limit. External fields also induce vacuum tensor condensates absent otherwise, and that is reflected by the non-zero vacuum magnetic susceptibility. The magnetic susceptibility of the vacuum is calculated in Chapter 4 also at strong coupling, which is analyzed in a comparison study against lattice data on the condensate susceptibility.

In the second part of my work I compare standard field theory resummation methods to the non-perturbative holographic models of the first part. In Chapter 5 I consider a possibility to apply the Erickson-Semenoff-Szabo-Zarembo (ESSZ) resummation to a non-supersymmetric theory; in Chapter 6 I estimate the contribution of Dyson-Schwinger resummed propagators to vacuum condensates. In the both latter cases I demonstrate partial or full failure of the resummed theory to exhibit some or any non-perturbative features. Thus I conclude superiority of holographic methods to study QCD in external fields when compared to Dyson-Schwinger and ESSZ resummation and suggest new experiments to check some of the duality predictions, namely, those of chiral magnetic effects in external fields.

0.2 Perturbative and Non-Perturbative Approaches to QCD: a Short Review

0.2.1 Condensates and Hadron Physics

Definition

One of the simplest and most effective ways to describe the non-perturbative effects in QCD are vacuum condensates. In general, the theoretical basis for the use of condensates [16] is the Wilsonian operator product expansion (OPE), which reads as

$$i\int d^4x e^{iqx}\left\langle \mathcal{O}^A(x)\mathcal{O}^B(0)\right\rangle = \sum_C C^{ABC}(q)\mathcal{O}^C. \tag{5}$$

The condensates still retain a great phenomenological significance and do indeed explain a lot of facts which would otherwise be beyond our understanding. The notion of condensate was first introduced by Shifman, Vainshtein and Zakharov in [17]. They have noticed that the sum rules

$$\frac{1}{\pi}\int\limits_{4m_q^2}^{\infty}\frac{ds\ \operatorname{Im}\Pi_{QCD}}{(s+q^2)^{n+1}} = \frac{1}{\pi}\int\limits_{\text{threshold}}^{\infty}\frac{ds\ \operatorname{Im}\Pi_{phys}}{(s+q^2)^{n+1}} \tag{6}$$

manifest a discrepancy in the fifth order in n for ϕ mesons; here Π_{QCD} is the perturbative vacuum polarization, and $\Pi_{phys}(s)$ is directly related to the experimental observable – the branching ratio

$$R(s) = \frac{\sigma(e^+e^-\to \text{hadrons})}{\sigma(e^+e^-\to\mu^+\mu^-)} = \frac{\sigma(e^+e^-\to \text{hadrons})}{\frac{4\pi\alpha^2}{3s}} \tag{7}$$

in the following way

$$\operatorname{Im}\Pi(s) = \frac{1}{3}\alpha s R(s), \tag{8}$$

the left-hand side being an integral in the Euclidean domain, the right-hand side – a Minkowskian (physical) direct observable. The discrepancy was very effectively cured by the revolutionary suggestion that the vacuum polarization Π, apart from the standard perturbative (PT) logarithmic terms

$$\Pi_{PT} = -\frac{1}{4\pi^2}\left(1+\frac{\alpha_s}{\pi}\right)\ln\frac{q^2}{\mu^2}, \tag{9}$$

acquires *a power correction* $\delta\Pi$, which in the simplest case contains $1/q^4$ terms:

$$\delta\Pi = \Pi_{\text{power}} = \frac{\alpha_s}{12\pi}\frac{\langle \operatorname{tr} G^2\rangle}{q^4} + \frac{2m_q\langle\bar{q}q\rangle}{q^4}. \tag{10}$$

Generally, the polarization function in QCD looks like

$$\Pi(q^2) = \Pi_{PT} + \sum_{k=2...5} C_k \left(\frac{\mu^2}{q^2}\right)^k, \tag{11}$$

where the *power corrections* $\left(\frac{\mu^2}{q^2}\right)^k$ come from the contribution of the *condensates*. It is believed by many [18] that asymptotic freedom and running of the coupling is broken not by the higher α_s terms, but rather by the power corrections.

The gluon condensate, apart from other meanings it has in theory, is thought of as some soft field, stopping the singular increase of QCD coupling in the IR [19]. A standard value of the gluon condensate is taken to be

$$\langle \frac{\alpha_s}{\pi} \operatorname{tr} G^2 \rangle \leq 0.01 \text{GeV}^4 \tag{12}$$

Unusually high estimates for the gluon condensate

$$0.04 \leq \langle \frac{\alpha_s}{\pi} \operatorname{tr} G^2 \rangle \leq 0.105 \text{GeV}^4 \tag{13}$$

from the analysis of J/Ψ and Υ meson families were suggested in [20]. Yet this result was sharply criticized by Ioffe in [21] as unreliable for not taking into account the finiteness of mesonic widths in the sum rules. Ioffe gives himself the value

$$0.04 \leq \langle \frac{\alpha_s}{\pi} \operatorname{tr} G^2 \rangle \leq 0.005 \pm 0.004 \text{GeV}^4. \tag{14}$$

Condensate Properties in External Fields

Basic non-perturbative properties of QCD condensates in external fields have been known from field theory. Among these count:

- Magnetic catalysis of (explicit) chiral symmetry breaking. The mass grows [22] as

$$m_q^2 = 2|e_q B| \left(c_q \alpha_s\right)^{2/3} e^{-\frac{4N_c\pi}{\alpha_s(N_c^2-1)\log(1/c_q\alpha_s)}}, \tag{15}$$

  where $c_q = \frac{e}{2\pi e_q}$, e is the electron charge, e_q is q-th quark electric charge, m_q is the quark mass.

- Chiral condensate growth [23]

$$\Delta\Sigma(H) = \Sigma(0) \frac{eB \log 2}{16\pi^2 f_\pi^2} I_H \left(\frac{m_\pi^2}{eB}\right), \tag{16}$$

  where the function $I(y)$ can be easily constructed numerically from its definition

$$I_H(y) = -\frac{1}{\log 2} \int_0^\infty \frac{dz}{z^2} e^{-yz} \left[\frac{z}{\sinh z} - 1\right]. \tag{17}$$

- Chiral condensate growth in the regime [24] of a large magnetic field $H \gg m_\pi^2$

$$\Delta\Sigma(H) = \Sigma(0)\frac{eH\log 2}{16\pi^2 f_\pi^2}. \tag{18}$$

Low-Energy Theorems

Furthermore, the condensates lead to a number of very interesting statements in field theory. In particular, the following low-energy theorems are valid.

Dilatation Ward Identity. Eq. (52) in [25] states the following theorem (dilatation Ward identity) holds

$$\lim_{q\to 0} i\int e^{iqx}d^4x\left\langle T\left\{\mathcal{O}(x),\frac{\beta(\alpha_s)}{4\alpha_s}\operatorname{tr}G^2(0)\right\}\right\rangle = (-d)\langle\mathcal{O}\rangle\left[1+\text{mass-dependent terms}\right], \tag{19}$$

where d is the canonical dimension of the operator $\mathcal{O}$, the one-loop beta-function is normalized as $\beta(\alpha_s) = -\frac{b\alpha_s^2}{2\pi}$, $b = \frac{11}{3}N_c - \frac{2}{3}N_f$. Identities for higher correlators are also available:

$$i^2\int d^4xd^4y\left\langle T\left\{\mathcal{O}(x),\frac{\beta(\alpha_s)}{4\alpha_s}\operatorname{tr}G^2(y),\frac{\beta(\alpha_s)}{4\alpha_s}\operatorname{tr}G^2(0)\right\}\right\rangle = (-d)^2\langle\mathcal{O}\rangle\left[1+\text{mass-dep. terms}\right]. \tag{20}$$

For the gluon field strength operators we obtain:

$$i\int\left\langle T\left\{\frac{3\alpha_s}{4\pi}\operatorname{tr}G^2(x),\frac{3\alpha_s}{4\pi}\operatorname{tr}G^2(0)\right\}\right\rangle = \frac{18}{b}\left\langle\frac{\alpha_s}{\pi}\operatorname{tr}G^2\right\rangle, \tag{21}$$

the latter is proven in Appendix B of [25]. In fact, the left-hand side of the equation above is the zero-frequency limit of the gluon correlator.

Gluonia in Self-Dual Fields. In *self-dual fields* for correlators defined as

$$\begin{aligned} S(q^2) &= i\int d^4x e^{iqx}\langle\operatorname{tr}G^2(x)\operatorname{tr}G^2(0)\rangle, \\ P(q^2) &= i\int d^4x e^{iqx}\langle\operatorname{tr}G\tilde{G}(x)\operatorname{tr}G\tilde{G}(0)\rangle, \end{aligned} \tag{22}$$

it is true that [26]

$$S+P = \alpha_s^2q^4\left\{\frac{1}{4\pi^2\log\frac{\mu^2}{q^2}}+\frac{4}{g^2q^2}\langle 2O_1-O_2\rangle\right\}, \tag{23}$$

where O_1 and O_2 are the higher-order gluon field operators

$$\begin{aligned} O_1 &= (f^{abc}G^b_{\mu\alpha}G^b_{\nu\alpha})^2, \\ O_2 &= (f^{abc}G^b_{\mu\nu}G^b_{\alpha\beta})^2. \end{aligned} \tag{24}$$

Another interesting low-energy theorem in a self-dual field is the following correlator of the energy-momentum components $\theta_{\mu\nu}$ which becomes zero in a self-dual field up to contact terms

$$\Pi_{\mu\nu,\mu',\nu'}(q) = 0 \quad (+\text{contact terms}\dots), \tag{25}$$

where

$$\Pi_{\mu\nu,\mu'\nu'}(q) = i\int e^{iqx}\langle T\{\theta_{\mu\nu}(x),\theta_{\mu'\nu'}(0)\}\rangle, \tag{26}$$

the energy-momentum tensor is defined as $\theta_{\mu\nu} = -G^a_{\mu\alpha}G^a_{\nu\alpha} + \frac{g_{\mu\nu}}{4}G^a_{\alpha\beta}G^a_{\alpha\beta}$.

Two-Point Gluonium Correlators. Interesting low-energy theorems on two-point correlation functions [27] are

$$\begin{aligned} \frac{i}{V_4}\int d^4x d^4y\,\langle \delta_{ij}S_0(x)S_0(y) - P_i(x)P_j(y)\rangle &= -\frac{G_\pi^2\delta_{ij}}{m_\pi^2} + \delta_{ij}\frac{B^2}{8\pi^2}(L_3 - 2L_4 + 3) = \\ &= 2\delta_{ij}\int d\lambda\left(\frac{m\frac{\partial}{\partial m}\rho(\lambda,m)}{(\lambda^2+m^2)} - \frac{2m^2\rho(\lambda,m)}{(\lambda^2+m^2)^2}\right), \end{aligned} \tag{27}$$

where S_i, P_i are scalar and pseudoscalar currents that have been obtained [28] from AdS/QCD duality as well; L_i are chiral perturbation theory coefficients.

Gluonium Correlators and Leading Logs from Field Theory. The following perturbative expressions can be explicitly calculated for gluonium correlators [29]

$$S(q^2) = 16i\int d^4x e^{iqx}\langle T\theta^\mu_\mu(x)\theta^\nu_\nu(0)\rangle = \sum_A C_A\langle\mathcal{O}_A\rangle, \tag{28}$$

where operators $\mathcal{O}_A$ are

$$\begin{aligned} \mathcal{O}_A &= \hat{1}, \\ \mathcal{O}_4 &= \tfrac{\alpha_s}{\pi}\,\mathrm{tr}\,G^2, \\ \mathcal{O}_6 &= g^3 f^{abc}G^a_{\mu\nu}G^b_{\nu\lambda}G^c_{\lambda\mu}, \\ \mathcal{O}_8 &= 14(\alpha_s f_{abc}G^a_{\mu\rho}G^b_{\nu\rho})^2 - (f_{abc}G^a_{\mu\nu}G^b_{\rho\lambda})^2, \end{aligned} \tag{29}$$

and the OPE coefficients up to two loops are

$$\begin{aligned} C_0 &= -2\left(\tfrac{\alpha_s}{\pi}\right)^2 Q^4\log\tfrac{Q^2}{\mu^2}\left\{1 + \tfrac{59}{4}\tfrac{\alpha_s}{\pi} + \tfrac{\beta_1}{2}\left(\tfrac{\alpha_s}{\pi}\right)\log\tfrac{Q^2}{\mu^2}\right\}, \\ C_4 &= 4\pi\alpha_s\left\{1 + \tfrac{49}{12}\tfrac{\alpha_s}{\pi} + \tfrac{\beta_1}{2}\left(\tfrac{\alpha_s}{\pi}\right)\log\tfrac{Q^2}{\mu^2}\right\}, \\ C_6 &= 2\tfrac{\alpha_s}{\pi}\left\{1 - \tfrac{29}{12}\alpha_s\right\}, \\ C_8 &= 1, \end{aligned} \tag{30}$$

where $Q^2 = -q^2$, μ is the renormalization scale.

Gluonium Correlators from Holography. In the work [30] the gluonium propagator

$$\Pi(q^2) = i \int e^{iqx} \langle \mathrm{tr}\, G^2(x)\, \mathrm{tr}\, G^2(0) \rangle d^4x \tag{31}$$

was calculated with the non-perturbative correction:

$$\Pi(q^2) = -\frac{2}{\pi^2} q^4 \left[\log \frac{q^2}{\lambda^2} + \frac{4\lambda^2}{q^2} \log \frac{q^2}{\lambda^2} + \frac{20}{3} \frac{\lambda^4}{q^4} \right], \tag{32}$$

for the sake of normalization here I quote the condensates of the leading gluonic operators

$$\begin{aligned} \langle \mathrm{tr}\, G^2 \rangle &= -\frac{10}{3\pi^2} \lambda^4, \\ \langle \mathrm{tr}\, gG^3 \rangle &= \frac{4}{3\pi^2} \lambda^6, \\ \langle \mathrm{tr}\, G^4 \rangle &= -\frac{8}{15\pi^3 \alpha_s} \lambda^8. \end{aligned} \tag{33}$$

The smeared D3-background [31] has lead to a very interesting example of the $\langle \mathrm{tr}\, G^2(x)\, \mathrm{tr}\, G^2(0) \rangle$ correlator without the log term:

$$\Pi(q^2) = -\frac{N_c^2}{32\pi^2} q^4 \psi \left(\frac{1}{2} + \frac{1}{2} \sqrt{1 - \frac{L^4 q^2}{l^2}} \right), \tag{34}$$

where L is AdS radius, l is the average distance between the branes, and $\frac{l}{L} \ll 1$. The gluonium propagator was calculated in the soft-wall AdS/QCD model in [32].

Decoupling Relation. For light quarks we have, as derived in [25] (eq. 102):

$$\frac{d}{dm_q} \left\langle \frac{\alpha_s}{\pi} \mathrm{tr}\, G^2 \right\rangle = -\frac{24}{b} \langle \bar{q} q \rangle. \tag{35}$$

This low-energy theorem for heavy quarks is recovered also in an independent manner from the Cornwall-Jackiw-Tomboulis potential in [33]. For heavy quarks it is true that

$$\langle \bar{q} q \rangle = -\frac{1}{12} \left\langle \frac{\alpha_s}{\pi} \mathrm{tr}\, G^2 \right\rangle. \tag{36}$$

the derivation of this relation is found in [16], eq. 6.25, p. 438. The factors 12 and 24 in the equations above are symmetry factors and come from a direct diagrammatic estimate of Feynman diagrams with corresponding external legs ending in vacuum fields. Let us stress that the factors 12 and 24 are universal, they do not contain N_c or N_f.

A slightly different form of the argument, from which the relation (36) emerges is the following. Consider the trace of the energy-momentum tensor of a gauge theory. For low quark mass there is a beta-function contribution from the quark, for heavy quarks there is only the gluonic contribution to the beta-function, yet there is a quark chiral condensate present:

$$\theta^\mu_\mu = \begin{cases} \left(\frac{11}{3}N_c - \frac{2}{3}\right)\frac{\alpha_s}{8\pi}\,\mathrm{tr}\,G^2, \\ \\ \left(\frac{11}{3}N_c\right)\frac{\alpha_s}{8\pi}\,\mathrm{tr}\,G^2 + m\bar{q}q. \end{cases} \tag{37}$$

When the two are equated, the necessary relation (36) appears. Equating small and large m domains happens on the ground that we select the scale at which the heavy quarks "decouple" from the one-loop polarization operator. Hence this theorem is also known as decoupling relation. A picture of the condensate as a function of the quark mass is given in [25], Fig. 18, p. 366.

0.2.2 Gluon Condensate and Holography

Different Holographic Approaches to Condensates and Pions

As mentioned above, condensates are not inherent to the AdS/CFT setup, thus it must be supplied with additional elements. In current literature there are several different approaches to pions and condensates, which are not quite compatible with each other, yet all of them remain popular since they yield reasonable results on meson masses, decay constants and coupling constants. In Section 0.1.2 I have already given the basic distinction between the two most widely-used classes models, the top-down and bottom-up models. Now I shall list the most common versions and modifications of them, briefly reviewing their successes and failures.

- **Top-down models:**

  - The $D3/D7$ model has been formulated in [15]. The idea of the model is to represent the fermionic (or mesonic via the quark-hadron duality) degrees of freedom in QCD by a probe brane, whose action is that by Dirac–Born–Infeld. Dynamical variables are the brane embedding coordinate $X^8 + iX^9 = w(\rho)e^{i\phi}$, and bulk vector fields A_μ, where w fluctuations are identified on the boundary with scalar mesons, and those of ϕ with pseudoscalars, fluctuations of the vector field are identified with vector mesons, while axial-vector mesons are absent in

this model. The scheme of brane embedding into the background and the physics corresponding to different sets of modes is illustrated in Fig. (7).

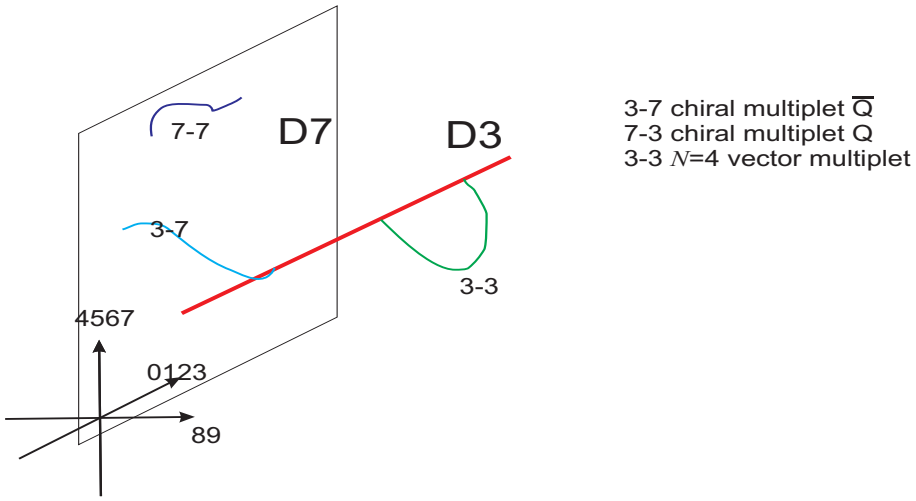

Figure 7: A scheme of an embedding of a D7 brane into the D3 backgrounds; shown are strings, whose oscillations correspond to the particles of specific sectors of the theory.

  - Sakai–Sugimoto: The $D4/D8/\overline{D8}$ model [34] is formulated on the similar physical principles as the $D3/D7$ model above, yet a different background is used (type IIA) and a different probe object is placed therein (a pair of $D8$ branes). The embedding coordinate is not a dynamical variable any more, dynamical variables are now two sets of bulk vector fields A_L, A_R. The holonomy of A_5 corresponds to pion on the boundary, $A_L \pm A_R$ correspond to vector and axial-vector mesons. The quark mass, pion mass and condensate cannot be explicitly introduced in this model, yet the description of meson spectra and coupling constants is amazingly well fitting experimental data.

- **Bottom-up models:** Mostly, terms "bottom-up" and "AdS/QCD" are synonyms. The AdS/QCD has the full set of fields given explicitly as an *ad hoc* model: $X = ve^{i\frac{\pi}{f_\pi}}$, which contains the dynamics of scalar and pseudoscalar mesons, bulk vector fields F_V, F_A correspond to vector and pseudo-vector mesons. The main difference between the classes of phenomenological AdS/QCD models is the type of chiral symmetry breaking. It is characterized by by:

  - Presence or absence of a scalar ("tachyon") field.
  - IR boundary condition.

- Joining two branes in the IR.
- If we regard AdS/QCD as a development of Sakai–Sugimoto, then an X (tachyon) field arises from gauging the action to the $A_5 = 0$ gauge. If we regard it as a development of the $D3/D7$, X is related to the embedding coordinate.
- The so-called improved holographic setup [35] has a peculiar set of fields. Apart from A_L, A_R it has a tachyonic field τ in the 5-dimensional DBI action, which is analogous to the embedding coordinate in the $D3/D7$ model.

Hard-Wall AdS/QCD Approach

The hard-wall AdS/QCD is due to Erlich, Katz, Son, Stephanov [13], Da Rold and Pomarol [36]. The model includes left- and right-handed vector $SU(N_f)_{L,R}$ adjoint fields L_μ, R_μ, corresponding to vector and axial-vector mesons, and a scalar X ("tachyon") bifundamental $SU(N_f)_L \times SU(N_f)_R$ field, corresponding to the scalar and axial mesons. The name "hard-wall" comes from the boundary conditions that set an infinitely high wall in the IR end. The hard-wall model was one of the first models that gave extensive experiment-comparable predictions. Its obvious disadvantage is the absence of the Regge spectrum for mesons; masses of resonances are rather organized as $m^2 \sim n^2$. The soft-wall model allows one to introduce the quark mass and the chiral condensate via the asymptotics of X in the UV. Although the hard-wall is now considered to have been mostly superceded by the soft-wall and other approaches, let us mention its most interesting developments. The form factors and the wave functions of the vector mesons were found in [37]. The deconfinement transition temperature in the hard-wall approach was obtained in [38]. Scalar and pseudoscalar two point correlators, meson masses and interactions were calculated in [39]. Effects of the gluon condensate upon chiral perturbation theory coefficients L_i are studied in the hard-wall model in [40] by means of quartic deformation of the metric. Self-bound objects, that is, classical solutions corresponding to the bound states with strong interactions, were studied in the hard-wall model in [41], and used for modelling nuclei. Surprisingly, the gluon condensate has been shown to be of little importance for the meson spectra in the hard-wall QCD model [42].

Soft-Wall AdS /QCD

Definition. The original reason to introduce the soft-wall [43] (quadratic dilaton) model (Karch-Katz-Son-Stephanov, KKSS) was to cure the meson spectrum. In the hard wall model the spectrum was $m_n^2 \sim n^2$. The soft-wall model has a dilaton $\phi = z^2$, with the metric being $ds^2 = \frac{dx^2+dz^2}{z^2}$. This yields qualitatively a correct Regge trajectory $m_n^2 \sim n$.

The enormous development of this model is discussed below.

Spectrum. A comparison of heavy quarkonia masses obtained from the soft-wall, hard-wall and braneless approaches has shown that the soft-wall approach is closer to experiment than the other two [44]. Glueball spectra were obtained in the soft-wall model in [45, 46], where it was found that the scalar and pseudoscalar glueballs are degenerate, whereas the vector glueballs are heavier then those. A "dynamical" version of the soft-wall model was considered in [47] where a tachyon field was taken into account. Linear Regge trajectories were obtained for heavy mesons and the tachyon field was interpreted in terms of non-critical string theory tachyon. It was claimed in [48] that soft-wall QCD predicts vector dominance breakdown due to the fact that vector meson couplings to other hadrons grow linearly with the increase of the radial excitation number n. A version of the soft-wall AdS/QCD with an additional UV cutoff, suggested in [49], has improved the ρ spectrum, with typical theory vs. experiment discrepancies becoming less then 10% instead of ca. 20% in the original soft-wall model. The soft-wall AdS/QCD was modified in [50] in such a way that it allows to independently break chiral symmetry spontaneously and explicitly; meson spectra are in good agreement with the experiment (up to 10%) except for the lowest ρ and f states. The heavy vector meson state spectral function at finite temperature from soft-wall AdS/QCD was found in [51] to be in good agreement with the lattice.

Interactions. In [52] it was shown that the effective quadratic dilaton behavior can be derived from the instanton gas model; the instanton size plays the role of the fifth coordinate in the field-theoretical approach. The QCD string tension was calculated as a function of temperature in the soft-wall AdS/QCD in [53]. Quartic and fourth-order in z corrections to the soft-wall quadratic dilaton, which account for the back-reaction and contain quark mass and condensate were suggested in [54]. The quark-quark potential in this back-reaction geometry was further studied in [55]. Form-factors for the ρ-meson obtained from the soft-wall model have been shown to be more realistic than those of the hard-wall [56]. The pion form-factor was calculated for spacelike momenta in [57] for both hard- and soft-wall models; it was found that the soft-wall model is a more realistic approximation. DIS structure functions were found in [58], for the soft-wall and hard-wall AdS/QCD similar results were observed. Light mesons were studied in the soft-wall model in [59], where it was found that a $1/q^2$ term (coupled to the dimension-two condensate) is present in the holographic sum rule, which is absent in the normal AdS/QCD. An absence of renormalons was demonstrated in [60] (the model used there for the Wilson loop calculation is equivalent, for that purpose, to the soft-wall AdS/QCD). In [61] a yet unresolved problem of the soft-wall AdS/QCD was noticed, namely, that the strong

couplings of scalar mesons to pairs of light pseudoscalars are too small compared to the experimental values. Virtual Compton scattering in the soft-wall model is studied in [62].

Thermodynamics and Kinetics. The deconfinement transition temperature was obtained in [38]; the dilaton running being fixed by the Regge curve, the numeric value for the transition temperature (ca. 340 MeV) is available, which is close to the lattice result. The jet quenching parameter was obtained from soft-wall AdS/QCD in [63] to be $3.5\frac{\mathrm{GeV}^2}{\mathrm{fm}}$ at the phase transition temperature. Viscosity and entropy in the soft-wall model were shown to violate the conformality bound in [64]; corrections to the viscosity due to the dilaton flow coefficient c (the latter defined from dilaton asymptotics $\phi = e^{cz^2}$) were found. Liu, Rajagopal and Shi, working in a kind of a soft-wall model have shown [65] that the drag and momentum diffusion constants, as well as the screening length for a quark-antiquark pair, become infrared insensitive in the relativistic limit, thus endowing with greater robustness the holographic results for these values. Agreement between the 4d picture of the confinement-deconfinement phase transition and the 5d Hawking-Page phase transition was demonstrated in [66]. The quark number susceptibility was calculated in [67] and has been shown to be identical in hard and soft wall models, zero at small temperatures (confinement phase), and $\sim T^2$ at large (deconfining) temperatures. The quark number susceptibility was calculated in [68] for both the hard- and the soft-wall AdS/QCD in the Reissner–Nordström background. It was found that both backgrounds exhibit the expected peak at $T = T_c$, yet the hard-wall model is pathological in the sense that at $\mu = 0$ the susceptibility does not depend on T any more, which is unphysical; in the soft-wall model this pathology is cured and the quark number susceptibility grows with temperature. From the analysis of the spectral functions of scalar, pseudoscalar, vector, pseudovector mesons in the soft-wall model, it was found [69] that the pseudovector melts earlier than the vector does, while the scalar and the pseudoscalar melt at the same temperature, but still below that of the vector.

Modified AdS/QCD Models

Pomarol–Wulzer Approach. The model by Pomarol and Wulzer is focussed at baryons. It is a version of AdS/QCD with a Chern-Simons term. The average precision of the model on a wide range of observables (interaction vertices) is claimed to be 16% against experiment. Nucleon form-factors have been calculated in [70], producing an agreement around 30% against experiment.

Forkel–Beyer–Frederico Approach. A *sui generis* modification of AdS/QCD was proposed by Forkel, Beyer and Frederico [71]. It is an AdS/QCD approach with a constant dilaton and an IR deformed warp factor. The parameters of the deformation are chosen in such a way that a linear baryon Regge trajectory is observed. The baryons are modelled by an *ad hoc* fermion, introduced into the bulk action; its spectrum results in the tower of the boundary baryons. The model is claimed to be the first in which both the linear Regge trajectories for the mesons and the baryons have been observed. It has received various developments. In [72] a $\frac{c}{z^2}$ term was added to the dilaton potential and a $z-$dependent mass was introduced, which lets chiral symmetry be broken independently both spontaneously and explicitly. For axials, vectors and pseudoscalars, masses and decay constants were calculated; the lowest ones disagree greatly, whereas all the rest exhibit 10-20% agreement with experiment.

Hirn-Sanz approach An "interpolation" between the hard-wall and the soft-wall AdS/QCD was suggested by Hirn and Sanz [73]. The model is ideologically closer to $D4/D8/\overline{D8}$, since it does not have a scalar field, analogous to the embedding coordinate in $D3/D7$, $D3/D5$ or to the X field in hard/soft wall AdS/QCD. The set of fields it features includes massless pions, higher-resonance radial excitations of pions, vectors and axial-vectors. Chiral symmetry breaking is performed by the IR boundary conditions. The pions arise as the holonomy of the A_5 field. The model predicts a quadratic, not a Regge behaviour of mesonic resonance masses m_n^2, however, the authors argue that this is admissible, since no-one has proven that linear trajectories must persist for all possible resonances. The Weinberg sum rules are nicely reproduced (up to the 0.1% level at some instances), and the vector meson dominance is strongly supported. The model also predicts (with different degree of success) the chiral Lagrangian interaction coefficients L_i. There are problems in this model with the condensates; the authors advocate the idea to modify the metric differently for scalar and vector fields, and then to adjust coefficients so that the Novikov–Shifman–Zakharov sum rules would be satisfied. The program is fulfilled in [74], yet in such a construction, where the geometry is different for vectors and axials, can be viewed as standing out of the standard holographic paradigm. The Froissart bound is satisfied. The axial electromagnetic form factor is found to be identically zero. A correct N_c scaling of f_i, L_i and the vector meson mass is observed. The AdS five-dimensional computations are also compared with a flat-space five-dimensional model; the AdS meson mass results are better fitting the experiment, yet the results for L_i are comparable. Developments of the Hirn-Sanz model include e.g. a pion-gamma-rho form factor calculation [75]. The neutron mass, isocalar electric radius, axial coupling and isovector magnetic moment have

been computed in [76] from the Hirn-Sanz model. Four-point flavour correlators were calculated in [77].

Sakai–Sugimoto model

A huge amount of literature is dedicated to the Sakai–Sugimoto model [34].

Meson Spectrum Vector and axial-vector meson masses were found with no more than 15% discrepance against experiment in a generalized embedding with non-anti-podal branes [78]. Meson mass shifts were studied in [79]. The repulsive nucleon-nucleon $1/r^2$ potential core was found in [80]. A picture of pionic dominance was proposed near the phase transition point [81]. The tachyon field introduced into the Sakai–Sugimoto model in [82] is claimed to account for chiral symmetry breaking dynamics. In this modified Sakai–Sugimoto model with a tachyonic profile the Gell-Mann–Oakes–Renner relation is claimed to be established [83]. Low-energy pion-pion scattering amplitudes from holography were found in [84] to be in satisfactory agreement with experiment. Meson-baryonic couplings were obtained in [85] for higher resonances. The quark mass was explicitly introduced into the Sakai–Sugimoto model in [86] by means of adding a special D4-brane far away from the stack of QCD branes; the Gell-Mann–Oakes–Renner relation is shown to be fulfilled in such a setting. The quark mass is introduced by means of open strings in [87].

Baryon Spectrum An excited nucleon spectrum with a precision up to 5% against experiment was obtained in [88]. Mass splittings of baryons exhibit rather poor coincidence (up to 50% error) with experiment in the Sakai–Sugimoto model with the strange quark mass added [89]. A very good precision (4% against experiment and lattice) in the baryon mass shift due to quark/lightest pion mass is reported in [90].

Interactions A technique for integrating out the higher Kaluza-Klein modes was suggested in [91] that allowed to calculate the pion electromagnetic form factors in the Sakai–Sugimoto model, which were inaccessible before due to complications with the infinite sum over the KK tower, leading to a good agreement with experiment ($\chi^2/\text{d.o.f.} = 2.8$). Deep inelastic scattering of vector and axial vector mesons is studied in [92] in the Sakai–Sugimoto model; the Callan-Gross relation is shown to be satisfied holographically. The n-body nuclear forces from Sakai–Sugimoto were shown to be of the order $\sim N_c(r^2)^{-n}$ [93]. The leading order hadronic contribution to the muonic $(g-2)$ was obtained in [94], the value of it is given as $a = 470 \cdot 10^{-10}$, whereas the current experimental value from

$e^+e^- \to \pi^+\pi^-$ is $a_{\pi\pi} = 515 \cdot 10^{-10}$. Holographic vector and axial-vector meson form-factors were shown in [95] to have relevance to experiment also at high q^2. A critical analysis of the Sakai–Sugimoto model against the Pomarol–Wulzer model was carried out in [96]; it was shown there that a universal ratio of baryon form-factors [97] fails in the Sakai–Sugimoto model, but survives in the Pomarol–Wulzer model [76]. An excellent agreement with experiment is reported [98], for the Regge regime of the p, p and $p, \overline{p}$ scattering cross-section, where the Pomeron exchange is modelled within the Sakai–Sugimoto model. At arbitrary distances the nucleon-nucleon potential was found in [99] to be universally $1/r^2$ repulsive at small r and $1/r^3$ attractive at long distances. The $1/r^2$ repulsion was also found in [100]. Proton and neutron magnetic moments are shown in [101] to be holographically related in a model-independent way. An agreement of 20-25% against experiment is found in [102] for baryonic radii and form-factors. Electric form factor sum rules are shown to be satisfied up to several % in [103] by means of "resumming" the vector meson resonance tower in taking the first four resonances.

Thermodynamics A new phase of hadronic matter was claimed to have been predicted from Sakai–Sugimoto, in which baryons with semi-integer Skyrmionic ("dyonic") numbers live in the phase with the restored chiral symmetry, light quark mesons live in the colour-confined phase [104]. The baryon binding energy as a function of temperature was found in [105]. The Sakai–Sugimoto and the Nambu–Jona-Lasinio models were compared in [106], close resemblance between them was found at low values of the chemical potential and the temperature, whereas at a large chemical potential they essentially disagree. The baryon number susceptibility is reported at 20-30% agreement against the lattice in [107]. Zero sound and linear scaling of the heat capacity are reported in the Sakai–Sugimoto model at finite chemical potential, which is interpreted as formation of a Fermi liquid state. The confined phase of Sakai–Sugimoto is found in [108] to be an incompressible and static baryonic insulator with a gap, whereas the deconfined state resembles a diffusive conductor with restored chiral symmetry. It is argued in [109] that the degree of inhomogeneity of the nuclear matter phase (observed at values of the baryon chemical potential above the transition point) can be arbitrarily large. Baryonic matter is considered in [67] as one large Skyrmion; pion dominance is reported near the phase transition point, and all meson vector fields disappear. Swelling of baryons in dense matter was observed in [110]. Instanton expansion breakdown below phase transition temperature was reported in [111]. The equation of state is shown to coincide with that of chiral perturbation theory at finite μ and T in [112]. Essential difference is found in gluon penetration length and quark transverse momentum diffusion constant as functions of temperature and incoming parti-

cle energy in [113]; it is speculated that heavy-ion experiments could distinguish between the two.

Magnetic Properties. The chiral magnetic effect was predicted holographically in the Sakai–Sugimoto model by [114, 115, 116, 117]. A state with the phase of the chiral condensate rotating in space, that is, the so-called spiral chiral magnetic state, was found in [118]. Magnetization of the quark-gluon plasma is studied in [119]; a magnetic phase transition is reported, partially resembling metamagnetism (i.e. an increase in the magnetization of a material with a small change in an externally applied magnetic field). In the framework of the open Wilson line paradigm, chiral symmetry breaking parameters are studied in external magnetic and electric fields, as well as temperature [120]. It is found, as expected, that the electric field decreases chiral symmetry breaking, whereas a magnetic field enhances it; a chiral phase transition is observed at some temperature. Saturation of the dimensionless magnetization is observed in [121], where the Meissner effect in the Sakai–Sugimoto model is studied [122]. Saturation of magnetization is observed in [123] at large magnetic fields. Chiral condensate enhancement was noticed in [124] in a magnetic field.

Light-Front Holography (Brodsky – de Teramond approach)

The method formulated in [125] is based on employing a step-function-like warp factor $A(z)$ in the integral over the holographic coordinate, which makes this setup close to the MIT bag model. Brodsky and de Teramond show [126] that the hadron light-cone wave-function, dependent on the light-cone coordinate ζ, can be identified with the 5-dimensional string amplitude $\phi(z)$, with the fifth coordinate identified $z = \zeta$. Numerous developments have followed since. This model allows a derivation of the Schrödinger equation for the spectra of hadrons of arbitrary spin and orbital momentum [127]. Light mesons and baryon spectra are calculated in [128]. The pion form factor was obtained in [129]. Gravitational form-factors of composite hadrons were calculated in [130]. Light-front holography predicts correctly (compared to lattice and Dyson-Schwinger) the running of the non-perturbative QCD coupling [131]. A confining potential was introduced into this model in [132].

Improved Holography

Gürsoy and Kiritsis Proposal Holographic duals of theories with condensates are an intense field of research presently. One of such schemes was proposed by Gürsoy and Kiritsis [133, 35]. The idea is to use a five-dimensional action with a specific dilaton

potential, containing both gluon condensate and running coupling. The bulk action is

$$S = N_c^2 \int d^5x\sqrt{-g}\left[R - \frac{4}{3}g^{\mu\nu}\partial_\mu\Phi\partial_\nu\Phi + V(\Phi)\right], \tag{38}$$

where the potential $V(\Phi)$ is guessed, not derived, the metric is

$$ds^2 = dr^2 + e^{2A(r)}dx^2, \tag{39}$$

and the dilaton Φ has the following asymptotics

$$\begin{array}{rcl} \Phi(u) & = & -\log(-\log(r\Lambda)),\ r \to 0, \\ A(r) & = & -\log(r/l). \end{array} \tag{40}$$

Spectrum. The "improved holography" work [35] has generated a large series of follow-ups, developments and improvements, on the base of the same set of degrees of freedom, with an *ad hoc* potential for the dilaton made responsible for reproducing the beta-function, and various geometries. In [133] a general criterion of confinement in an improved holographic QCD setup was derived. Satisfactory linear Regge glueball trajectories were found. Using this "dynamic holography" in [134, 135], meson masses and decay widths were calculated with precision of ca. 5%. Spectra of hadrons of spin 1/2 and 3/2 were obtained in this model in [136, 137] with 5-10% accuracy. On the basis of the improved holographic QCD, a fermionic extension by means of Sen's tachyonic action was supposed in [138], which allowed a satisfactory calculation of mesonic masses.

Interactions and Thermodynamics. In [139] the dependence of the confinement-deconfinement transitions on the type of the IR behavior of the background was studied. In [140] it was shown that the quark potentials in the improved holography by Gürsoy, Kiritsis and Nitti fit lattice results better than those obtained without the RG improvement. In [141] the thermal gluon condensate was calculated, and it was shown that the physics of the phase transition in the improved holography is very close to pure YM. Glueball masses were predicted at a 3% precision level (compared to lattice) from the improved holographic QCD in [142]. The quark-quark potential in this framework was studied in [143, 144], with additional quadratic corrections (motivated by string-tension) added to the warp factor.

A review of the "dynamic holography" related topics was recently published in [145].

"Braneless" Approach

Gluon Condensate in the Csaki Model. One of the first systematic studies of backgrounds with condensates for the purpose of QCD applications was done by Csaki and

Reece in [146] and is known as "braneless approach". The idea is to consider the five-dimensional action

$$S = \frac{1}{2\kappa^2}\int d^5x\sqrt{g}\left(-R + \frac{12}{L^2} + \frac{1}{2}g^{\mu\nu}\partial_\mu\phi\partial_\nu\phi\right), \tag{41}$$

where in the Einstein frame the metric and the dilaton are

$$\begin{aligned} ds^2 &= \left(\frac{L}{z}\right)^2\sqrt{1-\left(\frac{z}{z_c}\right)^8}, \\ \phi(z) &= \sqrt{\frac{3}{2}}\log\left(\frac{1+\left(\frac{z}{z_c}\right)^4}{1-\left(\frac{z}{z_c}\right)^4}\right), \end{aligned} \tag{42}$$

and the gluon condensate is

$$\langle \mathrm{tr}\, G^2\rangle = 4\sqrt{3}\sqrt{\frac{R^3}{\kappa^2}}\frac{1}{z_c^4}. \tag{43}$$

This has allowed the authors of the model to extract the gluonium propagator (the correlator of gluon field strength)

$$\int d^4x e^{iqx}\langle \mathrm{tr}\, G^2(x)\,\mathrm{tr}\, G^2(0)\rangle = -\frac{N_c^2-1}{4\pi^2}q^4\log\frac{q^2}{\mu^2}, \tag{44}$$

which allows to fix the overall coefficient in front of the condensate as

$$\langle \mathrm{tr}\, G^2\rangle = \frac{8}{\pi z_c^4}\sqrt{3(N_c^2-1)}. \tag{45}$$

Dilaton Reconstruction from QCD Within the braneless approach, an inverted logic ("from known properties of QCD to the background") allows one to reconstruct such a potential for the dilaton that it reproduces both running of the coupling and presence of the condensate

$$\begin{aligned} V(\phi) &= -\frac{6}{L^2}e^{\pm\sqrt{\frac{2}{3}}\phi} - \frac{12}{L^2}, \\ \phi(z) &= \mp\sqrt{3}2\log\log\frac{z_0}{z}, \\ A(z) &= \log\frac{z}{L} - \frac{1}{4}\log\log\frac{z_0}{z}. \end{aligned} \tag{46}$$

This metric is reminiscent of the solutions by Kirsch and Vaman [147], which arise in a top-down approach. The condensate is expressed in this background as

$$\langle \mathrm{tr}\, G^2\rangle = \frac{N_c^2-1}{11N_c}\frac{8}{z_0^4}, \tag{47}$$

and the running coupling is

$$\alpha_s = \frac{2\pi}{\frac{11}{3}N_c \log z_0 Q}. \tag{48}$$

An unusual feature of [146] is that it suggests a framework for dimension 6 condensates, usually neglected both in field theory and holography.

Developments and Parallels with the Migdal Approach The approach by Csaki and Reece was further developed by many others. The dissociation of mesons and monopole-antimonopole bound states was studied in Csaki's "braneless" approach in [42]. In [148] it was noticed that the braneless approach has problems with the gluonium spectrum, namely, that at the large values of the numeric parameter $Q > 4/3$ (for the "improved" holography by Kiritsis et al. $Q = 4/3$) the gluonium spectrum is ill-defined. It was noted in [149] that there is an amazing similarity between the correlator relations in the field-theoretic Migdal approach [150] and in the holographic setup by Csaki and Reece. Other interesting parallels with the Migdal meromorphic program and AdS/CFT were noticed in [151]. In [152] the Migdal approach was compared to the soft-wall AdS/QCD; a close relationship between the Migdal ideas and the quark-hadron duality background was noticed.

Ready-made Condensate Backgrounds for Top-Down $D3/D7$ Models

The typical ("popular") backgrounds on the market for studying non-conformality effects in D3/D7 models are:

- Dilaton flow (dilaton wall) by Gubser, Kehagias and Sfetsos;
- Yang-Mills* by Babington et al.;
- Constable–Myers;
- Liu–Tseytlin;
- Nojiri and Odintsov.

Some of these have further variations and modifications.

Gubser–Kehagias–Sfetsos. One of the first non-conformal backgrounds, introduced into AdS/CFT was that by Gubser [153]. Originally it was intended to explain confinement, yet it came also useful for gluon condensate introduction. Shortly before Gubser the

background was obtained by Kehagias and Sfetsos [154] in a less convenient parametrization. In [155] the properties of Gubser's solution were shown to be universal for a wide class of five-dimensional actions (e.g. those with extra scalars in the Lagrangian). The solution by Gubser has made possible the formulation of the idea of a holography describing a flow between two theories, the IR and the UV [156]. In [42] meson spectra were studied in Gubser background via AdS/QCD. The Wilson loop in Gubser geometry with finite temperature was studied in [157], where effects of gluon condensate on quark-quark potential were calculated. In [158] a consistent picture of chiral symmetry breaking by $D7$-branes in the Gubser background was suggested. In [159] it was shown that confinement and chiral symmetry breaking in this background are not intrinsically unrelated. Non-trivial estimates of mesonic spectra in the $D7$ model in this background were done in [160]. Meson and monopole-antimonopole melting in this background was studied in [42]. Hadronic spectra in the presence of baryon chemical potential in dilaton flow geometry were studied in [161].

Constable–Myers. Another popular solution of the IIB string theory is the Constable-Myers background [162]. It has also generated a large flow of follow-up papers, calculating all kinds of observables. The $D7$ embeddings were shown by Apreda, Erdmenger and Evans to be stable in this background [163, 164]. Masses of heavy-light mesons in this background in the $D7$ model were obtained in [165]. The quark condensate, pion decay constant and higher order Gasser-Leutwyler coefficients were calculated for the $D7$ model in Constable–Myers background in [166]. The chiral condensate and meson spectrum in the $D7$ model in this background were obtained in [15].

Nojiri and Odintsov Background. An early generalization of the background was constructed by Nojiri and Odintsov in [167]; the solution was given implicitly, and shown to manifest confinement, running coupling and possess a gluon condensate.

$\mathcal{N} = 2^*$ **background.** A different deformation of AdS/CFT was suggested by Erdmenger, Crooks and Evans [168]. It is also known as Yang–Mills* background. It included an additional scalar operator, which led to the scaling factor in the metric $ds^2 = e^{2A}dx^2 + dr^2$ which looks like

$$e^A = \frac{\rho^4}{\rho^6 - 1}, \tag{49}$$

where in the UV asymptotics $\rho = 1 + ve^{-2r} + rm^2e^{-2r}$. D7 embeddings were shown to be stable in this background [163].

Other Backgrounds with Gluon Condensate

Other Models with Log-running Coupling. In [169] the log-running of the coupling is reached by putting a stack of $D3$ branes in a $0B$ theory on top of a conifold, which results in a gravity-dual of a non-SUSY gauge theory.

Type 0 theories. A simple classical solution for type 0 theories was constructed in [170], which is dual to some non-supersymmetric theory. This solution was developed further in [171] to a consistent picture of a flow of a conformal theory into a non-conformal one.

A non-maximal SUSY Background. Typically, such a background is UV-asymptotically AdS and something different in the IR, thus providing a "holographical renormgroup flow" between the two boundaries. In [172] such a background in IIB type string theory was proposed, which also incorporated a gluino condensate, analogous to the chiral condensate in a non-supersymmetric theory.

Beyond the Quenched Approximation.

An extensive review on unquenching the fermions in AdS/CFT is available in the work [173]. Here we briefly review some of developments in the field.

Dynamic Holography. A so-called "dynamic holographic QCD" was formulated in [174] by de Paula, Frederico, Forkel and Beyer as a development of the "improved AdS/QCD". The main issue of this "dynamical holography" is additional deformation of the warp factor (49):

$$A(z) = \log z + z^{\lambda}, \tag{50}$$

where $\lambda > 0$ is an extra parameter.

Back-reacted AdS/QCD. Back-reacted geometry of the type

$$A(z) = \log(z) + \frac{m_q^2}{24} z^2 + \frac{m_q \sigma}{16} z^4 + \frac{\sigma^2}{24} z^6, \tag{51}$$

(factor A is defined as in (39)), i.e. the one in which the effects of the scalar field due to the quark mass and the chiral condensate (though not to the gluon condensate) upon the metric have been partially taken into account, was considered in [54]. A fully back-reacted geometry is claimed to have been found for a three-flavoured AdS/QCD in [175]. In this approach, the condensate and the mass are contained in the scalar field, which then

influences the warp factor. The influence is UV-negligible, whereas it essentially modifies the geometry in the IR. Yet the effect of back-reaction upon the mass spectrum is almost unobserved, and does not decrease the discrepancy between theory and experiment.

Back-reacted $D3/D7$. A comprehensive model of the back-reaction in a $D3/D7$ system was suggested in [147], where a self-consistent metric for that system was derived both numerically and, in an approximation, analytically. The feature of this solution is that it reproduces the fermionic leading log in the beta-function exactly. The N_f dependence of the Regge curves is obtained (Regge curves going down at large N_f). In [176] it is argued that this type of back-reaction should extend to $D7$ branes as well, not just to the $D3$ background. Unquenched flavours in the Klebanov-Witten model with massless quarks were considered in [177, 178]. Such a background is found to describe the screening of color charges [179].

Thermodynamics with Backreaction. Quark-gluon plasma properties were studied in [180] in an unquenched approximation within the $D3/D7$ model with massive quarks. It was shown that $\frac{\eta}{s}$ remains unmodified, whereas jet quenching and friction coefficients are increased, the correction in $\frac{N_f}{N_c}$ reaching 20-30%. The corresponding backreacted background was obtained approximately analytically as an expansion up to $(N_f/N_c)^2$.

Spectra at Backreaction. In [181] screening of mesonic masses was found as a function of N_c/N_f in a back-reacted background of the Klebanov-Witten type. The backreaction in the Sakai–Sugimoto model was studied in [182]; in particular, it was found that no tachyonic modes arise in the mesonic spectrum due to the backreaction, and that the original embedding remains a solution in the back-reacted metric.

Other Back-reacted Solutions. Backreacted solutions in 2+1 dimensions for an $\mathcal{N} = 2$ geometry were found in [183]. A 2+1 dimensional $\mathcal{N} = 1$ background, deformed by N_f smeared $D5$ branes was also found in [184]. The non-deformed solution are NS5-branes wrapping a 3-sphere, and the deformation is induced by $D5$ branes. Backreaction due to a $D7$ embedding into the Polchinski-Strassler geometry was calculated up to $O(m^2)$ in [185, 186]. In [187] an unquenched N_f $D5$ background for a 3+1d $\mathcal{N} = 2$ dual geometry was obtained.

0.2.3 Chiral Condensate and Holography

Chiral Theory and Sum Rules from Holography

The chiral Lagrangian was derived in [73] from AdS/QCD with quite satisfactory precision in chiral perturbation theory parameters L_i's. In [188] it was obtained that the shear sum rule for finite-temperature systems can be reproduced from duality in the case of the $\mathcal{N} = 4$ background, but does not hold exactly in non-conformal backgrounds.

Wilson loop and gluon condensate are related via the following theorem

$$\log W = -\sum_n c_n \alpha_s^n - \frac{\pi^2}{36} Z \,\mathrm{tr}\, G^2 s^2, \tag{52}$$

where $s = \pi a^2$ is the surface area of the loop, $Z^{-1} = \frac{\beta}{\beta^{(1)}}$, β is the beta-function, index (1) points out to its one-loop piece. This relation was confirmed holographically in [189].

Vector dominance was established from holography on an extensive set of comprehensive examples in [190] in a model close to Sakai – Sugimoto.

0.2.4 Condensates and Field Theory Resummations

The idea of relating condensates to somehow (e.g. Dyson-Schwinger) resummed field theory has not so far been very popular. Apart from my present work, we can mention [191], where it is claimed that the chiral condensate has been obtained at a finite chemical potential from the Dyson–Schwinger equations. Yet it should be noted that the authors of that work solve only the quark equation, whereas the gluon propagator is not dynamical, but substituted by an Ansatz, thus the significance of the result essentially decreases, since it cannot reproduce the condensate in a model-independent way. A consistent scheme of defining the chiral condensate from both the full coupled set of the Dyson-Schwinger equations (the gluon and the quark propagators, the quark-gluon vertex) and the Bethe-Salpeter equation for pion has been elaborated in [192].

Part I

Holography

Chapter 1

Chiral Magnetic Effect in Soft-Wall AdS/QCD

The essence of the chiral magnetic effect is the generation of an electric current along an external magnetic field. Recently it has been studied by Rebhan *et al.* within the Sakai–Sugimoto model, where it was shown to be zero. As an alternative, the chiral magnetic effect is calculated by me in this Chapter in the soft-wall AdS/QCD and a non-zero result is found with natural boundary conditions.

1.1 Introduction

The chiral magnetic effect [193, 6] is best described as a generation of an electric current by a magnetic field in a topologically nontrivial background. The standard field-theoretical argumentation is the following. Let us consider QCD with massless quarks, so that left and right quarks can be dealt with independently, and suppose that a chiral chemical potential μ_5 is present, accounting for a certain topologically nontrivial background. The topologically nontrivial field configuration will change chirality, and an external magnetic field $\mathbf{B} = (0, 0, B)$ will order spins parallel to itself. Thus a non-zero vector current arises, which is given by Fukushima, Kharzeev and Warringa [6]

$$J_3^V = \frac{\mu_5 B}{2\pi^2} \equiv \mathcal{J}_{FKW}. \tag{1.1}$$

During recent years holography has become one of the main alternative tools for analyzing of non-perturbative QCD. Different conductivities of quark matter, including chiral magnetic conductivity, have already been analyzed in a variety of holographic models. Electric conductivity in the $D3/D7$ model was examined by Karch and O'Bannon in [194]. Axial, ohmic and Hall conductivity in a magnetic field were calculated on the basis of the

Kubo formula and correlator analysis for the Sakai-Sugimoto model in [123, 195]. One of the holographic results for the electric current in [123] is 1/2 of the QCD weak coupling result (1.1).

An attempt to describe the chiral magnetic effect for the vector current in the Sakai-Sugimoto model has been made recently in [117]. The result at zero frequency, where only the Yang–Mills part of the action was used, exactly amounts to the weak coupling QCD effect; non-zero frequencies have also been considered. In [116] a more sophisticated anomaly subtraction scheme was suggested. It was argued that if one uses the Bardeen term subtraction, then one gets a zero effect for the vector current, otherwise one gets 2/3 of the weak-coupling effect. The reason for adding the Bardeen term to the action was to cure the pathological behavior of the vector anomaly.

The experimental status of the problem is discussed in [196]. Presently it is claimed that the effect is present, yet the exact proportionality coefficient c in $J_3^V = c \cdot \frac{\mu_5 B}{2\pi^2}$ cannot be inferred from it. Lattice estimates are also close to 2/3 [197] of the weak-coupling effect. The discussion of the effect in the framework of NJL model can be found in [198].

The present Chapter aims at comparing the field theoretical result as well as the derivation of [116] to the chiral magnetic effect as derived in the framework of soft-wall AdS/QCD. The question whether the effect is present in a holographic model or not, turns out to be quite delicate. The Chapter is organized as follows. In Section 1.2 I consider the analysis of the gauge sector of the soft-wall model and confirm the result of [116]. In Section 1.3 I discuss the contribution of scalars and pseudoscalars and focus on their boundary conditions in the 5d equations of motion. The results of this Chapter are summarized in Section 1.4.

1.2 The Soft-Wall Model

1.2.1 Gauge Part of the Action

Consider the gauge field sector of the soft-wall AdS/QCD model [13] taking into account the Chern-Simons action $\int A \wedge F \wedge F$. Let us begin with an action of Abelian fields L and

R with a coupling g_5 that has the following form:

$$\begin{aligned} S &= S_{YM}[L] + S_{YM}[R] + S_{CS}[L] - S_{CS}[R] && (1.2)\\ S_{YM}[A] &= -\frac{1}{8g_5^2}\int e^{-\phi} F \wedge *F = -\frac{1}{8g_5^2}\int dz\ d^4x\ e^{-\phi}\sqrt{g} F_{MN}F^{MN} && (1.3)\\ S_{CS}[A] &= -\frac{k\cdot N_c}{24\pi^2}\int A\wedge F\wedge F - \frac{1}{2}A\wedge A\wedge A\wedge F + \frac{1}{10}A\wedge A\wedge A\wedge A\wedge A \\ &= -\frac{k\cdot N_c}{24\pi^2}\int dz\ d^4x\ \epsilon^{MNPQR}A_M F_{NP}F_{QR}. && (1.4) \end{aligned}$$

Here k is an integer that scales the CS term and effectively the magnetic field. The canonical normalization of the CS term is $k = 1$, but it will be kept for the sake of generality. The metric tensor is the following:

$$ds^2 = g_{MN}dX^M dX^N = \frac{R^2}{z^2}\eta_{MN}dX^M dX^N = \frac{R^2}{z^2}(-dz^2 + dx_\mu dx^\mu). \quad (1.5)$$

In the $A_z = 0$ gauge the YM action acquires the form

$$\begin{aligned} S_{YM}[A] &= -\frac{R}{4g_5^2}\int dz\ d^4x\ \left\{\frac{e^{-\phi}}{z}A_\mu(\Box\eta^{\mu\nu} - \partial^\mu\partial^\nu)A_\nu + A_\mu\partial_z\left(\frac{e^{-\phi}}{z}\ \partial_z\right)A^\mu\right\} \\ &+ \frac{R}{4g_5^2}\int d^4x\ \frac{e^{-\phi}}{z}A_\mu\partial_z A^\mu\Big|_{z=0}^{z=\infty}. && (1.6) \end{aligned}$$

From the YM part of the action one gets

$$\frac{\delta S_{YM}[A]}{\delta A_\mu} = -\frac{R}{2g_5^2}\left\{\frac{e^{-\phi}}{z}(\Box\eta^{\mu\nu} - \partial^\mu\partial^\nu)A_\nu + \partial_z\left(\frac{e^{-\phi}}{z}\partial_z A^\mu\right)\right\}. \quad (1.7)$$

Varying the volume term of the action one obtains

$$\frac{\delta S_{CS}[A]}{\delta A_\mu} = \frac{k\cdot N_c}{2\pi^2}\ \epsilon^{\mu\nu\rho\sigma}\ \partial_z A_\nu F_{\rho\sigma}. \quad (1.8)$$

Taking into account $\dfrac{R}{g_5^2} = \dfrac{N_c}{12\pi^2}$, the equations of motion for the fields L and R are obtained

$$\partial_z\left(\frac{e^{-\phi(z)}}{z}\partial_z L^\mu\right) - 24k\epsilon^{\mu\nu\rho\sigma}\ \partial_z L_\nu\partial_\rho L_\sigma = 0, \quad (1.9)$$

$$\partial_z\left(\frac{e^{-\phi(z)}}{z}\partial_z R^\mu\right) + 24k\epsilon^{\mu\nu\rho\sigma}\ \partial_z R_\nu\partial_\rho R_\sigma = 0 \quad (1.10)$$

with the following boundary conditions

$$L_0(0) = \mu_L, \qquad R_0(0) = \mu_R, \tag{1.11}$$

$$L_3(0) = j_L, \qquad R_3(0) = j_R, \tag{1.12}$$

$$L_1(0, x_2) = -\frac{1}{2} x_2 B, \qquad R_1(0, x_2) = -\frac{1}{2} x_2 B, \tag{1.13}$$

$$L_\mu(\infty) = R_\mu(\infty), \qquad \partial_z L_\mu(\infty) = -\partial_z R_\mu(\infty), \tag{1.14}$$

here $\mu = \frac{1}{2}(\mu_L + \mu_R), \mu_5 = \frac{1}{2}(\mu_L - \mu_R)$, and $j_{L,R}$ are the gauge field boundary values, a variation with respect to which gives the currents

$$\frac{\delta S[L,R]}{\delta L_3(z=0)} = \frac{1}{V_{4D}} \frac{\partial S[L,R]}{\partial j_L} = \mathcal{J}_L, \tag{1.15}$$

$$\frac{\delta S[L,R]}{\delta R_3(z=0)} = \frac{1}{V_{4D}} \frac{\partial S[L,R]}{\partial j_R} = \mathcal{J}_R. \tag{1.16}$$

Conditions (1.14) arise, since both the left- and the right-handed gauge fields are associated with a single gauge field in the Sakai–Sugimoto model [199, 200]. In that model regions of positive and negative values of the holographic coordinate $\rho = 1/z$ correspond to left-handed $D8$ and right-handed $\bar{D}8$ branes, respectively. Since the gauge field is smooth and continuous at $\rho = 0$, a boundary condition (1.14) is obtained at $z = 1/\rho = \infty$.

Denoting $\beta = 12kB$ one can get the following set of e.o.m.'s

$$\partial_z \left(\frac{e^{-\phi(z)}}{z} \, \partial_z L_0 \right) = \beta \partial_z L_3, \qquad \partial_z \left(\frac{e^{-\phi(z)}}{z} \, \partial_z L_3 \right) = \beta \partial_z L_0, \tag{1.17}$$

$$\partial_z \left(\frac{e^{-\phi(z)}}{z} \, \partial_z R_0 \right) = -\beta \partial_z R_3, \qquad \partial_z \left(\frac{e^{-\phi(z)}}{z} \, \partial_z R_3 \right) = -\beta \partial_z R_0, \tag{1.18}$$

$$\partial_z \left(\frac{e^{-\phi(z)}}{z} \, \partial_z L_1 \right) = 0, \qquad \partial_z \left(\frac{e^{-\phi(z)}}{z} \, \partial_z R_1 \right) = 0. \tag{1.19}$$

The solution is the following

$$L_0(z) = \mu_L + \left(\mu_5 - \frac{1}{2} j_5 \right) \left(e^{-|\beta| w(z)} - 1 \right), \quad L_3(z) = j_L - \left(\mu_5 - \frac{1}{2} j_5 \right) \left(e^{-|\beta| w(z)} - 1 \right),$$

$$R_0(z) = \mu_R - \left(\mu_5 + \frac{1}{2} j_5 \right) \left(e^{-|\beta| w(z)} - 1 \right), \quad R_3(z) = j_R - \left(\mu_5 + \frac{1}{2} j_5 \right) \left(e^{-|\beta| w(z)} - 1 \right),$$

$$R_1(z, x_2) = -\frac{1}{2} x_2 B, \qquad L_1(z, x_2) = -\frac{1}{2} x_2 B, \tag{1.20}$$

here $j = j_L + j_R, j_5 = j_L - j_R$, and $w(z) = \int\limits_0^z du \; u \; e^{\phi(u)}$, $\dfrac{e^{-\phi(z)}}{z} \; w'(z) = 1$.

1.2.2 On-shell Action and Symmetry Currents

Let us now compute the on-shell action with the gauge fields given by (1.20) for both left- and right-handed gauge fields. Its Yang–Mills part is given as

$$\begin{aligned} S_{YM}[A] &= -\int dz\ d^4x\ \frac{e^{-\lambda z^2}}{z}\frac{R}{8g_5^2}\ \eta^{AB}\eta^{MN}F_{AM}F_{BN} \\ &= -\frac{R}{8g_5^2}\int dz\ d^4x\ \frac{e^{-\lambda z^2}}{z}\left\{-2\eta^{\alpha\beta}\partial_z A_\alpha \partial_z A_\beta + \eta^{\alpha\beta}\eta^{\mu\nu}F_{\alpha\mu}F_{\beta\nu}\right\} \\ &= -\frac{R}{4g_5^2}\frac{B^2}{4}V_{4D}\int dz\ \frac{e^{-\lambda z^2}}{z} \end{aligned} \tag{1.21}$$

The Chern–Simons part of the action is

$$\begin{aligned} S_{CS}[A] &= \frac{k\cdot N_c}{6\pi^2}\int dz\ d^4x\ \epsilon^{\mu\nu\rho\sigma}\ A_\mu \partial_z A_\nu F_{\rho\sigma} \\ &= \frac{k\cdot N_c}{3\pi^2}\int dz\ d^4x\ \left(A_0\partial_z A_3 - A_3\partial_z A_0\right)F_{12}. \end{aligned} \tag{1.22}$$

Recall that $w(z)=\int\limits_0^z du\ u\ e^{\phi(u)}, w(0)=0, w(\infty)=\infty$. Then the solutions (1.20) have the following form

$$\begin{aligned} &L_0(z)=\mu+\frac{1}{2}j_5+\left(\mu_5-\frac{1}{2}j_5\right)e^{-|\beta|w(z)}, \quad L_3(z)=\mu_5+\frac{1}{2}j-\left(\mu_5-\frac{1}{2}j_5\right)e^{-|\beta|w(z)}, \\ &R_0(z)=\mu+\frac{1}{2}j_5-\left(\mu_5+\frac{1}{2}j_5\right)e^{-|\beta|w(z)}, \quad R_3(z)=\mu_5+\frac{1}{2}j-\left(\mu_5+\frac{1}{2}j_5\right)e^{-|\beta|w(z)}, \\ &F_{12}^L=\frac{1}{2}B, \qquad\qquad F_{12}^R=\frac{1}{2}B. \end{aligned} \tag{1.23}$$

Upon substituting (1.23) into (1.22) the on-shell CS action becomes

$$\begin{aligned} S_{CS}[L] &= \frac{k\cdot N_c}{3\pi^2}\int dz\ d^4x\ F_{12}^L\left(L_0\partial_z L_3 - L_3\partial_z L_0\right) \\ &= \frac{k\cdot N_c}{6\pi^2}BV_{4D}\left(\mu\mu_5+\mu_5^2-\frac{1}{2}\mu j_5+\frac{1}{2}\mu_5 j-\frac{1}{4}j_5^2-\frac{1}{4}jj_5\right), \end{aligned} \tag{1.24}$$

and

$$\begin{aligned} S_{CS}[R] &= \frac{k\cdot N_c}{3\pi^2}\int dz\ d^4x\ F_{12}^R\left(R_0\partial_z R_3 - R_3\partial_z R_0\right) \\ &= \frac{k\cdot N_c}{6\pi^2}BV_{4D}\left(\mu\mu_5-\mu_5^2+\frac{1}{2}\mu j_5-\frac{1}{2}\mu_5 j+\frac{1}{4}j_5^2-\frac{1}{4}jj_5\right). \end{aligned} \tag{1.25}$$

The symmetry currents $\mathcal{J}_L, \mathcal{J}_R$ are equal to the partial derivatives of the action with respect to j_L, j_R

$$\mathcal{J}_L = \frac{1}{V_{4D}}\frac{\partial S}{\partial j_L} = \frac{1}{V_{4D}}\left(\frac{\partial j}{\partial j_L}\frac{\partial S}{\partial j} + \frac{\partial j_5}{\partial j_L}\frac{\partial S}{\partial j_5}\right) = \frac{1}{V_{4D}}\left(\frac{\partial S}{\partial j} + \frac{\partial S}{\partial j_5}\right), \tag{1.26}$$

$$\mathcal{J}_R = \frac{1}{V_{4D}}\frac{\partial S}{\partial j_R} = \frac{1}{V_{4D}}\left(\frac{\partial j}{\partial j_R}\frac{\partial S}{\partial j} + \frac{\partial j_5}{\partial j_R}\frac{\partial S}{\partial j_5}\right) = \frac{1}{V_{4D}}\left(\frac{\partial S}{\partial j} - \frac{\partial S}{\partial j_5}\right), \tag{1.27}$$

$$\mathcal{J} = \frac{2}{V_{4D}}\frac{\partial S}{\partial j}\ ,\ \mathcal{J}_5 = \frac{2}{V_{4D}}\frac{\partial S}{\partial j_5}\ . \tag{1.28}$$

As can be seen from (1.21), the YM part of the action does not depend on the current sources. The CS part, on the other hand, equals

$$S_{CS} = S_{CS}[L] - S_{CS}[R] = \frac{k\cdot N_c}{6\pi^2}BV_{4D}\left(2\mu_5^2 - \frac{1}{2}j_5^2 + \mu_5 j - \mu j_5\right). \tag{1.29}$$

From eqs. (1.28,1.29) one obtains

$$\mathcal{J} = \frac{k\cdot N_c}{3\pi^2}B\mu_5, \tag{1.30}$$

$$\mathcal{J}_5 = -\frac{k\cdot N_c}{3\pi^2}B(\mu + j_5). \tag{1.31}$$

If one sets $k = 1$, a standard normalization of the CS action (1.4) is recovered and the result (1.30) is in agreement with [116] without the Bardeen counterterm. The axial supercurrent introduced in [116] is an equivalent of my j_5. If it is interpreted as a source for the axial current it has to be set to zero. Minimizing the action with respect to it is analogous to setting the axial current (1.31) to zero. It is interesting that the answer does not depend on j, which probably justifies its absence in [116].

1.2.3 The Divergence of the Vector Current

In this section a general formula for the left and right symmetry currents $\mathcal{J}_{L,R}$ will be derived. An approach to calculating currents different yet equivalent to the one of the previous section will be used here. The current definition is the following (for the current $\mathcal{J}_{L,R} \equiv \mathcal{J}^3_{L,R}$ it is the same as in (1.28)):

$$\mathcal{J}^\mu_L(x) = \frac{\delta S}{\delta L_\mu(z=0,x)},\ \mathcal{J}^\mu_R(x) = \frac{\delta S}{\delta R_\mu(z=0,x)}. \tag{1.32}$$

The variation of the action $\delta S = \delta S_{YM} + \delta S_{CS}$ can be split into two parts – one proportional to the equations of motion and one reducible to a surface term

$$\delta S_{YM}[A] = \delta S^{vol}_{YM}[A] - \frac{R}{2g_5^2}\int d^4x \frac{e^{-\phi(z)}}{z}\ \partial_z A^\mu \delta A_\mu\Big|_{z=0}, \tag{1.33}$$

$$\delta S_{CS}[A] = \delta S^{vol}_{CS}[A] + \frac{k\cdot N_c}{6\pi^2}\int d^4x\ \epsilon^{\mu\nu\rho\sigma}A_\nu F_{\rho\sigma}\delta A_\mu\Big|_{z=0}. \tag{1.34}$$

The 5D parts are equal to zero on-shell, so that one gets

$$\mathcal{J}^{\mu}_{L}(x) = -\frac{R}{2g_5^2}\frac{e^{-\phi(z)}}{z}\,\partial_z L^{\mu} + \frac{k\cdot N_c}{6\pi^2}\,\epsilon^{\mu\nu\rho\sigma}\,L_{\nu}F^{L}_{\rho\sigma}, \tag{1.35}$$

$$\mathcal{J}^{\mu}_{R}(x) = -\frac{R}{2g_5^2}\frac{e^{-\phi(z)}}{z}\,\partial_z R^{\mu} - \frac{k\cdot N_c}{6\pi^2}\,\epsilon^{\mu\nu\rho\sigma}\,R_{\nu}F^{R}_{\rho\sigma}. \tag{1.36}$$

Recalling that $\dfrac{R}{g_5^2}=\dfrac{N_c}{12\pi^2}$ and $V_\mu = L_\mu + R_\mu$ the following expression for the divergence of the vector current is obtained

$$\begin{aligned}\partial_\mu\mathcal{J}^{\mu} &= \partial_\mu(\mathcal{J}^{\mu}_{L}+\mathcal{J}^{\mu}_{R}) = -\frac{N_c}{24\pi^2}\frac{e^{-\phi(z)}}{z}\,\partial_z\partial_\mu V^{\mu} + \frac{k\cdot N_c}{6\pi^2}\,\epsilon^{\mu\nu\rho\sigma}\,(\partial_\mu L_\nu F^{L}_{\rho\sigma} - \partial_\mu R_\nu F^{R}_{\rho\sigma})\\ &= -\frac{N_c}{24\pi^2}\frac{e^{-\phi(z)}}{z}\,\partial_z\partial_\mu V^{\mu} + \frac{k\cdot N_c}{3\pi^2}\,\epsilon^{\mu\nu\rho\sigma}\,\partial_\mu V_\nu\partial_\rho A_\sigma.\end{aligned} \tag{1.37}$$

To express the divergence of the vector field V_μ another equation of motion generated by $\dfrac{\delta S}{\delta A_z}$ will be needed

$$\begin{aligned}\frac{\delta S_{YM}[A]}{\delta A_z} &= \frac{R}{2g_5^2}\frac{e^{-\phi(z)}}{z}\,\partial_z\partial_\mu A^{\mu} = \frac{N_c}{24\pi^2}\frac{e^{-\phi(z)}}{z}\,\partial_z\partial_\mu A^{\mu},\\ \frac{\delta S_{CS}[A]}{\delta A_z} &= -\frac{kN_c}{24\pi^2}\frac{\delta}{\delta A_z}\int d^4x\,dz\;\epsilon^{\mu\nu\rho\sigma}(A_z F_{\mu\nu}F_{\rho\sigma} - 4A_\mu F_{z\nu}F_{\rho\sigma}) =\\ &= -\frac{kN_c}{2\pi^2}\,\epsilon^{\mu\nu\rho\sigma}\,\partial_\mu A_\nu\partial_\rho A_\sigma.\end{aligned} \tag{1.38}$$

The corresponding e.o.m.'s assume the form:

$$\frac{e^{-\phi(z)}}{z}\,\partial_z\partial_\mu L^{\mu} = 12k\epsilon^{\mu\nu\rho\sigma}\,\partial_\mu L_\nu\partial_\rho L_\sigma, \qquad \frac{e^{-\phi(z)}}{z}\,\partial_z\partial_\mu R^{\mu} = 12k\epsilon^{\mu\nu\rho\sigma}\,\partial_\mu R_\nu\partial_\rho R_\sigma,$$

$$\frac{e^{-\phi(z)}}{z}\,\partial_z\partial_\mu V^{\mu} = 12k\epsilon^{\mu\nu\rho\sigma}\,\partial_\mu V_\nu\partial_\rho A_\sigma. \tag{1.39}$$

Thus the divergence in (1.37) equals:

$$\partial_\mu\mathcal{J}^{\mu} = -\frac{kN_c}{6\pi^2}\,\epsilon^{\mu\nu\rho\sigma}\,\partial_\mu V_\nu\partial_\rho A_\sigma. \tag{1.40}$$

1.2.4 The Bardeen Counterterm

The Bardeen counterterm has a dimensionless prefactor c that is determined from the following condition

$$\partial_\mu\mathcal{J}^{\mu}_{subtracted} = \partial_\mu\mathcal{J}^{\mu} + \partial_\mu\mathcal{J}^{\mu}_{Bardeen} = 0, \tag{1.41}$$

where the counterterm has the form

$$S_{Bardeen} = c\int d^4x\epsilon^{\mu\nu\rho\sigma}L_\mu R_\nu(F^{L}_{\rho\sigma}+F^{R}_{\rho\sigma}). \tag{1.42}$$

It may be interpreted as a surface counterterm in the spirit of the holographic renormalization. In our case

$$\begin{aligned} S_{Bardeen} &= -2c\int d^4x(L_0R_3 - L_3R_0)\partial_2 V_1\Big|_{z=0} = 2cBV_{4D}\ (L_0R_3 - L_3R_0)|_{z=0} = \\ &= 2cBV_{4D}(\mu_L j_R - \mu_R j_L) = 2cBV_{4D}(\mu_5 j - \mu j_5), \end{aligned} \tag{1.43}$$

hence

$$\mathcal{J}_{Bardeen} = 4cB\mu_5,\ \mathcal{J}_{Bardeen\ 5} = -4cB\mu. \tag{1.44}$$

The general expression for the currents is the following:

$$\begin{aligned} \delta S_{Bardeen} &= \int d^4x\,(\mathcal{J}^\mu_{Bardeen\ L}\ \delta L_\mu + \mathcal{J}^\mu_{Bardeen\ R}\ \delta R_\mu,)\,, \\ \mathcal{J}^\mu_{Bardeen\ L} &= 2c\epsilon^{\mu\nu\rho\sigma}\left(R_\nu\partial_\rho R_\sigma + 2R_\nu\partial_\rho L_\sigma + L_\sigma\partial_\rho R_\nu\right), \\ \mathcal{J}^\mu_{Bardeen\ R} &= -2c\epsilon^{\mu\nu\rho\sigma}\left(L_\nu\partial_\rho L_\sigma + 2L_\nu\partial_\rho R_\sigma + R_\sigma\partial_\rho L_\nu\right), \\ \mathcal{J}^\mu_{Bardeen} &= 2c\epsilon^{\mu\nu\rho\sigma}\left(R_\nu\partial_\rho R_\sigma - L_\nu\partial_\rho L_\sigma - 3L_\nu\partial_\rho R_\sigma + 3R_\nu\partial_\rho L_\sigma\right). \end{aligned} \tag{1.45}$$

The divergence of the Bardeen current equals:

$$\partial_\mu\mathcal{J}^\mu_{Bardeen} = -2c\epsilon^{\mu\nu\rho\sigma}\partial_\mu V_\nu\partial_\rho A_\sigma. \tag{1.46}$$

Based on (1.40, 1.41, 1.46) one gets

$$c = -\frac{kN_c}{12\pi^2}. \tag{1.47}$$

As a result, the subtracted current turns out to be zero (1.30, 1.44, 1.47):

$$\mathcal{J}_{subtracted} = \mathcal{J} + \mathcal{J}_{Bardeen} = \frac{kN_c}{3\pi^2}B\mu_5 + 4cB\mu_5 = \frac{kN_c}{3\pi^2}B\mu_5 + 4\left(-\frac{kN_c}{12\pi^2}\right)B\mu_5 = 0. \tag{1.48}$$

1.3 Scalars and Pseudoscalars

1.3.1 Kinetic Term and Potential

Let us consider now the scalar–pseudoscalar sector, which was first omitted from our considerations. The bilinear part is

$$S_X = \int d^4x dz\ e^{-\phi}\ R^3\left[\frac{1}{z^3}(D^\mu X)^\dagger D^\mu X + \frac{3}{z^5}|X|^2\right], \tag{1.49}$$

where $D_\mu = \partial_\mu X - iL_\mu X + iXR_\mu$; field X is related to pion field via

$$X = \exp\left(i\frac{\pi^a t^a}{f_\pi}\right)\frac{1}{2}v(z). \tag{1.50}$$

What is crucial for our case is that there is a scalar interaction with gauge fields. It can be thought of in two different ways. If one works in $A_z = 0$ gauge (both $L_z = 0$ and $R_z = 0$), than the pion is identified with the phase of the field X as in (1.50), and the interaction term is

$$S_{XAA} = \frac{N_c}{24\pi^2}\ \mathrm{tr} \int d^4x dz\ \partial_\mu V_\nu \partial_\lambda V_\rho \frac{\partial_\alpha \pi}{f_\pi}\ \epsilon^{\mu\nu\lambda\rho\alpha}. \tag{1.51}$$

If, however, one does not impose this gauge, then the holonomy of the axial field $\int A_z dz$ is itself the pion field, and the term (1.51) arises directly from Chern–Simons. Note there is no double-counting here: when dealing with Chern-Simons solely (as was the case in the Sakai-Sugimoto model of [116]), A_z can always be set to zero. This is impossible without inducing a phase of X in the true AdS/QCD model by Erlich–Katz–Son–Stephanov [13] which is used here. Thus the phase is properly absent in [116], and should be present in our model.

Taking the action (1.51) and differentiating it over F_{z3}, one gets the following contribution to the current

$$\mathcal{J}_{XAA} = \frac{N_c}{2\pi^2}\frac{1}{3} B \frac{\partial_0 \pi(x)}{f_\pi}. \tag{1.52}$$

Special care concerns the boundary conditions. I argue that the linear in time "rotating" boundary conditions are appropriate. Let us remind the PCAC relation connecting the axial current and the pion field

$$\bar{\Psi}\gamma_\nu\gamma_5\Psi \Leftrightarrow f_\pi \partial_\nu \pi, \tag{1.53}$$

which implies that one adds the following term in the pion Lagrangian

$$\mu_5 f_\pi \partial_0 \pi. \tag{1.54}$$

This term changes the pion canonical momentum and the condition of the vanishing of the canonical momentum yields the rotating boundary condition

$$P = \partial_0 \pi + \mu_5 f_\pi = 0. \tag{1.55}$$

Collecting all the terms one gets

$$\begin{aligned} \mathcal{J}_{full,\ subtracted} &= \mathcal{J} + \mathcal{J}_{Bardeen} + \mathcal{J}_{XAA} = \tfrac{1}{3}\mathcal{J}_{FKW}, \\ \mathcal{J}_{full,\ nonsubtracted} &= \mathcal{J} + \mathcal{J}_{XAA} = \mathcal{J}_{FKW}. \end{aligned} \tag{1.56}$$

1.3.2 Chern-Simons Action with Scalars

The result of the previous section can be justified from a somewhat different point of view. Let us once more consider the Chern–Simons action

$$S_{CS} = \frac{-kN_c}{24\pi^2}\left(\int L\wedge dL\wedge dL - \int R\wedge dR\wedge dR\right). \tag{1.57}$$

Its gauge transformation ($L \to L + d\alpha_L$, $R \to R + d\alpha_R$) is proportional to a surface term

$$S_{CS} \to S_{CS} + \frac{-kN_c}{24\pi^2}\left(\int d\alpha_L\wedge dL\wedge dL - \int d\alpha_R\wedge dR\wedge dR\right). \tag{1.58}$$

While in the standard field theory this is satisfactory, in my particular consideration this boundary term is nonzero and the gauge invariance is violated. When the component A_z is gauged out, one has to introduce in some other way the pion back into the Chern–Simons action. One may proceed in the following way. An explicitly gauge invariant Chern–Simons term is defined as

$$\bar{S}_{CS} = \frac{-kN_c}{24\pi^2}\left(\int (L + d\phi_L)\wedge dL\wedge dL - \int (R + d\phi_R)\wedge dR\wedge dR\right), \tag{1.59}$$

where $\phi_{L,R}$ are scalar fields that transform so as to keep the combinations within the brackets invariant, $\phi_{L,R} \to \phi_{L,R} - \alpha_{L,R}$. This means that the combination $f_\pi\,(\phi_R - \phi_L)$ may be associated with the five-dimensional pion in the gauge in which A_z is set to zero.

As in the previous section, arguments can be made in favor of setting the scalar fields proportional to the chemical potentials on the ultraviolet holographic boundary at $z = 0$

$$\phi_{L,R}|_{z=0} = -\frac{1}{2}\mu_{L,R}\cdot t. \tag{1.60}$$

To clarify the infrared behavior ($z \to \infty$) of the scalars, let us turn once more to the Sakai–Sugimoto model [199, 200], in which the infrared region is the area where the $D8$ and $\bar{D}8$ branes connect. There the Chern–Simons action is a single integral over both $D8$ and $\bar{D}8$ branes

$$S_{CS} \sim \int A\wedge dA\wedge dA, \tag{1.61}$$

where the holographic coordinate $\rho = 1/z$ runs from $-\infty$ (right $\bar{D}8$ brane) to ∞ (left $D8$ brane) and the gauge field A is associated with the left-handed field L of the Erlich–Katz–Son–Stephanov model at $\rho > 0$ and with the right-handed field R at $\rho < 0$.

I might undertake a similar procedure of making this action explicitly gauge invariant by adding a single scalar ϕ

$$\bar{S}_{CS} \sim \int (A + d\phi)\wedge dA\wedge dA, \tag{1.62}$$

and this scalar field will be analogous to ϕ_L (ϕ_R) for positive (negative) values of ρ.

Now, since the field ϕ is smooth and continuous at $\rho = 0$ a boundary condition is obtained for the $\phi_{L,R}$ fields in my setup

$$\text{for all } x_\mu \ \phi_L|_{z=\infty} = \phi_R|_{z=\infty} \,. \tag{1.63}$$

It is quite analogous to the condition (1.14). In what follows it will be assumed that the gauge fields are adiabatically tuned out in the temporal positive and negative infinities. Let us simplify the modification of the Chern–Simons action $S_{\phi AA} = \bar{S}_{CS} - S_{CS}$ which happens to be a surface term

$$\begin{aligned} S_{\phi AA} &= \frac{-kN_c}{24\pi^2}\left(\int d\phi_L \wedge dL \wedge dL - \int d\phi_R \wedge dR \wedge dR\right) \\ &= \frac{kN_c}{6\pi^2} B\left(\int dz\ d^4x\ \partial_t\phi_L\partial_z L_3 - \int dz\ d^4x\ \partial_t\phi_R\partial_z R_3\right). \end{aligned} \tag{1.64}$$

If the surface terms that arise at temporal infinities $\sim \int dz\ d^3x \{L,R\}_3 \partial_z \phi_{L,R}\big|_{t=-\infty}^{t=+\infty}$ are neglected, the following is obtained

$$\begin{aligned} S_{\phi AA} &= \frac{kN_c}{6\pi^2} B\left[-\left(j_L\partial_t\phi_L - j_R\partial_t\phi_R\right)\Big|_{z=0}\right. \\ &+ \left.\left(\mu_5 + \frac{1}{2}j_L + \frac{1}{2}j_R\right)\left(\partial_t\phi_L - \partial_t\phi_R\right)\Big|_{z=\infty}\right]. \end{aligned} \tag{1.65}$$

Due to the boundary condition (1.63), the second term vanishes and another contribution to the current is found

$$\mathcal{J}_{\phi AA} = \frac{kN_c}{6\pi^2} B\mu_5. \tag{1.66}$$

The total current now equals

$$\mathcal{J}_{full,\ subtracted} = \mathcal{J} + \mathcal{J}_{Bardeen} + \mathcal{J}_{\phi AA} = \frac{1}{3}\frac{kN_c}{2\pi^2} B\mu_5, \tag{1.67}$$

$$\mathcal{J}_{full,\ nonsubtracted} = \mathcal{J} + \mathcal{J}_{\phi AA} = \frac{kN_c}{2\pi^2} B\mu_5. \tag{1.68}$$

Here is a summary of all the contributions to the chiral magnetic effect (1.28,1.44, 1.45,-1.48,1.66, 1.68,1.67).

Term in the action	Yang–Mills		Chern–Simons		Bardeen counterterm	Scalars in CS
	bulk	boundary	bulk	boundary		
Contribution to the current	$-\frac{1}{3}\frac{N_c}{2\pi^2}B\mu_5$	$\frac{1}{3}\frac{N_c}{2\pi^2}B\mu_5$	$\frac{1}{3}\frac{N_c}{2\pi^2}B\mu_5$	$\frac{1}{3}\frac{N_c}{2\pi^2}B\mu_5$	$-\frac{2}{3}\frac{N_c}{2\pi^2}B\mu_5$	$\frac{1}{3}\frac{N_c}{2\pi^2}B\mu_5$

Action taken into account	Total		Total without scalars	
	subtracted	nonsubtracted	subtracted	nonsubtracted
Resulting current, in terms of $\frac{N_c}{2\pi^2}B\mu_5$	$\frac{1}{3}$	1	0	$\frac{2}{3}$

1.4 Summary

In this Chapter the holographic derivation of the chiral magnetic effect has been revisited in the soft-wall AdS/QCD model. Unlike the estimate via the Sakai-Sugimoto model [116], in the soft-wall model the effect is present under reasonable boundary conditions. Let us stress here that in no way do I argue against the result by Rebhan *et al.* [116]; on the contrary, I confirm it independently; the difference between my model and theirs is the presence of an additional contribution from the scalar part of the action. Putting it loosely, scalars act as "catalysts" for the effect, the value of which is determined however not by those, but by the Chern–Simons term. Thus the effect is still topological in its nature, as it is within the standard paradigm; though triggered by scalars, it is a robust prediction in the sense of its independence on the Lagrangian of the scalars. Notice that the effect is trivially absent in the D3/D7 model due to the different form of the Chern-Simons term.

Some comments are due about other recent attempts to obtain the chiral magnetic effect in a consistent way. Rubakov's paper [201] deals with the proper introduction of the chiral chemical potential in the theory under consideration. It was argued that μ_5 has to be coupled to the conserved chiral current, that is the initial fermionic current has to be modified by the anomalous contribution; in order to compare this argument with our approach note that our additional contribution involving the scalar does the same job. Indeed, I have argued that vanishing of the canonical momentum of the scalar implies that the scalar field has a constant time gradient proportional to μ_5. Substituting this expression for the gradient of the scalar into my additional CS term, I get the expression

for the conserved current discussed in [201].

In another paper [115] it has been argued that a nontrivial contribution to the holographic CME in the Lagrangian without scalars comes from the singular gauge configurations at the horizon. This statement is still to be clarified. Comparing this point to my approach with the scalar field, I can assume that the nontrivial effect due to this field may somehow be related with the singular solutions in [115] and could influence the choice of the gauge. This point certainly needs further clarification.

It is well-known from the study of the triangle diagram that there is an ambiguity in the regularization which allows to obtain either conserved vector or axial currents. In the standard situation demanding the conserved vector current, I get the anomaly in the axial current. In the study of the chiral magnetic effect I can assume that the axial current is conserved instead of introducing the chiral chemical potential. It is this unusual viewpoint that amounts to the discussion on the role of the Bardeen counterterm.

In my model I focus on the scalar Goldstone-Wilczek contribution to the vector current, which is familiar in the chiral theory. This GW contribution has been overlooked in the previous papers on this issue. For generality I have presented the different answers which correspond to different ways to account for the Bardeen counterterm.

Rubakov calculates the value of current for a differently defined chemical potential. Namely, his "axial chemical potential" is related to a conserved chiral charge, whereas ours is not. The difference manifests itself in whether we include the Bardeen counterterm into the calculation – it should be taken into account if I treat the axial chemical potential as a temporal component of a gauge field.

On the other hand, if the Bardeen counterterm is left out, our result may be compared with Rubakov's. In that case the present result agrees with both the weak-coupling and with Rubakov's results. Furthermore, the scalar field contribution in my calculation corresponds to the anomalous term in the conserved chiral charge according to Rubakov.

The said ambiguity is that between a choice of different models, not within our model itself; the coefficients in the action of both our and Rubakov's model are topologically fixed.

My calculations allow to extract an expression for the axial current $J_5 = -\frac{1}{3}\frac{N_c \mu}{2\pi^2 B}$ (with the Bardeen counterterm left out) which is different from one in the paper by Metlitski and Zhitnitsky [202]. This is not surprising, since in their paper they consider the regularization corresponding to the conserved vector current, which is necessary to introduce the standard, not the chiral chemical potential.

Chapter 2

Low-Energy Theorems in Holography

2.1 Introduction

The purpose of this Chapter is to compare holography to field theory by considering a set of statements, known as low-energy theorems, about one- and two-point functions of a strongly coupled gauge theory on both sides of the correspondence. I report nice non-trivial agreement in two important cases: the dilatation Ward identities and the decoupling theorem. Apart from demonstrating validity of low-energy theorems, a particular result of our analysis is a statement on the IR universality of theories dual to various backgrounds with scale.

Firstly, I want to see explicitly the realization of the QCD dilatation Ward indentities [203]:

$$\int d^4x \langle T(x) O(0) \rangle = -\dim(O) \langle O \rangle, \tag{2.1}$$

where $T \equiv T^\mu_\mu$ is the energy-momentum trace on the boundary. This is trivially fulfilled in the conformal metric dual to the trivial vacuum (for an explicitly written down correlator of energy-momentum components see e.g. [204]); one cannot expect anything else on the r.h.s. other than 0, since there are no condensates in the theory. Thus for a nontrivial test one needs a background different from the AdS in the IR by having a gluon condensate. I use the self-dual background [205] in this part of our work. This check is a necessary prerequisite to testing the typical AdS/QCD models with scale on validity of low-energy theorems. To perform the test of dilatation Ward identities, I calculate the two-point correlators: $\langle \mathrm{tr}\, G^2(x)\, \mathrm{tr}\, G^2(0) \rangle$, $\langle \mathrm{tr}\, G^2(x)\, \mathrm{tr}\, G\tilde{G}(0) \rangle$, $\langle T(x)\, \mathrm{tr}\, G^2(0) \rangle$, $\langle T(x)\, \mathrm{tr}\, G\tilde{G}(0) \rangle$, $\langle T_{\mu\nu}(x) T_{\alpha\beta}(0) \rangle$.

The analysis of correlators is easily extended to non-zero frequency, which opens us a way to constructing useful quantities, first of all, η/s via $\langle T_{xy} T_{xy} \rangle$ [206, 207, 208, 209].

Here our main result after holographic renormalization is the predictable absence of q-corrections to $\frac{\eta}{s}(q,\omega)\,|_{T\to 0} = \frac{1}{4\pi}$. Our analysis of correlators allows us to extract meson transport coefficients in a self-dual background with temperature.

Secondly, I check the relationship between two-point and one point functions in gauge theory with fermions, known as decoupling relation $\langle \mathrm{tr}\frac{\alpha_s}{\pi}G^2\rangle = -12m\langle\overline{\psi}\psi\rangle$. Fermions are introduced into the system via the $D3/D7$ model. Again, a non-trivial check is possible only for an IR-non-trivial metric; I use three different backgrounds with gluon condensate in this part of the work; remarkable universality and agreement with the standard field theory is observed.

2.2 Normalization of Operators

Definition of the Model. In the Einstein frame the bulk IIB action is [205]

$$S_{10} = \frac{1}{g_s^2(2\pi)^7\alpha'^4}\int d^{10}x\sqrt{g_{10}}\left(R - \frac{1}{2}(\partial_\mu\phi)^2 - \frac{1}{2}e^{2\phi}(\partial_\mu C)^2 - \frac{1}{2}|F_5|^2\right), \tag{2.2}$$

where R is the curvature, ϕ is the dilaton, F_5 is the 5-form, C is the axion.

Introduction of fermions. I follow what is known as the Karch-Katz model in different backgrounds, in the quenched approximation $N_f \ll N_c$. One can write down the Dirac–Born–Infeld action for the $D7$ brane embedding in the Einstein frame

$$S_{D7} = \frac{1}{(2\pi)^7\alpha'^4}\int d^8\xi\; e^{\phi}\sqrt{\det_{\alpha\beta}(\partial_\alpha X^\mu\partial_\beta X^\nu g_{\mu\nu} + B_{\alpha\beta})}. \tag{2.3}$$

I keep here an external Kalb-Ramond field, which will later turn out to be useful to study the properties of the quark condensate with regard to an Abelian background in this theory. The embedding of $D7$ is made as shown in the following table:

$AdS_5\times S^5$	0	1	2	3	4	5	6	7	8	9
$D7$	+	+	+	+	+	+	+	+	−	−

. (2.4)

One can get an image of the corresponding physics in Fig. (7), where the string modes generating specific sectors of the spectrum are shown. I look for the embeddings of the form

$$X^9 = w(\rho),\; X^8 = 0, \tag{2.5}$$

where the embedding function w, worldsheet coordinates ξ_i and targetspace coordinates r,ρ are related as

$$\begin{aligned} w^2(\rho) &= r^2 - \rho^2,\\ \rho &= \sqrt{\xi_5^2+\xi_6^2+\xi_7^2+\xi_8^2}. \end{aligned} \tag{2.6}$$

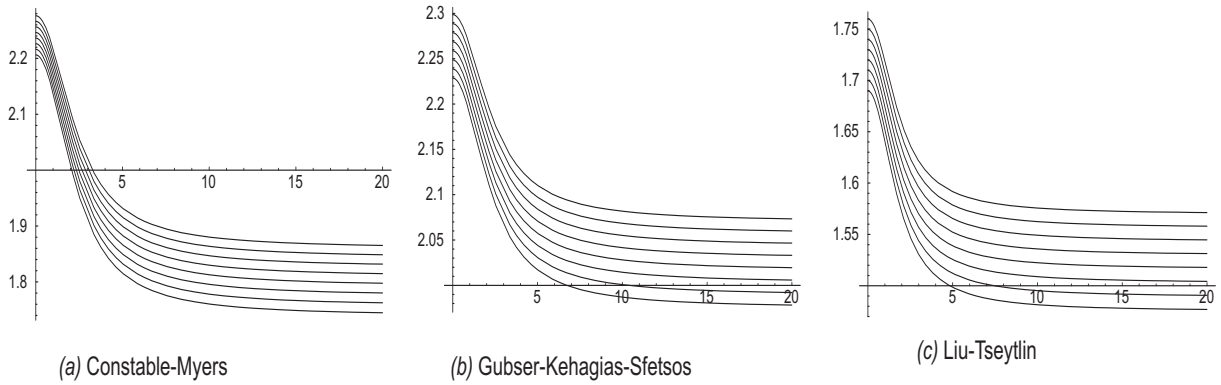

Figure 2.1: Embeddings of the spectator D7 brane into Constable–Myers, Gubser and Liu-Tseytlin backgrounds.

Liu–Tseytlin background. The holography description of gauge theories has originally been formulated for $\mathcal{N}=4$ SYM dual to strings on $AdS_5 \times S_5$ [7]. Various attempts have been made to generalize it to backgrounds corresponding to non-vacuum states of $\mathcal{N}=4$ SYM or to non-conformal and non-supersymmetric theories.

Among the generalized backgrounds for holography, those possessing self-duality are of special interest. Namely, by virtue of self-duality, they are still supersymmetric and thus still correspond to the same theory on the boundary. However, they can possess scale parameters which make them closer to real-world physics. The archetypal example of such a background is the Liu–Tseytlin background [205]. It has a scale – the scale of the gluon condensate, yet it remains supersymmetric since the metric is self-dual; the latter self-duality is provided by the presence of a non-trivial axion field. Despite the presence of the scale, it is conformal (in the UV); in the IR the dilaton singularity is determined by the condensate. This is not bad for mimicking some features of QCD gluodynamics: there is UV asymptotic freedom, and the IR is (at least partially) driven by condensate. Physically this background is understood as a "smeared" $D(-1)$ brane (i.e. instanton distribution with constant density) with a usual stack of $D3$-branes. Since the $D(-1)$ brane is an instanton in 10D, the resulting 4d theory can be considered as having an instanton-gas type of vacuum, which is advantageous for QCD purposes. Moreover, this background is confining (in the sense of a Wilson loop linear behaviour at large temporal separation), and the string tension is proportional to the condensate. Of course, I do not claim to produce any real QCD results in this framework, but it is generally believed to be a very useful toy model.

For the Liu–Tseytlin background [205] the metric in the Einstein frame looks like the

standard conformal solution

$$ds^2 = g_{0\mu\nu}dx^\mu dx^\nu = R^2\left(\frac{dx^{\mu 2}}{\sqrt{h_3}} + \sqrt{h_3}\,\frac{dz^2 + z^2 d\Omega_5^2}{z^4}\right), \tag{2.7}$$

but the dilaton is modified by the smeared instanton (nonzero density of $D(-1)$)

$$e^\phi = h_{-1}, \tag{2.8}$$

and the axion is present

$$C_0 = \frac{1}{h_{-1}} - 1; \tag{2.9}$$

the $D3$ and $D(-1)$ form-factors are:

$$h_3 = z^4, \tag{2.10}$$

and

$$h_{-1} = 1 + qz^4. \tag{2.11}$$

The parameter q is the crucial quantity for us, since it measures the degree of IR-non-conformality of the theory (remember that in the UV, the theory is conformal and its β-function is zero).

Here I employ the Liu-Tseytlin background to test dilatation Ward identities in Section 2.3.1, and to test decoupling the relation on it in Section 2.3.2.

Constable – Myers background. The Constable – Myers background in the Einstein frame has the metric

$$ds^2 = \frac{\left(\frac{b^4+r^4}{r^4-b^4}\right)^{\frac{1}{8b^4}}}{\sqrt{h_3}}dx_\mu^2 + \frac{(r^4-b^4)\left(\frac{b^4+r^4}{r^4-b^4}\right)^{\frac{1}{4}\left(2-\frac{1}{2b^4}\right)}\sqrt{\left(\frac{b^4+r^4}{r^4-b^4}\right)^{\frac{1}{2b^4}}-1}}{r^4}\left(dr^2 + r^2 d\Omega_5^2\right), \tag{2.12}$$

where

$$h_3 = \left(\frac{b^4+r^4}{r^4-b^4}\right)^{\frac{1}{2b^4}} - 1, \tag{2.13}$$

and the dilaton is

$$e^\phi = \left(\frac{b^4+r^4}{r^4-b^4}\right)^{\frac{1}{2}\sqrt{10-\frac{1}{4b^8}}}, \tag{2.14}$$

the axion is zero, and $F_5 = \epsilon_5 \frac{1}{h_3}$, where ϵ_5 is the unitary antisymmetric tensor in the S_5 directions.

Gubser–Kehagias–Sfetsos. One of the first non-conformal backgrounds, introduced into AdS/CFT, was that by Gubser [153]:

$$ds^2 = \sqrt[4]{1-\frac{b^8}{r^8}}r^2 dx_\mu^2 + \frac{1}{r^2}\left(dr^2 + r^2 d\Omega_5^2\right), \tag{2.15}$$

the dilaton in this background is

$$e^\phi = \left(\frac{\frac{r^4}{b^4}+1}{\frac{r^4}{b^4}-1}\right)^{\sqrt{\frac{3}{2}}}, \tag{2.16}$$

and the axion is zero. Originally it was intended to explain confinement, yet it came also useful for the gluon condensate introduction. Shortly before Gubser the background was obtained by Kehagias and Sfetsos [154] in a less convenient parametrization.

Recipes of AdS/CFT. I consider now the general rules for two-point functions. What is calculated is the matrix of correlators

$$M_{ij} = \langle O_i O_j\rangle|_{(p)} = \frac{\delta^2 S_{full}}{\delta\bar{\Phi}_i(p)\delta\bar{\Phi}_j(-p)}. \tag{2.17}$$

The standard wisdom on finding a Green function means setting an action of the type

$$S_{bulk} = \int d^4x dz \phi'^2 g^{zz}\sqrt{g} \tag{2.18}$$

out onto the boundary as

$$S_{boundary} = \int d^4x \phi\phi' g^{zz}\sqrt{g}|_{z\to 0} \tag{2.19}$$

and calculating a correlator in terms of bulk-to-boundary Green functions $G(x,z)$ of a field ϕ as

$$\langle O(x)O(0)\rangle = G(x,z)\partial_z G(0,z)|_{z=0}. \tag{2.20}$$

In our case two additional difficulties arise. First, the correct boundary term should be supplemented by the Gibbons–Hawking term [204], which makes a theory defined on a manifold with boundary being globally diffeomorphism-invariant. Second, the bilinear action of fields' fluctuations is non-diagonal, this means that I shall be dealing with a matrix of Green functions rather than with separately-treatable ones.

Let us define the Green function matrix. Namely, if the field Φ_i has a bulk solution $\Phi_i(z)$, satisfying $z^{\delta_i}\Phi_i(z)|_{z\to 0} = \bar{\Phi}_i$, then by definition

$$K_{ij}(z) = \frac{\delta\Phi_j(z)}{\delta\bar{\Phi}_i}. \tag{2.21}$$

Let us establish the correct boundary term. The full action of our bulk theory is actually [204]

$$S_{full} = S_{10d} + S_{div} + S_{4d} \tag{2.22}$$

where the Gibbons–Hawking term

$$S_{4d} = -2\partial_z \int d^4x\sqrt{-g_4} - c\int d^4x\sqrt{-g_4}, \tag{2.23}$$

here

$$g_4 = \det(g_{ij}),\ i = 0, 1, 2, 3. \tag{2.24}$$

The constant c can be fixed arbitrarily to our convenience, e.g. as in eq. (4.15) in [204]. The other piece which one has to take into account is the full divergence term S_{div}, which does not affect the equations of motion, but does change the appearance of the action and makes it diagonal in terms of physical degrees of freedom of the graviton. It is the well-known fluctuation term

$$S_{div} = \frac{3}{2}\partial_\mu W^\mu, \tag{2.25}$$

the vector W^μ is (see [210], Vol.II, §96)

$$W^\mu = \sqrt{-g}\left(g^{\alpha\beta}\delta\Gamma^\mu_{\alpha\beta} - g^{\alpha\mu}\delta\Gamma^\beta_{\alpha\beta}\right), \tag{2.26}$$

where $\delta\Gamma^\mu_{\alpha\beta} = \Gamma^\mu_{\alpha\beta}(g+h) - \Gamma^\mu_{\alpha\beta}(g)$. Consider now the second variation of these actions in fluctuation fields; denote these second-order expressions as $S^{(2)}_{10d}$, $S^{(2)}_{div}$, $S^{(2)}_{4d}$, respectively; they contain both fields and their derivatives. The two-point correlator is then

$$\langle O_i O_j\rangle = K_{ik}\frac{\partial^2\mathcal{L}}{\partial\Phi'_k\partial\Phi'_m}\partial_z K_{jm} + K_{ik}\frac{\partial^2 S^{(2)}_{4d}}{\partial\Phi_k\partial\Phi'_m}\partial_z K_{jm} + K_{ik}\frac{\partial^2 S^{(2)}_{4d}}{\partial\Phi_k\partial\Phi_m}K_{jm}, \tag{2.27}$$

here $\mathcal{L}$ is the Lagrangian density of the bulk action:

$$S_{bulk} = S^{(2)}_{10d} + S^{(2)}_{div} = \int dz\,\mathcal{L}. \tag{2.28}$$

The above structure is obvious from the following reasons. Consider the bulk action

$$\delta^2 S_{bulk} = \frac{\delta\Phi_m(z)}{\delta\bar{\Phi}_j}\frac{\delta^2 S_{bulk}}{\delta\Phi_m\delta\Phi_k}\frac{\delta\Phi_k(z)}{\delta\bar{\Phi}_i}, \tag{2.29}$$

where

$$\frac{\delta^2 S_{bulk}}{\delta\Phi_m\delta\Phi_k} = \int dz\left[\frac{\partial^2 L}{\partial\Phi'_m\partial\Phi'_k}\partial_z\delta\Phi_m\partial_z\delta\Phi_k + \frac{\partial^2 L}{\partial\Phi_m\partial\Phi'_k}\delta\Phi_m\partial_z\delta\Phi_k + \frac{\partial^2 L}{\partial\Phi_m\partial\Phi_k}\delta\Phi_m\delta\Phi_k\right]. \tag{2.30}$$

Taking into account that Green functions of field fluctuations by definition satisfy equations:

$$\left[-\partial_z \frac{\partial^2 L}{\partial \Phi'_m \partial \Phi'_k}\partial_z + \frac{\partial^2 L}{\partial \Phi_m \partial \Phi'_k}\partial_z + \frac{\partial^2 L}{\partial \Phi_m \partial \Phi_k}\right]\delta\Phi_k(z) = 0, \tag{2.31}$$

one sees that the only contribution of S_{bulk} into the correlator will be, after taking off the derivative and integration, the term:

$$\delta^2 S_{bulk} = \delta\Phi_m(z)\frac{\partial^2 L}{\partial \Phi'_m \partial \Phi'_k}\partial_z \delta\Phi_k(z). \tag{2.32}$$

Now remembering the definition of the Green function matrix

$$K_{mj} = \frac{\delta\Phi_m(z)}{\delta\bar{\Phi}_j}, \tag{2.33}$$

one arrives exactly at (2.27). Then there is a purely boundary term (Hawking-Gibbons term). It does not require the above procedure, since it already sits on 4d. Then it contributes the following:

$$\delta^2 S_{4d} = \frac{\partial^2 S_{4d}}{\partial \Phi'_m \partial \Phi_k}\partial_z \delta\Phi_m \delta\Phi_k + \frac{\partial^2 S_{4d}}{\partial \Phi_m \partial \Phi_k}\delta\Phi_m \delta\Phi_k. \tag{2.34}$$

The action S_{4d} contains no more than one derivative term, which is due to normal differentiating of extrinsic curvature, thus $\frac{\partial^2 L}{\partial \Phi'^2} = 0$. This contributes the other two terms into the correlator (2.27).

Normalization of Gluon Field Strength. Firstly consider the dilaton field. According to the AdS/CFT dictionary it is stated that the fluctuation $\delta\phi(z, Q)$ of the dilaton field

$$\phi(z, Q) = \phi_0(z) + \delta\phi(z, Q) \tag{2.35}$$

is dual to the operator O_ϕ, proportional to the QCD scalar gluonic operator $\mathrm{tr}(G^2) \equiv \frac{1}{\lambda_\phi} O_\phi$. I can fix the normalization constant λ_ϕ by comparing the two-point functions

$$\langle O_\phi O_\phi \rangle = \lambda_\phi^2 \langle \mathrm{tr}(G^2)\,\mathrm{tr}(G^2)\rangle. \tag{2.36}$$

At large momenta the leading behavior of the gluonic correlator in QCD is [211]:

$$\langle \mathrm{tr}(G^2)(Q)\,\mathrm{tr}(G^2)(-Q)\rangle = \frac{N_c^2 - 1}{4\pi^2} Q^4 \ln(Q^2\epsilon^2). \tag{2.37}$$

To obtain a two-point function from holography, I take the second variation of the action computed on a classical solution. In the vicinity of the boundary of AdS_5 (at large r) the action for the fluctuation is:

$$S_5 = \frac{\pi^3 R^8}{g_s^2 (2\pi)^7 \alpha'^4} \int d^4x dz \frac{1}{z^3} \frac{1}{2} \left[-(\partial_z \delta\phi)^2 - \partial_\mu \delta\phi \partial^\mu \delta\phi + 2e^{\phi_0} \delta\phi (\partial_z C)^2 \right]. \tag{2.38}$$

Here coordinates have been changed $z = \frac{R^2}{r^2}$, so that $r^2 = \rho^2$ and π^3 is the volume of the S_5 sphere, R^8 came from the determinant of the metric ($\sqrt{g} = \frac{R^{10}}{z^5}$). The last term containing the profile of the axion field is negligible at the boundary (small z) because $\partial_z C(z) \sim z^3$. The bulk-to-boundary propagator of $\phi(z, Q)$ can be found at small z and large Q^2. It is

$$\varphi(z, Q) = \frac{Q^2 z^2}{2} K_2(Qz), \qquad \varphi(0, Q) = 1, \tag{2.39}$$

where K_i is the McDonald function. Now the second variation of the action can be computed. It is

$$\langle O_\phi O_\phi \rangle = \frac{\delta^2 S_{cl}}{\delta\phi_0 \delta\phi_0} = \frac{\pi^3 R^8}{g_s^2 (2\pi)^7 \alpha'^4} \frac{1}{2} \varphi(z, Q) \frac{\partial_z \varphi(z, Q)}{z^3} \bigg|_{z=\epsilon} = \frac{N_c^2}{4(2\pi)^2} \frac{1}{8} Q^4 \ln(Q^2 \epsilon^2), \tag{2.40}$$

where the definition $R^4 = 4\pi g_s \alpha'^2 N_c$ was used together with the asymptotics of the Bessel function of the second kind. Comparing this result with the expression of QCD one finds

$$O_\phi = \frac{1}{4\sqrt{2}} \operatorname{tr}(G^2). \tag{2.41}$$

To establish a relation between gluon condensate and the expansion coefficient of the dilaton field, the vacuum expectation value of O_ϕ is computed at zero momentum taking the first variation of the action with respect to the boundary value of the field ϕ_0. At zero momentum near the boundary the dilaton field behaves as

$$\phi(z) = \phi_0 + \phi_4 z^4. \tag{2.42}$$

One finds

$$\langle O_\phi \rangle = \frac{\delta S_{cl}}{\delta\phi_0} = \frac{\pi^3 R^8}{g_s^2 (2\pi)^7 \alpha'^4} \frac{1}{2} \varphi(z, Q) \frac{\partial_z \phi(z, Q)}{z^3} \bigg|_{z=\epsilon} = \frac{N_c^2}{4(2\pi)^2} \, 4\phi_4. \tag{2.43}$$

After all, the expression for the gluon condensate is obtained

$$\langle \operatorname{tr}(G^2) \rangle = 4\sqrt{2} O_\phi = N_c^2 \frac{4\sqrt{2}}{(2\pi)^2} \phi_4. \tag{2.44}$$

Normalization of "Quark" Operators. Next, following the same steps I explore the scalar field w dual to the diquark operator $\bar{q}q$. It is described by the action of the D7 brane, for which w is the embedding coordinate. In the Einstein frame the action is [212]

$$S_8 = -\frac{1}{g_s(2\pi)^7\alpha'^4}\int d^8\xi e^{\phi}\sqrt{\det(\partial_a X^\mu \partial_b X^\nu g^{(10)}_{\mu\nu})}. \tag{2.45}$$

For the fluctuations of the scalar field w it gives

$$S_5 = -\frac{2\pi^2 R^4}{g_s(2\pi)^7\alpha'^4}\int d^4x dz e^{\phi}\left[\frac{1}{2z}(\partial_z w)^2 + \frac{1}{2z}\partial_\mu w \partial^\mu w\right]. \tag{2.46}$$

Here $2\pi^2$ is a volume of a 3-sphere and R^4 comes again from the determinant of the metric $\sqrt{g^{(8)}} = \frac{R^6}{z^3}$. In the limit of large momenta near the boundary the bulk-to-boundary propagator is

$$\tilde{w}(z,Q) = Qz\ K_1(Qz), \qquad \tilde{\omega}(0,Q) = 1. \tag{2.47}$$

The scalar field is dual to the operator O_w, which is proportional to $\bar{q}q = \frac{1}{\lambda_w}O_w$. The two-point function of O_w is computed to fix this proportionality

$$\begin{aligned}\langle O_w O_w\rangle &= \frac{\delta^2 S_{8cl}}{\delta w_0 \delta w_0} = \frac{2\pi^2 R^4}{g_s(2\pi)^7\alpha'^4}\ e^{\phi}\frac{1}{2}\tilde{w}(z,Q)\frac{\partial_z\tilde{w}(z,Q)}{z}|_{z=\epsilon} = \\ &= \frac{N_c}{2(2\pi)^4\alpha'^2}\frac{1}{2}Q^2\ln(Q^2\epsilon^2)|_{z=\epsilon}.\end{aligned} \tag{2.48}$$

Here the fact is used that $e^{\phi}|_{boundary} = 1$ and again $R^4 = 4\pi g_s\alpha'^2 N_c$. This result is compared with the QCD calculation (see eq. 4.27 in [16]),

$$\langle \bar{q}q(Q)\ \bar{q}q(-Q)\rangle = \frac{N_c}{16\pi^2}Q^2\ln(Q^2\epsilon^2), \tag{2.49}$$

and it found that

$$O_w = \frac{1}{2\pi\alpha'}\bar{q}q. \tag{2.50}$$

At this stage the boundary value of the field $w_0 = w|_{z=0}$ can be identified. It is the source of $O_w = \lambda_w(\bar{q}q)$, so it is proportional to the quark mass $w_0 = \frac{1}{\lambda_w}M$. Thus one can state

$$M = \frac{1}{2\pi\alpha'}w_0. \tag{2.51}$$

To identify the quark condensate $\langle\bar{q}q\rangle$, the expectation value of O_w is computed at $Q = 0$. In this limit near the boundary the field is expressed as

$$w(z) = w_0 + w_2 z^2. \tag{2.52}$$

The result is

$$\langle O_w\rangle = \frac{\delta S_{8cl}}{\delta w_0} = \frac{2\pi^2 R^4}{g_s(2\pi)^7\alpha'^4}\ e^{\phi}\ \frac{1}{2}\tilde{w}(z,Q)\frac{\partial_z w(z,Q)}{z}\bigg|_{z=\epsilon} = \frac{N_c}{2(2\pi)^4\alpha'^2}2w_2. \tag{2.53}$$

The following normalization for the quark condensate is found

$$\langle \bar{q}q \rangle = \frac{1}{\lambda_w} \langle O_w \rangle = \frac{N_c}{(2\pi\alpha')^3} w_2. \tag{2.54}$$

2.3 Low-Energy Theorems

2.3.1 Dilatation Ward Identities in a Self-Dual Background

Correlators at Zero Frequency

The infinitesimal fluctuations of the fields on the bulk couple to the operators $\operatorname{tr} G^2$, $\operatorname{tr} G\tilde{G}$, $T_{\mu\nu}$ in the boundary theory. The latter is thought to be $\mathcal{N} = 4$ SYM, whose gauge field part of the action is normalized here as

$$S_{4d} = \frac{1}{2g_{YM}^2} \int d^4x \left(\operatorname{tr} G^2 - \frac{i\theta}{16\pi^2} \operatorname{tr} G\tilde{G} \right), \tag{2.55}$$

with non-trivial condensates switched on:

$$\langle \operatorname{tr} G^2 \rangle = \langle \operatorname{tr} G\tilde{G} \rangle = N_c \frac{q}{\pi^2}. \tag{2.56}$$

Fluctuation terms are defined as

$$\begin{aligned} \phi &= \phi_c + \varphi, \\ C &= C_0 + \xi, \\ g &= g_{0\mu\nu} + h_{\mu\nu}. \end{aligned} \tag{2.57}$$

The following interaction term is considered to provide a correspondence with the boundary theory:

$$S_{int} = \int d^4x \left[\frac{1}{2} T_{\mu\nu} \bar{h}^{\mu\nu} - e^{-\phi_c} \left(\bar{\varphi} \operatorname{tr} G^2 + \bar{\xi} \operatorname{tr} G\tilde{G} \right) \right], \tag{2.58}$$

which, after introduction of useful self-dual and anti-self-dual components

$$G^{\pm} = \frac{G \pm \tilde{G}}{2} \tag{2.59}$$

and splitting axion and dilaton fluctuations into a new couple of variables

$$\eta^{\pm} = \eta \pm \xi, \tag{2.60}$$

becomes

$$S_{int} = \int d^4x \left[\frac{1}{2} T_{\mu\nu} \bar{h}^{\mu\nu} - e^{-\phi_c} \left(\bar{\eta}^{+} \operatorname{tr} G^{+2} + \bar{\eta}^{-} \operatorname{tr} G^{-2} \right) \right]. \tag{2.61}$$

Here bars denote four-dimensional sources, which are proportional to boundary values of five-dimensional fields:

$$\bar{h}_{\mu\nu} = z^2 h_{\mu\nu}|_{z=0},\ \bar{\eta}^{\pm} = \eta^{\pm}|_{z=0},\ \bar{\varphi} = \varphi|_{z=0}. \tag{2.62}$$

Fluctuations of F_5 are fully determined by h^μ_μ, thus there is no independent source for them.

Let us choose the gauge $h_{5\mu} = 0$, $k^\mu h_{\mu\nu} = 0$, $u^\mu h_{\mu\nu} = 0$, where the wave-vector $k = (\omega, 0, 0, k)$, the constant vector u is $u = (1, 0, 0, 0)$. I work with five fields:

$$\bar{\Phi}_i = (\eta^+, \bar{h}_{11} + \bar{h}_{22}, \bar{h}_{11} - \bar{h}_{22}, \bar{h}_{12}, \eta^-), \tag{2.63}$$

$i = 1, \ldots 5$, each coupled to the corresponding $\mathcal{O}_i$ operator[1]

$$O_i = \left(\frac{1}{g_s^2} \operatorname{tr} G^{+2}, \frac{1}{8} T^\mu_\mu, \frac{3}{8} T_{11} - \frac{1}{8} T_{22} - \frac{1}{8} T_{33} - \frac{1}{8} T_{00}, T_{xy}, \frac{1}{g_s^2} \operatorname{tr} G^{-2} \right) \tag{2.64}$$

via

$$S_{int} = \int d^4x dz \sum_{i=1}^{5} \mathcal{O}_i \Phi_i. \tag{2.65}$$

The correctly defined double-derivative piece of the fluctuation action in the bulk is

$$S^{(2),\text{double deriv.}}_{10d+div} = \int d^4x dz \left(\frac{1}{z^3} \Phi_1' \Phi_5' + \frac{z}{8} \Phi_2'^2 + \frac{z}{8} \Phi_3'^2 + \frac{z}{2} \Phi_4'^2 \right). \tag{2.66}$$

One should not be misled by its diagonal structure; beside the diagonal terms with double derivatives, the full bilinear action contains terms which make it non-diagonal.

The boundary Gibbons-Hawking action term is

$$S^{(2),\text{derivatives}}_{4d} = \int d^4x \frac{1}{8} \left(4c\, h_{xy}(z)^2 + 16 z h'_{xy}(z) h_{xy}(z) + \Phi_2(z) \left(c\, \Phi_2(z) + 4 z \Phi_2'(z) \right) \right). \tag{2.67}$$

The full system of equations upon Green functions (2.31) in the given background (2.7)–(2.11) is cumbersome and therefore is given in the Appendix, Eq. (2.114). Note that for the F_5 form one always has $\delta F = -2/r^3 \Phi_2$, which solves automatically the equations for this field and at the same time retains the constancy of the Ramond-Ramond flow $\int_{S^5} F_5 = N_c$.

It is instructive to start with zero-frequency correlators (setting $\omega = 0$ in (2.114)), since the subsequent introduction of ω in the next section, finding oscillatory (Bessel-function) solutions instead of rational ones and sending then $\omega \to 0$ is an additional check of validity

[1]Some of these operators, e.g. the O_3 are not of immediate interest; however, it costs no additional effort to incorporate them into the calculation, so I work the correlators out for them as well.

of our procedure. At zero frequency, the most general solution is the one given in the Appendix, Eq. (2.115).

Here a very peculiar situation is encountered: out of the ten modes, quite unexpectedly six are IR finite $(C_1, C_4, C_5, C_6, C_7, C_9)$, and the remaining four are infinite. Since the Green function matrix (2.21) requires us to be able to differentiate properly over boundary values of fields, such an ambiguity cannot be tolerated, and must somehow be cured. To do that, an *ad hoc* additional condition is imposed that makes the resulting correlator matrix symmetric: $C_5 = C_6/2$. We stress that apart from arguing from the result, there is no scientific way at this stage of the calculation to justify this additional constraint. The Green function matrix is then:

$$K_{ij} = \begin{array}{|c|c|c|c|c|c|} \hline & \frac{\mathrm{tr}\, G^{+2}}{g_s^2} & \frac{1}{8}T^\mu_\mu & \mathcal{O}_3 & \mathcal{O}_4 & \frac{\mathrm{tr}\, G^{+2}}{g_s^2} \\ \hline \frac{\mathrm{tr}\, G^{+2}}{g_s^2} & qz^4 - q\epsilon^4 + 1 & 0 & 0 & 0 & 0 \\ \hline \frac{1}{8}T^\mu_\mu & 0 & \frac{1}{z^2} & 0 & 0 & 0 \\ \hline \mathcal{O}_3 & 0 & 0 & \frac{1}{z^2} & 0 & 0 \\ \hline \mathcal{O}_4 & 0 & 0 & 0 & \frac{1}{z^2} & 0 \\ \hline \frac{\mathrm{tr}\, G^{-2}}{g_s^2} & -2q\left(\epsilon^4 - z^4\right) & 0 & 0 & 0 & qz^4 - q\epsilon^4 + 1 \\ \hline \end{array} \tag{2.68}$$

As a result, combining our knowledge of the Green function matrix (2.68), the boundary action (2.67) and the derivative piece of the bulk action (2.66) the correlator matrix is obtained:

$$M = \begin{array}{|c|c|c|c|c|c|} \hline & \frac{\mathrm{tr}\, G^{+2}}{g_s^2} & \frac{1}{8}T^\mu_\mu & \mathcal{O}_3 & \mathcal{O}_4 & \frac{\mathrm{tr}\, G^{+2}}{g_s^2} \\ \hline \frac{\mathrm{tr}\, G^{+2}}{g_s^2} & -4q & -2q & 0 & 0 & -2q \\ \hline \frac{1}{8}T^\mu_\mu & -2q & -\frac{1}{4\epsilon^4} & 0 & 0 & 0 \\ \hline \mathcal{O}_3 & 0 & 0 & -\frac{1}{4\epsilon^4} & 0 & 0 \\ \hline \mathcal{O}_4 & 0 & 0 & 0 & -\frac{1}{\epsilon^4} & 0 \\ \hline \frac{\mathrm{tr}\, G^{+2}}{g_s^2} & -2q & 0 & 0 & 0 & 0 \\ \hline \end{array} \tag{2.69}$$

Some comments are due here. The singular terms $\frac{1}{\epsilon^4}$ are expected on general grounds; they are subtracted away by the holographic renormalization procedure, quite analogous to field-theoretical subtraction. An asymmetry in $O_1 \leftrightarrow O_5$ is also expected: what I consider is a self-dual configuration, therefore, self-dual and anti-self-dual operators develop different properties.

Checking Ward Identities

Having obtained the matrix elements, the low-energy theorems can be established. After due normalization one has

$$\begin{cases} \int d^4x \left\langle \dfrac{\operatorname{tr} G^{+2}(x)}{g^2} T(0) \right\rangle &= 4 \left\langle \dfrac{\operatorname{tr} G^{+2}(0)}{g^2} \right\rangle, \\ \int d^4x \left\langle \dfrac{\operatorname{tr} G^{-2}(x)}{g^2} T(0) \right\rangle &= 0, \\ \int d^4x \left\langle \dfrac{\operatorname{tr} G^2(x)}{g^2} \dfrac{\operatorname{tr} G^2(0)}{g^2} \right\rangle &= \dfrac{1}{2} \dfrac{1}{4\pi^2} \left\langle \dfrac{\operatorname{tr} G^2}{g^2} \right\rangle, \\ \int d^4x \left\langle \dfrac{\operatorname{tr} G^2(x)}{g^2} \dfrac{\operatorname{tr} G\tilde{G}(0)}{g^2} \right\rangle &= \dfrac{1}{4} \dfrac{1}{4\pi^2} \left\langle \dfrac{\operatorname{tr} G^2}{g^2} \right\rangle, \\ \int d^4x \left\langle \dfrac{\operatorname{tr} G\tilde{G}(x)}{g^2} \dfrac{\operatorname{tr} G\tilde{G}(0)}{g^2} \right\rangle &= 0. \end{cases} \tag{2.70}$$

Here one can see that the first and the second lines of the equations above constitute exactly the statement of the low-energy theorems

$$\langle \hat{\mathcal{O}} T \rangle = \dim(\hat{\mathcal{O}}) \langle \hat{\mathcal{O}} \rangle. \tag{2.71}$$

The gluonium propagators, i.e. correlators of $\operatorname{tr} G^2$ and $\operatorname{tr} G\tilde{G}$ between themselves (i.e. not with T) are more difficult for interpretation. In section (2.3.1) the relation (21) was obtained as a low-energy theorem in field theory exactly for the correlator calculated here from duality. Comparing the two, one immediately sees that both have the RHS proportional to the one-loop gluon function. On the other hand, the presence of the beta-function makes the two quite different. In the Liu–Tseytlin background the dilaton does not contain any logarithmic terms. Therefore, formally the beta-function is zero. Coupling is still running though. Field-theoretically such a situation is understood as running due to instantons solely. It is known that generally instantons provide power-corrections to the running of the coupling, and the leading term is always the log. This is not the case with the theory dual to the Liu-Tseytlin background, where only the instanton is present. Therefore, instead of trying to relate the RHS of the third equation in (2.70) to the beta-function coefficient in (21), one has rather to think on modifying the standard LE theorems for the case when power corrections are the dominant or the sole contributors to the running of the coupling; the same refers to lines 4 and 5 in (2.70), that is, scalar-pseudoscalar and pseudoscalar-pseudoscalar correlators. Here one should remember that

the field-theoretical LE theorem $\int\langle \mathrm{tr}\, G^2\, \mathrm{tr}\, G^2\rangle \sim 1/\beta_0\, \mathrm{tr}\langle G^2\rangle$ is a consequence of the form of the *operator identity* (dilatation anomaly) $\theta^\mu_\mu = \beta\, \mathrm{tr}\, G^2$. The anomaly is no more here in this peculiar form. Instead, going along the ideas of eq. 2.17 in [203], one may get something like

$$\theta^\mu_\mu(p) \sim \frac{(\mathrm{tr}\, G^2)^2}{p^4}. \tag{2.72}$$

Then there is no beta-function coefficient in the denominator, and there is no paradox: instead of questioning the validity of holography for this specific theory, I emphasize a totally different type of LE relations, if such exist at all. Note also that the dilatation Ward identity $\int \theta^\mu_\mu(x)\mathcal{O}(0) \sim \dim(\mathcal{O})\langle\mathcal{O}\rangle$ is a consequence of a Callan–Symanzik equation solution for the operator O, looking approximately as

$$\langle O\rangle \sim \left(Me^{-\frac{8\pi^2}{\beta_0 g_0^2}}\right)^{\dim(O)}, \tag{2.73}$$

where M is the renormalization scale. Again, since everything runs due to power contribution and not due to the log term, the solution might be quite different. Note that writing $\langle \mathrm{tr}\, G^2\rangle$ in the RHS, while having a pseudoscalar in the LHS, is not a misprint or mistake: the background field is self-dual, and what one obtains is a number $\sim q$, which is the value of both $\langle \mathrm{tr}\, G^2\rangle$ and $\langle \mathrm{tr}\, G\tilde{G}\rangle$.

Correlators at Finite Frequency

Now let us analyze the finite-frequency solutions. The solutions are given in the Appendix, eq. (2.116); only relevant modes are shown. Unlike the $\omega = 0$ solutions, which were exact solutions, here $\Phi_2(z)$ and $\Phi_5(z)$ are powerlog expansions in ω and r. Since I am interested in the near-UV behaviour of Green functions, and eventually expand the correlator matrix in powers of ω, this approximation is reasonable. The matrix of correlators becomes:

$M =$

	$\frac{\mathrm{tr}\, G^{+2}}{g_s^2}$	$\frac{1}{8}T^\mu_\mu$	$\mathcal{O}_3$	$\mathcal{O}_4$	$\frac{\mathrm{tr}\, G^{+2}}{g_s^2}$
$\frac{\mathrm{tr}\, G^{+2}}{g_s^2}$	$-4q$	$-2q$	0	0	$\frac{\log(\omega e)\omega^4}{8} - 2q$
$\frac{1}{8}T^\mu_\mu$	$-2q$	$-\frac{\log(\omega e)\omega^4}{32}$	0	0	0
$\mathcal{O}_3$	0	0	$-\frac{\log(\omega e)\omega^4}{32}$	0	0
$\mathcal{O}_4$	0	0	0	$-\frac{\log(\omega e)\omega^4}{32}$	0
$\frac{\mathrm{tr}\, G^{+2}}{g_s^2}$	$\frac{\log(\omega e)\omega^4}{8} - 2q$	0	0	0	0

(2.74)

The most interesting physical implication of this correlator matrix comes from the $\langle T_{xy}T_{xy}\rangle$ element. It is proportional to $\frac{\eta}{s}|_{T=0}$, and here its independence of q is observed. This fact is

not trivial from dimensional considerations, since one does not possess another dimensional parameter, ω. Thus it has been established that

$$\frac{\eta}{s}(q,\omega)\Big|_{T=0} = \frac{1}{4\pi}. \tag{2.75}$$

As a bonus of this calculation, in Section 2.4 the matrix of quarkonium transport coefficients is easily elaborated based on the above correlator matrix.

2.3.2 Decoupling Theorem in Backgrounds with Gluon Condensate

Physics of Decoupling

The other low-energy theorem of interest is known as "decoupling relation". It can be found in [16], eq. (6.25):

$$\left\langle \frac{\alpha_s}{\pi} G^a_{\mu\nu} G^a_{\mu\nu} \right\rangle = -12 m_q \langle \bar{q} q \rangle. \tag{2.76}$$

The derivation of this relation is somewhat intuitive, but let us still restate the arguments by Shifman, Vainshtein and Zakharov. For vacuum expectation values of different operators pertinent to light quarks, the parameter of expansion is the quark mass. For heavy quarks one expands in the inverse quark mass and sets the external momentum to $Q^2 \sim 0$. Let us suppose there exists a quark for which both expansions, small and large m are true. As it is in particular a "heavy" quark, the quark condensate can be done perturbatively from the triangle diagram with gluons as "vacuum sources", shown in Fig. (2.2). Then,

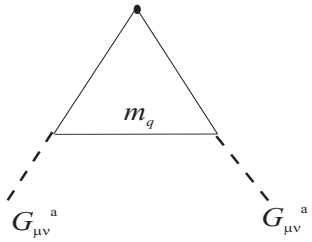

Figure 2.2: Vacuum diagram with heavy quarks depicting $\langle \overline{\psi}\psi \rangle$ as gluon-driven quantity.

using the statement above on the smoothness of the transition between light and heavy quarks, one can argue that the relation will retain its validity if the quark condensate is taken as for light quarks, whereas the mass is that of some heavy-light transition point. To check the decoupling theorem we study the ratio $\frac{M\langle \bar{q} q \rangle}{\frac{g^2_{YM}}{4\pi^2}\langle \mathrm{tr}(G^2) \rangle}$, which, when expressed in terms of the parameters of the bulk solutions, turns out to be

$$\frac{M\langle\bar{q}q\rangle}{\frac{g_{YM}^2}{4\pi^2}\langle \mathrm{tr}(G^2)\rangle} = \frac{(2\pi)}{N_c 4\sqrt{2}\alpha'^2 g_{YM}^2}\frac{w_0 w_2}{\phi_4}, \tag{2.77}$$

coefficients w_0, w_2, ϕ_4 defined in (2.42), (2.52). It is convenient to express all the coefficients via the expansion parameters in the coordinate $r = \frac{R^2}{z}$. Let us denote them $\phi = \phi_0 + \frac{b}{r^4}, w = a + \frac{c}{r^2}$. Obviously, these are related to the former by $\phi_4 = \frac{b}{R^8}, \omega_2 = \frac{c}{R^4}$. Recalling, that $R^4 = 4\pi g_s \alpha'^2 N_c$ and $g_{YM}^2 = 4\pi g_s$, one obtains

$$-\frac{M\langle\bar{q}q\rangle}{\frac{g_{YM}^2}{4\pi^2}\langle \mathrm{tr}(G^2)\rangle} = \frac{g_{YM}^2\alpha'^2 N_c 4\pi^2 (2\pi)^2 N_c}{N_c 4\sqrt{2} g_{YM}^2 2\pi\alpha'(2\pi)^3\alpha'}\frac{ac}{b} = \frac{1}{4\sqrt{2}}\frac{ac}{b} \tag{2.78}$$

For the theorem

$$\frac{M\langle\bar{q}q\rangle}{\frac{g_{YM}^2}{4\pi^2}\langle \mathrm{tr}(G^2)\rangle} = -\frac{1}{12}, \tag{2.79}$$

to hold, the solution asymptotics a, b, c must satisfy

$$\frac{ac}{b} = \frac{\sqrt{2}}{3}. \tag{2.80}$$

This is the most practical form of the decoupling theorem, and will be tested directly in the next section.

Decoupling in Specific Backgrounds – Numerics

Let us try to establish this relation holographically. It shall be done in different backgrounds, those by Constable and Myers, by Gubser and by Liu and Tseytlin.

Using these definitions, equations of motion (3.10) are easily constructed upon the embedding coordinate $w(r)$, and we solve them numerically at different values of the vacuum parameters and fields. Knowing these embeddings, quark masses and condensates are easily extracted according to (2.44), (2.51), (2.54).

The most convenient object for our analysis is the dimensionless ratio $\frac{ac}{b}$, expected from (2.80) to be equal $\frac{\sqrt{2}}{3}$. The ratio of these coefficients, obtained numerically, is shown in Fig. (2.3) for the Gubser background. Similar pictures are observed for the other two backgrounds. Each point represents an individual "measurement", that is, a calculation of a $D7$-brane embedding, whence the values for mass and condensates follow. By fitting the "experimental" points, the value of the ratio and a statistical error margin thereof are estimated.

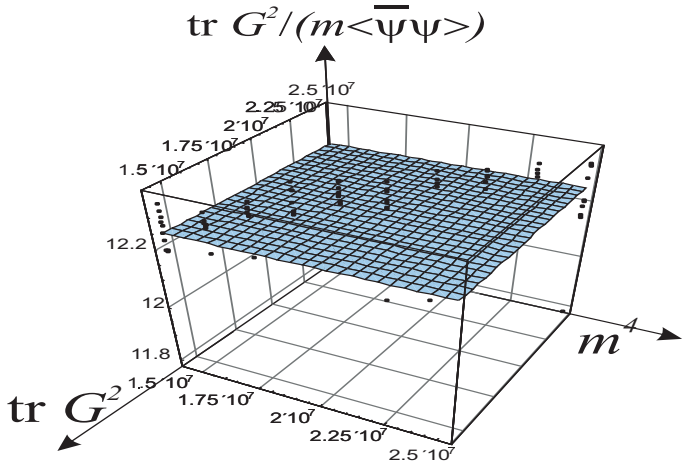

Figure 2.3: Dependence of the ratio $\frac{m\langle\overline{\psi}\psi\rangle}{\langle \mathrm{tr}\, G^2\rangle}$ on the quark mass

The following results are obtained numerically for the dimensionless ratio $\frac{ac}{b}$ one is looking for:

$$\frac{ac}{b} = \begin{cases} \text{Constable–Myers} & 0.4711 \pm 0.0002, \\ \text{Gubser} & 0.4694 \pm 0.0004, \\ \text{Liu-Tseytlin} & 0.4746 \pm 0.0008. \end{cases} \tag{2.81}$$

Comparing the results to the correct analytic value $\sqrt{2}/3 \approx 0.47140$, an impressive agreement is seen up to the third decimal point. The obvious universality of the three different metrics might signal that decoupling theorem is insensitive to the details of IR physics.

The susceptibility with respect to the Kalb–Ramond field (which effectively represents the electromagnetic gauge field) can also be easily extracted by switching on a magnetic $B_{\alpha\beta}$. For a small B field one has

$$\frac{ac}{b}\Big|_B - \frac{ac}{b}\Big|_{B=0} = \begin{cases} \text{Constable–Myers} & 0.00014(2\pi\alpha')^2 B^2, \\ \text{Gubser} & 0.00017(2\pi\alpha')^2 B^2, \\ \text{Liu-Tseytlin} & 0.00040(2\pi\alpha')^2 . B^2 \end{cases} \tag{2.82}$$

The decoupling theorem is not expected to be independent of an external Abelian field. However, field-theoretically what one expects is a linear dependence after Smilga and Shushpanov [24], whereas a quadratic dependence is seen here.

2.4 Quarkonium Transport in Self-Dual Background

2.4.1 Self-Dual Background at Zero Temperature

Here I review the method of [213] for calculating quarkonium transport properties. The basic result of this discussion is a decoupled structure, in which the contributions of the fermionic part of the action will be separated from those of the gluodynamics part according to the pattern

$$\text{meson kin. coeff.} = \begin{bmatrix}\text{meson mass shift}\\ \text{(D7 contribution)}\end{bmatrix} \times \begin{bmatrix}\text{two-point correlator}\\ \text{(D3 contribution)}\end{bmatrix}. \tag{2.83}$$

Consider a complex field φ of a slowly moving meson of velocity v, coupled to some operators of the gluodynamic sector,

$$L = \varphi^+ v\partial_t\varphi + \sum_n c_n\varphi^+\mathcal{O}_n\varphi, \tag{2.84}$$

where the coefficients c_n are defined e.g. from the $D7$ action of a dual model, which secures the existence of mesons. The latter are understood as eigenmodes of fluctuations above the classical solution of the $D7$ equations of motion. Interaction terms modify the spectra of eigenmodes in the bulk; in terms of the boundary theory this amounts to a meson mass shift. Coefficients C_n are then introduced as "susceptibility" of mass with regard to switching on operators $\mathcal{O}_n$:

$$\delta M = -c_n\langle\mathcal{O}_n\rangle. \tag{2.85}$$

Considering one-particle dynamics one can obtain from (2.84)

$$\frac{dp_i}{dt} = \mathcal{F}_i, \tag{2.86}$$

where

$$\mathcal{F}_i = \int d^3x\varphi^+\nabla_i c_n\mathcal{O}_n\varphi, \tag{2.87}$$

while a correlator of two forces is directly related to the transport coefficient

$$\kappa = \frac{1}{3}\int dt\langle\mathcal{F}(t)\mathcal{F}(0)\rangle. \tag{2.88}$$

One can integrate field φ out of these relations and obtain finally

$$\kappa = \frac{1}{3}\int k^2 d^3k c_n^2\frac{2T}{\omega}\mathrm{Im}\,\langle\mathcal{O}_n\mathcal{O}_n\rangle|_k\,, \tag{2.89}$$

where

$$\langle\mathcal{O}_n\mathcal{O}_n\rangle|_k = \int d^4x\theta(t)e^{i(\omega t-\vec{k}\vec{x})}\langle\mathcal{O}_n(x)\mathcal{O}_n(0)\rangle. \tag{2.90}$$

Here the contributions of flavour dynamics and pure gluodynamics are decoupled; below I proceed in calculating the gluodynamical part (the two-point correlator); the coefficients c_n being responsible for mass shifts are known in literature.

2.4.2 Self-Dual Background at Finite Temperature

It is possible to obtain quarkonium diffusion and relaxation coefficients at finite temperature and condensate, extending the work [213] towards the background of [214]. This background has the metric

$$ds^2 = R^2\left(\frac{1-r^4\pi^4T^4}{r^2}dt^2+\frac{dx_3^2}{r^2}+\frac{dr^2}{r^2(1-r^4\pi^4T^4)}\right)+R^2d\Omega_5^2, \tag{2.91}$$

the dilaton is

$$e^{\phi} = 1+\frac{q}{\pi T^4}\log\left(\frac{1}{1-r^4\pi^4T^4}\right), \tag{2.92}$$

the axion is related to the dilaton in the same way as in the zero-temperature Liu-Tseytlin background

$$C = e^{-\phi}-1. \tag{2.93}$$

Quarkonium transport coefficients are quantities which feel both the fermionic piece of the action (some embedded brane) and the gluodynamics. From the former comes the mass susceptibility to the condensate, from the latter – correlators of interest. In principle, it would make a good sense to work in a back-reacted metric (e.g. like Kirsch, Vaman; or Paredes, Cotrone et al.), however this must be postponed till the method is fully technically developed for a well-controllable Ghoroku–Liu–Tseyltin metric. For convenience I further use the variable

$$u = r^2\pi^2T^2, \tag{2.94}$$

which lives in the interval $(0,1)$. A reduced sector of the fluctuations is considered, namely, those of fields $\eta^+,\eta^-,h_{11}+h_{22}$. The equations of motion are given in Appendix, (2.117).

It can be seen now that the problem of fields coupling to each other is additionally burdened by the presence of finite temperature. Yet a diagonalization of these equations is possible by means of the following functional transformation $(\eta^+,h,\eta^-)\to(\overline{\eta}^+,\overline{h},\overline{\eta}^-)$

$$\begin{cases} \overline{\eta}^+(u) &= \eta^+(u), \\ \overline{h}(u) &= h(u)+q\left(C_1-\pi^2\log\left(1-u^2\right)\right)\eta^+(u), \\ \overline{\eta}^-(u) &= qh(u)\left(F_1-\frac{\log\left(1-u^2\right)}{2\pi^2}\right)+\eta^-(u)+ \\ & \quad +q\left(\frac{1}{4}q\log^2\left(1-u^2\right)-\frac{qC_1\log\left(1-u^2\right)}{2\pi^2}+C_2\right)\eta^+(u). \end{cases} \tag{2.95}$$

Now for each of the variables an equation can be written down, similar to that for the simple dilaton modes:

$$\varphi''(u)+\frac{u\left(u^3+6u+4\omega^2+4k^2\left(u^2-1\right)\right)-3}{4u^2\left(u^2-1\right)^2}\varphi(u)=0, \tag{2.96}$$

for which the transport coefficient is known; I calculate it independently, and found it to be in agreement with the previous results [213]

$$\frac{2\omega}{T}G_{\phi,\phi}=\pi^2k^4e^{-2C_\gamma k/T}, \tag{2.97}$$

where $C_\gamma=4\sqrt{\frac{2}{\pi}}\Gamma\left(\frac{5}{4}\right)^2\approx 2.62$. The knowledge of the diagonalization matrix A defined as

$$\begin{pmatrix}\bar{\eta}^+\\ \bar{h}\\ \bar{\eta}^-\end{pmatrix}=\left(\hat{1}+qA\right)\begin{pmatrix}\eta^+\\ h\\ \eta^-\end{pmatrix} \tag{2.98}$$

allows us to transform these results (at $q=0$) into a non-zero-condensate background:

$$\langle\Phi_i\Phi_j\rangle=(\hat{1}+qA)\langle\Phi_i'\Phi_j'\rangle_{q=0}(\hat{1}+qA)^+, \tag{2.99}$$

where the zero-condensate solutions are rotated to the non-zero-condensate by the following rotation matrix in mode space:

$$A=\begin{pmatrix}0 & 0 & 0\\ \pi^2 & 0 & 0\\ 0 & 1/2/\pi^2 & 0\end{pmatrix}, \tag{2.100}$$

and the non-perturbed matrix of finite-temperature correlators is diagonal

$$\langle\Phi_i\Phi_j\rangle_{q=0}=\begin{pmatrix}\langle\operatorname{tr}G^{+2}\operatorname{tr}G^{+2}\rangle & 0 & 0\\ 0 & \langle TT\rangle & 0\\ 0 & 0 & \langle\operatorname{tr}G^{-2}\operatorname{tr}G^{-2}\rangle\end{pmatrix}, \tag{2.101}$$

whence one easily gets the mesonic transport coefficient by use of the following formula:

$$\kappa=\sum_{\mathcal{O}}c_{\mathcal{O}}^2\frac{1}{3}\frac{\pi}{2}\int k^2\frac{d^3k}{(2\pi)^3}\frac{2\omega}{T}\langle\Phi_{\mathcal{O}}\Phi_{\mathcal{O}}\rangle, \tag{2.102}$$

where the respective mass susceptibility coefficients are obtained from considering the fermionic fluctuations coming from the embedded $D7$ brane piece of the action, and are defined via

$$\delta M=-c_{\mathcal{O}}\langle\mathcal{O}\rangle, \tag{2.103}$$

M is referring to the mass of quarkonium.

The correlators themselves are obtained in the following way, which is illustrated on the example of the dilaton. Three domains are considered: UV, IR and the intermediate domain (we denote the latter QC for quasiclassics, since semiclassical approximate solutions will be valid therein). The physical limitations are infalling boundary condition on the horizon and a reflected wave in the UV, which reduces the number of unknown coefficients from 6 to 4. Then we have matching conditions separate for each of the modes in the matching regions between the UV and the QC, and between the QC and the IR. This provides additional 4 constraints, thus the system is fully defined. In the UV the general solution to the EOM is

$$\phi = \frac{2uI_2\left(2\sqrt{u}\sqrt{k^2-\omega^2}\right)C_1}{k^2-\omega^2} + 2u\left(k^2-\omega^2\right)K_2\left(2\sqrt{u}\sqrt{k^2-\omega^2}\right)C_2. \tag{2.104}$$

Taking the UV asymptotic ($u \to 0$) of ϕ, it is clear that physical boundary conditions are $C_1 = B, C_2 = 1$, where B is related to the correlator straightforwardly:

$$\frac{2\omega}{T}G_{\phi\phi} = \frac{\operatorname{Im} B}{\omega}. \tag{2.105}$$

On the contrary, expanding it for large k, one gets the form appropriate for matching with QC:

$$\phi = e^{-2k\sqrt{u}}\sqrt{\pi}k^{-29/2}u^{-5/4} - \frac{Be^{2k\sqrt{u}}k^{-9/2}u^{-5/4}}{\sqrt{\pi}}. \tag{2.106}$$

The quasiclassical equation has the approximate potential

$$V_{QC} = \frac{k^2}{u\left(1-u^2\right)}, \tag{2.107}$$

which allows to obtain the wave-functions in the standard way

$$\psi_{1,2} = \frac{e^{\pm\int p dx}}{\sqrt{p}}, \tag{2.108}$$

where

$$p = \sqrt{V_{QC} - E}. \tag{2.109}$$

The quasiclassical solution near $u = 0$ and $u = 1$ is

$$\begin{aligned}
\phi_{QC,u\to 0} &= -\frac{ie^{-2k\sqrt{u}}\left(e^{4k\sqrt{u}}A_1 + A_2\right)}{\sqrt{k}\sqrt[4]{u}}, \\
\phi_{QC,u\to 1} &= -\frac{ie^{-\sqrt{2}k\left(\sqrt{1-u}+1\right)}\left(e^{2\sqrt{2}k}A_1 + e^{2k\sqrt{2(1-u)}}A_2\right)}{\sqrt{k}\sqrt[4]{2-2u}}.
\end{aligned} \tag{2.110}$$

The IR solution with an infalling boundary condition has only one degree of freedom:

$$\phi_{IR} = \left(e^{\sqrt{2}k\sqrt{1-u}}\csc(\pi\omega + e^{-\sqrt{2}k\sqrt{1-u}}\right)\frac{\sqrt{\pi}C}{2^{3/4}\sqrt{k}\sqrt[4]{1-u}}. \tag{2.111}$$

Equating the QC solution branches with those of IR and UV solutions, one obtains

$$\mathrm{Im}B = \pi^2 k^4 e^{-2C_\gamma k/T}, \tag{2.112}$$

as already stated above. Taking the integral over phase space (2.102) and performing linear transformation of correlator matrix (2.99), the transport coefficient is obtained

$$\kappa = \frac{1}{3}T^9\frac{60\Gamma\left(\frac{3}{4}\right)^6}{\pi^2\Gamma\left(\frac{1}{4}\right)^6}\left[c_{\mathrm{tr}\,G^{+2}}(1+2q\pi^2) + c_T(1+q\pi^2) + c_{\mathrm{tr}\,G^{-2}}\right], \tag{2.113}$$

where c_i are found in [213], $c_{\mathrm{tr}\,G^2} = \frac{8}{5\pi}\left(\frac{2\pi}{M_0}\right)^3$, $c_T = \frac{12}{5\pi}\left(\frac{2\pi}{M_0}\right)^3$, M_0 being the meson mass.

2.5 Discussion

Let us restate the main results of this Chapter:

- The low-energy theorem $\int\langle T\mathcal{O}\rangle = \dim(\mathcal{O})\langle\mathcal{O}\rangle$ is satisfied in holography with condensates for the pure glue sector.
- A universal constant value has been established for the ratio $\frac{m\langle\overline{\psi}\psi\rangle}{\langle\mathrm{tr}\,G^2\rangle}$ in duality with a good precision (0.5%), thus supporting the validity of the decoupling relationship in holographic models of QCD.

Additional "bonus" results, which follow from our calculations without having been designated as original objectives:

- A non-trivial relation between two-point and one-point functions $\int\langle G^2G^2\rangle = const\langle G^2\rangle$ has been established.
- Shear and bulk viscosities have been shown to be independent of condensates.

2.6 Appendix: Equations of Motion

Equations of motion for the Liu–Tseytlin background.

$$
\begin{cases}
z\left(\left(q\omega z^4+\omega\right)^2-32q^2z^6\right)\eta_+(z)+ \\
\quad+\left(qz^4+1\right)\left(\left(11qz^4+3\right)\eta'_+(z)-z\left(qz^4+1\right)\eta''_+(z)\right)=0, \\
\\
32q^2\eta_+(z)z^6+\left(qz^4+1\right)\left(\left(qz^4+1\right)\left(z^2\omega^2+4\right)\Phi_2(z)- \right. \\
\quad\left.-z\left(8q\eta'_+(z)z^2+\left(qz^4+1\right)\left(\Phi'_2(z)+z\Phi''_2(z)\right)\right)\right)=0, \\
\\
\left(z^2\omega^2+4\right)\Phi_2(z)-z\left(\Phi'_2(z)+z\Phi''_2(z)\right)=0, \\
\\
\left(z^2\omega^2+4\right)h_{xy}(z)-z\left(h'_{xy}(z)+zh''_{xy}(z)\right)=0, \\
\\
-32q^2\eta_+(z)z^7+\left(q\omega z^4+\omega\right)^2\eta_-(z)z- \\
\quad-\left(qz^4+1\right)\left(8q\Phi_2(z)z^5+\left(4q\Phi'_2(z)z^5+\left(qz^4+1\right)\eta''_-(z)\right)z+\left(5qz^4-3\right)\eta'_-(z)\right)=0.
\end{cases}
\tag{2.114}
$$

Solutions for the EOM in the Liu–Tseytlin case:

$$
\begin{pmatrix}\Phi_1\\ \Phi_2\\ \Phi_3\\ \Phi_4\\ \Phi_5\end{pmatrix}=\begin{pmatrix}C_2\left(qz^4+1\right)^2+C_1\left(qz^4+1\right)\\ \frac{-q^2C_2z^8+C_3z^4+C_4}{z^2}\\ \frac{C_8z^4+C_7}{z^2}\\ \frac{C_{10}z^4+C_9}{z^2}\\ qC_5-\frac{C_6q^2+\left(q\left(qz^4+2\right)z^4+2\right)(4q(C_1+C_2)+2C_3)}{4q(qz^4+1)}\end{pmatrix}
\tag{2.115}
$$

Solution modes for non-zero frequency:

$$\Phi_1 = \tfrac{1}{2}q\omega^2 K_2(z\omega)C_1 z^6 + \tfrac{1}{2}\omega^2 K_2(z\omega)C_1 z^2,$$

$$\begin{aligned}\Phi_2 = C_1 \Big[& \tfrac{\gamma q\omega^8 z^{10}}{6144} - \tfrac{161 q\omega^8 z^{10}}{552960} + \\ & + \tfrac{q\omega^8 \log(z) z^{10}}{6144} + \tfrac{q\omega^8 \log(\omega) z^{10}}{6144} - \tfrac{q\omega^8 \log(16) z^{10}}{92160} - \\ & - \tfrac{q\omega^8 \log(8) z^{10}}{27648} - \tfrac{q\omega^8 \log(4) z^{10}}{184320} + \tfrac{1}{192}\gamma q\omega^6 z^8 - \tfrac{169 q\omega^6 z^8}{23040} + \\ & + \tfrac{1}{192}q\omega^6 \log(z) z^8 + \tfrac{1}{192}q\omega^6 \log(\omega) z^8 - \tfrac{1}{960}q\omega^6 \log(16) z^8 - \\ & - \tfrac{q\omega^6 \log(4) z^8}{1920} + \tfrac{1}{16}\gamma q\omega^4 z^6 - \tfrac{17}{384}q\omega^4 z^6 + \tfrac{1}{16}q\omega^4 \log(z) z^6 + \\ & + \tfrac{1}{16}q\omega^4 \log(\omega) z^6 - \tfrac{1}{32}q\omega^4 \log(4) z^6 + \tfrac{1}{3}q\omega^2 z^4 \Big] + \tfrac{1}{2}\omega^2 K_2(z\omega)C_2,\end{aligned} \tag{2.116}$$

$$\Phi_3 = \frac{1}{2}\omega^2 K_2(z\omega)C_7,$$

$$\Phi_4 = \frac{1}{2}\omega^2 K_2(z\omega)C_9,$$

$$\begin{aligned}\Phi_5 = & -\frac{1}{12}q\omega^2 C_1 z^6 + \frac{1}{6}q\omega^2 C_4 z^6 - qC_1 z^4 - \frac{8qI_2(z\omega)C_1 z^2}{(qz^4+1)\,\omega^2} - \frac{\omega^2 K_2(z\omega)C_1 z^2}{qz^4+1} + \\ & + \frac{4q^2 I_2(z\omega)C_6 z^2}{(qz^4+1)\,\omega^2} + \frac{q\omega^2 K_2(z\omega)C_6 z^2}{8\,(qz^4+1)}.\end{aligned}$$

The thermal version of Liu–Tseytlin backgrounds leads to equations of motion:

$$\begin{cases} \frac{\left(u\left(u^3+6u+4\omega^2+4k^2\left(u^2-1\right)\right)-3\right)\eta^+}{4u^2(u^2-1)^2} + \eta^{+\prime\prime} = 0, \\ \\ -4q\,(u^2+1)\,h(u)u^2 + 4\,(u^2-1)\left(2quh' + \pi^2\,(u^2-1)\,\eta^{-\prime\prime}\right)u^2 + \\ +\pi^2\,(u\,(u^3+6u+4\omega^2+4k^2\,(u^2-1))-3)\,\eta^- = 0, \\ \\ 4\left(h''\,(u^2-1)^2 + 2\pi^2 q\left(2u\,(u^2-1)\,\eta^{+\prime} - (u^2+1)\,\eta^+(u)\right)\right)u^2 + \\ +\,(u\,(u^3+6u+4\omega^2+4k^2\,(u^2-1))-3)\,h = 0. \end{cases} \tag{2.117}$$

Chapter 3

Chiral Condensate Scaling in a Magnetic Field

The chiral condensate is studied in this Chapter under the influence of an external Abelian magnetic field. I work here within the D3/D7 Karch–Katz model of flavoured AdS/CFT with supersymmetry broken by the Gubser–Kehagias–Sfetsos deformations and by the self-dual supersymmetric Liu-Tseytlin deformation of the background. It is shown in this Chapter that this setting yields for different types of metrics a universal quadratic dependence of the condensate on the field, rather than the non-analytic (linear in field) dependence, typical for chiral perturbation theory in the exact chiral limit. I argue that the analytic (quadratic) result must be put into correspondence with the leading-order in the $1/N_c$ decomposition for the condensate, whereas the existing chiral perturbation theory result, which is linear in field strength, is $1/N_c$ suppressed.

Introduction

The behavior of the QCD vacuum in strong electromagnetic fields has recently attracted a great deal of attention (e.g. [215, 22]), reinvigorating the subject which had been started by [216]. Lattice simulations [217, 218], Simonov's string model [219] are just a few of the recent studies of QCD vacuum in external fields to be mentioned here. In this Thesis I try to compare the description of the condensate from the perspective of duality with that from the point of view of resummed field theory. This Chapter is organized as follows. In the following Section 3.1 the condensates' scaling in external fields is reviewed. It is explained why traditional field-theoretical approaches are still demanding a non-perturbative insight, possibly coming from the realm of dual models. Then in Section 3.2 a short description of the specific dual model is given, which we are going to apply. In the subsequent Section

3.3 the numerical calculations are presented. We conclude in 6.5.

3.1 Motivation

The QCD vacuum is quantitatively described by its chiral condensate, gluonic condensate, pion decay constant and some other physical quantities. Below we shall revisit the properties of some of these objects in the electromagnetic background.

3.1.1 Chiral Condensate in Field Theory

The QCD chiral condensate $\langle\bar{q}q\rangle$ is the order parameter of chiral symmetry breaking. Important ideas of chiral symmetry breaking catalysis were being developed by Gusynin, Miransky and Shovkovy. In [22, 220, 221] an enhancement of chiral condensates was studied by them in $2+1$ and $3+1$-dimensional Nambu—Jona-Lasinio-like models.

The issue of condensates in an external magnetic field was resolved field-theoretically by Schramm, Mueller and Schramm [222], and by Smilga and Shushpanov in [223]. For small magnetic fields H, and in an exact chiral limit, the chiral condensate scales as

$$\langle\bar{q}q\rangle_H = \langle\bar{q}q\rangle_0 \left(1 + \frac{eH\ln 2}{16\pi^2 f_\pi^2}\right). \tag{3.1}$$

Note that the linear term in H has a $\frac{1}{N_c}$ factor, for $f_\pi^2 \sim N_c$ A second-loop correction to this result was calculated by Shushpanov and Agasian [224]. It is instructive to compare this low-energy QCD computation with a Nambu—Jona-Lasinio model computation made by Klevansky and Lemmer [225]

$$\langle\bar{q}q\rangle_H = \langle\bar{q}q\rangle_0 \left(1 + c\frac{e^2H^2}{(\langle\bar{q}q\rangle_0)^{4/3}}\right), \tag{3.2}$$

where c is some model-dependent coefficient. The linear dependence (3.1) by Smilga and Shushpanov is non-analytic (has a square-root type cut) in terms of the invariants of the external field, i.e. is organized as $\sim\sqrt{F^2}$. This might seem to be inconsistent from a first view. However, this non-analyticity is of vital importance. It means there are no other massive parameters in the low-energy domain, where the chiral perturbation theory is valid. The non-analyticity of (3.1) is a direct signature of the π-meson being a Goldstone particle. If the chiral limit is violated, the dependence will be analytic. One must work here in the exact chiral limit, for otherwise all other massive hadronic states in the vacuum energy loops must be taken into account. The Nambu—Jona-Lasinio model is at the same time seen to be deficient to describe full QCD, as it does not reproduce the correct non-analytic behaviour of the condensate, representing the Goldstone particles.

Chiral condensates in arbitrary electromagnetic fields were calculated by Cohen, McGady and Werbos in [23]. They have obtained expressions for electric, magnetic, and arbitrary configurations of constant fields. Their results are basically obtained in the same Heisenberg-Euler technique type as those of Smilga and Shushpanov, and perfectly reproduce the latter as a particular case.

3.1.2 Limitations of Traditional Approaches

The above chiral perturbation theory results have the status of exact low-energy theorems. However, they have their domain of applicability, as explained in the review paper by Ioffe [226]. The one-loop result has been reminded above. This means there will be next-order loop corrections in chiral perturbation theory to this value. Chiral perturbation theory has also limitations due to the fact that quarks' and gluons' degrees of freedom are fully absent in it. Therefore, other models have to be considered to be compared with chiral perturbation theory estimates.

The subject of this Thesis is comparison of AdS/CFT-motivated model with the traditional field-theoretical approach. The flavoured AdS/CFT correspondence in an external magnetic field was studied by Filev et al. in [227]. They produce a spectrum of mesons from pure-AdS background, which satisfies the Gell-Mann–Oakes–Renner relation. In [228] thermodynamic properties of the gauge theory in a magnetic field have been studied in the same framework. Properties of the theory in an electric field were obtained in [229] by the same method.

AdS/CFT with flavours in external fields and at finite temperatures have also been studied in [230]. The authors calculate a number of external-field-dependent properties for a supersymmetric background, such as meson masses in electric and magnetic fields. The Sakai—Sugimoto model in external fields was studied in [231]. It has been concluded that the Sakai—Sugimoto model is consistent with the picture of magnetic catalysis of chiral symmetry breaking. Phase transitions in the Sakai—Sugimoto models due to switching on of electric and magnetic fields were discussed in [232]. Pair production in an electric field in Sakai—Sugimoto model was studied in [233].

3.1.3 Chiral Symmetry Breaking and Holography

Klebanov and Strassler Conifold Deformation. An early attempt of describing chiral symmetry breaking was done by Distler and Zamora [234], where additional *ad hoc* complex scalar fields, dual to scalar operator $\overline{\psi}\psi$ were added into the bulk Lagrangian. The earliest widely recognized picture of chiral symmetry breaking in duality was suggested by

the Klebanov and Strassler, who holographically described chiral symmetry breaking by deforming the conifold of the Klebanov–Tseytlin background [235]. Conifold-type solutions with additional matter have been used for chiral symmetry breaking modelling by a number of authors. By means of a $D7$ embedding into the Klebanov–Strassler background chiral symmetry breaking was realized in [236]. Chiral symmetry breaking was described in terms of embedding a stack of $D7 - \overline{D7}$ into the Klebanov-Witten background by Kuperstein and Sonnenschein [237].

D7 Non-Trivial Embedding. A gravity dual of chiral symmetry breaking organized by means of $D7$-brane embedding was first suggested in [238]. Holographic studies of the chiral phase transition in [239] within pure AdS with fermions as $D7$-branes have shown that at zero chemical potentials QCD with massless quarks exhibits a first-order phase transition, whereas with massive quarks there is a crossover. Chiral symmetry breaking in Klebanov-Witten background is realized via a $D7 - \overline{D}7$ brane configuration. The soft-wall model in its naive version predicts chiral symmetry restoration in the mass spectrum, which is not supported in QCD; the soft-wall model modification [240] eliminates this by means of considering an exact kink-like solution to the tachyon field equations. The chiral condensate dependence on the quark mass and external field for the Liu-Tseytlin background was obtained in [241].

Chiral Condensate in the Sakai–Sugimoto Model. Chiral phase transitions in a wide class of generalized Sakai–Sugimoto models are studied extensively in [242]. Condensation of the tachyon field added to the Sakai–Sugimoto system is interpreted in terms of spontaneous chiral symmetry breaking in [82]. An inconsistency in introducing a scalar field, responsible for spontaneous and explicit chiral symmetry breaking was claimed in [243], where the appearance of complex values of the mass and condensate was claimed to have been observed.

A proposal by Aharony and Kutasov is used in [120] to define a gravity dual of a Wilson loop in the Sakai-Sugimoto model. Following this definition, the condensate of Wilson loops is regarded in [244] as the chiral symmetry breaking order parameter, its behaviour as a function of temperature and chemical potential is established holographically in a type of Sakai-Sugimoto model (the so-called holographic Nambu-Jona-Lasinio model).

Scale Dependence Paradox. A serious problem with chiral symmetry breaking was observed in [245], namely, in real-life QCD condensate and quark mass are scale-dependent, whereas such a dependence is absent in hard-wall AdS/QCD, which makes many of the claims to success of the model superfluous; the work also criticizes the typical assertion

that the tachyon is related to the condensate and mass simply as

$$X \to mz + \langle \overline{\psi}\psi \rangle z^3, \tag{3.3}$$

whereas the correct identification is claimed to be

$$X \to amz + \langle \overline{\psi}\psi \rangle z^3/a, \tag{3.4}$$

where a is originally not fixed, yet can be obtained form a two-point function as $a = \frac{\sqrt{N_c}}{2\pi}$.

3.2 D7 Brane with a Maxwell Field in a Deformed AdS Background

In this Chapter a modelling of the chiral condensate is discussed by means of a class of simple models already discussed previously, that features many of the basic QCD characteristics: confinement, conformal symmetry breaking and spontaneous chiral symmetry breaking, namely, the $D3/D7$ model that has been described in Chapter 2, Section 2.2. We take the action of the $D3/D7$ in the Gubser–Kehagias–Sfetsos background, (2.15)-(2.16). We also study the Liu–Tseytlin self-dual supersymmetric deformation, Eqs. (2.7)-(2.11). We put the fermionic degrees of freedom into a magnetic field and observe the behaviour of condensates.

As we already mentioned in the preceding Chapter, the dynamics of the brane is described by a Dirac—Born—Infeld action

$$S_{D7} = \mu_7 \int d^8\xi \sqrt{\det_{\alpha,\beta}\left(2\pi B_{\alpha\beta} + 2\pi\alpha' F_{\alpha\beta} + g_{\mu\nu}\frac{\partial X^\mu}{\partial \xi^\alpha}\frac{\partial X^\nu}{\partial \xi^\beta}\right)} + \mu_{ChS}\int d^8\xi C_4 \wedge F \wedge B \tag{3.5}$$

Here $B_{\mu\nu}$ is the Kalb—Ramond field, defined in the bulk, which is projected to the brane as $B_{\alpha\beta}$ and $F_{\alpha\beta}$ is the usual Maxwell field on the brane. A constant field $F_{23} = -F_{32} = B$ is chosen, all other field components being zero. Classically the Chern–Simons part of the action

$$S_{ChS} = \frac{1}{2(2\pi)^5\alpha'^2}\int d^8\xi P[F_5] \wedge F \wedge F, \tag{3.6}$$

where P is projection of S^5 onto S^3, is identically zero, since F_5 is directed over S_5, and the Kalb–Ramond field F has only one non-zero component, F_{23}. It might give a contribution into the oscillations describing mesonic masses. We work in the approximation $N_c \gg N_f$, so that the backreaction can be safely neglected.

We remind the reader that the D7 brane runs through the directions of coordinates $x_0, x_1, x_2, x_3, w_1, w_2, w_3, w_4$. These coordinates are respectively $\xi_1 \ldots \xi_8$ internal coordinates of the brane world-volume. The brane doesn't run through the remaining w_5, w_6.

The latter coordinates are embedding coordinates of the brane into the targetspace. They are functions of ξ_i. Solutions in the form $w_5 = w(\rho), w_6 = 0$ will be sought, where

$$\rho = \sqrt{w_1^2 + w_2^2 + w_3^2 + w_4^2}. \tag{3.7}$$

With such an Ansatz, the DBI action is organized as

$$S = \mu_7 \int e^{\phi(\rho)} \rho^3 g_{11}(r) g_{55}(r)^2 \sqrt{\left(B^2 + g_{11}(r)^2\right)\left(w'(\rho)^2 + 1\right)}, \tag{3.8}$$

where

$$r = \sqrt{\rho^2 + w^2(\rho)}. \tag{3.9}$$

The equations of motion with a non-zero field B for the embedding coordinate w will look like

$$\begin{aligned}
&2w\Big(-\rho\left(w^2+1\right)\Big(\Big(-\sqrt{r}g_{11}\left(3B^2+2g_{11}^2\right)\left(g_{11}'\right)^2+\left(B^4+3g_{11}^2B^2+2g_{11}^4\right)g_{11}'-\\
&-\sqrt{r}\left(B^4+3g_{11}^2B^2+2g_{11}^4\right)g_{11}''\Big)g_{55}^2+2\left(B^2+g_{11}^2\right)\left(\left(g_{55}'-\sqrt{r}g_{55}''\right)g_{11}^3-4\sqrt{r}g_{11}'g_{55}'g_{11}^2+\right.\\
&\left.+B^2\left(g_{55}'-\sqrt{r}g_{55}''\right)g_{11}-2B^2\sqrt{r}g_{11}'g_{55}'\right)g_{55}-2\sqrt{r}g_{11}\left(B^2+g_{11}^2\right)^2\left(g_{55}'\right)^2\Big)w^2+\\
&+2\sqrt{r}\rho^2\left(w^2+1\right)g_{11}\left(B^2+g_{11}^2\right)^2\left(g_{55}'\right)^2+\\
&+r\rho\left(w^2+1\right)\left(B^2+g_{11}^2\right)g_{55}\left(\left(B^2+2g_{11}^2\right)g_{55}g_{11}'+2g_{11}\left(B^2+g_{11}^2\right)g_{55}'\right)+\\
&+g_{55}^2\Big(\sqrt{r}\left(w^2+1\right)g_{11}\left(3B^2+2g_{11}^2\right)\left(g_{11}'\right)^2\rho^2+\sqrt{r}\left(w^2+1\right)\left(B^4+3g_{11}^2B^2+\right.\\
&\left.+2g_{11}^4\right)g_{11}''\rho^2+\left(B^4+3g_{11}^2B^2+2g_{11}^4\right)g_{11}'\left(r\rho ww''+\left(w^2+1\right)\left(-\rho^2+r\phi'(\rho)\rho+3r\right)\right)\Big)+\\
&+2\left(B^2+g_{11}^2\right)g_{55}\left(\left(\sqrt{r}\left(w^2+1\right)g_{55}''\rho^2+\right.\right.\\
&\left.\left.+g_{55}'\left(r\rho ww''+\left(w^2+1\right)\left(-\rho^2+r\phi'(\rho)\rho+3r\right)\right)\right)g_{11}^3\right.\\
&+4\sqrt{r}\rho^2\left(w^2+1\right)g_{11}'g_{55}'g_{11}^2+B^2\left(\sqrt{r}\left(w^2+1\right)g_{55}''\rho^2+g_{55}'\left(r\rho ww''+\right.\right.\\
&\left.\left.\left.+\left(w^2+1\right)\left(-\rho^2+r\phi'(\rho)\rho+3r\right)\right)\right)g_{11}+2B^2\sqrt{r}\rho^2\left(w^2+1\right)g_{11}'g_{55}'\right)\Big)=0.
\end{aligned} \tag{3.10}$$

The known functions $g_{00}(r), g_{55}(r), \phi(r)$, which have to be supplied for each of the backgrounds in study, have been left arbitrary on purpose, since when specific values are inserted, the equations would look even more cumbersome. The both interrelated variables r and ρ have been left for brevity.

The equations of motion are solved numerically in the next section. First quark masses and condensates are extracted and fitted with appropriate interpolation functions.

3.3 Condensate

The standard lore is: one must search for physical solutions of these non-linear second-order differential equations, which have the following asymptotics in the infinity:

$$w(\rho) = m + \frac{c}{\rho^2}. \tag{3.11}$$

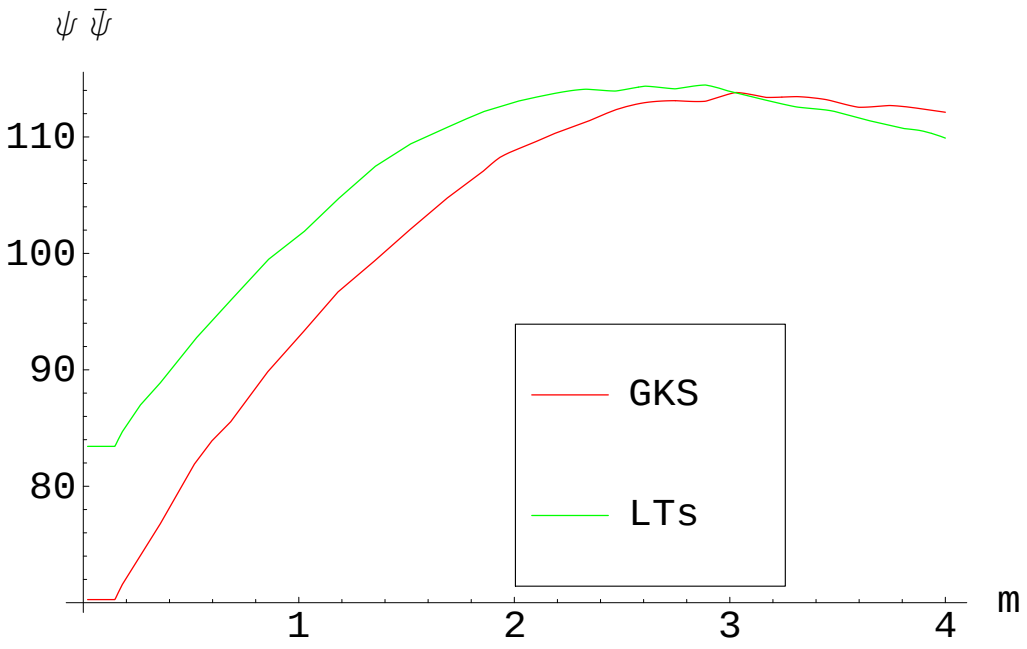

Figure 3.1: Dependence of the condensate on the mass. "GKS" stands for the Gubser–Kehagias–Sfetsos background, "LTs" for the Liu–Tseytlin background.

Then the parameters m and c correspond to the quark mass and chiral condensate:

$$\begin{aligned} m_q &= \tfrac{m}{2\pi\alpha'}, \\ \langle\bar{q}q\rangle &= \tfrac{c}{(2\pi\alpha')^3}, \end{aligned} \tag{3.12}$$

where α' is the string tension parameter. Contrary to the physical solutions, the unphysical ones are those ending in the singularity of the metrics, or going to infinity at $\rho \to 0$. The singularity is marked by an ellipse denoted "singularity" in Fig. (2.1). Physical solutions can be defined by boundary condition $w'(0) = 0$. It happens that the generic solutions are unphysical ones.

To obtain physical solutions, one imposes

$$\begin{cases} w'(0) = 0, \\ w(0) = w_0 = const. \end{cases} \tag{3.13}$$

For each value of w_0 above some value this will yield a curve from the family shown in Fig. (2.1), the asymptotic behaviour of which will reveal some definite m and c. This allows one to build the dependence of the condensate on quark mass Fig. (3.1). Doing the same thing with different values of the magnetic field B, one gets a shifted curve. It is a subtlety of this method that in order to understand how the condensate shifts in

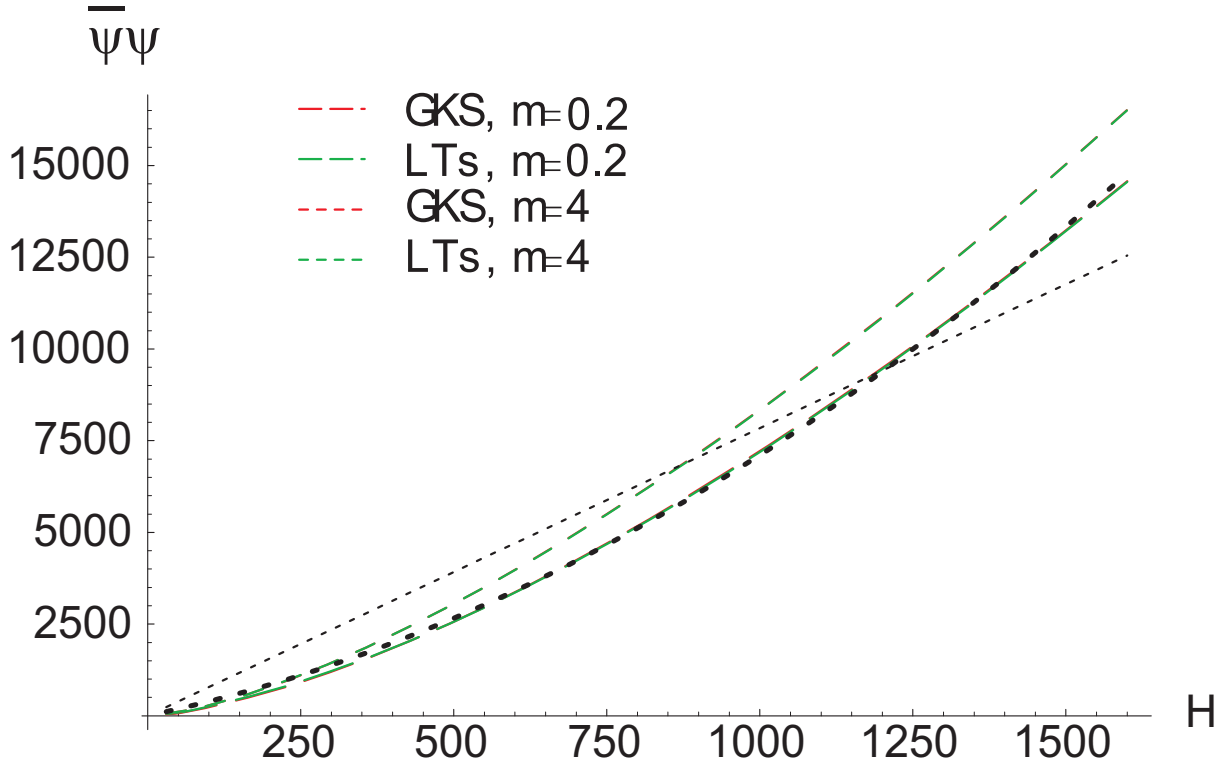

Figure 3.2: Magnetic catalysis of chiral symmetry breaking in the Karch—Katz model in different backgrounds, chiral limit and non-zero mass case. Abbreviations: "GKS" stands for the Gubser–Kehagias–Sfetsos background, "LTs" for the Liu–Tseytlin background.

the field, one must take a section of Fig. (3.1) at a constant m rather than follow some fixed w_0 value; fixing w_0 makes no physical sense at all. The resulting dependence of the condensate on the field is shown in Fig. (3.2) for the two backgrounds.

We analyze this "experimental" dependence. One could expect either linear (as in true QCD) or quadratic (as in NJL) condensate growth with the field. In our case, an approximation with a quadratic polynomial comes out to be quite effective. In Fig. (3.2) one can see the comparison between the linear and quadratic approximations, and judge in favor of the latter.

This quadratic dependence on the field value corresponds very nicely to the picture of magnetic catalysis of chiral symmetry breaking in [221, 22] in NJL models. On the other hand, it does not correspond to the linear condensate shift, predicted by the low-energy QCD effective action by Smilga and Shushpanov [223]. This phenomenon may be given a nice qualitative explanation. The condensate expression (3.1) is a part of the series in powers of $\frac{1}{N_c}$, for $f_\pi \sim \sqrt{N_c}$. It starts with the $\frac{1}{N_c}$ term. There may be a term, dependent on field, and containing $\frac{1}{N_c}$ in the zeroth power. To our best knowledge, such terms have

not been reported in chiral perturbation theory. On the contrary, dual models restore the missing leading-order $\frac{1}{N_c}$ contribution.

3.4 Summary

A qualitative conclusion can be drawn upon analyzing the dependence of the chiral condensate on the magnetic field. We can see that the linear field dependence of the QCD condensate from chiral perturbation theory is not reproduced at all. Instead, a quadratic dependence is retrieved. It is universal for the two backgrounds under considerations. Our conjecture to explain this phenomenon is very simple. The chiral perturbation theory estimate, as given in the cited references, misses the leading-order in $\frac{1}{N_c}$. It starts with the next-to-leading order in $\frac{1}{N_c}$. On the other hand, duality might reproduce the leading-order effect. Nevertheless, the search for a true dual model of QCD must still be in progress. One of possible improvements of the model would be to take into account back-reaction effects. In our setting, the $D7$ brane was a probe brane, a self-consistent supergravity solution in a background of a stack of $D3$ branes and a $D7$ brane would be advantageous.

Chapter 4

Vacuum Magnetization in Strong Fields

4.1 Notion of Vacuum and Condensate Magnetization

In statistical physics [210] the magnetization of matter is defined as the derivative of the free energy F over field B

$$M = -\left(\frac{\partial F}{\partial B}\right)_{T,V,N} \tag{4.1}$$

and magnetic the susceptibility χ as

$$\chi = \frac{\partial M}{\partial B}. \tag{4.2}$$

In a relativistic field theory, the magnetic susceptibility of the chiral condensate is defined as

$$\langle \bar{\psi}\sigma^{\mu\nu}\psi\rangle = \chi(F)F^{\mu\nu}\langle\bar{\psi}\psi\rangle_0. \tag{4.3}$$

where F is the external field strength. It is important to note here that the condensate $\langle\bar{\psi}\psi\rangle_0$ is taken at $B = 0$. The two definitions of magnetization are not universally equivalent; actually one could speak of two different quantities, which may or may not coincide. To distinguish between them, we shall refer to (4.1) and its derivative as *vacuum* magnetization and susceptibility, and to (4.3) and other definitions via matrix element as *condensate* magnetization or susceptibility.

The definition (4.3) includes all possible contributions to the vacuum response to the field. As "contributions" are meant the diamagnetic and the paramagnetic pieces, the

former related to charge effects, the latter to spin effects. To eliminate diamagnetism, one can also consider

$$\langle\bar{\psi}\sigma^{\mu\nu}\psi\rangle = \chi_{para}(F)F^{\mu\nu}\langle\bar{\psi}\psi\rangle_B, \tag{4.4}$$

where $\langle\bar{\psi}\psi\rangle_B$ is the condensate in presence of the field [24]. It is generally believed that lattice calculations provide us only with the paramagnetic part of χ. For a non-relativistic fermion gas, a theorem relating χ_{dia} and χ_{para} holds

$$\chi_{dia} = -\frac{1}{3}\chi_{para}, \tag{4.5}$$

however, there is no evidence that it holds for the QCD vacuum as well. The standard lore about condensate susceptibility is [246]

$$\chi(0) = -\frac{N_c}{4\pi^2 f_\pi^2} = \frac{1}{(335\text{MeV})^2}. \tag{4.6}$$

The numerical value of χ defined from sum rules [247] is

$$\chi(0) = \frac{1}{(475\text{MeV})^2}. \tag{4.7}$$

Again, in this case only the small-field value $\chi(0)$ could be determined. An experimental determination [248] of $\chi(0)$ by a light-cone sum rule analysis of the branching ratios of radiative meson decays has led to

$$\chi(0) = \frac{1}{(590\text{MeV})^2}. \tag{4.8}$$

The definition of magnetization used in the lattice paper [249] is a condensate magnetization

$$M = \frac{\langle\overline{\psi}\sigma^{12}\psi\rangle}{\langle\overline{\psi}\psi\rangle}, \tag{4.9}$$

let us for definiteness choose the magnetic field $\vec{B} = (0, 0, F_{12})$. Let us try to understand when and how condensate magnetization can be related to vacuum magnetization. As known, the energy of the magnetic field interacting with a magnetized medium is [250] (chap.VII, eq. 37)

$$W = \int d^3x \left[-\left\langle \frac{e}{2m}\overline{\psi}\sigma^{\mu\nu}F^{ext}_{\mu\nu}\psi \right\rangle - \left\langle \frac{e}{m}\overline{\psi}(k)\left(\vec{k}'\vec{A}^{ext}(q)\right)\psi(k') \right\rangle \right], \tag{4.10}$$

where we have taken into account $A_0^{ext} = 0$. In our case the external field is constant, hence $q = 0, k = k'$. Although non-locality of the vacuum has been known since [251], here we work in the approximation of a local vacuum. Thus the "momentum" of the vacuum state

$|\psi\rangle$ is zero. There are no real particles, since temperature and chemical potential are zero. Therefore, $k' = 0$. Had we had a thermal quark gas, the situation would be completely different.

Diamagnetic contributions to the vacuum energy still arise at the one-loop level, since virtual quarks do have $k' \neq 0$. In QED this would be the leading effect; the Euler–Heisenberg Lagrangian is the archetypal example of the electron gas diamagnetism phenomenon. Yet in QCD the leading effect is the tree-level effect we deal in this Chapter with. Diamagnetism could become important only at very large values of the field, when the *field-induced* condensate of $\langle\overline{\psi}\psi\rangle$, which is given in Eq. 7 of [252], is large; the condensate of free fermions in a magnetic field is

$$\langle\overline{\psi}\psi\rangle = -\frac{m^3}{4\pi^2} + \frac{m^3}{4\pi^2}\log\left(\frac{m^2}{2eB}\right) - \frac{eBm}{4\pi^2}\log\left(\frac{m^2}{2eB}\right) - \frac{eBm}{2\pi^2}\left(\log\left(\Gamma\left(\frac{m^2}{2eB}\right)\right) - \frac{1}{2}\log(2\pi)\right), \tag{4.11}$$

whence it follows that the condensate is essentially non-analytical at zero field, therefore, non-perturbatively small at low fields. Therefore, for a homogeneous QCD vacuum with zero temperature and zero particle density in a purely magnetic field we are left with the spin (i.e. paramagnetic) contribution solely:

$$W = \int d^3x \left\langle -\frac{e}{2m}\overline{\psi}\sigma^{\mu\nu}F_{\mu\nu}\psi \right\rangle. \tag{4.12}$$

Then the tensor condensate is

$$\langle\overline{\psi}\sigma^{12}\psi\rangle = -\frac{2m}{e}\frac{\partial W}{\partial F_{12}}\frac{1}{V_3}. \tag{4.13}$$

The argumentation we have made above clearly indicates: vacuum magnetization may coincide with condensate magnetization only for very heavy quarks in a zero temperature, zero chemical potential theory.

Let us define the paramagnetic vacuum susceptibility holographically. Of course, this will be vacuum rather than condensate magnetization, since in all of the $D7$ and similar models describing fermionic degrees of freedom in holography, we lack a mode coupled to an antisymmetric tensor of rank 2. Holographically we have direct access to the bulk action

$$S = Wt = V_3 t\int \mathcal{L}d\rho, \tag{4.14}$$

where ρ is the holographic coordinate, $\mathcal{L}$ is the effective action density, $V_3 t$ is the four-volume. Then we have

$$M = -\frac{2m}{\langle\overline{\psi}\psi\rangle}\int d\rho\frac{\partial\mathcal{L}}{\partial B}. \tag{4.15}$$

This will be of direct use below for any $\mathcal{L}$ specific for a given background. One can easily obtain a vacuum magnetization for free fermions very much in the same way as $\langle\overline{\psi}\psi\rangle$ was obtained in [252]. The matrix element $\langle\overline{\psi}\sigma_{12}\psi\rangle$ is different from the latter only in changing

$$\operatorname*{tr}_{\text{Dirac}} e^{ie\frac{s}{2}F_{\mu\nu}} \to \operatorname*{tr}_{\text{Dirac}} \sigma_{12} e^{ie\frac{s}{2}F_{\mu\nu}} \tag{4.16}$$

in the Schwinger proper time integral, that is, one makes the change

$$\coth s \to 1 \tag{4.17}$$

in the expression for the condensate, leaving the rest of the Schwinger integral untouched. Following their eq. (5) we have

$$\langle\overline{\psi}\sigma_{12}\psi\rangle = \frac{eBm}{4\pi^2}\int\frac{ds}{s}e^{-\frac{m^2}{eB}s} = \frac{eBm}{4\pi^2}\log\left(\frac{m^2}{eB}\right). \tag{4.18}$$

Recent lattice simulations [249] have revealed a very interesting picture of condensate magnetization saturation at high values of the magnetic field B. The picture was suggested to have an explanation in terms of a classical (Langevin) law

$$\mu^{Langevin} = \mu_\infty\left(\coth\frac{3\chi_0 qB}{\mu_\infty} - \frac{\mu_\infty}{3\chi_0 qB}\right), \tag{4.19}$$

or in terms of a quantum (Brillouin) law

$$\mu^{Brillouin} = \mu_\infty\left(2\coth\frac{2\chi_0 qB}{\mu_\infty} - \coth\frac{\chi_0 qB}{\mu_\infty}\right). \tag{4.20}$$

It is remarkable that actually a third form of condensate magnetization dependence, not based on any known simple theoretical model, fits to lattice data with a much better χ^2 criterion:

$$\mu^{trig}(B) = \frac{2\mu_\infty}{\pi}\arctan\frac{\pi\chi_0 qB}{2\mu_\infty}. \tag{4.21}$$

It remains a challenge to understand why such a dependence emerges and what it may mean in the field-theoretic or dual context. A comparison of lattice data and theoretical model is shown in Fig. (4.1).

Vacuum magnetization can be easily extracted from dual models. Given the classical action

$$S_F = \int d^{p+1}\sigma\sqrt{\det_{\alpha\beta}\left(g_{\mu\nu}\partial_\alpha X^\mu\partial_\beta X^\nu + 2\pi B_{\alpha\beta}\right)} \tag{4.22}$$

of some embedding of Dp-brane, corresponding to adjoint fermionic degrees of freedom, in the presence of a Kalb-Ramond field B, the vacuum magnetization is related to it via (4.15).

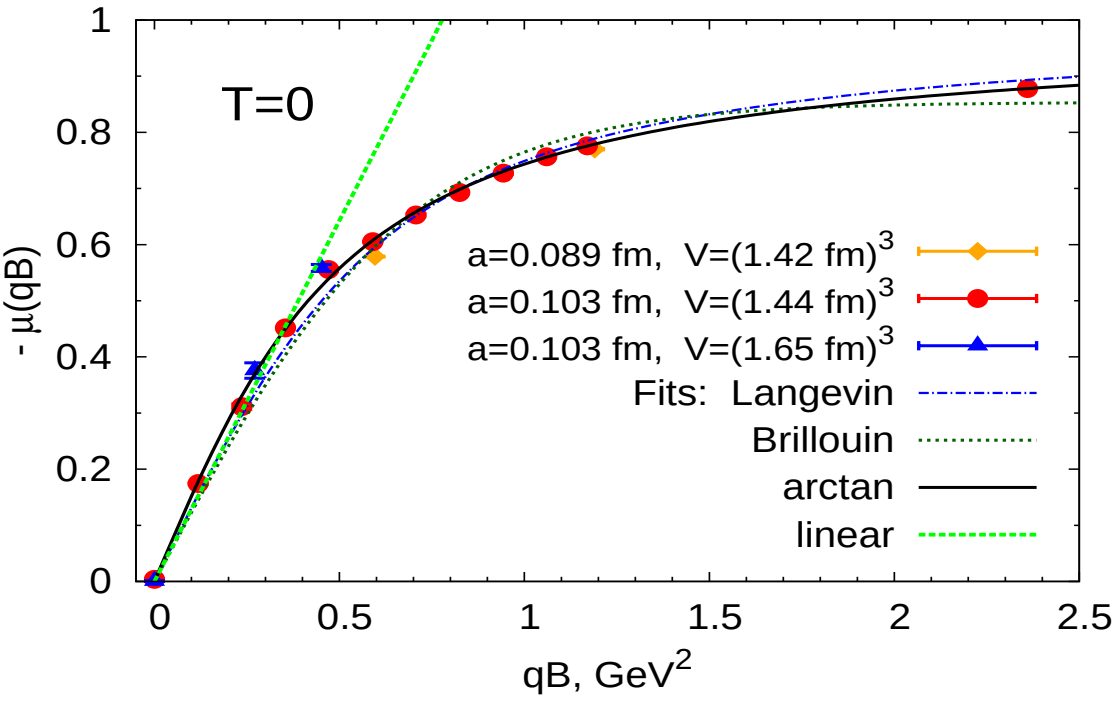

Figure 4.1: Condensate magnetization from the lattice, compared to Langevin, Brillouin, and "arctan" models. Plot taken from [249].

The response of holographic QCD to electric and magnetic fields has been studied during the last years extensively. We are interested in this Chapter in vacuum magnetization only. Bergman, Lifschytz and Lippert in a series of papers studied these problems in the Sakai–Sugimoto $D4$-$D8$-$\bar{D}8$ model. In the standard Sakai–Sugimoto framework, as described above, no saturation was obtained in [232]. In [123] holographic QCD in the confined phase was studied at a non-zero chemical potential. It has been shown that turning on the magnetic field induces a gradient for the pseudoscalar, which carries baryons and becomes a dominant phase at large fields. In [119] it has been shown that in the deconfined phase the fermions possess a first-order phase transition, where their vacuum magnetization makes a leap with increase of the field.

In the $D3/D7$ model in pure AdS space, the following asymptotic was derived [228] for large quark masses m

$$\mu(B) \sim \frac{B}{2} - \frac{B}{2}\log\frac{B}{2} + \frac{B(1+2B^2)}{24}, \tag{4.23}$$

where B is the dimensionless magnetic field strength. This behavior of vacuum susceptibility and vacuum magnetization is shown in Fig. (4.2). Again, no saturation is present.

Magnetic susceptibility of QCD condensate has been studied within AdS/QCD in [253].

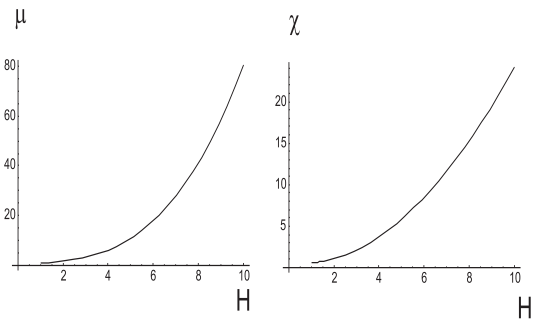

Figure 4.2: Vacuum susceptibility and vacuum magnetization from the $D3/D7$ model in pure AdS at large quark mass from [228].

For small fields, the value

$$\chi(0) = -2.15\frac{N_c}{8\pi^2} \tag{4.24}$$

has been obtained, in good agreement with Vainshtein's result.

4.2 Vacuum Magnetization from Holography

In the preceding Section I have analyzed some of the previous holographic studies of condensate/vacuum/baryonic matter magnetization and susceptibility. We have seen so far that none of the holographic models for vacuum magnetization reproduce the saturation property of condensate magnetization fully; perhaps, there is a good ground to believe they should in fact not coincide, being physically different objects.

We use here the $D3/D7$ model which we defined in Chapter 2, Section 2.2. We use the action (2.3), obtain equations of motion (3.10), find the sets of solutions for different backgrounds, shown in Fig. (2.1). From those, using (3.12) for the quark condensate and the quark mass, we easily evaluate the vacuum magnetization according to (4.15) in the three backgrounds under consideration (Constable–Myers (2.12)–(2.14), Gubser–Kehagias–Sfetsos (2.15)–(2.16), Liu–Tseytlin, (2.7)–(2.11)); the magnetization is shown in Fig. (4.3). The asymptotic behavior at small fields is linear, at large fields it is an unexpected

$$M = \frac{c}{\sqrt{B}}. \tag{4.25}$$

This asymptotic is shown in Fig. (4.4).

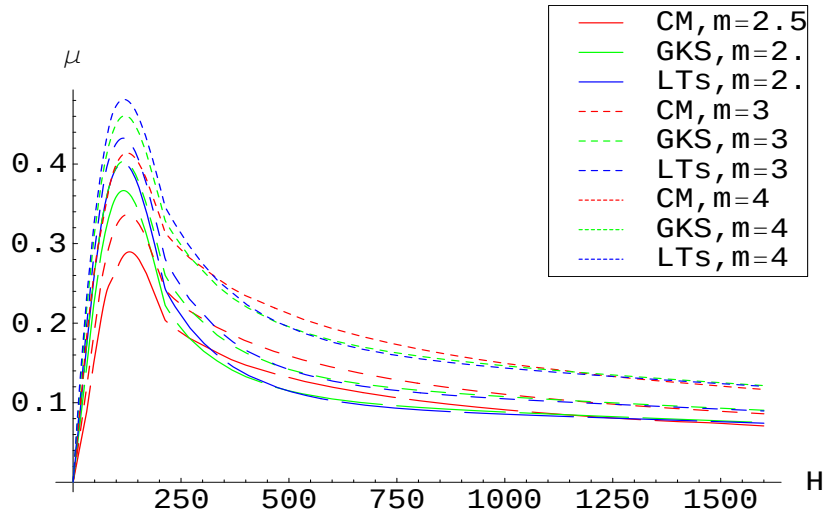

Figure 4.3: Vacuum magnetization from $D3/D7$ model in the Constable–Myers metric (abbreviated as "CM" in the Figure), the Gubser–Kehagias–Sfetsos metric ("GKS") and the Liu–Tseytlin metric ("LTs"), at different values of quark mass ($m = 2.5, 3, 4$).

The value of the constant c is very close for all the three metrics:

$$c = \begin{cases} 4.689, \text{Constable} - \text{Myers}, \\ 4.602, \text{Gubser} \\ 4.604, \text{Liu} - \text{Tseytlin}. \end{cases} \tag{4.26}$$

At small values of the field we have

$$\mu = \chi_0 B, \tag{4.27}$$

where the linear vacuum susceptibility is

$$\chi_0 = \begin{cases} 0.0052, \text{Constable} - \text{Myers}, \\ 0.0062, \text{Gubser}, \\ 0.0065, \text{Liu} - \text{Tseytlin}. \end{cases} \tag{4.28}$$

thus the linear vacuum susceptibility is very close in all of the three models. These results are different from those by [249], yet we see the presence of saturation of vacuum magnetization at large fields. What the lattice is definitely lacking is the maximum point; moreover, the vacuum magnetization on the lattice saturates at a non-zero value.

Note that such a strange behavior of the vacuum susceptibility has been observed in [254] for the transversal magnetization of matter $M_\perp$, see Fig. 2b. This effect for

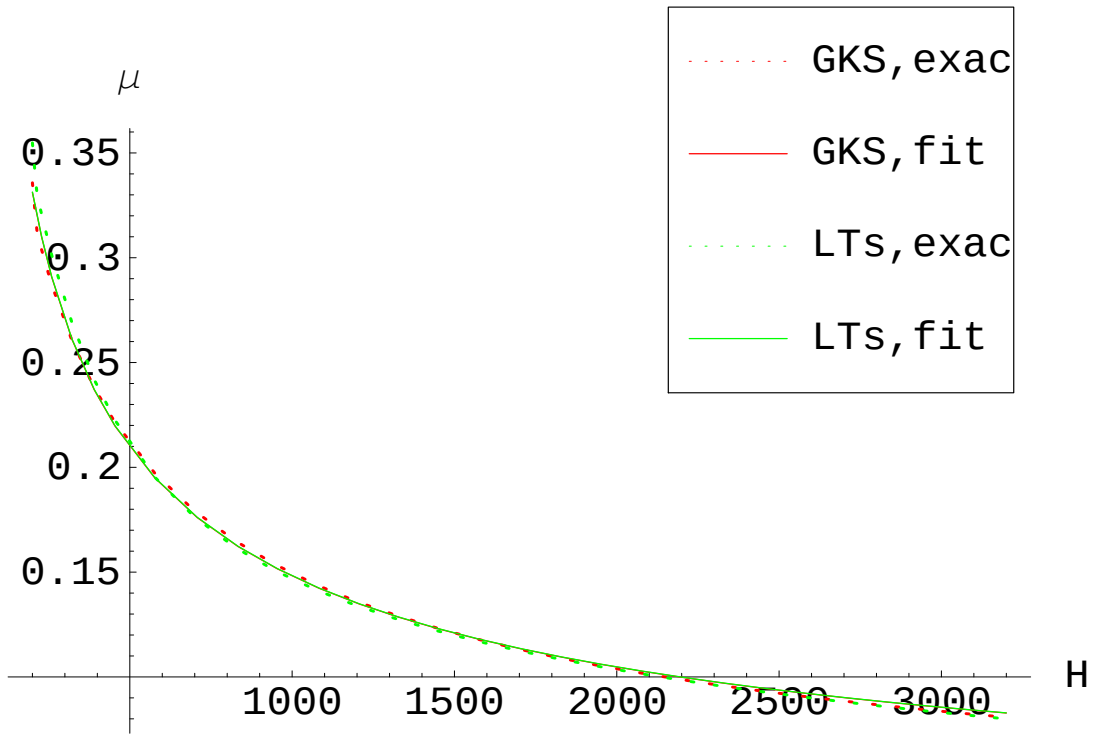

Figure 4.4: Asymptotic behavior of the vacuum magnetization at large fields: exact results and fits. "CM" stands for the Constable–Myers metric, "GKS" for the Gubser–Kehagias–Sfetsos metric, "LTs" for the Liu–Tseytlin metric.

longitudinal magnetization has been observed for doped silicon and denoted as matter magnetization inversion in [255], Fig. 1. A remarkably similar curve was observed in $YBa_2Cu_3O_7$ in the non-superconducting phase, see Fig. 1 in [256]. A family of analogous curves with a maximum at some $B = B_{max}$ and further diminishing magnetization for $Bi_2Sr_2CaCu_2O_{8+\delta}$ above T_c in magnetic fields is demonstrated in [257], for $Bi_2Sr_2CaCu_2O_8$, $Bi_2Sr_{2-y}La_yCuO_6$ and $La_{2-x}Sr_xCuO_4$. The plot is reproduced in Fig. (4.5)[1].

Speaking somewhat loosely, this result could possibly fit into the paradigm of the *electromagnetically* superconducting QCD vacuum [258]. Note that this picture does not have anything to do with the dual color superconductivity, which is one of the archetypal models of QCD.

The issue of QCD *electromagnetic* superconductivity is widely discussed in current literature. The idea of electromagnetic superconductivity for quark matter was proposed by [259]. For cold and dense quark matter it has been realized by Bailin and Love that

[1]I thank Dr. Phuan Ong for his kind permission to reproduce this Figure.

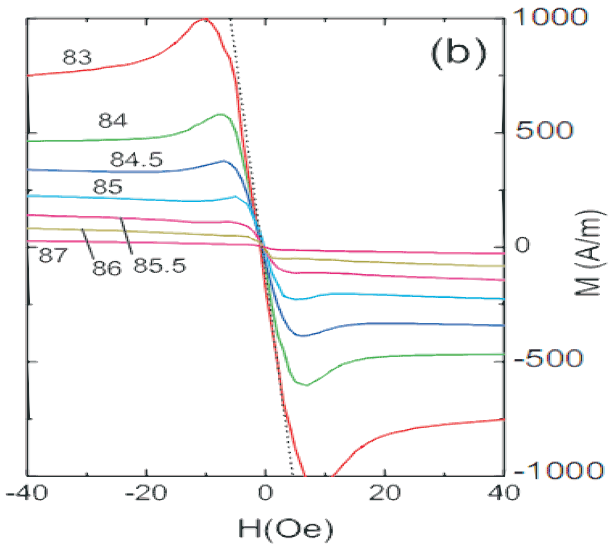

Figure 4.5: Experimental measurements from [257]: magnetization M of $Bi_2Sr_2CaCu_2O_{8+\delta}$ as a function of the field B, at different temperatures (given by numbers next to curves).

it must be a superfluid and electromagnetically superconducting phase [260, 261]. The situation was described as most fitting to the physics of neutron stars. In these early papers the critical magnetic field was calculated for the quark matter; it was found four orders of magnitudes smaller than that on the surface of neutron stars, thus presumably rendering the neutron star electromagnetically superconducting. Both s-wave (for u and d quarks) and p-wave (for s-quarks) were considered.

The case of interest for us is the electromagnetic superconductivity of the QCD vacuum, as opposed to a hot and dense medium. In [258] a prediction is made that the QCD vacuum becomes inhomogeneously (longitudinally) electromagnetically superconducting in the normal electromagnetic sense ($\rho^{\pm}$ meant as charges) after a second order phase transition at $\sqrt{B} > 0.6\text{GeV}$. This electromagnetic superconductivity transition in a strong magnetic field in the vacuum is related to a ρ-meson condensation. Thus at the phase transition point a discontinuity in magnetic vacuum susceptibility should be observed. We do not observe a true discontinuity, yet there is a significant fall-off and change of the asymptotic behavior at some B_c, which is rather abrupt, when the $M \sim B$ law is changed to $M \sim \frac{1}{\sqrt{B}}$; thus, if there were indeed a different phase above the value of the critical point, it would be reached via a crossover rather than a true transition. The numerical value of the critical point can be obtained by comparing to the known value of the gluon condensate in each of the respective metrics, $\langle \frac{\alpha}{\pi} \operatorname{tr} G^2 \rangle \sim 0.01\text{GeV}^2$. The estimate we can

give is

$$\sqrt{B_c} \sim 2GeV. \tag{4.29}$$

Another dimensionful quantity we can compare against is the linear vacuum susceptibility. We obtain a result which is an order of magnitude smaller than the experimental value (4.8):

$$\chi_0 = \begin{cases} 2.7 \text{ GeV}^{-2}, \text{experiment}, \\ 0.14 \text{ GeV}^{-2}, \text{holography}. \end{cases} \tag{4.30}$$

4.3 Discussion

This Chapter states the problem rather than fixes it. The problem generally may be formulated as follows: at large fields the magnetization of the QCD vacuum and baryonic matter is expected to saturate to

$$\mu(B)|_{B\to\infty} = 1. \tag{4.31}$$

Evidence for that is given both from lattice behaviour of the condensate magnetization and from standard solid-state results like the Brillouin law. Although neither is an exact physical equivalent of vacuum magnetization, one could speculate that the paramagnetic saturation to unity due to ordering all the available spins is universal. This is not what is observed in holography. In the cases considered, namely for my calculations with the Gubser metric, with the Constable–Myers metric, with the Tseytlin metric, the $D3/D7$ and for the Sakai–Sugimoto model results from literature, everything points to a very interesting non-Brillouin behaviour. In all of the $D3/D7$ cases done here (Gubser, Constable–Myers, Liu–Tseytlin), the vacuum magnetization rises to a certain B_c linearly, then falls of as $1/\sqrt{B}$. This is very untypical for normal matter, yet we find two examples, which resemble this behaviour: one is the QCD phase transition to an electromagnetically superconducting state at zero density and large magnetic field [258], the other one is a an anomalous (high T_c) cuprate superconductor below the phase transition point (where such a behaviour is observed for diamagnetism, not for paramagnetism as done here). We do not claim presently having observed an electromagnetically superconducting behavior in these models, yet a possibility of it should not be excluded, and the strange behaviour of vacuum magnetization could be considered as a hint thereto.

Another unsolved problem is the numerical value of the dimensionful parameters, B_c and χ_0. For B_c only a conjecture exists based on rho-meson effective electromagnetic superconductivity of the QCD vacuum; our B_c is definitely much greater than the expected B_c on a ρ-meson scale. For χ_0 there exist both experimental and theoretical well-established

values; our χ_0 is ridiculously small. This may be an artefact of setting a physical scale. If, instead of using $\mathrm{tr}\, G^2$ for fixing the scale, we use χ_0 itself

$$\chi_0 \equiv 2.7\mathrm{GeV}^{-2}, \tag{4.32}$$

then we arrive at

$$\sqrt{B_c} = 580MeV, \tag{4.33}$$

which is not that bad compared to $\sqrt{B_c} = 600$MeV from [258]. The values are different, yet at present level of possible errors, generated by different estimates for χ_0 – (4.6), (4.7), (4.8), it is impossible to make any speculation on this difference. Perhaps, the main lesson we learn from this comparison is that we roughly land into the ρ-meson range.

The other important conclusion is independent of the conjectured superconductivity state and tells us something about the holography itself. Namely, for these three metrics, different in the IR, the numerical results are almost universal, which makes it possible to speculate on them defining a universality class of holographic models. The relevance of the universality class to QCD is only partial, as one sees from spectrum and from the above considerations of magnetization properties, yet the result is in some sense "model-independent".

Part II

Resummed Field Theory

Chapter 5

A Novel Resummation of Wilson Loops

I study in this Chapter the confinement property of the pure SU(3) gauge theory, combining in this effort non-perturbative gluon and ghost propagators obtained as solutions of Dyson–Schwinger equations, with solutions of an integral ladder diagram summation type equation for the Wilson loop. I obtain the string potential and an effective UV coupling.

5.1 Overview

The problem of explaining the quark confinement has been of foremost importance since the formulation of $SU(N)$ Yang–Mills dynamics. The principal manifestation of confinement is the linear growth of the potential between color charges. This is known to be a property of the Wilson loop [262]. However, it has been impossible so far to reach this in an analytic *ab initio* calculation in a $3+1$ dimensional Yang–Mills. Along with other efforts, estimates for the $SU(N)$ string spectra have been done e.g. in [263], but those were performed on the lattice in 2+1 dimensions. We want to deal with this challenging problem by combining:

- the Erickson–Semenoff–Szabo–Zarembo (ESSZ) [3, 264] formulation for the Bethe–Salpeter type equation for Wilson loops, with
- Dyson–Schwinger equations (DSE) for the gluon and ghost propagator in the Landau gauge [265, 266].

I solve DSE for gluons and ghosts in the pure glue two-point sector. Then I insert the resulting coupling $\alpha = g^2/4\pi$ and the gluon propagator into the ESSZ equation for

a rectangular (non-supersymmetric) Wilson loop, and solve this integral equation, which yields the Wilson potential.

The ESSZ type ladder (or rainbow) diagram summation has long been a major tool for extracting the non-perturbative information about the dynamics of a gauge theory. However the strength of this method is more evident in the $\mathcal{N} = 4$ supersymmetric Yang–Mills due to the higher order vertex correction cancelation. In principle the use of the ESSZ ladder summation in our context of non-supersymmetric Yang–Mills is doubtful, and we will make several efforts to establish this approach: we will study the vertex correction terms by comparing the leading order (LO) contribution to the next to LO (NLO) contribution of the three-gluon vertex, and we will consider the convergence of the entire procedure by evaluating the string tension at different DSE scale fixing points.

Within the Yang–Mills, the DSE for propagators and vertex functions have been studied in great depth, for a review see [266, 265] and references therein. The relation of DSE to lattice results is discussed in [267]. An alternative related method of the functional renormalization group has been discussed in [268]. Dyson–Schwinger equations for fermions were extensively used in [269, 270, 271, 272] for hadron physics applications. The relevant results on three-point functions are seen in [273], and on the quark propagator in [265], the question of confinement inherent alone in DSE are discussed in [274, 275, 276], the uniqueness of the infrared (IR) scaling of Green functions was established and gluon propagator IR non-singularity was strictly supported in [277, 278], while the IR universality established in [279].

Below in section 5.2 we describe the ESSZ equations in a pure Yang–Mills theory with an arbitrary propagator (form-factor). In section 5.3 we present DSE and our solution, our results are in agreement with the standard state-of-the art calculations of ghost and gluon propagators in the Landau gauge. In section 5.4 we evaluate the ESSZ truncated Wilson loop, employing the DSE propagators from section 5.3 and check the significance of the NLO vertex correction. In section 5.5 we discuss the reasons why a confining potential is not observed either in the pure-glue two-point sector of DSE, or ESSZ solely, yet it is seen in the combination thereof.

5.2 ESSZ Equation

The Wilson loop

$$W(C) = \langle \mathrm{tr}\ \ \mathrm{Pexp}\left\{ \oint_C A_\mu(x) dx^\mu \right\} \rangle \tag{5.1}$$

contains information about the behaviour of quarks in the theory, and the quark-antiquark potential is

$$V(L) = -\lim_{T\to\infty} \frac{1}{T} \ln W(C_{T,L}), \tag{5.2}$$

where $C_{T,L}$ is a rectangular Wilson loop in the (x^0, x^1) plane, with T being loop temporal length, and L loop spatial length, $T \gg L$.

The Wilson loop (5.1) can be represented in terms of a perturbative expansion, which can be found e.g. in the review [280]. A set of Feynman rules for Wilson loops can be found in [281], which will be of use to us below. A perturbative treatment of Wilson loops is not useful in the non-Abelian case, and especially in the present context, as it yields obviously wrong results for the Yang–Mills theory, for which it predicts a Coulomb-type potential [280]. A large-N_c partial summation of ladder diagrams has been proposed in [3, 264] and performed for a circular and a rectangular loop in the $\mathcal{N} = 4$ supersymmetric model (SUSY). This method is adapted here to a non-SUSY theory, for the case that the partial summation of a perturbation theory (PT) series for propagators has already been performed in terms of solving DSE.

Consider a trapezoidal loop $W(C) = \Gamma(T_1, T_2; L)$ with long parallel temporal sides of lengths T_1, T_2, separated by a spatial distance L. Then the requirement that adding a propagator to the summed expression does not change it leads to the following integral equation for the sum of all ladder diagrams:

$$\begin{aligned} \Gamma(T_1, T_2, L) &= 1 + \frac{g^2 N_c}{4\pi^2} \int^{T_1} dt_1 \int^{T_2} dt_2 \times \\ &\quad \times \Gamma(t_1, t_2, L) D_{\mu\nu}((x_1 - x_2)^2) \dot{x}_1^\mu \dot{x}_2^\nu, \end{aligned} \tag{5.3}$$

dots denote derivatives in $t_{1,2}$, respectively, where $x_1^\mu = x_1^\mu(t_1)$, $x_2^\nu = x_2^\nu(t_2)$ are paths running over the Wilson loop as functions of t_1, t_2. For a rectangular loop $x_1 = (-L/2, t_1, 0, 0)$, $x_2 = (L/2, t_2, 0, 0)$. One should note here that the propagator connecting the long sides of the loop is just one of the possible corrections to be added even at the level of g^2. The loop has 4 sides, so in principle there could be 10 different propagator corrections (we consider each side separately when integrating over the loop). Corrections which start and end on the same side will lead to the perimeter divergence, which is irrelevant for the present discussion of the potential. Corrections which include one of the shorter sides are suppressed by their measure L, which satisfies $L << T$. We believe that this constitutes the approximation which restricts us from taking the limit of $L \to \infty$. Therefore, when claiming confinement, we shall not be able to claim it asymptotically, but only within a certain range of distances.

A term not considered here is the tad-pole contribution like the one discussed in [282]. The tadpoles are arising on the lattice due to the higher powers of the field vector potential A^a_μ coming from the expansion of Wilson loop. Our method is essentially devised to resum the non-linear contributions coming from Wilson loops. Thus in our case that the tad-pole term would lead to double-counting. Note that our approach based on ladder partial summation of the perturbative series is valid in the $1/N_c$ approximation. The latter is often used but is not yet fully established.

The configuration space propagator is related to the momentum-space form-factor $F(p^2)$, introduced in the next Section 5.3 by:

$$D_{\mu\nu}(x^2) = \frac{1}{(2\pi)^4}\int \frac{d^4p e^{-ipx}}{p^2} F(p^2)\left(g_{\mu\nu} - \frac{p_\mu p_\nu}{p^2}\right). \tag{5.4}$$

For simplicity we write $D_{\mu\nu}(x^2)\dot{x}_1^\mu \dot{x}_2^\nu \equiv D(x^2)$. Boundary conditions imposed upon Γ are

$$\Gamma(T,0;L) = \Gamma(0,T;L) = 1. \tag{5.5}$$

These boundary conditions are valid within the approximation, in which the gluon propagator is inserted between the long temporal sides solely, which is exactly our case. The potential is related to $\Gamma(T_1,T_2;L)$ in the following way

$$V(L) = -\lim_{T\to\infty}\frac{1}{T}\ln\Gamma\left(T,T;L\right). \tag{5.6}$$

Equation (5.3) is depicted symbolically in Fig. (5.1). Obviously, if we write down the first term for $\Gamma(T_1,T_2;L)$ in the g^2 expansion of the solution, we shall reproduce the perturbative result for the Wilson loop.

The central filled square in Fig. (5.1) symbolizes an irreducible kernel, containing (potentially) all the possible loop corrections. Combining the equation for the Wilson loop and Dyson–Schwinger does not lead to double-counting, because the class of ladder diagrams, summed for the Wilson loop, does not contain any iterations inside each particular propagator. Since the Dyson–Schwinger formalism does not contain any geometric degrees of freedom, related to the loop, Dyson–Schwinger does not resum any contributions of Wilson type. However, one could imagine a reformulation of our approach in which the Dyson–Schwinger equations include a Wilson line in order to secure gauge invariance (which we did not do); in that case the overcounting problem would of course be present. A convenient way of solving (5.3) is to consider the equivalent differential equation:

$$\frac{\partial^2\Gamma(t_1,t_2;L)}{\partial t_1\partial t_2} = \frac{g^2N_c}{4\pi^2}D\left((t_1-t_2)^2+L^2\right)\Gamma(t_1,t_2;L), \tag{5.7}$$

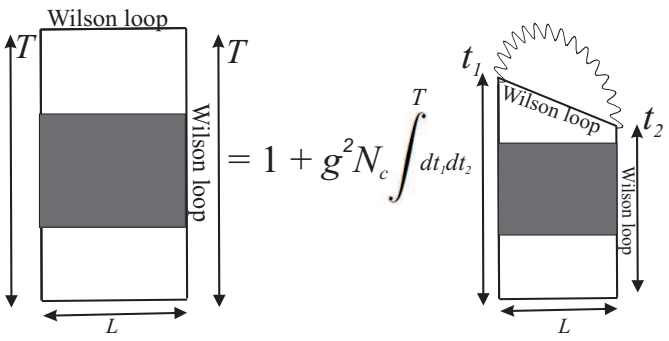

Figure 5.1: Summation of ladder/rainbows for a Wilson loop.

We now introduce the variables $x = (t_1 - t_2)/L,\ y = (t_1 + t_2)/L$. With this Ansatz the separation of variables becomes possible, and using the form:

$$\Gamma = \sum_n \psi_n(x) e^{\frac{\Omega_n y}{2L}} \tag{5.8}$$

we will be solving the 1d-equation

$$-\frac{d^2}{dx^2}\psi_n(x) + U(x;L)\psi_n(x) = -\frac{\Omega_n^2}{4}\psi_n(x), \tag{5.9}$$

with the effective potential

$$U(x;L) = -\frac{g^2 N_c}{4\pi^2} L^2 D\left(L^2(1+x^2)\right). \tag{5.10}$$

We are solely interested in the unique ground state solution of (5.9), since the Wilson quark-quark potential is

$$V(L) = -\lim_{T\to\infty}\frac{1}{T}\log\sum_n \psi_n(x) e^{\frac{\Omega_n T}{L}} = -\frac{\Omega_0}{L}. \tag{5.11}$$

A degeneracy in solutions of (5.9) may arise and thus complicate the situation, however, we have never observed it in our numeric calculations shown below in section 5.4.

It is now evident, that in order to complete the Wilson potential evaluation we need the propagator D and the coupling $\alpha = g^2/4\pi$ derived from DSE in order to be able to evaluate $V = -\Omega_0(L)/L$.

5.3 Dyson–Schwinger Equations

We now obtain the nonperturbative input to the ESSZ equations, i.e. the Dyson–Schwinger improved gluon propagator and coupling α. The difference between DSE and the simple renormalization group (RG) improved quantity is in the IR and medium momentum ranges, their ultra violet (UV) behaviour being identical (up to 1 loop at least). Our DSE procedure uses the technique described in [283, 284], the reader familiar with this may skip the current section where we demonstrate that the results of [283, 284] are independently reproduced by us.

I employ in this Chapter the Newton-method based numerical technique described in [285]. We solve a system for ghost and gluon propagators, corresponding to the representation seen in Fig. (5.2). Here bulbs denote dressing of the propagators, and transparent bulbs – dressing of vertices.

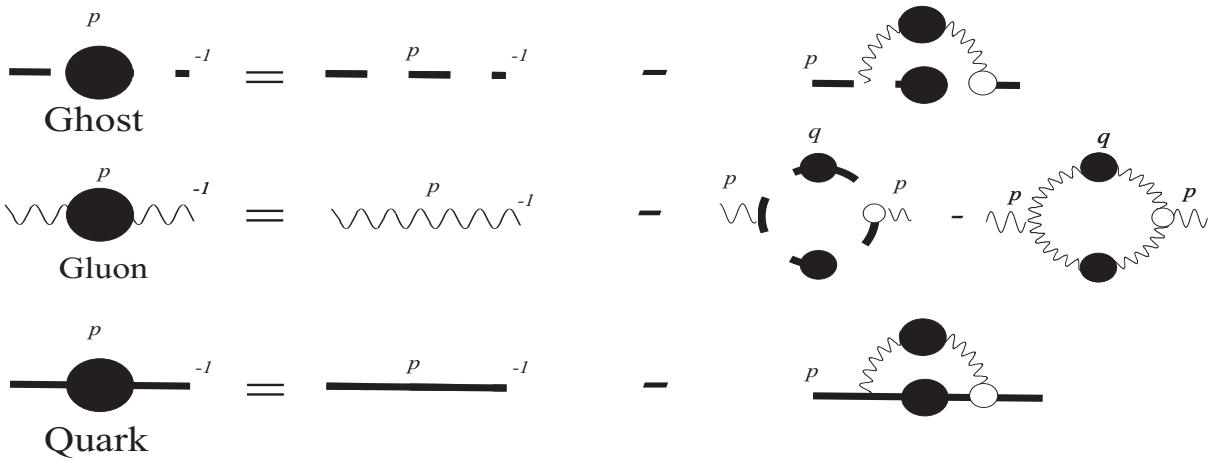

Figure 5.2: Diagrammatic representation of DSE.

These equations can be written in the form:

$$\begin{cases} \dfrac{1}{G(p^2)} - \dfrac{1}{G(\bar{\mu}_c^2)} = -\left(\Sigma(p^2) - \Sigma(\bar{\mu}_c^2)\right), \\ \dfrac{1}{F(p^2)} - \dfrac{1}{F(\bar{\mu}_g^2)} = -\left(\Pi(p^2) - \Pi(\bar{\mu}_g^2)\right), \end{cases} \tag{5.12}$$

where vacuum polarization is

$$\Pi(p^2) = \Pi^{2c}(p^2) + \Pi^{2g}(p^2), \tag{5.13}$$

$$\Pi^{2c}(p^2) = N_c g^2 \int \frac{d^d q}{(2\pi)^d} M_0(p^2, q^2, r^2) G(q^2) G(r^2),$$
$$\Pi^{2g}(p^2) = N_c g^2 \int \frac{d^d q}{(2\pi)^4} Q_0(p^2, q^2, r^2) F(q^2) F(r^2), \tag{5.14}$$

and self-energy is

$$\Sigma(p^2) = N_c g^2 \int K_0(p^2, q^2, r^2) G(q^2) F(r^2) \frac{d^d q}{(2\pi)^d}. \tag{5.15}$$

Fermion equations shown in the Figure will be explicitly written down and used in the next Chapter; in this Chapter pure gluodynamics is considered. Here $\bar{\mu}_{g,c}$ are the subtraction points, $\bar{\mu}_c = 0$, $\bar{\mu}_g = \bar{\mu}$, $\bar{\mu}$ is the limit of the interval $p^2 \in (0, \bar{\mu}^2)$ in the momentum space, where we solve the DSE, the coupling g^2 is meant to be the $g^2(\bar{\mu}^2)$. F is the gluon propagator form-factor in the Landau gauge, defined via the relation

$$D^{F\,ab}_{\mu\nu}(p) = \delta^{ab} \left(g_{\mu\nu} - \frac{p_\mu p_\nu}{p^2} \right) \frac{F(p^2)}{p^2 + i\epsilon}, \tag{5.16}$$

and the ghost propagator the non-trivial behaviour is described by the form-factor G

$$D^{G\,ab}(p) = \frac{\delta^{ab}}{p^2 + i\epsilon} G(p^2). \tag{5.17}$$

The variable z is the logarithmic variable

$$z = \ln \frac{p^2}{\mu^2}, \tag{5.18}$$

and the scale μ is yet to be defined upon solving the Dyson–Schwinger equations from comparing the obtained coupling $\alpha_{DSE}(z)$ to the known values of $\alpha_{PDG}(p^2)$ at point M:

$$\alpha_{DSE}(\ln(M^2/\mu^2)) = \alpha_{PDG}(M^2). \tag{5.19}$$

The coupling constant $g^2/4\pi \equiv \alpha$ is expressed in terms of G, F solely [286, 287], as the vertex is finite in the Landau gauge (at one-loop level)

$$\alpha_{\rm DSE}(\ln(p^2)) = \alpha_{\rm DSE}(\bar{\mu}) F(p^2) G^2(p^2). \tag{5.20}$$

In our case, we shall use a varying scale fixing point M, so that we can prove that our results are independent of scale fixing point choice, within the error margin of our procedure.

The kernels M_0, K_0, Q_0 are known in literature, but for self-containedness of the Chapter we show them here:

$$\begin{aligned} K_0(x, y, \theta) &= \frac{y^2 \sin^4(\theta)}{\left(-2\cos(\theta)\sqrt{xy} + x + y\right)^2}, \\ M_0(x, y, \theta) &= -\frac{y^2 \sin^4(\theta)}{3x\left(-2\cos(\theta)\sqrt{xy} + x + y\right)}, \end{aligned} \tag{5.21}$$

$$
\begin{aligned}
Q_0(x,y,\theta) = &-\frac{1}{12x\left(-2\cos(\theta)\sqrt{xy}+x+y\right)^2}\times \\
&\left\{y\sin^2(\theta)\left[2\cos(2\theta)\left(6x^2+31xy+6y^2\right)-\right.\right. \\
&-12x\cos(3\theta)\sqrt{xy}+xy\cos(4\theta)-48\cos(\theta)\sqrt{xy}(x+y)- \\
&\left.\left.-12y\cos(3\theta)\sqrt{xy}+3x^2+27xy+3y^2\right]\right\}.
\end{aligned}
\tag{5.22}
$$

For convenience, the variables $x = p^2$, $y = q^2$ are introduced; the variable θ is defined via $(p-q)^2 = x+y-2\sqrt{xy}\cos\theta$. We neglect the effects of non-trivial dressing of the vertices, since these do not essentially back-react the IR structure of the propagator themselves, and we do not apply them anywhere in the ESSZ summation. Had we been doing next-order corrections to ESSZ, we would certainly have required the modifications of e.g. triple-gluon vertex as well.

To solve the Dyson–Schwinger equations we use the Ansatz [283, 284]:

$$
F(z) = \begin{cases} \exp\left(\sum\limits_i^{\bar{n}} a_i T_i(z)\right),\ z \in (\ln\epsilon, \ln\bar{\mu}^2), \\ F(\bar{\mu})\left(1+\omega\log\dfrac{p^2}{\bar{\mu}^2}\right)^{\gamma},\ z > \ln\bar{\mu}^2, \\ Az^{2\kappa},\ z < \ln\epsilon, \end{cases}
\tag{5.23}
$$

$$
G(z) = \begin{cases} \exp\left(\sum\limits_i^{\bar{n}} b_i T_i(z)\right),\ z \in (\ln\epsilon, \ln\bar{\mu}^2), \\ G(\sigma)\left(1+\omega\ln\dfrac{p^2}{\bar{\mu}^2}\right)^{\delta},\ z > \ln\bar{\mu}^2, \\ Bz^{-\kappa},\ z < \epsilon. \end{cases}
$$

Here T_i are Tschebyschev polynomials, a_i, b_i are unknown coefficients yet to be determined from the numerical solution, $\bar{n}$ is the number of polynomials used (mostly $\bar{n} = 30$ has been used here, allowing a precision of 10^{-10} for coefficients), $\delta = -9/44$, $\gamma = -1-2\delta$, $\omega = 11N_c\alpha(\sigma)/(12\pi)$. The IR scaling κ is chosen to be the standard [288, 289]

$$
\kappa = 0.59 \tag{5.24}
$$

for the case of the Brown–Pennington truncation with $\zeta = 1$ [284] (for discussion of the meaning of ζ see [290]), which is our case (ζ already set to its number value everywhere). Following [265], we employ the renormalization constant $\mathcal{Z}_1$ redefinition, so that no momentum dependence could possibly enter it, that is

$$\mathcal{Z}_1 = \frac{G(y)^{(1-a/\delta-2a)}}{F(y)^{(1+a)}} \frac{G(y)^{(1-b/\delta-2b)}}{F(y)^{(1+b)}}. \tag{5.25}$$

Again, following [265] we choose

$$a = b = 3\delta, \tag{5.26}$$

which minimizes its momentum dependence. The renormalization constant $\mathcal{Z}_1$ refers to the piece with the ghost loop in vacuum polarization. The equations are solved by using Newton's method, very clearly described for this particular application by Bloch [285].

The results of the solution are propagator form factors F, G, shown in Fig. (5.3) on the left, the IR behavior of the propagators corresponds to the standard ghost enhancement and gluon suppression. The coupling α obtained from DSE (5.20) is shown on the right in Fig. (5.3). We compare it to the standard coupling from the Particle Data Group [291], and note that the both coincide very well in the UV. We note here that the IR fixed point seen in the Figure is

$$\alpha(0) \approx 3 \tag{5.27}$$

for $N_c = 3$, which is consistent with the up-to-date Dyson–Schwinger results reported by other groups [265, 266].

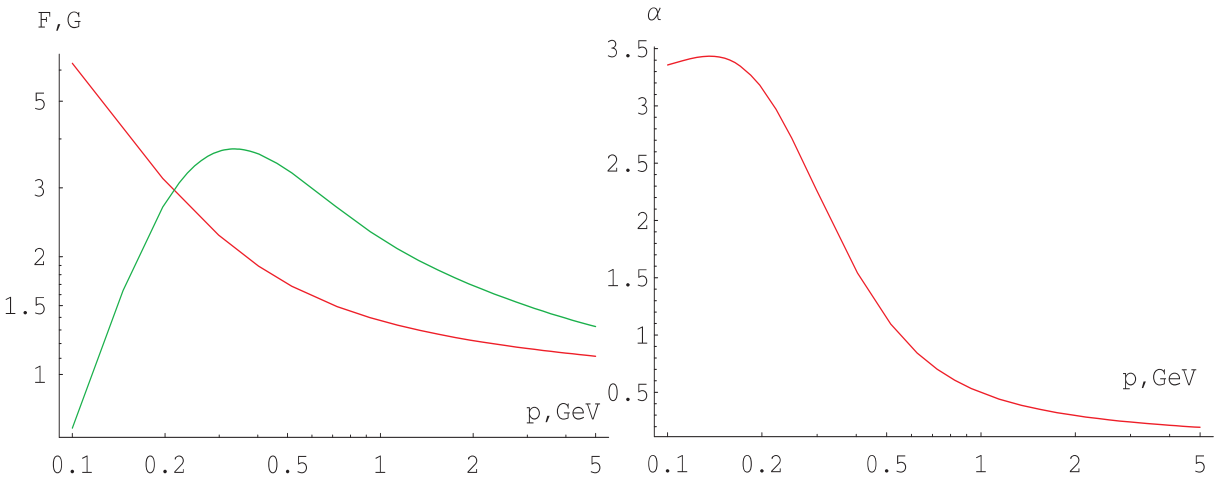

Figure 5.3: Ghost (red line) and gluon (green line) propagator form factors obtained in DSE in Landau gauge; running coupling from the DSE.

5.4 Solving ESSZ Equation

We have to find the lowest eigenvalue of a Schrödinger equation (5.9)

$$\left(-\frac{1}{2}\frac{d^2}{dx^2}+U(x;L)\right)\psi(x)=\mathcal{E}\psi(x) \tag{5.28}$$

where the auxillary potential $U(x)$ is related by a linear integral transform to the gluon form-factor as

$$\begin{aligned} U(x) = &-\frac{2\pi\alpha N_c}{(1+x^2)^2}\frac{1}{(2\pi)^2}\int\frac{du}{u}\times \\ &\big(uJ_1(u)-(1-3x^2)J_2(u)\big)\,F\left(\ln\left(\frac{u^2}{L^2\mu^2(1+x^2)}\right)\right), \end{aligned} \tag{5.29}$$

where μ is defined at point M as given in Eq. (5.19), M varying from 1 to 10 GeV, u is a dummy scalar dimensionless integration variable. The coupling α, in the sense of the DSE approach, is taken here at the scale of $\frac{2\pi}{L}$. We solve the Schrödinger equation with the shooting method and find its ground state. Special care is taken to make sure this state is not degenerate. As a result we get the potential $V(L)=-\frac{2\sqrt{2|\mathcal{E}|}}{L}$. The potential is defined up to an additive constant, so we shift it to provide convenient comparison to existent results. It is shown in Fig. (5.4) below, and is compared with lattice results by Gubarev et al. [292] and Necco [293]. The linear IR behaviour of the potential can be clearly seen from the figure. We fit the potential by the standard expression

$$V(L)=-\frac{4}{3}\frac{\alpha_0}{L}+c_0+\sigma L. \tag{5.30}$$

We demonstrate in Fig. (5.5) that the linear part of the potential is indeed clearly present, comparing the approximation we make with a purely Coulomb approximation. We then consider this question in a more systematic way in Table (5.1), where we evaluate χ^2/DOF for several possible analytic forms of the potential. The 'experimental' error for the potential is taken from the error of string tension, which is estimated below. The linear "confinement"-type dependence is the one with the acceptable confidence level. This study demonstrates that the additional potential component is best described by a linear dependence of the potential and that it is the variation of the Coulomb part of the potential which misleads the eye to think that there is a nonlinear behavior.

The dependence of the string tension σ on the scale fixing point choice is shown in Fig. (5.6). We see that the variance of σ does not exceed that of different lattice

Table 5.1: χ^2 for different approximations

Model	χ^2/DOF
$ax + b + c/x$	0.29
$ax^2 + b + c/x$	2.6
$b + c/x$	19

Table 5.2: Comparison of string tension from different sources

Author	Year	σ,GeV/fm
Bali et al. [294]	2000	1.27
Necco [293]	2003	1.10
Gubarev et al. [292]	2007	0.978
Weise et al. [295]	2009	1.07
Present work	2009	1.07 ± 0.1

results, shown in the table (5.2). The error we quote arises from an average of results obtained at different scale fixing points. This yields $\alpha_0 = 0.24$ and $\sigma = 1.07 \pm 0.1$.

The key result, the linear confining potential comes as a surprise. It invites the question, how large are the corrections coming from the three-point vertex? One actually should not have thought that the Yang–Mills can be described with an ESSZ partial summation structure. Considering the vertex, the auxillary potential is then modified:

$$U(x) = U^{(1)}(x) + 4\pi\alpha N_c U^{(2)}(x), \tag{5.31}$$

where $U^{(2)}(x)$ comes, in the leading $1/N_c$ order, from the Wilson loop diagram shown in Fig. (5.7).

Calculating the diagram in Landau gauge with rules as defined in [281] we obtain:

$$\begin{aligned} U^{(2)}(t_1, t_2) = &\int d^4y \int_0^1 dt_3 \frac{1}{(y-x_1)^2(y-x_2)^2(y-x_3)^2} \times \\ &\left[(u_1u_2)(u_3y)\left(\frac{1}{(y-x_1)^2} - \frac{1}{(y-x_2)^2}\right) + \text{cyclic permut.}\right] \end{aligned} \tag{5.32}$$

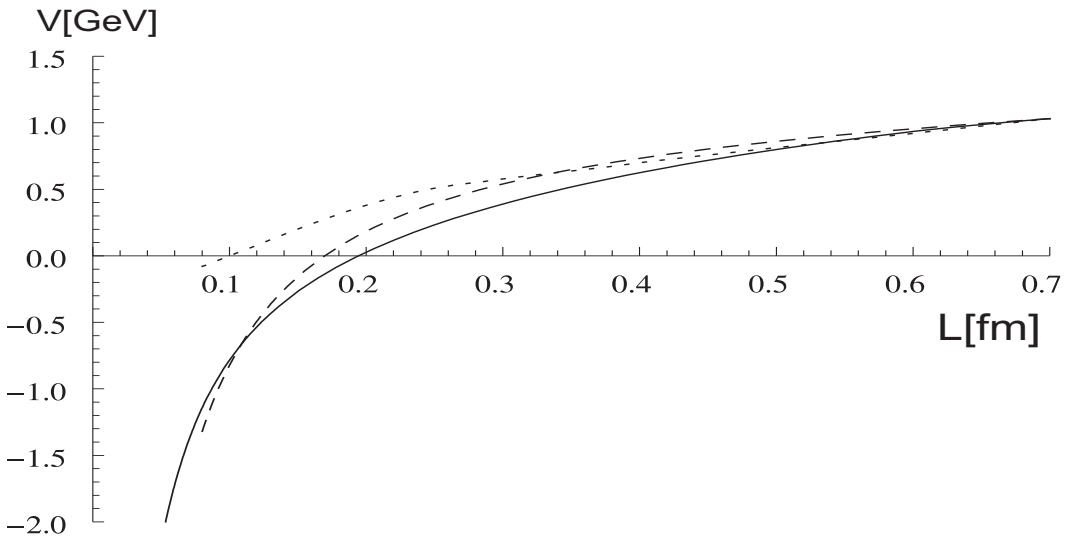

Figure 5.4: Potential as function of distance, solid line: our result, dashed line: result by Necco, 2003 [293], dotted line: result by Gubarev et al. 2007 [292].

with

$$\begin{cases} x_1 = (-L/2, t_1, 0, 0) \\ x_2 = (L/2, t_2, 0, 0) \\ x_3 = (-L/2 + Lt_3, t_1 + t_3(t_2 - t_1), 0, 0) \\ u_1 = (0, 1, 0, 0) \\ u_2 = (0, 1, 0, 0) \\ u_3 = (L, t_2 - t_1, 0, 0) \end{cases} . \tag{5.33}$$

The additional integral is taken over the intermediate gluon leg coordinate x_3 on the loop and over the position of the three-gluon vertex in spacetime; x_1 and x_2 are the same points

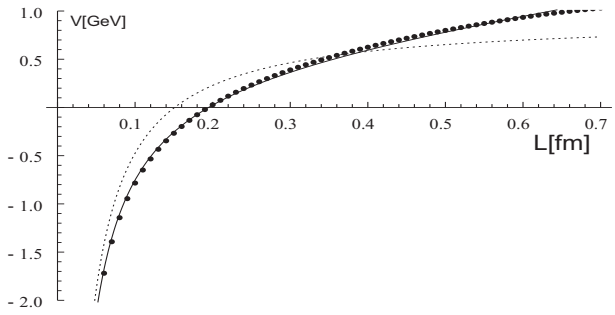

Figure 5.5: Comparison of the approximations. Thick black dots are my numeric results, continuous curve: approximation $V(x) = ax + b + c/x$; dashed curve: $V(x) = b + c/x$.

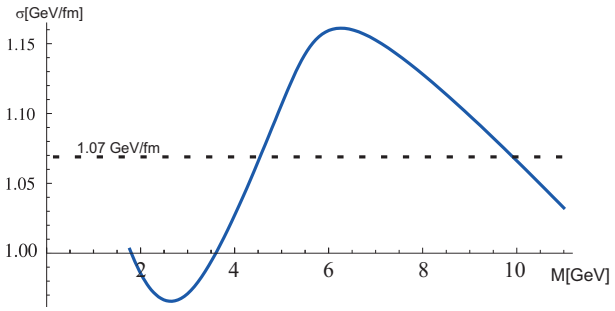

Figure 5.6: Dependence of string tension σ on the scale fixing point M.

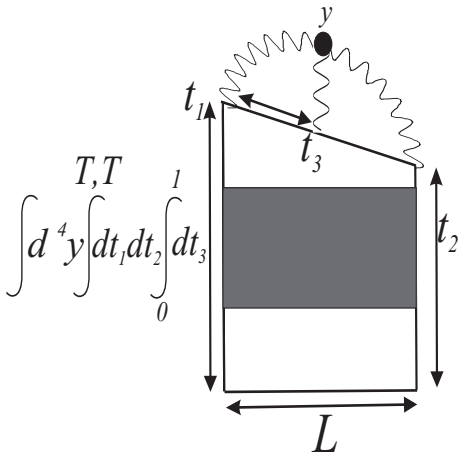

Figure 5.7: The terms in the ESSZ equations generating a two-loop correction to the auxiliary potential $U^{(2)}(x)$.

as before. The loop in the NLO must keep its form for consistency with the LO.

A numerical evaluation of this integral shows that within the whole range of values of t_1, t_2 with which we work, $U^{(2)}(t_1, t_2) = U^{(2)}(t_1 - t_2) \equiv U^{(2)}(x)$. This makes a separation of variables still possible and provides an extra test for the validity of our model. Numerical values of $U^{(2)}(x)$ are such that $U^{(2)}(x)/U^{(1)}(x) \lessapprox 10^{-3}$, which makes its contribution to an auxiliary potential ground state negligible. This allows us to justify the use of the ESSZ equation in the non-SUSY case: a vertex correction is present but numerically suppressed.

5.5 Summary

The ESSZ approach to SUSY-Wilson-loops has worked very well in [3, 264]. The reason for that is the absence of NLO corrections in the maximally supersymmetric theory. At

a small coupling their result has restored the perturbatively known IR singularity structure. Moreover, the calculation originally performed in the small coupling limit, could be continued into the large coupling limit. At large coupling the solution to the ESSZ equation reproduces almost exactly the gravity dual result [296, 297, 298] (up to an overall numerical factor very close to unity). Actually this result, though obtained in a different theory, has been guiding our $SU(N)$ Yang–Mills treatment: as we are dealing with the IR strongly coupled theory, we are certainly out of order of applicability of any perturbative treatment, and even summation of diagrams would be suspicious.

The reason why the ESSZ equation has never been applied to non-SUSY contents is obvious. It is clear from [3, 264] that when a perturbative propagator input is being used, only a non-confining Wilson loop, with a Coulomb-type potential may be obtained. This follows from the fact that dependence on the Wilson loop spatial size L may be scaled out of the ESSZ equation, so that any potentials one gets from it are Coulombic, varying from each other by coupling rather than by a distance dependence. Thus such a result would have been *a priori* useless in understanding anything about the strong coupling IR regime of gauge theory, where confinement governs the dynamics. This maybe the reason why summation à la ESSZ has not before been employed in the pure Yang–Mills theory.

A description of a single Wilson loop, from which one can obtain the $SU(N)$ potential and provide a criterion of confinement, has not been done so far in terms of the two-point sector of DSE hierarchy. Thus this Chapter closes an essential gap in the literature. The main reason for this gap was the theorem by West [299], stating that confinement is provided by a very IR-singular propagator $D(q^2) \sim 1/q^4$. We know however that the gluon propagator is regular in the IR in the DSE approach.

My work is based on a combined analysis of Green functions and Wilson loops, allowing thus a study of the spatial Yang–Mills potential. This distinguishes our approach from several earlier papers, where gluon non-propagation was considered instead of confinement and related to the analytic properties of Green functions, in particular, to the IR scaling κ, Eq. (5.24). These other works use the word "confinement" as in the original paper [262] when they mean to say of "non-propagation". Known is the so-called Kugo–Ojima criterion for colour non-propagation $\kappa > 0$ [300], the Zwanziger criterion of ghost non-propagation $\kappa > 0$ and gluon non-propagation $\kappa > 1/2$ [301]. A claim has been made [302] for $\kappa > 1/4$ to be a quark confinement criterion by an analysis of the Polyakov loop and the effective QCD action in an external field. All these results are about gluon non-propagation rather than the properties of a colour charge confining interaction.

Returning to the discussion of my results, I note that the reliability thereof may be questioned in what concerns the DSE input. The first issue is the truncation of the DSE

system we solve to the level of two-point functions. This truncation is justified, since the ghost-gluon vertex does not acquire one-loop corrections in Landau gauge. It has been proven that the three-point gluon and quark-gluon functions do not change the ghost dominance property [273], even though they are important for bound states [303]. In this sense, vertex functions are unimportant for our particular context.

Another question is whether the Green functions obtained from DSE are physically relevant within the Wilson loop context we are discussing. We note that it is mostly the medium-energy range that provides the important contribution into the auxiliary potential $U(x;L)$, rather than the perhaps more model dependent IR piece. The Wilson loop thus depends on medium energy range values of the propagators, where the DSE behaviour is the same as on the lattice. There are unresolved questions regarding a comparison of IR scaling [304] within lattice and DSE. These issues have yet to be understood and resolved, although they do not affect our results materially.

The observables σ, α we compute are in principle gauge invariant, when taken to all loop orders. Our results are obtained in Landau gauge, which, as noted, is a convenient choice. The ESSZ summation, as any ladder diagram summation, relies on a selective diagram sum, so it may not necessarily be order-by-order gauge-invariant. It should be possible to check gauge-invariance explicitly at the one loop level, we however do not do that here, since this transcends the scope of the present Chapter. We think that the possibility for the observable we consider to be gauge invariant at one-loop level comes from the fact that several gauge-dependent objects are combined.

I speculate here *à propos* that a nonperturbative summation *a la* ESSZ could improve significantly the properties of a correlator of gluon strengths with Wilson lines

$$\mathcal{F}(x) = \langle \mathrm{tr}\, F_{\mu\nu}(x) U(C) F^{\mu\nu}(0) U^{+}(C) \rangle \tag{5.34}$$

$U(C)$ being a phase factor

$$U(C) = \mathrm{Pexp}\left\{ ig \int\limits_{C} A_\mu dx^\mu \right\}, \tag{5.35}$$

which differs from the Wilson loop since the path is connecting the arguments in (5.34) i.e. points x and 0. (5.34) had recently been of great interest [305], as it represents an important vacuum property. As far as we know, a Bethe–Salpeter equation for this kind of correlator has not been developed yet. We attempted to evaluate it perturbatively [306]. The present effort arose from this earlier one but should have actually anteceded it, since then the required framework for the ESSZ summation may have been at hand.

A hypothesis should be considered that using a relevant component of the non-perturbative input from Dyson–Schwinger equations, one may be able to obtain a self-consistent

picture of the Yang–Mills vacuum with all the higher correlation functions, colour confinement and condensates, which is supported at the simplest LO level by the presented calculation.

To conclude, combining a Dyson–Schwinger summation for gluon and ghost propagators with the Ericson–Semenoff–Szabo–Zarembo summation (truncation) for the Wilson loop, I have obtained the string tension and have further demonstrated that its value is nearly not dependent on the selection of the DSE scale fixing point, thus establishing the internal consistency of this novel description of confinement. The string tension determined by our method for the pure SU(3) gauge theory is $\sigma = 1.07 \pm 0.1$ GeV/fm. The UV Coulomb behavior is governed by $\alpha_0 \approx 0.24$.

One can actually be quite amazed that our method has worked so well in the $SU(3)$ Yang–Mills approach, without supersymmetry, thus with vertices non-compensated. One can speculate that the two truncated summations are complementary, ESSZ taking care of the ladders and the DSE taking care of rainbows in the vertices. Among interesting further steps in the development of this framework we recognize the formulation and evaluation of a similar ESSZ equation for the correlator of two gluons, having in mind its application to the non-local gluon condensate (5.34). Another, perhaps more challenging further development could be to solve the ESSZ and the DSE jointly, without the separation into partial systems.

Chapter 6

Dyson–Schwinger Equations, Non-Local Condensates and Effective Actions

I obtain in this Chapter the QCD quark condensate from a consideration of unquenched quark dynamics in the Dyson–Schwinger gluon vacuum. I consider the non-local extension of the condensate and determine the quark virtuality. I also obtain the condensate-driven contribution of the non-perturbative QCD to the Euler–Heisenberg Lagrangian of QED in external electromagnetic fields.

6.1 Overview

A method relying on the Dyson–Schwinger equations (DSE) for obtaining the (non-local) quark condensate and Euler-Heisenberg type effective action with quarks in loops is described here. A self-consistent scheme for that is developed, based on a full set of DSE with dynamical quarks, ghosts and gluons. This approach is built on methods and prescriptions we adapt from Fischer [307], and already partially explained in Chapter 5.

The non-local quark condensate was considered by Shuryak in [5], and further developments followed soon after [308, 251, 309]. The gauge invariant NLC is defined by

$$C(x^2) \equiv \langle \bar{q}(x) E(x;0) q(0) \rangle, \tag{6.1}$$

where the Wilson phase factor is defined as

$$E(x;0) = \mathrm{Pexp}\left(ie \int\limits_{\mathcal{C}} A_\mu(x) dx^\mu \right), \tag{6.2}$$

and the contour $\mathcal{C}$ connects points x and 0. In this Chapter we focus our attention on the first terms in powers of x which are independent of the Wilson line contributions. Wilson line terms are in general very important, and such contributions should be evaluated self-consistently [310, 311], which may be done by the Ericson – Semenoff – Szabo – Zarembo (ESSZ) technique used by me in the previous Chapter 5. It has been shown within the instanton vacuum model [312] that the form of the NLC is nearly independent on possible irregularities of the path, such as a cusp and thus in general the path can be represented by a straight line.

The initial motivation for introducing a NLC came from its influence on the hadron phenomenology. For this reason NLC has been decomposed into the local condensates (LC) and the measure of the quark fluctuations in vacuum, known as the quark virtuality (QV). This quantity related to NLC, is defined as

$$\lambda_q^2 = \frac{\langle \bar{q} D_\mu^2 q \rangle}{\langle \bar{q} q \rangle}, \tag{6.3}$$

(here D_μ is the covariant derivative), arising in the standard operator product expansion (OPE) of the NLC as the coefficient in front of the quadratic term:

$$C(x^2) = \langle \bar{q}(0) q(0) \rangle \left[1 + \frac{x^2}{4} \frac{\langle \bar{q} D^2 q \rangle}{\langle \bar{q} q \rangle} \right]. \tag{6.4}$$

Quark virtuality is related to the gluon-quark trilinear (local) condensate

$$\frac{\langle \bar{q} D^2 q \rangle}{\langle \bar{q} q \rangle} \sim \langle \bar{q} g \sigma_{\mu\nu} G^{\mu\nu} q \rangle. \tag{6.5}$$

and thus can be counted as an independent vacuum structure parameter, characterizing the non-perturbative QCD vacuum. The standard estimate for λ_q^2 by Chernyak and Zhitnitsky [313] is $\lambda_q^2 \approx 0.4 \pm 0.1 \mathrm{GeV}^2$. There are other estimates, however, e.g. within an instanton liquid model [314], the corrected value of which is given in [310, 315] as $\lambda_q^2 \sim 0.7 \mathrm{GeV}^2$. We note that these numerical values for the correlation length are comparable with the typical hadronic scale.

Our effort to relate DSE and NLC is not the first. An attempt to derive self-consistent equations upon condensates was made by Pauchy Hwang [316] in the large-$1/N_c$ limit. A non-local quark condensate has been obtained within the flat-bottom potential approach to the Dyson–Schwinger equations, where a typical correlation length of $3 \mathrm{GeV}^{-1}$ has been obtained [317]. The Dyson–Schwinger equations are solved in [318] for the quark dynamical mass and wave-function (no gluons or ghosts solved dynamically; gluon propagator mimicked by an Ansatz, rainbow approximation applied to quark equations); using

propagators, the quark-quark non-local condensate and the quark-quark-gluon local condensates are calculated, the typical correlation length obtained is 0.5 GeV^{-1}. The same methods were used in [319], where virtualities $\lambda^2_{u,d} = 0.7\mathrm{GeV}^2, \lambda^2_s = 1.6\ \mathrm{GeV}^2$ are reported. These results are confirmed in [320] and completed with the gluon virtuality as well $\lambda^2_g = 0.2\alpha_s^{-\frac{1}{2}} - 1.0\alpha_s^3\ \mathrm{GeV}^2$, the latter exhibiting a strong scale dependence via the coupling constant. The Dyson–Schwinger equations were solved in a similar approximation (no dynamical gluons and ghosts) in [321]; however, surprisingly large values of virtualities have been reported: $\lambda^2_{u,d} = 12 \ldots 16\ \mathrm{GeV}^2, \lambda^2_s = 14 \ldots 18\ \mathrm{GeV}^2$. Till now, there has been no self-consistent treatment of the non-local condensates based on DSE with gluons. We consider this to be a disadvantage of the scheme, since quark fluctuations in vacuum are driven by gluons. We will present our result for QV as function of quark mass.

I describe the DSE methodology and calculate the propagators in the next section (6.2), the non-local condensate (NLC) and its response to an external field is studied in section (6.3). In section (6.4) I do the Euler-Heisenberg type effective action for quarks with non-perturbative DSE propagators in external fields and compare our results to the meson based evaluation. I conclude the Chapter in section (6.5).

6.2 Dyson–Schwinger Equations

6.2.1 Formulation of DSE with Quarks

In this section the technique of obtaining quark and gluon propagators in a self-consistent way is reviewed. As in the previous Chpater, Fisher's DSE technique is used, which was described in [307], and it is shown that the propagators are reproduced by us in the case with quarks as well – they have already been reproduced the gluodynamics sector above. The Newton optimization method is applied here, based on the numerical procedure described in the previous Chapter. The system for ghost, gluon and quark propagators is solved, as shown in Fig. (5.2). Propagator dressing is shown by bulbs, and that of vertices – by transparent bulbs. The gluon propagator is parameterized in Landau gauge by the form-factor F, defined via the relation (5.16), and the ghost by formfactor defined by (5.17). The quark propagator is defined as

$$S(p) = \frac{1}{A(p)} \frac{1}{\not{p} + M(p)}. \tag{6.6}$$

Finding the scalar form-factors F, G, A, M will yield non-perturbative information on the physical quarks and gluons.

DSE for this system can be written in the form:

$$\begin{cases} \dfrac{1}{G(p^2)} - \dfrac{1}{G(\bar{\mu}_c^2)} = -\left(\Sigma(p^2) - \Sigma(\bar{\mu}_c^2)\right), \\ \dfrac{1}{F(p^2)} - \dfrac{1}{F(\bar{\mu}_g^2)} = -\left(\Pi(p^2) - \Pi(\bar{\mu}_g^2)\right), \\ \dfrac{1}{A(x)} = 1 - \dfrac{\Pi_A(x)}{A(x)} + \Pi_A(\bar{\mu}_g^2) \\ M(x)A(x) = M(\bar{\mu}_g^2) + \Pi_M(x) - \Pi_M(\bar{\mu}_g^2) \end{cases} \tag{6.7}$$

Here $\bar{\mu}_{g,c}$ are the points of subtraction, $\bar{\mu}_c = 0$, $\bar{\mu}_g = \bar{\mu}$, $\bar{\mu}$ is the limit of the interval $p^2 \in (0, \bar{\mu}^2)$ in the momentum space where we solve the DSE, the coupling g^2 is meant to be taken at point μ: $g^2(\bar{\mu}^2)$. The gluon vacuum polarization is given in (5.13), the ghost self-energy is (5.15). The quark self-energy is conveniently split into functions Π_A and Π_M, given below:

$$\begin{aligned} \Pi_M = \frac{1}{3\pi^3}\int d^4y \Bigg\{ & \frac{\alpha(z)}{z(y+M^2(y))}\frac{G(z)^{-2d-d/\delta}}{F(z)^d}\frac{1}{A(y)} \\ & \Bigg[\frac{3}{2}\left(A(x)+A(y)\right)M(y) + \frac{1}{2}\left(\Delta A(x,y)M(y) - \right. \\ & \left. -\Delta B(x,y)\right)\left(-z+2(x+y)-(x-y)^2/z\right) + \\ & + \frac{3}{2}(A(x)-A(y))M(y)\Omega(x,y)(x-y)\Bigg]\Bigg\} \end{aligned} \tag{6.8}$$

and

$$\begin{aligned} \Pi_A = \frac{1}{3\pi^3}\int d^4y \Bigg\{ & \frac{\alpha(z)}{xz(y+M^2(y))}\frac{G(z)^{-2d-d/\delta}}{F(z)^d}\frac{1}{A(y)} \\ & \Bigg[\left(-z+\frac{x+y}{2}+\frac{(x-y)^2}{2z}\right)\frac{A(x)+A(y)}{2} - \\ & - \left(\frac{\Delta A(x,y)}{2}(x+y) + \Delta B(x,y)M(y)\right)\times \\ & \times\left(-\tfrac{z}{2} + (x+y) - \tfrac{(x-y)^2}{2z}\right) + \\ & + \frac{3}{2}\left(A(x)-A(y)\right)\Omega(x,y)\left(\frac{x^2-y^2}{2} - z\frac{x-y}{2}\right)\Bigg]\Bigg\}, \end{aligned} \tag{6.9}$$

yielding the last two equations of (6.7). Here auxiliary functions $\Delta A, \Delta B, \Omega, \Delta\Omega$ have been introduced:

$$\begin{aligned} \Delta A(x,y) &= \frac{A(x)-A(y)}{x-y}, \\ B(x) &= M(x)A(x), \\ \Delta B(x,y) &= \frac{B(x)-B(y)}{x-y}, \\ \Omega(x,y) &= \frac{x+y}{(x-y)^2+(M^2(x)+M^2(y))^2}. \end{aligned} \tag{6.10}$$

The constructions (6.8), (6.9), are taken from [307], we have fixed here a typo originally present in Eq. (6.8). The parameter d is related to the Ansatz for the quark-gluon vertex that is used. There is no unambiguous way of choosing this parameter, since there is no fully consistent way of truncating DSE without violating some of the worthy properties of the original full tower of equations, and we refer the reader to [307] for a comprehensive discussion on that point. The variable z is a logarithmic variable

$$z = \ln \frac{p^2}{\mu^2}, \tag{6.11}$$

and the scale μ is yet to be defined as in (5.19); in everything what concerns the scale and coupling constant definition we follow Chapter 5.

The kernels M_0, K_0, Q_0 are given in (5.21)-(5.22). Scalar variables $x = p^2$, $y = q^2$ are introduced as in Chapter 5.

To solve DSE we use Ansätze similar to (5.23) for $M(p), A(p)$, the rest of the procedure remains exactly as it was. The coupling and gluon propagators are little modified compared to the previous chapter, so we do not show the figures for them here again.

Quark wave-functions were obtained for one quark at a time solving in a self-consistent way the DSE, i.e. these are unquenched quarks. They are quite similar to the quenched approximation where quark DSE is solved for a given glue DSE solution. The wave function form factors are shown in Fig. (6.1). Wave-function form factors become perturbatively unity; within an error margin they are no more distinguishable in the UV, although they exhibit a different and non-trivial behavior in the IR.

The quark masses are shown in Fig. (6.2). Physically it is important that UV anomalous dimensions of all the quarks are rendered the same in Fig. (6.2) , which confirms the validity of the procedure. This can be seen from the dashed parallel lines in Fig. (6.2). In general, in this Section, we confirm all the current knowledge on the DSE with quarks. We improve the numerical convergence by smoothing the numerical cut-off on integrals

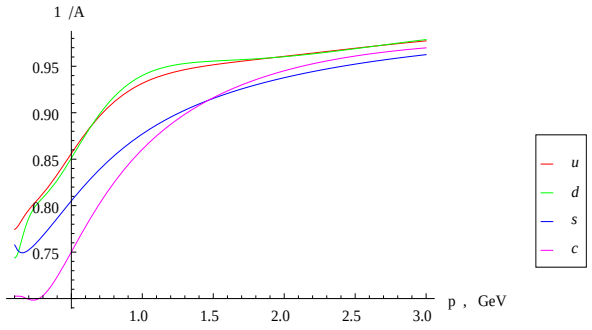

Figure 6.1: Wave-function (propagator) form factors $A(p)$ for flavors u(red), d(green), s(blue), c(magenta) (lines from top to bottom at $p = 0.5$ GeV.

by superimposing varying limits, which procedure removes Fourier transform 'echos' from the results.

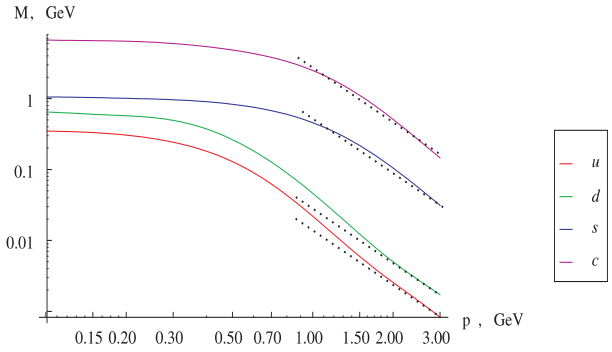

Figure 6.2: Quark mass $M(p)$ for flavors u, d, s, c. Punctured parallel tangent lines demonstrate that anomalous dimension is mass-independent.

6.3 Non-local Condensate

6.3.1 Dependence on Mass of the Condensate Shape

In this Section we calculate the non-local condensate omitting the Wilson line, study its behavior under external fields and compute the vacuum response due to the presence of non-local condensates to external fields.

The nonlocal condensate-related vacuum expectation value (C-VEV)

$$C_0(x) = \langle \bar{\psi}(x)\psi(0)\rangle, \tag{6.12}$$

where the local condensate $C(0)$ satisfies $C(0) = C_0(0)$, can be related to the propagator as

$$C_0(x) = \frac{1}{(2\pi)^4} N_c \sum_i^{N_f} \int d^4p \frac{e^{ipx}}{A_i(p)} \frac{4M_i(p)}{p^2 + M_i^2} - (\text{PT}). \tag{6.13}$$

However, the separation the perturbative (PT) part from the non-perturbative propagator is not well-defined. Moreover, some argue that the non-perturbative procedure is producing only the non-perturbative quark propagator and that there is no PT subtraction needed. We do not have a good argument to support this reasoning, or, alternatively, a PT part subtraction, thus we follow the former approach. This also does not introduce additional procedure ambiguity. Accordingly, it should be remembered when evaluating our results that the full non-perturbative understanding of the QCD vacuum cannot be reached on grounds of Dyson-Schwinger equations alone, without applying additional resummation procedures, e.g. the ESSZ-resummation [322]. For this reason our results should be treated as a first qualitative estimate, and not yet as exact predictions.

Despite any of the above shortcomings, the results obtained are surprizing. The C-VEV is shown in Fig. (6.3), where it can be seen from top to bottom (at $x \to 0$) beginning with the heavy quark $\langle \bar{c}(x)c(0)\rangle$, $\langle \bar{s}(x)s(0)\rangle$ $\langle \bar{d}(x)d(0)\rangle$, $\langle \bar{u}(x)u(0)\rangle$. Numerical difficulties prevent one from reaching a higher mass than 500 MeV for charm (at scale of 2 GeV). The non-local condensate exhibits some oscillatory behaviour within $2 < x < 10$ GeV^{-1}. It can be believed that these C-VEV oscillations are due to the numeric uncertainty. At this large distance the sequence of the C-VEV has reversed with smallest quark mass leading to largest values of C-VEV.

6.3.2 Local Quark Condensate and Quark Virtuality Dependence on Mass

The standard wisdom [16] about condensate dependence on mass for heavy quarks is

$$\langle \bar{q}q\rangle = -\frac{1}{12m_q}\langle \alpha G^2\rangle, \tag{6.14}$$

which I checked holographically in Section (2.3.2). This relation is usually derived from requiring continuity between heavy and light quarks' properties, imposed at the scale of about 0.2 GeV. The behavior of our propagators and wave functions is continuous, yet the

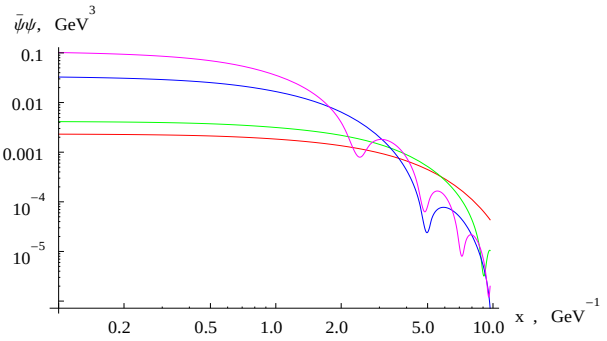

Figure 6.3: Non-local condensate for u, d, c, s quarks (red, green, blue and magenta curves correspondingly).

dependence on mass we observe is completely different. Another well regarded relation is [226]

$$\langle \bar{s}s \rangle \sim 0.8 \langle \bar{u}u \rangle. \tag{6.15}$$

Note that in my evaluation the local condensate is independent of the Wilson line integral and thus our results for $x \to 0$ while still the PT subtraction dependent are more secure. For c and s quarks the values one sees in Fig. (6.3) are considerably larger than expected. Moreover, it is found that our condensates increase with mass and do not decrease, as was expected based on the above low-energy theorem. The condensate dependence on mass was studied by means of a DSE analysis also in [323, 324].

The values of the condensate is fitted surprisingly well by a simple power law

$$\overline{q}q(m) = 0.2 \text{ GeV}^3 \left(\frac{m}{1\text{GeV}} \right)^{0.73}, \tag{6.16}$$

not at all expected from any qualitative QCD model we know. The mass dependence of condensate is illustrated in Fig. (6.4). The dashed line is the expected light quark value, the thick line the c, s expectations of Eq.(6.14). Note that these results are obtained by considering one quark at a time and solving self-consistently DSE (unquenched single quarks).

It seems that with increasing mass quarks can probe better the non-local glue vacuum fluctuations and thus their response strength increases. The non-locality of the glue vacuum structure is usually not considered in the qualitative condensate models. However, there is no argument to align the light quark local condensate as a function of m with the heavy quark condensate. It can be also noted that when dealing with realistic quarks, their physical magnetic moments must be taken into account. However, this effect diminishes with quark mass and cannot explain the heavy quark condensate behavior.

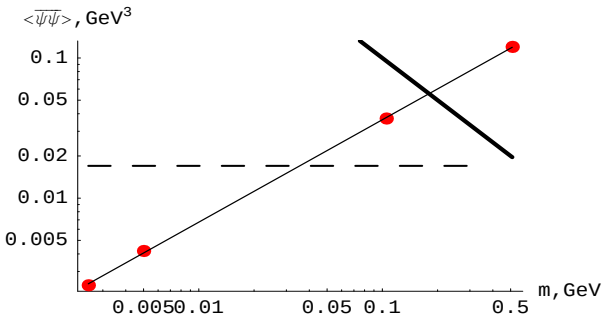

Figure 6.4: Local condensate mass dependence. Red dots are DSE results, the thick line represents the estimate (6.14) for heavy quarks, while the dashed line stands for the standard $\langle \bar{u}u \rangle$ value, the thin line indicates the power-law approximation (6.16).

In another attempt to understand this strange behavior, one could suggest that heavy quarks are worse represented by Dyson–Schwinger equations, since they tend to decouple and thus a one-loop approximation becomes almost free, but at higher loops they might become again important, thus yielding the DSE approach invalid. However, this explanation is not valid, since a comparison of quenched approximation to the unquenched shows very little difference between the two. Thus the issue of condensate dependence on mass in the DSE scheme presented here remains an open question.

Should this behavior be true, this strong dependence on mass of the light quark condensate would deeply impact the chiral model analysis of quark masses, where a cornerstone assumption is that light quark condensates have equal values.

The quark virtuality dependence on mass is given in the table 6.1 below and is shown in Fig. (6.5). We note the highly regular behavior, following the fit

$$\lambda_q^2 = 0.39\,\mathrm{GeV}^2 \left(\frac{m_q}{1\mathrm{GeV}}\right)^{1.07} \tag{6.17}$$

shown in Fig. (6.5) For comparison recall that virtualities $\lambda_{u,d}^2 = 0.7\,\mathrm{GeV}^2, \lambda_s^2 = 1.6\,\mathrm{GeV}^2$ were reported [320], as discussed in Section 1. Recall also $\lambda_q^2 \approx 0.4 \pm 0.1\mathrm{GeV}^2$ [313] and $\lambda_q^2 \sim 1.2\,\mathrm{GeV}^2$ [325].

6.3.3 Condensate Response to an External Field

The character of the condensate dependence on the external field can also be established. Considering the diagram shown in Fig. (6.6), F^2-order term in the non-local condensate can be derived

$$\langle \bar{\psi}\psi \rangle_F = \langle \bar{\psi}\psi \rangle_0 + F^2 f_1(x) - F_{\nu\alpha}F_\mu^\alpha \frac{\partial^2}{\partial_\nu \partial_\mu} f_2(x), \tag{6.18}$$

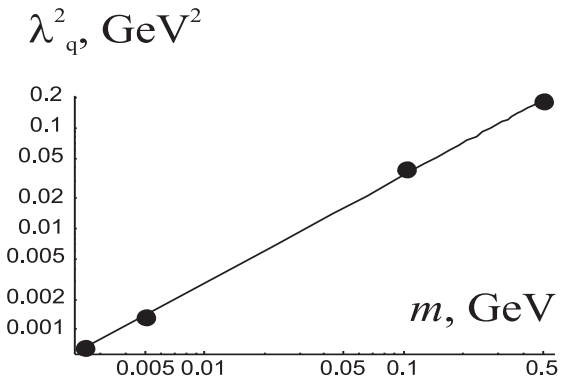

Figure 6.5: Quark virtuality dependence on the quark mass.

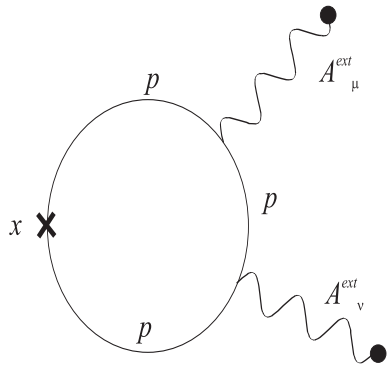

Figure 6.6: Diagram describing the condensate sensitivity to the field.

where moments f_1, f_2 are

$$f_1(x) = \frac{1}{(2\pi)^4}\int \frac{e^{ipx}d^4p}{A^3(p)}\frac{(-8)m(p)}{(p^2+m^2(p))^3},$$
$$f_2(x) = \frac{1}{(2\pi)^4}\int \frac{e^{ipx}d^4p}{A^3(p)}\frac{(-16)m(p)}{(p^2+m^2(p))^4}. \tag{6.19}$$

Notice here that not only the character of the condensate dependence on x changes due to the field being switched on, but it acquires anisotropy. The function f_1 is shown in Fig. (6.7). It deserves attention that smallest quark masses bring largest response to the field, which is quite reasonable. The resulting parameters are shown in the table (6.1). It can be seen from analysis of f_1 that already fields of order of magnitude of 10^{-1} GeV^2 may put the local condensate to zero. This is comparable to the prediction of critical fields

Table 6.1: Main characteristics of the condensate: the local amplitude $C(0)$, the virtuality λ^2, condensate amplitude variation $\frac{\delta C(0)}{\delta F^2}$, the virtuality variation $\frac{\delta\lambda_q^2}{\delta F^2}$, the infrared exponent a ($\langle\bar\psi(x)\psi(0)\rangle \sim e^{-ax}$), the variation of the infrared exponent $\frac{\delta a}{\delta F^2}$. Mass value $m = 0.51$ in the fourth line is not a misprint against the expected $m = 1.27$ GeV, but was the largest mass at the 2 GeV scale available to us.

m_q, GeV	q	$C(0)$, GeV	λ_q^2, GeV^2	$\frac{\delta C(0)}{\delta F^2}$, GeV^{-1}	$\frac{\delta\lambda_q^2}{\delta F^2}$, GeV^{-2}	a, GeV	$\frac{\delta a}{\delta F^2}$, GeV^{-3}
0.0025	2/3	0.00239	0.00066	0.037	0.00082	0.40	0.20
0.005	1/3	0.0042	0.0013	0.023	0.00094	0.65	0.20
0.105	1/3	0.037	0.039	0.015	0.0017	1.04	0.22
0.51	2/3	0.12	0.18	0.0064	0.0015	1.04	0.37

for condensate

$$F_{\rm cr} = \frac{m_\pi^2}{\log 2} \tag{6.20}$$

by Smilga and Shushpanov [24].

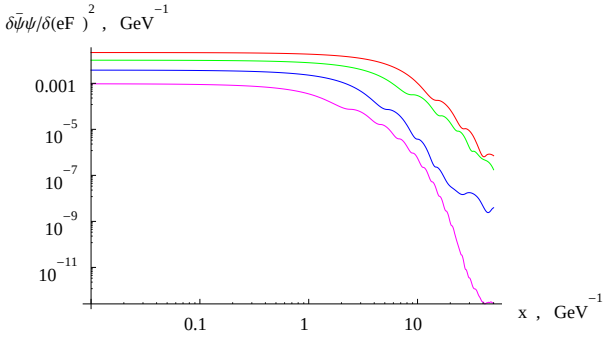

Figure 6.7: Factor $f_1(x)$ as a function of the distance, describing the nonlocality of the condensate sensitivity to an external field.

Long-distance correlations will be even more sensitive to fields, since f_1 decreases slower than the condensate itself, thus making the pion wave-function a nice candidate for an analysis in an external field.

6.4 Effective Action due to Condensates

One of the simplest nonlinear processes of QED is photon-photon scattering, shown in Fig. (6.8). In the language of the Euler–Heisenberg effective action, the following term is responsible for this kind of processes

$$\begin{aligned}\mathcal{L} &= a(F_{\mu\nu}F^{\mu\nu})^2 + F^{\nu}_{\mu}F^{\lambda}_{\nu}F^{\rho}_{\lambda}F^{\mu}_{\rho} = \\ &= A(F_{\mu\nu}F^{\mu\nu})^2 + B(F_{\mu\nu}\tilde{F}^{\mu\nu})^2.\end{aligned} \tag{6.21}$$

Coefficients a, b are in case of QED

$$\begin{aligned}a &= -\frac{\alpha^2}{36m^4}, \\ b &= \frac{7\alpha^2}{90m^4},\end{aligned} \tag{6.22}$$

and A, B are linearly related to them: $A = a + b/2, B = b$. These coefficients are calculate din this section for the condensate contribution of the QCD vacuum into QCD-related photon-photon scattering. It will be clear at the end that the contribution is larger than expected, compared to standard (perturbative) contribution due to hadrons. However, the magnitude of the effects is very small compared to what is experimentally accessible today, and in the foreseeable future in the domain of intense laser physics.

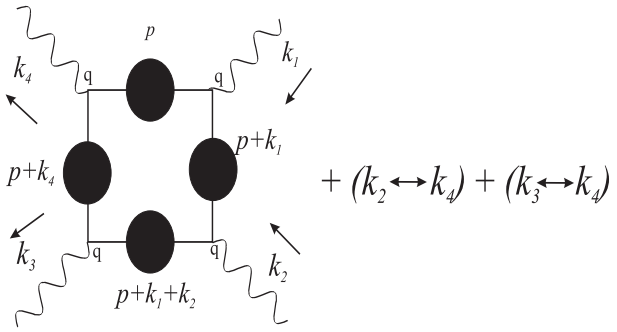

Figure 6.8: Leading nonlinear term in the Euler–Heisenberg effective action, k_i are incoming momenta, q quark charges.

Strictly speaking, when dealing with realistic quarks, their physical magnetic moments must be taken into account. In the effective action quark magnetic moments would invoke a contribution of the type $\mu_q^4 F^{\mu_1\nu_1}F^{\mu_2\nu_2}F^{\mu_3\nu_3}F^{\mu_4\nu_4}\,\mathrm{tr}[\sigma^{\mu_1\nu_1}\sigma^{\mu_2\nu_2}\sigma^{\mu_3\nu_3}\sigma^{\mu_4\nu_4}]$. Noting that the

outcome might be non-negligible, this contribution is left aside, since it requires a serious modification of the DSE solution scheme and complicated issues of truncation validity.

To achieve the result the diagram Fig. (6.8) is calculated with propagators obtained in the previous section, which are responsible for condensates. The condensate and the free terms are not separated at the level of each propagator, but rather the full diagram is done with the full propagators, and then compared to the perturbative terms (a, b already given above, multiplied by respective quark charges). As the momentum dependence of the full diagram on the s, t, u invariants would be known only numerically as a result of a calculation, containing numerical data for propagators, we use the following trick. The scattering amplitudes $M(e_1, e_2, e_3, e_4)$ are worked out, given as

$$\begin{aligned}\tilde{M}_{\mu\nu\lambda\rho}(k_1,k_2,k_3,k_4) = e^4 \int \frac{d^4p}{(2\pi)^4} \,\mathrm{tr}\,[S(p)\gamma^\mu S(p+k_1)\gamma^\nu \times \\ \times \quad S(p+k_1+k_2)\gamma^\lambda S(p+k_4)\gamma^\rho]\,.\end{aligned} \tag{6.23}$$

For the scattering amplitudes at small values of the photon frequencies ω we extract the coefficient at the ω^4 term:

$$\tilde{M}_{\mu\nu\lambda\rho}(k_1,k_2,k_3,k_4)e_1^\mu e_2^\nu e_3^\lambda e_4^\rho = M_0 + \omega^4\alpha^2 M(e_1,e_2,e_3,e_4), \tag{6.24}$$

for two specific sets of polarization vectors, namely, $(e_{1\perp}, e_{2\perp}, e_{3\perp}, e_{4\perp})$ and $(e_{1\parallel}, e_{2\parallel}, e_{3\perp}, e_{4\perp})$, ($e_{i\perp}$ denotes the polarization orthogonal to the reaction plane, and $e_{1\parallel}$ the polarization in the reaction plane), at specific values for θ (namely, forward scattering $\theta = \pi$). These can be expressed as the following scalar integrals

$$\begin{aligned}&M(e_{1\perp}, e_{2\perp}, e_{3\perp}, e_{4\perp}) = \\ &= \int_0^\infty \frac{32p^3dp}{15\left[p^2+M(p)^2\right]^8 A(p)^3}\left[19p^8 + 75M(p)^2p^6 - \right. \\ &\left. -10M(p)^4p^4 - 330M(p)^6p^2 + 30M(p)^8\right],\end{aligned} \tag{6.25}$$

$$\begin{aligned}&M(e_{1\parallel}, e_{2\parallel}, e_{3\perp}, e_{4\perp}) = \\ &= -\int_0^\infty \frac{32p^3dp}{15\left[p^2+M(p)^2\right]^8 A(p)^3}\left[7p^8 - 25M(p)^2p^6 - \right. \\ &\left. -40M(p)^4p^4 + 60M(p)^6p^2 - 30M(p)^8\right].\end{aligned} \tag{6.26}$$

Table 6.2: Coefficients a, b, A, B of non-linear terms in the effective action. The "perturbative" (PT) line shows for comparison the coefficients a_0, b_0, A_0, B_0 for mass m in the loops which can be thought of approximately as $\Lambda \sim 300$ GeV; our results are shown as dimensionless ratios against a_0, b_0, A_0, B_0. Quarks charges $q_i = 2/3, 1/3$ are included into the coefficients.

	a_0	b_0	A_0	B_0
PT	$-\frac{1}{36m^4}$	$\frac{7}{90m^4}$	$\frac{1}{90m^4}$	$\frac{7}{90m^4}$
flavor	a/a_0	b/b_0	A/A_0	B/B_0
u	0.07732	0.09317	0.1328	0.09317
d	0.00302	0.00337	0.00425	0.00337
s	0.00019	0.00022	0.0003	0.00022
c	0.00064	0.0007	0.00085	0.0007

Polarization vectors have been

$$\begin{aligned} e_\parallel &= \{0,0,1,0\}, \\ e_\perp &= \{0,0,0,1\}, \end{aligned} \tag{6.27}$$

with center-of-mass kinematics

$$\begin{aligned} k_1 &= \omega\{1,1,0,0\}, \\ k_2 &= \omega\{1,-1,0,0\}, \\ k_3 &= \omega\{1,\cos\theta,\sin\theta,0\}, \\ k_4 &= \omega\{1,-\cos\theta,-\sin\theta,0\}. \end{aligned} \tag{6.28}$$

In the expansion we used the fact that ω is believed to be small, therefore, all non-perturbative momentum-dependent factors $(M(p), A(p))$ are taken at the point p.

On the other hand, the coefficients $M(\dots)$ are known from (6.21) by direct analysis

$$\begin{aligned} M(e_{1\perp}, e_{2\perp}, e_{3\perp}, e_{4\perp}) &= 64(2a+b), \\ M(e_{1\parallel}, e_{2\parallel}, e_{3\perp}, e_{4\perp}) &= 16(4a+b). \end{aligned} \tag{6.29}$$

Thus a simple comparison of (6.25) and (6.29) yields values for a, b and A, B. They are shown in Table (6.2). This Table is quite instructive. First of all, the contributions are comparable with the expected hadronic ones. The range of the latter can be estimated roughly within $1/90m_\pi^4 \dots 1/90m_\rho^4 \sim 40 \dots 0.05$ GeV^{-4}. Quarks with large bare masses yield less, as expected on general grounds.

6.5 Discussion

Solving the one quark-gluon-ghost Dyson-Schwinger equations, the quark non-local condensate and quark virtuality have been obtained as functions of the quark mass. The mass dependence of the condensate disagrees with current qualitative wisdom, and with our holographic proof of decoupling, given in Section (2.3.2). An explanation for why this is the case has not been found. The growth of the quark condensate with $m^{0.73}, m < 500\,\mathrm{MeV}$ implies a significant difference between all mass condensates above and beyond any expectations.

Regarding the influence of an external field on the condensate I predict that fields of order of magnitude of 10^{-1} GeV^2 can actually destroy the local condensate, and even smaller fields can destroy the non-local x-dependent condensate at $x \neq 0$. This result may have direct impact on the pion wave function in external fields. Pimikov, Bakulev and Stefanis [326] show that the non-locality of the condensates is needed in a study of the non-perturbative contributions to the pion form factor. This shows how our results influence the study of dynamics of the pion wave function in external fields.

In addition I predict that light quarks make important non-perturbative contributions to the photon-photon scattering amplitude, comparable with the corresponding perturbative contributions based on loops with light mesons. This effect is driven by the condensate non-locality. The present non-perturbative evaluation suggests that the critical field, above which the non-linear QCD-QED effects can be seen, is several times lower than the typical hadronic scale. Even so, experiments to probe the QCD vacuum with intense laser fields are far beyond the foreseeable future.

I have outlined in the text an opportunity for further theoretical advance, which must first focus on the resolution of the mass dependence of quark condensate and better understanding of the related quark virtuality. The relatively large effects which external fields can impart on the QCD vacuum must be confirmed in the context of such an improved theoretical framework.

6.6 A Recently Proposed Experiment

In the paper [2] is has been suggested that a very precise measurement of the real part of the vacuum polarization can be reached in the following experiment. Consider a laser creating a very narrow bunch of high intensity, which we shall call target, and another one, creating a wider bunch of low intensity, which we shall call probe. The setup is shown symbolically in Fig. (6.9). The thin target bunch will effectively act as a diffraction object

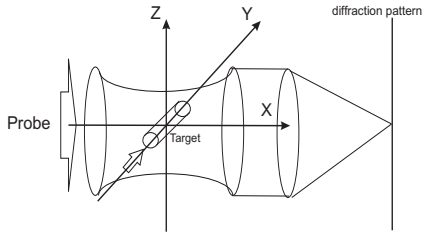

Figure 6.9: Experiment suggested in [2]

for the probe laser, since it will have a refraction index different from that of the rest of the medium. The diffraction pattern of it can then be observed on the diffraction screen. This will measure the phase difference acquired by the laser by means of passing through the area of intensive field, where vacuum polarization effects are significant.

The effects of QCD will be due to the diagrams of (6.10). The effect of the one-

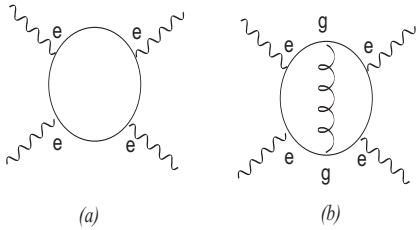

Figure 6.10: One- and two-loop contributions to photon-photon scattering.

loop diagrams Fig.6.10(a) is absolutely the same as in QED, modulo charges and group-theoretical factors. The diagram Fig.6.10(b) is specifically QCD, where a gluon runs inside. The contributions of Fig. 6.10(a) to the effective action is [327]:

$$\mathcal{L}^{(4)} = N_c \frac{2}{45} \frac{\alpha^2}{m_q^4} \left[(\vec{E}^2 - \vec{H}^2)^2 + 7(\vec{E}\vec{H})^2 \right], \tag{6.30}$$

and Fig.6.10(b) contributes

$$\mathcal{L}^{(6)} = \frac{\alpha_s}{\pi} \frac{\alpha^2}{m_q^4} \left[\frac{16}{81} (\vec{E}^2 - \vec{H}^2)^2 + \frac{263}{162} (\vec{E}\vec{H})^2 \right], \tag{6.31}$$

where α_s is the QCD coupling. Here a comment on the applicability of the standard effective action QED paradigm to QCD is due.

Perturbation theory with the quarks is applicable in QCD mostly in the high-energy range. The standard lore is that low energy QCD is dominated by pions, and treatment by means of chiral perturbation theory is prescribed in most of the low-energy QCD manuals [328]. The low-energy theory is properly described by the effective Lagrangian

$$\mathcal{L} = \frac{f_\pi^2}{4} \operatorname{tr} D_\mu U D^\mu U^+ + \frac{\Sigma}{2} \operatorname{tr} M U^+ + h.c., \tag{6.32}$$

where $\Sigma = \overline{\psi}\psi$, M is the quark mass matrix, $U = e^{i\frac{\tau^a \pi_a}{f_\pi}}$, π_a is a pion field. An example of a typical treatment of low-energy QCD with vacuum loops in external fields is the Smilga-Shushpanov theorem on a condensate in an external field [24]. From that point of view it would be simply wrong to do the quark vacuum loop which is done in (6.30), (6.31).

Let us though conjecture the validity of quark loops in this low-energy domain when we deal with four-gamma scattering. We argue that a zero-point function resummed in an external field is different from the four-point function we are interested in, with small but finite external momenta $\sim$ 1eV. E.g. if we were doing a two-point function at such a scale, we would say there is no logarithmic term, since the threshold is high above, but still there is a power-like term $\frac{m_q^2}{q^2}$ in the vacuum polarization function $\Pi(q^2)$, and the mass would be the quark mass, not the pion mass.

Finally, QCD at low energy is a strongly coupled theory, thus a high-order term with gluon propagators can yield a contribution larger than that of low-order terms. All this sets the perturbation theory in powers of α_s for such a low-energy observable as effective action under serious doubts.

The fate of higher-loop (full, planar, non-planar, ladder...) corrections to scattering amplitudes has been a subject of immense speculations, conjectures [329] (especially in supersymmetric theories), ladder summations [330], ladder cancellations [331] direct semi-classical estimates [332], and still remain a point of very intense discussion nowadays; since there is no all-loop massive QED prediction, we cannot make use of these estimates here.

Then, the coupling being large indeed, we cannot make any claim that the next-order term will not exceed the second-loop approximation. Then, we have no other way of incorporating QCD corrections, so let us adhere to the only feasible way of estimating it. It will serve the experiment as a rough guide to what the expected QCD results may be.

Now let us write down the refraction index tensor from (6.30), (6.31). Define the refraction index coefficients n_0, n_1, n_2 as

$$n_{ij} = \delta_{ij} + n_1 \frac{(E^2 - H^2)}{m_q^4} \delta_{ij} + n_2 \frac{H_i H_j}{m_q^4}. \tag{6.33}$$

Then

$$n_1 = N_c\alpha^2\left(\frac{2}{3}\right)^4\left[\frac{4}{45}+\frac{\alpha_s}{\pi}\frac{32}{81}\right], \tag{6.34}$$

and

$$n_2 = N_c\alpha^2\left(\frac{2}{3}\right)^4\left[\frac{14}{45}+\frac{\alpha_s}{\pi}\frac{232}{162}\right]. \tag{6.35}$$

Taking into account that α_s is taken in the very IR limit, we use $\alpha_s = 3.4$ as obtained in our Dyson-Schwinger analysis. Then

$$n_1 = 0.51N_c\alpha^2\left(\frac{2}{3}\right)^4, \tag{6.36}$$

and

$$n_2 = 1.86N_c\alpha^2\left(\frac{2}{3}\right)^4. \tag{6.37}$$

Compare this to pure QED

$$n_1 = \alpha^2\frac{m_q^4}{m_e^4}\left[\frac{4}{45}\right], \tag{6.38}$$

and

$$n_2 = \alpha^2\frac{m_q^4}{m_e^4}\left[\frac{14}{45}\right]. \tag{6.39}$$

At $m_u = 1.5$ MeV (lowest possible, as given in PDG tables) one gets that $n_{QCD} \sim 10^{-3}n_{QED}$.

Analyzing the data from the experiment schematically shown in Fig. (6.9), we can find an interesting evidence of QCD processes of vacuum polarization. Namely, let us estimate the limiting precision. As given in [2], the shift of the refraction index for laser pulse of energy E_t passing through a volume Vol_3 in the presence of vacuum polarization n is

$$\delta n = n\frac{E_t}{m_q^4\mathrm{Vol}_3}. \tag{6.40}$$

The volume is roughly $\mathrm{Vol}_3 = 1\mu\mathrm{m}^3$, energy $E_t = 10^4 J$, the limit of measurement of δn is better than 10^{-11}. Taking QED $n = 1.2\cdot 10^{-12}$ we get $\delta n \sim 10^{-8}$, which shall be perfectly visible in the setup. Taking the QCD estimate, we have $\delta n \sim 10^{-11}$, which is still visible. This opens a door to measuring the QCD vacuum polarization at the very IR by optical means. Two basic methods can be suggested then:

- Measure n_{full}, subtract n_{QED} and try to identify the rest with n_{QCD}.
- Use the birefringence phenomenon, get $n^1_{full}, n^1_{QCD}, n^2_{full}, n^2_{QCD}$, build ratios n^2_{full}/n^1_{full}, n^2_{QED}/n^1_{QED}.

The method of ratios could seem attractive since it potentially kills different effects of dressing the quark propagator etc (pretty much in the similar way as in quarkonium physics one cancels the unknown wavefunction by considering a ratio of decay widths). Yet the ratios are not that different: $\frac{n_1}{n_2}|_{full} = 0.124$, $\frac{n_1}{n_2}|_{QED} = 0.142$, thus it might be better to try to accurately subtract the known QED part and ascribe the remnant to QCD, which will be of course plagued with greater experimental errors in this case, since it will be a 10^{-3} of the original observable δn, thus a precision of at least 10^{-4} is necessary for the measurement of a refraction index shift.

6.7 The $\gamma\gamma$ Scattering in Holography

It makes perfect sense to ask oneself if the refraction index shift due to fermions or mesons in the loops is present in holography. The fermionic action is a Dirac–Born–Infeld action (2.3), which is non-linear in the Maxwell field living on the brane, and it makes no great trouble to extract the corresponding coefficient, analogous to the four-photon term in the Euler–Heisenberg action.

We follow here a simplified analysis, in which we consider the background allowing introduction of chirality-breaking solutions (that is, $m \equiv \frac{w(\rho)|_{\rho\to\infty}}{2\pi\alpha'} \neq 0$) to be not very different from AdS in the UV. This will alow us to make analytic estimates for the effective action coefficients. We thus neglect the dependence of the classical solution itself, that is, we put $w(\rho, H) = w(\rho)$. To evaluate the action on the classical solutions we finally put $w(\rho) = const$, and relate this constant to mass. The action (2.3) is

$$S = \frac{1}{(2\pi)^7\alpha'^4}\int d^4x \int \rho^3 d\rho\sqrt{1+w'^2} \times \begin{cases} \sqrt{1+\dfrac{(2\pi\alpha')^2e^2H^2R^4}{(\rho^2+w^2)^2}}, & \text{magnetic case,} \\ \sqrt{1+\dfrac{(2\pi\alpha')^2e^4(\vec{E}\vec{H})^2R^8}{(\rho^2+w^2)^4}}, & \text{self-dual case.} \end{cases} \tag{6.41}$$

The second-order in e term in the expansion of the holographic Dirac–Born–Infeld action, elaborated in [333], contains a log-term and thus corresponds to quark charge renormalization.

By expanding the action in terms of the field invariants and writing out the fourth-order coefficient, we get the coefficients n_1, n_2 defined as

$$n_{ij} = \delta_{ij} + n_1\alpha^2\frac{(E^2-H^2)}{m_q^4}\delta_{ij} + n_2\alpha^2\frac{H_iH_j}{m_q^4}. \tag{6.42}$$

in the vacuum refraction index n_{ij}.

$$\begin{aligned} n_1 &= 2\frac{N_c\lambda}{4\pi^3}\frac{1}{24} \approx 0.006 N_c, \\ n_2 &= \frac{N_c\lambda}{4\pi^3}\frac{1}{96} \approx 0.001 N_c. \end{aligned} \quad , \tag{6.43}$$

where λ is 't Hooft constant ($\lambda = \frac{g^2_{YM}N_c}{4\pi}$). For comparison the values of these coefficients in the Euler–Heisenberg effective action for quarks are

$$\begin{aligned} n_1 &\approx 0.088 N_c, \\ n_2 &\approx 0.311 N_c. \end{aligned} \tag{6.44}$$

For a rough estimate, the DSE value of α_s has been taken; anyway, the dual theory has yet nothing to do with QCD. As already noticed, a pure AdS cannot provide a successful model of QCD vacuum, since it describes a theory with a completely different spectrum. Therefore, the ideology of this section – to consider the $\frac{F^4}{m^4}$ terms – is tested below on the three other metrics which have been employed throughout the work as more or less realistic models of the QCD. One has to adhere to numerical solutions, precisely as was done in the previous Chapters. The $\frac{1}{m^4}$ dependence (shown in Fig. (6.11)), as well as the F^4 dependence will have also to be extracted numerically by means of fitting. The results

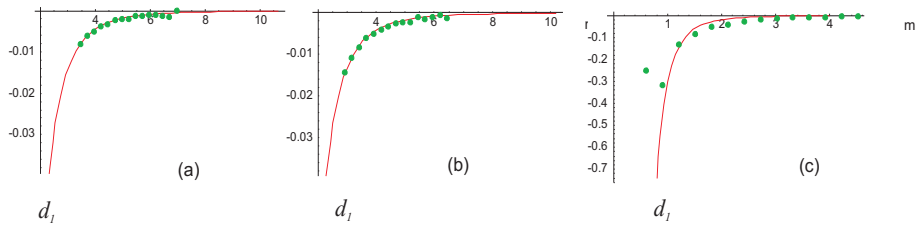

Figure 6.11: Dependence of the effective action coefficient d_1 (defined from $n = 1 + d_1 e^4 (E^2 - H^2)^2$) on m, compared to an $1/m^4$ fit, (a) – Liu–Tseytlin, (b) – Gubser, (c) – Constable–Myers backgrounds.

are in this case:

$$n_1 \approx \begin{cases} 0.044 N_c, \text{Constable} - \text{Myers}, \\ 0.14 N_c, \text{Gubser}, \\ 0.16 N_c, \text{Liu} - \text{Tseytlin}. \end{cases} \tag{6.45}$$

Comparing the results for the conformal and the non-conformal backgrounds to the Euler–Heisenberg effective action, one can note first of all that the non-conformal metrics yield a dimensionless coefficient much closer to the Euler–Heisenberg. The numerical

estimate for the refraction index contribution will depend not only on the model, but on the selected quark mass (current quark or constituent quark). For definiteness, let us indicate the order of magnitude of the effect. The contribution to the refraction index is

$$\delta n = c_1 \frac{H^4}{H_{cr}^4}, \tag{6.46}$$

where e.g. for the Liu–Tseytlin model, taken with current quarks masses (ca. 5 MeV), $c_1 \approx 10^{-5}$, and H_c is the electron critical field. However, a better logic would be to use this effect (which can be observed as a discrepancy between the QED and the experimental value of vacuum nonlinearity) for definition of the mass. By comparing n_1 and n_2 one can make sure whether the QCD non-linearity can or cannot be fully described by the QCD Euler–Heisenberg, or may be described by the Dirac–Born–Infeld action. By comparing the absolute values of n_1, n_2 to the estimates given in this Section, one can obtain an estimate of the effective quark mass.

6.8 Phantom QCD Effects

In this subsection I reexamine a claim made in [334] that QCD condensate effects can in fact overcome the *electron* QED one-loop effect. Similarly, in [335] it was claimed that QCD effects are at least similar in magnitude results to *electron* QED. Note that both works have been implying the same attitude to the quarks vs. pions dilemma as we do, thus a comparison is not hindered.

It is shown that these estimates are based on an inappropriate use of the small-field limit. The idea of the calculation [334] is to compare two types of one-loop contributions: four legs, all of them being photons, and six legs, four of them also photons, the remaining two being vacuum condensate gluons, considered as a kind of constant external field background, characterized by its field strength vacuum expectation value $\mathrm{tr}\, G^2 = 0.01$ GeV^4. The purely photon piece is same as given above (6.30) with quarks inside. The "QED-QCD interference" term, which is shown in Fig. (6.12), is

$$L_{6legs}^{1-loop} = \left(\frac{2}{3}\right)^2 \frac{\pi^4}{m^8} \left[12 \left(\frac{\alpha}{\pi} F^2\right)^2 \left\langle \frac{\alpha_s}{\pi} G^2 \right\rangle + \frac{13}{2} \left(\frac{\alpha}{\pi} F\tilde{F}\right)^2 \left\langle \frac{\alpha_s}{\pi} G^2 \right\rangle \right]. \tag{6.47}$$

Hence it is derived that the second-order term (with gluons) strongly dominates over the first term:

$$\frac{L_{eff}[4-\mathrm{photon}, 2-\mathrm{gluons}]}{L_{eff}[4-\mathrm{photon}]} = \frac{24}{7} \frac{q^2 \pi^4}{m^4} \langle \frac{\alpha}{\pi} \mathrm{tr}\, G^2 \rangle \sim 10^4. \tag{6.48}$$

However, this cannot be true since the gluon field strength must be resummed, as shown in Fig. (6.13). It is obvious that the resummation must take place: the effective field

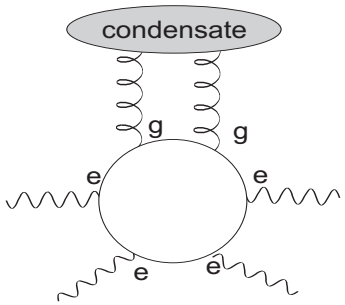

Figure 6.12: One-loop, four + two legs diagram, claimed to yield a larger contribution than the LO.

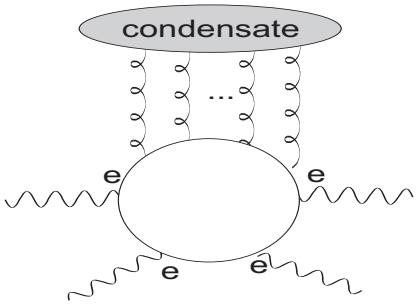

Figure 6.13: Four photon, resummed gluons diagram.

strength $\mathrm{tr}\, G^2 = 0.01\ \mathrm{GeV}^4$ should be compared with the quark mass scale $m_q^4 = 6 \cdot 10^{-10}\mathrm{GeV}^4$; the gluon vacuum field strength squared is 8 orders of magnitude greater than the corresponding Schwinger limit. The true value of the effective action for this case must necessarily be given by differentiating the Schwinger formula over the external electromagnetic field and then substituting necessary charges and symmetry factors in the remaining non-abelian part

$$L_{eff} \sim H^4 \frac{\partial^4}{\partial H^4} L_{eff}(H)|_{H\to G, e\to g} = \int_0^\infty (-2s) e^{-m^2 s} \mathrm{csch}^5(Hs)(11Hs\cosh(Hs)+ \\ + Hs\cosh(3Hs) - 2(3\sinh(Hs) + \sinh(3Hs))). \tag{6.49}$$

Inserting m_q and $\mathrm{tr}\, G^2$, we get

$$L_{eff}^{QCD,condens.} = q^4\alpha^2 H^2 \cdot (-9\mathrm{GeV}^4), \tag{6.50}$$

which is far smaller than

$$L_{eff}^{1\text{uarksinQED}} = q^4\alpha^2 H^2 \cdot (10^{10}\mathrm{GeV}^4). \tag{6.51}$$

Actually, this result of ours is present in [334] as well (eq. 26), and is given the correct interpretation, namely, of quarks effectively acquiring a large "effective mass" in the gluon condensate field. Yet this correct result is dismissed there on the ground of the short-rangedness of gluon correlations and stochastic character of the background. Thus this is not a valid reason to withdraw particularly the resummed correlation.

Firstly, if it were, it would similarly be a good reason to withdraw the two-gluon computation as well, which [334] does not do so far. Secondly, the short-rangedness of the gluon correlation strength must be taken into account only if it falls below the typical scale associated with the quark mass (that is, its size goes above the de Broglie wavelength size of the quark). However, the OPE predictions for the gluon field strength non-locality are well-known and exclude that possibility completely: $\langle \mathrm{tr}\, G^2(x)\, \mathrm{tr}\, G^2(0)\rangle \sim (1-\lambda^2 x^2)$, where $\lambda^2 \sim 0.2$ GeV^2; in the Dyson-Schwinger approach [306] one has $\lambda^2 \sim 1.1$ GeV. At large distances the correlator of gluon field strengths decreases as $\langle \mathrm{tr}\, G^2(x)\, \mathrm{tr}\, G^2(0)\rangle \sim e^{-ax}$, where the lattice estimate [336] is $a = 0.6$ GeV, the Dyson-Schwinger estimate [306] is $a = 1.3$ GeV. This makes a resummation for u and d quarks compulsory, since from the "point of view" of the quark, the field through which it virtually moves, is constant on the average. On the other hand, heavy quarks could already start noticing the non-locality and stochasticity of gluon fields, yet their contribution to the vacuum polarization effect is of no relevance, being strongly suppressed in mass. In other words, a light quark is "greater" in coordinate space (de Broglie wavelength is meant) than its typical inhomogeneity and therefore "moves" through them as through some average field (or one can say, a light quark "averages" the field over itself), whereas a heavy quark is "smaller" than the gluon field, thus it can "scatter" off the fluctuation of the gluon field, be deflected or refracted.

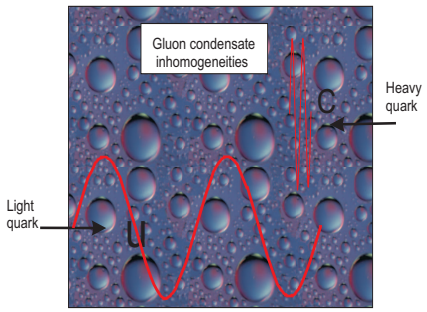

Figure 6.14: Symbolic picture of light and heavy quarks in the QCD vacuum with gluon field fluctuations.

In [335] a more elaborated model was used, namely, the Stochastic Vacuum Model, which assumed a Maxwell-type stochastic distribution of gluon fields, centered around the

experimentally-known value of the gluon condensate. Thus a QCD condensate-corrected Euler-Heisenberg Lagrangian was obtained (electric piece shown for simplicity)

$$\Delta L_{eff} = -\frac{2}{45}E^4 \sum_q \frac{64\sqrt{2\pi}}{5} \frac{\left\langle \frac{\alpha_s}{\pi} \operatorname{tr} G^2 \right\rangle^{1/2}}{m_q^2} \left(e_q\right)^2 , \tag{6.52}$$

where m_q, e_q are quark masses and charges, respectively; the authors evaluate it to

$$\Delta L_{eff} = 3.86 \frac{2}{45} \frac{E^4}{m_e^4} \tag{6.53}$$

where the mass of electron is shown to alleviate a comparison to QED. The $\sqrt{\langle \operatorname{tr} G^2 \rangle}$ term comes exactly after integrating the gluon fields G out with weight $\sim \frac{1}{G_0^{3/2}} e^{-G^2/G_0^2}$. Unlike [334], the gluon field is not dealt perturbatively from the very beginning. Eq. (39) is still exact in all tree orders of strong coupling at one-loop level and fourth-order in the electromagnetic field. Then strong-field limit is taken for gluons (which is justified), and Eq. (41) is already an approximation.

6.9 Abuse of Condensates

The argumentation of the previous section can be easily understood in terms of the renowned "Use and Misuse of Sum Rules" by Novikov, Shifman, Vainshtein, Voloshin and Zakharov [337]. The proper use of the condensate *power correction* occurs in the deeply Euclidean kinematics, as shown in Fig. (6.15). The incoming momenta are far

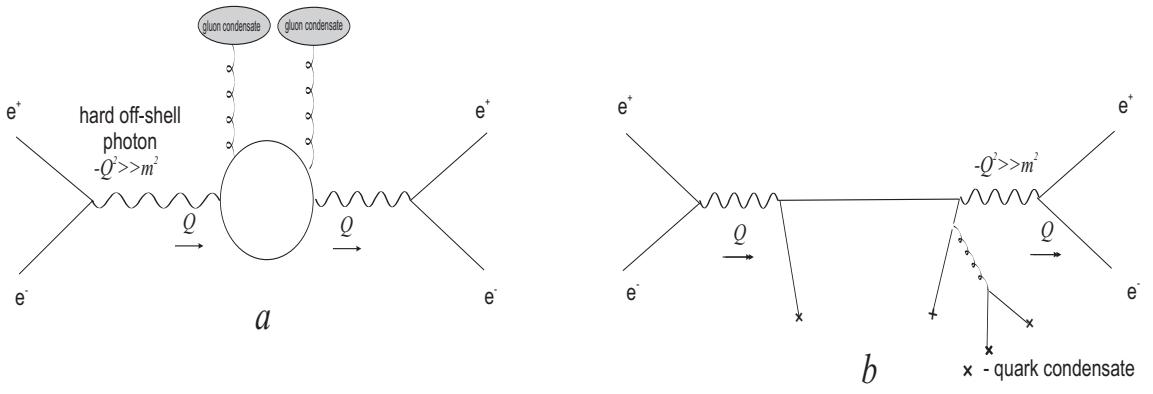

Figure 6.15: Contributions of (a) $\alpha_s \operatorname{tr} G^2$, (b) $\langle \overline{q}\gamma^\mu t^a q \overline{q}\gamma_\mu t_a q \rangle$

off-shell, since otherwise the ideology of small power corrections to large logs does not work; for the analysis of the vacuum polarization function in the case of electron-positron

scattering into hadrons this is perfectly fine, since the basic expression for sum rules here is

$$-\frac{1}{8\pi^2}\ln\frac{Q^2}{\mu^2}+\frac{1}{2Q^4}\langle\overline{q}q\rangle+\frac{1}{24Q^4}\left\langle\frac{\alpha_s}{\pi}\operatorname{tr}G^2\right\rangle=\frac{1}{\pi}\int\frac{\mathrm{Im}\Pi_{phys}(s)ds}{s+Q^2}. \tag{6.54}$$

It is of crucial importance that here, in the case of a hard incoming virtual photon ($Q^2\gtrsim 1\mathrm{GeV}^2$, whereas $\sqrt{\operatorname{tr}G^2}\lesssim 0.3\mathrm{GeV}^2$), the suppression parameter is not the smallness of the vacuum field (which is not small at all), but the largeness of the momentum. Then, the larger the momentum is, the smaller α_s, also improving the quality of the approximation. If one wants to resum the contributions of condensate and thus interpret $\sqrt{\operatorname{tr}G^2}$ as some effective mass, this is possible but totally pointless since $Q^4\gg\operatorname{tr}G^2$.

Now let us analyze our case, namely, very low-energy (1eV) $\gamma\gamma$ scattering. There is no suppression in α_s, and there is a huge enhancement in $1/Q^2$. This means that no accounting for single contributions with external condensate legs is allowed, but only the Euler-Heisenberg resummed action should be taken into account.

6.10 Instead of a Conclusion: What does QCD Contribute?

As a result of considering the possible QCD contributions to vacuum polarizations in the last two sections we come to the following conclusions:

- Vacuum polarization due to quarks can be observed by means of the experiment [2], provided it can measure the refraction index at the level

$$\frac{\delta n}{n}\sim 10^{-11} \tag{6.55}$$

- Next-to-leading-order QCD corrections to the QED leading-order (LO) quark loop are important and can exceed the LO result

- Condensate (tree-level) corrections [334] to the QED quark loop are irrelevant.

Chapter 7

Comparison: Resummations vs. Holography

7.1 Main Results

This Thesis has attempted to describe electromagnetic effects in QCD in two types of models, the holographic ones (Part I) and those based on resummation schemes (Part II). We have thus a basis for comparing the two with each other and with experiment. To summarize the main results in holography:

- The chiral magnetic effect is essentially different in five-dimensional models at strong coupling compared to the perturbative approach.
- The viscosity-to-entropy ratio and shear viscosity remain unchanged in the self-dual background with the gluon condensate.
- The quark condensate is scaled quadratically with the field, unlike the linear scaling in the resummed field theory.
- Ward identities for the scaling symmetry are satisfied in theories with condensates.
- The decoupling relation remains valid.
- The magnetization of vacuum saturates to zero.

Physically this means, in particular, that dual theories can give robust falsifiable predictions, which can be tested in experiment. The predictions for the chiral magnetic effect and for the viscosity are already in direct comparison with RHIC data. The predictions for the magnetization can be tested against the lattice data.

For the resummed theories the successes are more moderate:

- Decoupling explicitly fails in the Dyson–Schwinger resummation.
- The Erickson-Semenoff-Szabo-Zarembo resummation only partially restores the confinement property.
- Quadratic field scaling coefficients of gluon condensate obtained.

Discussing these results, it is instructive to look for the properties that are realized in both approaches and in experiment as well. Again, a caution should be taken against accepting the predictions about QCD from holography too literally. None of the existing holographic models claims to be the true dual theory of QCD. Yet basing on common features of holographic models with chiral perturbation theory, we may suggest an "effective theory ideology" for the holographic theories. Thinking about purely four-dimensional theories, we do encounter effective "strongly-coupled" *effective* theories; the typical examples are the Euler–Heisenberg action in the large-field limit and the chiral perturbation theory (where, strictly speaking, there is no coupling parameter at all, and small momentum acts as the series expansion parameter; the QCD coupling is of course not small in the IR area). Both these actions (Chiral PT and Euler–Heisenberg) have actually been pointed out to possess features similar to holographic models, and geometric setups were proposed to account for some of their properties. Thus strongly-coupled models are not absent from the range of commonly discussed theories. Therefore nothing strange or superficial is in comparing the two sides of the correspondence directly, insofar the strong-coupling regime is discussed.

The resummation schemes I deal with are not fully and uniquely determined either. All the functional resummations I have considered arise after an infinite tower of equations is truncated at some level. The ambiguity of truncations has been discussed above for each of the integral resummations. Then, a solution to a non-linear equation is not unique, and the fact that I have obtained some functions numerically as solutions of Dyson–Schwinger equations does not allow me to state that it is indeed the way to describe the dynamics of the system. The correlators which are yielded by the resummation equations are limited in the number of points; we might speculate however that the high-multiplicity processes are thus left beyond the reach of the non-perturbative scheme. The truncated set of the Dyson–Schwinger equations has problems with retaining both scaling invariance and gauge invariance simultaneously. Moreover, the Dyson–Schwinger equations ideology as advocated here: "take the DSE Green functions as the true non-perturbative Green functions and calculate any observable you want", surely is based on an intrinsically perturbative assumption, namely, that a representation via (dressed) Green functions is valid for all observables, which is at least questionable. Thus problems plague both sides of our

comparison.

I present the results of my comparison in the form of a concise table and comment on them in the next section[1]. The abbreviation "EH" stands for "Euler–Heisenberg".

Property	Holographic models	Resummation models	Experiment/Lattice
Decoupling relation is observed	+	−	+
The chiral condensate scaling with the magnetic field H	$\sim H^2$	$\sim H$(EH) $\sim H^2$(DSE)	$\sim H^{3/2}$
The chiral magnetic effect at strong coupling is exactly the same as at weak coupling	−	+	?
The magnetic susceptibility saturates to 1	+	−	+
The magnetic susceptibility saturates to 0	−	+	−
Small shear viscosity	+	−	+
Zero bulk viscosity	+	−	+
Confinement is present	+	+ (this work)	+
Quarkonium transport coefficients independent of condensates	+	?	?

7.2 Comments on Compared Values

7.2.1 Decoupling

Field theory is incapable of predicting the values of the condensates. Yet it can predict some interesting relations between them: decoupling relations and scaling low-energy the-

[1]The lattice result quoted in this fourth line of the table comes from the unpublished data by the DESY group, I thank Ingo Kirsch and Tigran Kalaydzhyan for their private communication.

orems. We reconstruct decoupling relations for gluonic operators in holography fully and we qualitatively support the decoupling relation numerically on a very high level of accuracy (better than 1%.) Note here that the resummed field theory fails completely to reproduce the simple decoupling ratio directly from the propagators. This is an important hint for validity of the idea that the propagator feels directly the presence of the condensate. Taken together with other discrepancies, observed under the hypothesis that the chiral condensate enters in some extractable way into the quark propagator, and the gluon condensate – into the gluon propagator, we should abandon this idea more or less completely. The full non-perturbative propagator, even if such a thing were simply available, does not shed much light upon the condensate of the corresponding field.

Here a moral can be drawn from our exercises with condensates in Dyson–Schwinger equations: very little information can be passed into the DSE system, and very little will proceed to the next stages of the calculation. The propagators are very robust; changes in boundary conditions or some other parameters alter them comparatively little (I do not discuss here a completely different set of solutions, provided by some authors). Then, even if the propagator function is greatly varied, little of this variation is felt by the functional-type observables, e.g. by the non-local condensate defined as functional on propagator. This insensitivity of observables to input data puts the whole procedure under a strong doubt.

On the other hand, special care should be taken on the holographic side of the correspondence in the proper identification of fields to some real-world objects like quark operators; since presently there is no exact "QCD" background, the results one gets are endangered by the possibility of misidentifying the QCD operators.

7.2.2 Wilson Line and Quark-Quark Potential

Holographically the three models of QCD I have been considering here possess confinement in the sense of the linear Wilson line scaling. The combined Dyson–Schwinger and Erickson–Semenov–Szabo–Zarembo resummations seem to provide linearity as well. Yet this linearity is bound by a limited range (up to 1 fm), and not prolonging further to the IR scale, where it rather goes to constant. This potential is certainly more realistic than a pure Coulomb, yet we know that physical reality is different. Even if at some point the potential formally saturates due to QCD string breaking, this is certainly not inside the double resummation model and cannot be expected from it; moreover, it would happen at greater spatial scales. Thus in what concerns Wilson loops, holography gives certainly a more reasonable-looking result than the resummation.

7.2.3 Linear Condensate Scaling

The linear condensate behavior in strong fields is an "experimental" (i.e. lattice) fact nowadays, supporting the Smilga–Shushpanov resummation. Basing on Dyson–Schwinger, we were destined to obtain a quadratic scaling, since whatever the mass function of the quark is, there is some mass in this model. On the other hand, the linearity of the Smilga–Shushpanov result vests fully in the masslessness of pion. Thus it can never be reached in such a way. Holographically we also see a wrong (quadratic) result already at an exactly zero mass; we explain that by an inconsistency of the $1/N_c$ orders of the holographic result with the field theory.

7.2.4 Magnetization

It has already been stated that the direct comparison between the vacuum magnetization that I have calculated and condensate magnetization, calculated on the lattice is impossible. Thus the difference in the behavior of the two observables does not signal that something is wrong with holography. Moreover, the speculations that the decreasing magnetization curve may be somehow related to the phenomenon of the quark vacuum electromagnetic superconductivity, are fitting into the ideas of recent findings of a rho-meson electromagnetically superconducting phase. I do not claim here that the anomalous behavior exactly means that the QCD vacuum becomes electromagnetically superconducting, yet there is certainly a lot of possible tests to do in that direction, both in the framework of the resummed field theories and holography.

7.3 Conclusion

One can see that the comparison is of course incomplete, since not all of the results are available for all of the three columns. The only result in which resummation models (and that is not the DSE resummation) supercede the holographic models is the Smilga–Shushpanov scaling, supported by recent lattice measurements [338].

The other achievement of the resummation ideology is confinement demonstration. Yet it is very limited and does not extend to the full range of distances. On the other hand, e.g. the Liu–Tseytlin model with which, in particular, I have worked, demonstrates a truly confining potential without problems at all sufficiently large distances. On the contrary, in the resummation paradigm the smallness of shear viscosity cannot be demonstrated, which is an elementary result in holography, and which I have confirmed here exactly for theories with condensates.

Open to discussion are the predictions of both field theory and holography for the chiral magnetic effect. Till experimental results become not only qualitative, but also quantitative for this phenomenon, we must withhold from judging on which theory is better describing it.

Thus the overall conclusion I draw in this Thesis is that despite many shortcomings, holography is a more apt tool for systematic studies of strongly-coupled theories rather than the resummation procedures via the Dyson–Schwinger equations.

7.4 Developments of Holographic Models

Holography as an effective model building approach describing the behavior of strongly-coupled systems is not limited by the QCD applications. In the last three years the new methods stemming from string theory have been applied to condensed matter systems with strongly-coupled electrons. AdS/CMT (Anti-de Sitter/Condensed Matter Theory) correspondence originated several years ago in the works [339] and [340]. The total amount of papers on AdS/CMT is about 250 presently, and it continues to grow quickly.

AdS/CMT has been an attempt to transfer the strong-coupling methods originally used for (supersymmetric) gauge field theories down to solid state physics. Surprisingly, this works for some regions, despite a completely different physics behind gravity on one side and the correlated electron (hole) gas in the condensed matter on the other. In superconductivity the p-wave order parameter and the nodes of fermion correlators have been studied within this methodology. Recently a progress was observed in holographically describing the non-standard phases of solids such as the Luttinger liquid, other types of the non-Fermi liquids, the strange metals, and HTSCs.

AdS/CMT methods applied to superconductors come under the name of the holographic superconductor, meaning a strongly interacting field theory that undergoes a condensation to a superconducting or a superfluid phase and that has in addition a dual gravitational description, see [341, 342, 343] for review.

The similarity of the phase diagrams along with the many observed non-Fermi liquid properties of the pseudogap region may suggest that there is a quantum critical point beneath the superconducting dome in the HTSC compounds. Some evidence for such a quantum critical point is reviewed in [344]. The field theory description can be applied in the finite region of the phase diagram around the critical point, moreover, this region expands as temperature grows.

The holographic models were shown to reproduce the spectral function of the “Marginal Fermi Liquid”, deduced from an analysis of the experimental data to describe the optimally

doped cuprates [345] as well as the ordinary Fermi-liquid for overdoped samples [346]. The gravity background of holographic models realizes geometrically the scaling properties and other symmetries of quantum critical points, and the models for both relativistic and non-relativistic types of symmetries have been developed. The advantage of holographic models is a relatively easy calculation of the dynamical real-time processes such as the optical, electrical and heat conductivities and dissipation.

Several holographic models for the d-wave superconductors were recently proposed [347, 348]. These models contain the field of spin 2 in the bulk, which has allowed the researchers to describe the d-wave superconductivity and to obtain the Fermi arcs. Holographically, this amounts to adding some peculiar matter on the five-dimensional side. These models are still not theoretically complete and require further significant work.

Acknowledgements

My most warm thanks to Professor Dietrich Habs for his keen guidance, constant encouragement, generous support, interest to my work, and courage for developing the theoretical QCD at a mostly experimental Chair. I am grateful to Priv.-Doz. Johanna Erdmenger for discussions, aid and guidance from her that made accomplishing this work possible. I gratefully acknowledge the great influence René Meyer has had upon my vision and understanding of $D3/D7$ models and the many interesting conversations we had on AdS/CFT. Collaboration with A. Gorsky, P. Kopnin and A. Krikun was crucial for working out the low-energy theorems of QCD from holography. Ein besonderer Dank geht an Priv.-Doz. Peter Thirolf, der die ganze Arbeit gelesen hat und die zahlreichen "a" und "the" auf ihre richtigen Stellen gestellt hat. I thank Peter Koroteev of Minnesota U. for always being the first from whom I heard criticism or comments on each new idea. The profound interest of Toshiki Tajima into the applications of holography towards the quark-gluon plasma physics and his insights on possible experiments with incredibly high fields are gratefully acknowledged. Thanks to Kensuke Homma for generously lending me his idea on considering the $D7$ DBI action as an analog of Euler–Heisenberg action. Part of this work originated during my collaboration with Prof. Johann Rafelski. My warmest thanks for enlightening discussions to my colleagues E. Akhdemov, R. Alkofer, M. Ammon, A. O'Bannon, E. Babichev, O. Bergman, L. Brits, P. Buividovich, V. Filev, C. Fischer, H. Fritzsch, S. Gärtner, A. Golovnev, G. Grigniani, N. Gromov, F. Gubarev, P. Hilz, Ho-Ung Yee, M. Kaminski, H. Kleinert, P. Koroteev, M. Konyushikhin, G. Lifschytz, L. Lipatov, D. Malyshev, D. Melnikov, V. Mikhailov, A.Yu. Morozov, A. Monin, R. Pasechnik, O. Pavlovsky, J. Pawlowski, M. Polikarpov, A. Rebhan, H. Reinhardt, R. Ruffini, W. Schulgin, I. Shenderovich, J. Shock, E. Shuryak, Shu Lin, S. Slizovsky, A. Starinets, M. Staudacher, J. Sonnenschein, G. Torrieri, M. Trusov, A. Vainshtein, V. Zakharov, K. Zarembo. My work in munich was funded by the DFG Cluster of Excellence MAP (Munich Centre of Advanced Photonics). Thanks to all colleagues from LMU-Munich, MPI-Munich, FU-Berlin, AEI-Potsdam, ITEP-Moscow and JINR-Dubna, with whom I had the pleasure to share scientific insights. Gratiam ago omnibus fratribus

et sororibus in ecclesia mea. My vision of QCD and holography was much formed by the 2006 Winter school in Jerusalem organized by David Gross, the 2007 SIS Program in Cambridge, the 2007 European RTN school in CERN, 2008 Krakow School organized by Michal Praszalowicz, the 2008 Confinement meeting in Mainz, the 2009 Potsdam integrability meeting, 2010 Munich String Theory School, the 2010 Les Houches "Physics in the plane" school, the 2010 String Theory Cargese school, the 2010 Vienna AdS/QCD workshop, the 2010 Quarks Seminar in Kolomna; I owe my deep gratitude to the organizers and participants of these meetings. I specially thank Prof. D.V. Shirkov for being the first who had introduced me to the beautiful world of the non-perturbative QCD. My interest to physics was inspired many years ago by my high school teacher, V.F. Potapov, whom I thank cordially. Lastly, and most importantly, I would like to thank my mother, Dr. Nadezhda Zayakina, for her life-long support and for her constant encouraging of my aspiration to discovery.

Bibliography

[1] M. Luzum and P. Romatschke, "Conformal Relativistic Viscous Hydrodynamics: Applications to RHIC results at $\sqrt{(}s_N N) = 200$GeV," *Phys. Rev.* **C78** (2008) 034915, 0804.4015.

[2] K. Homma, D. Habs, and T. Tajima, "Probing semi-macroscopic vacua by high fields of lasers," 1006.4533.

[3] J. K. Erickson, G. W. Semenoff, R. J. Szabo, and K. Zarembo, "Static potential in N = 4 supersymmetric Yang-Mills theory," *Phys. Rev.* **D61** (2000) 105006, hep-th/9911088.

[4] S. Jeon and L. G. Yaffe, "From Quantum Field Theory to Hydrodynamics: Transport Coefficients and Effective Kinetic Theory," *Phys. Rev.* **D53** (1996) 5799–5809, hep-ph/9512263.

[5] E. V. Shuryak, "The Role of Instantons in Quantum Chromodynamics. 2. Hadronic Structure," *Nucl. Phys.* **B203** (1982) 116.

[6] K. Fukushima, D. E. Kharzeev, and H. J. Warringa, "The Chiral Magnetic Effect," *Phys. Rev.* **D78** (2008) 074033, 0808.3382.

[7] J. M. Maldacena, "The large N limit of superconformal field theories and supergravity," *Adv. Theor. Math. Phys.* **2** (1998) 231–252, hep-th/9711200.

[8] E. Witten, "Anti-de Sitter space and holography," *Adv. Theor. Math. Phys.* **2** (1998) 253–291, hep-th/9802150.

[9] O. Aharony, S. S. Gubser, J. M. Maldacena, H. Ooguri, and Y. Oz, "Large N field theories, string theory and gravity," *Phys. Rept.* **323** (2000) 183–386, hep-th/9905111.

[10] E. D'Hoker and D. Z. Freedman, "Supersymmetric gauge theories and the AdS/CFT correspondence," hep-th/0201253.

[11] J. Erdmenger, (ed.), "String cosmology: Modern string theory concepts from the Big Bang to cosmic structure,". Weinheim, Germany: Wiley-VCH (2009) 313 p.

[12] **STAR** Collaboration, J. Adams *et al.*, "Experimental and theoretical challenges in the search for the quark gluon plasma: The STAR collaboration's critical assessment of the evidence from RHIC collisions," *Nucl. Phys.* **A757** (2005) 102–183, `nucl-ex/0501009`.

[13] J. Erlich, E. Katz, D. T. Son, and M. A. Stephanov, "QCD and a Holographic Model of Hadrons," *Phys. Rev. Lett.* **95** (2005) 261602, `hep-ph/0501128`.

[14] A. Karch and E. Katz, "Adding flavor to AdS/CFT," *JHEP* **06** (2002) 043, `hep-th/0205236`.

[15] J. Babington, J. Erdmenger, N. J. Evans, Z. Guralnik, and I. Kirsch, "Chiral symmetry breaking and pions in non-supersymmetric gauge / gravity duals," *Phys. Rev.* **D69** (2004) 066007, `hep-th/0306018`.

[16] M. A. Shifman, A. I. Vainshtein, and V. I. Zakharov, "QCD and Resonance Physics. Sum Rules," *Nucl. Phys.* **B147** (1979) 385–447.

[17] A. I. Vainshtein, V. I. Zakharov, and M. A. Shifman, "Gluon Condensate and Lepton Decays of Vector Mesons. (In Russian)," *JETP Lett.* **27** (1978) 55–58.

[18] M. A. Shifman, A. I. Vainshtein, and V. I. Zakharov, "QCD and Resonance Physics: Applications," *Nucl. Phys.* **B147** (1979) 448–518.

[19] V. I. Zakharov, "Gluon condensate and beyond," *Int. J. Mod. Phys.* **A14** (1999) 4865–4880, `hep-ph/9906264`.

[20] B. V. Geshkenbein, "Calculation of gluon and four-quark condensates from the operator product expansion," *Phys. Rev.* **D70** (2004) 074027.

[21] B. L. Ioffe, "QCD at low energies," *Prog. Part. Nucl. Phys.* **56** (2006) 232–277, `hep-ph/0502148`.

[22] V. A. Miransky and I. A. Shovkovy, "Magnetic catalysis and anisotropic confinement in QCD," *Phys. Rev.* **D66** (2002) 045006, `hep-ph/0205348`.

[23] T. D. Cohen, D. A. McGady, and E. S. Werbos, "The chiral condensate in a constant electromagnetic field," *Phys. Rev.* **C76** (2007) 055201, `0706.3208`.

[24] I. A. Shushpanov and A. V. Smilga, "Quark condensate in a magnetic field," *Phys. Lett.* **B402** (1997) 351–358, hep-ph/9703201.

[25] V. A. Novikov, M. A. Shifman, A. I. Vainshtein, and V. I. Zakharov, "Are All Hadrons Alike?," *Nucl. Phys.* **B191** (1981) 301.

[26] V. A. Novikov, M. A. Shifman, A. I. Vainshtein, and V. I. Zakharov, "Operator Expansion in Quantum Chromodynamics beyond Perturbation Theory," *Nucl. Phys.* **B174** (1980) 378.

[27] A. Gorsky, "Low energy theorems and the Dirac operator spectral density in QCD," *JETP Lett.* **71** (2000) 239–241, hep-ph/9812519.

[28] P. N. Kopnin, "Low-energy theorems and spectral density of the Dirac operator in AdS/QCD," *Phys. Rev.* **D80** (2009) 126005, 0907.1294.

[29] S. Narison, "Masses, decays and mixings of gluonia in QCD," *Nucl.Phys.* **B509** (1998) 312–356, hep-ph/9612457.

[30] H. Forkel, "Holographic glueball structure," *Phys. Rev.* **D78** (2008) 025001, 0711.1179.

[31] D. Z. Freedman, S. S. Gubser, K. Pilch, and N. P. Warner, "Continuous distributions of D3-branes and gauged supergravity," *JHEP* **07** (2000) 038, hep-th/9906194.

[32] P. Colangelo, F. De Fazio, F. Jugeau, and S. Nicotri, "Investigating AdS/QCD duality through scalar glueball correlators," *Int. J. Mod. Phys.* **A24** (2009) 4177–4192, 0711.4747.

[33] E. V. Gorbar and A. A. Natale, "Relating the quark and gluon condensates through the QCD vacuum energy," *Phys. Rev.* **D61** (2000) 054012, hep-ph/9906299.

[34] T. Sakai and S. Sugimoto, "Low energy hadron physics in holographic QCD," *Prog. Theor. Phys.* **113** (2005) 843–882, hep-th/0412141.

[35] U. Gursoy and E. Kiritsis, "Exploring improved holographic theories for QCD: Part I," *JHEP* **0802** (2008) 032, arXiv:0707.1324.

[36] L. Da Rold and A. Pomarol, "Chiral symmetry breaking from five dimensional spaces," *Nucl. Phys.* **B721** (2005) 79–97, hep-ph/0501218.

[37] H. R. Grigoryan and A. V. Radyushkin, "Form Factors and Wave Functions of Vector Mesons in Holographic QCD," *Phys. Lett.* **B650** (2007) 421–427, hep-ph/0703069.

[38] C. P. Herzog, "A holographic prediction of the deconfinement temperature," *Phys. Rev. Lett.* **98** (2007) 091601, hep-th/0608151.

[39] L. Da Rold and A. Pomarol, "The scalar and pseudoscalar sector in a five-dimensional approach to chiral symmetry breaking," *JHEP* **01** (2006) 157, hep-ph/0510268.

[40] L. Cappiello and G. D'Ambrosio, "On the Evaluation of Gluon Condensate Effects in the Holographic Approach to QCD," 0912.3721.

[41] K. K. Kim, Y. Kim, and Y. Ko, "Self-bound dense objects in holographic QCD," 1007.2470.

[42] Y. Ko, B.-H. Lee, and C. Park, "Meson spectra in a gluon condensate background," *JHEP* **04** (2010) 037, 0912.5274.

[43] A. Karch, E. Katz, D. T. Son, and M. A. Stephanov, "Linear Confinement and AdS/QCD," *Phys. Rev.* **D74** (2006) 015005, hep-ph/0602229.

[44] Y. Kim, J.-P. Lee, and S. H. Lee, "Heavy quarkonium in a holographic QCD model," *Phys. Rev.* **D75** (2007) 114008, hep-ph/0703172.

[45] P. Colangelo, F. De Fazio, F. Jugeau, and S. Nicotri, "On the light glueball spectrum in a holographic description of QCD," *Phys. Lett.* **B652** (2007) 73–78, hep-ph/0703316.

[46] F. Jugeau, "Holographic description of glueballs in a deformed AdS- dilaton background," *AIP Conf. Proc.* **964** (2007) 151–156, 0709.1093.

[47] B. Batell and T. Gherghetta, "Dynamical Soft-Wall AdS/QCD," *Phys. Rev.* **D78** (2008) 026002, 0801.4383.

[48] T. Huang and F. Zuo, "Couplings of the Rho Meson in a Holographic dual of QCD with Regge Trajectories," *Eur. Phys. J.* **C56** (2008) 75–80, 0708.0936.

[49] N. Evans and A. Tedder, "Perfecting the Ultra-violet of Holographic Descriptions of QCD," *Phys. Lett.* **B642** (2006) 546–550, hep-ph/0609112.

[50] T. Gherghetta, J. I. Kapusta, and T. M. Kelley, "Chiral symmetry breaking in the soft-wall AdS/QCD model," *Phys. Rev.* **D79** (2009) 076003, 0902.1998.

[51] M. Fujita, K. Fukushima, T. Misumi, and M. Murata, "Finite-temperature spectral function of the vector mesons in an AdS/QCD model," *Phys. Rev.* **D80** (2009) 035001, 0903.2316.

[52] E. Shuryak, "Building a 'holographic dual' to QCD in the AdS(5): Instantons and confinement," hep-th/0605219.

[53] O. Andreev and V. I. Zakharov, "The Spatial String Tension, Thermal Phase Transition, and AdS/QCD," *Phys. Lett.* **B645** (2007) 437–441, hep-ph/0607026.

[54] J. P. Shock, F. Wu, Y.-L. Wu, and Z.-F. Xie, "AdS/QCD Phenomenological Models from a Back-Reacted Geometry," *JHEP* **0703** (2007) 064, hep-ph/0611227.

[55] C. D. White, "The Cornell potential from general geometries in AdS / QCD," *Phys. Lett.* **B652** (2007) 79–85, hep-ph/0701157.

[56] H. R. Grigoryan and A. V. Radyushkin, "Structure of Vector Mesons in Holographic Model with Linear Confinement," *Phys. Rev.* **D76** (2007) 095007, 0706.1543.

[57] H. J. Kwee and R. F. Lebed, "Pion Form Factors in Holographic QCD," *JHEP* **01** (2008) 027, 0708.4054.

[58] C. A. Ballon Bayona, H. Boschi-Filho, and N. R. F. Braga, "Deep inelastic scattering from gauge string duality in the soft wall model," *JHEP* **03** (2008) 064, 0711.0221.

[59] P. Colangelo, F. De Fazio, F. Giannuzzi, F. Jugeau, and S. Nicotri, "Light scalar mesons in the soft-wall model of AdS/QCD," *Phys. Rev.* **D78** (2008) 055009, 0807.1054.

[60] O. Andreev and V. I. Zakharov, "Heavy-quark potentials and AdS/QCD," *Phys. Rev.* **D74** (2006) 025023, hep-ph/0604204.

[61] F. De Fazio, "Soft-wall model of AdS/QCD: The case of light scalar mesons," *PoS* **CONFINEMENT8** (2008) 128, 0812.3218.

[62] C. Marquet, C. Roiesnel, and S. Wallon, "Virtual Compton Scattering off a Spinless Target in AdS/QCD," *JHEP* **04** (2010) 051, 1002.0566.

[63] E. Nakano, S. Teraguchi, and W.-Y. Wen, "Drag Force, Jet Quenching, and AdS/QCD," *Phys. Rev.* **D75** (2007) 085016, hep-ph/0608274.

[64] Y.-h. Gao, W.-s. Xu, and D.-f. Zeng, "Viscosity and jet quenching from holographic model," 0707.0817.

[65] H. Liu, K. Rajagopal, and Y. Shi, "Robustness and Infrared Sensitivity of Various Observables in the Application of AdS/CFT to Heavy Ion Collisions," *JHEP* **08** (2008) 048, 0803.3214.

[66] K. Kajantie, T. Tahkokallio, and J.-T. Yee, "Thermodynamics of AdS/QCD," *JHEP* **01** (2007) 019, hep-ph/0609254.

[67] K. Jo, Y. Kim, H. K. Lee, and S.-J. Sin, "Quark number Susceptibility and Phase Transition in hQCD Models," *JHEP* **11** (2008) 040, 0810.0063.

[68] Y. Kim, Y. Matsuo, W. Sim, S. Takeuchi, and T. Tsukioka, "Quark Number Susceptibility with Finite Chemical Potential in Holographic QCD," *JHEP* **05** (2010) 038, 1001.5343.

[69] M. Fujita, T. Kikuchi, K. Fukushima, T. Misumi, and M. Murata, "Melting Spectral Functions of the Scalar and Vector Mesons in a Holographic QCD Model," *Phys. Rev.* **D81** (2010) 065024, 0911.2298.

[70] G. Panico and A. Wulzer, "Nucleon Form Factors from 5D Skyrmions," *Nucl. Phys.* **A825** (2009) 91–114, 0811.2211.

[71] H. Forkel, M. Beyer, and T. Frederico, "Linear square-mass trajectories of radially and orbitally excited hadrons in holographic QCD," *JHEP* **07** (2007) 077, 0705.1857.

[72] A. Vega and I. Schmidt, "Modes with variable mass as an alternative in AdS / QCD models with chiral symmetry breaking," 1005.3000.

[73] J. Hirn and V. Sanz, "Interpolating between low and high energy QCD via a 5D Yang-Mills model," *JHEP* **12** (2005) 030, hep-ph/0507049.

[74] J. Hirn, N. Rius, and V. Sanz, "Geometric approach to condensates in holographic QCD," *Phys. Rev.* **D73** (2006) 085005, hep-ph/0512240.

[75] F. Zuo, Y. Jia, and T. Huang, "$\gamma^*\rho^0 \to \pi^0$ Transition Form Factor in Extended AdS/QCD Models," *Eur. Phys. J.* **C67** (2010) 253–261, 0910.3990.

[76] A. Pomarol and A. Wulzer, "Baryon Physics in Holographic QCD," *Nucl. Phys.* **B809** (2009) 347–361, 0807.0316.

[77] T. Hambye, B. Hassanain, J. March-Russell, and M. Schvellinger, "Four-point functions and kaon decays in a minimal AdS/QCD model," *Phys. Rev.* **D76** (2007) 125017, hep-ph/0612010.

[78] S. Seki and J. Sonnenschein, "Comments on Baryons in Holographic QCD," *JHEP* **01** (2009) 053, 0810.1633.

[79] C. V. Johnson and A. Kundu, "Meson Spectra and Magnetic Fields in the Sakai-Sugimoto Model," *JHEP* **07** (2009) 103, 0904.4320.

[80] K. Hashimoto, T. Sakai, and S. Sugimoto, "Nuclear Force from String Theory," *Prog. Theor. Phys.* **122** (2009) 427–476, 0901.4449.

[81] K. Nawa, H. Suganuma, and T. Kojo, "Baryonic matter in holographic QCD," *Prog. Theor. Phys. Suppl.* **174** (2008) 347–352, 0806.3041.

[82] A. Dhar and P. Nag, "Sakai-Sugimoto model, Tachyon Condensation and Chiral symmetry Breaking," *JHEP* **01** (2008) 055, 0708.3233.

[83] A. Dhar and P. Nag, "Tachyon condensation and quark mass in modified Sakai-Sugimoto model," *Phys. Rev.* **D78** (2008) 066021, 0804.4807.

[84] R. Parthasarathy and K. S. Viswanathan, "Low Energy Pion-Pion Elastic Scattering in Sakai-Sugimoto Model," *Phys. Rev.* **D77** (2008) 115002, 0804.3446.

[85] J. Park and P. Yi, "A Holographic QCD and Excited Baryons from String Theory," *JHEP* **06** (2008) 011, 0804.2926.

[86] K. Hashimoto, T. Hirayama, F.-L. Lin, and H.-U. Yee, "Quark Mass Deformation of Holographic Massless QCD," *JHEP* **07** (2008) 089, 0803.4192.

[87] O. Aharony and D. Kutasov, "Holographic Duals of Long Open Strings," *Phys. Rev.* **D78** (2008) 026005, 0803.3547.

[88] P. Zhang, "Improving the Excited Nucleon Spectrum in Hard-Wall AdS/QCD," *Phys. Rev.* **D81** (2010) 114029, 1002.4352.

[89] K. Hashimoto, N. Iizuka, T. Ishii, and D. Kadoh, "Three-flavor quark mass dependence of baryon spectra in holographic QCD," *Phys. Lett.* **B691** (2010) 65–71, 0910.1179.

[90] K. Hashimoto, T. Hirayama, and D. K. Hong, "Quark Mass Dependence of Hadron Spectrum in Holographic QCD," *Phys. Rev.* **D81** (2010) 045016, 0906.0402.

[91] M. Harada, S. Matsuzaki, and K. Yamawaki, "Holographic QCD Integrated back to Hidden Local Symmetry," 1007.4715.

[92] C. A. B. Bayona, H. Boschi-Filho, N. R. F. Braga, and M. A. C. Torres, "Deep inelastic scattering for vector mesons in holographic D4-D8 model," 1007.2448.

[93] K. Hashimoto, N. Iizuka, and T. Nakatsukasa, "N-Body Nuclear Forces at Short Distances in Holographic QCD," *Phys. Rev.* **D81** (2010) 106003, 0911.1035.

[94] D. K. Hong, D. Kim, and S. Matsuzaki, "Holographic calculation of hadronic contributions to muon $g-2$," *Phys. Rev.* **D81** (2010) 073005, 0911.0560.

[95] C. A. Ballon Bayona, H. Boschi-Filho, N. R. F. Braga, and M. A. C. Torres, "Form factors of vector and axial-vector mesons in holographic D4-D8 model," *JHEP* **01** (2010) 052, 0911.0023.

[96] A. Cherman, T. D. Cohen, and M. Nielsen, "Tests of Universality of Baryon Form Factors in Holographic QCD," *Nucl. Phys. Proc. Suppl.* **199** (2010) 103–106, 0909.5359.

[97] A. Cherman, T. D. Cohen, and M. Nielsen, "Model Independent Tests of Skyrmions and Their Holographic Cousins," *Phys. Rev. Lett.* **103** (2009) 022001, 0903.2662.

[98] S. K. Domokos, J. A. Harvey, and N. Mann, "The Pomeron contribution to p p and p bar p scattering in AdS/QCD," *Phys. Rev.* **D80** (2009) 126015, 0907.1084.

[99] F. Jugeau, "Towards a consistent AdS/QCD dictionary," 0902.3864.

[100] K.-Y. Kim and I. Zahed, "Nucleon-Nucleon Potential from Holography," *JHEP* **03** (2009) 131, 0901.0012.

[101] K.-Y. Kim and I. Zahed, "Electromagnetic Baryon Form Factors from Holographic QCD," *JHEP* **09** (2008) 007, 0807.0033.

[102] K. Hashimoto, T. Sakai, and S. Sugimoto, "Holographic Baryons : Static Properties and Form Factors from Gauge/String Duality," *Prog. Theor. Phys.* **120** (2008) 1093–1137, 0806.3122.

[103] D. K. Hong, M. Rho, H.-U. Yee, and P. Yi, "Nucleon Form Factors and Hidden Symmetry in Holographic QCD," *Phys. Rev.* **D77** (2008) 014030, 0710.4615.

[104] M. Rho, "Cold Compressed Baryonic Matter with Hidden Local Symmetry and Holography," 1002.2503.

[105] J. Sadeghi, M. R. Pahlavani, S. Heshmatian, and R. Morad, "Baryon Binding Energy in Sakai-Sugimoto Model," 0910.3542.

[106] D. Yamada, "A Comparative Study of NJL and Sakai-Sugimoto Models," 0909.1494.

[107] K.-y. Kim and J. Liao, "On the Baryonic Density and Susceptibilities in a Holographic Model of QCD," *Nucl. Phys.* **B822** (2009) 201–218, 0906.2978.

[108] K.-Y. Kim and I. Zahed, "Baryonic Response of Dense Holographic QCD," *JHEP* **12** (2008) 075, 0811.0184.

[109] M. Rozali and L. Brits, "Holography and Fermions at a Finite Chemical Potential," *Can. J. Phys.* **87** (2009) 271–277, 0810.5321.

[110] H. Suganuma, K. Nawa, and T. Kojo, "Baryons and Baryonic Matter in Holographic QCD from Superstring," *Nucl. Phys. Proc. Suppl.* **186** (2009) 248–251, 0809.0805.

[111] A. Parnachev and A. R. Zhitnitsky, "Phase Transitions, theta Behavior and Instantons in QCD and its Holographic Model," *Phys. Rev.* **D78** (2008) 125002, 0806.1736.

[112] E. G. Thompson and D. T. Son, "Magnetized baryonic matter in holographic QCD," *Phys. Rev.* **D78** (2008) 066007, 0806.0367.

[113] Y. Pang, "Transverse momentum broadening of heavy quark and gluon energy loss in Sakai-Sugimoto model," *JHEP* **10** (2008) 041, 0805.4052.

[114] A. Rebhan, A. Schmitt, and S. Stricker, "Holographic chiral currents in a magnetic field," 1007.2494.

[115] A. Gynther, K. Landsteiner, F. Pena-Benitez, and A. Rebhan, "Holographic Anomalous Conductivities and the Chiral Magnetic Effect," 1005.2587.

[116] A. Rebhan, A. Schmitt, and S. A. Stricker, "Anomalies and the chiral magnetic effect in the Sakai- Sugimoto model," 0909.4782.

[117] H.-U. Yee, "Holographic Chiral Magnetic Conductivity," 0908.4189.

[118] K.-Y. Kim, B. Sahoo, and H.-U. Yee, "Holographic chiral magnetic spiral," 1007.1985.

[119] G. Lifschytz and M. Lippert, "Holographic Magnetic Phase Transition," 0906.3892.

[120] P. C. Argyres, M. Edalati, R. G. Leigh, and J. F. Vazquez-Poritz, "Open Wilson Lines and Chiral Condensates in Thermal Holographic QCD," *Phys. Rev.* **D79** (2009) 045022, 0811.4617.

[121] A. Rebhan, A. Schmitt, and S. A. Stricker, "Meson supercurrents and the Meissner effect in the Sakai- Sugimoto model," *JHEP* **05** (2009) 084, 0811.3533.

[122] M. Kulaxizi and A. Parnachev, "Holographic Responses of Fermion Matter," *Nucl. Phys.* **B815** (2009) 125–141, 0811.2262.

[123] O. Bergman, G. Lifschytz, and M. Lippert, "Magnetic properties of dense holographic QCD," *Phys. Rev.* **D79** (2009) 105024, 0806.0366.

[124] C. V. Johnson and A. Kundu, "External Fields and Chiral Symmetry Breaking in the Sakai- Sugimoto Model," *JHEP* **12** (2008) 053, 0803.0038.

[125] G. F. de Teramond and S. J. Brodsky, "The hadronic spectrum of a holographic dual of QCD," *Phys. Rev. Lett.* **94** (2005) 201601, hep-th/0501022.

[126] S. J. Brodsky and G. F. de Teramond, "Hadronic spectra and light-front wavefunctions in holographic QCD," *Phys. Rev. Lett.* **96** (2006) 201601, hep-ph/0602252.

[127] G. F. de Teramond and S. J. Brodsky, "Light-Front Holography: A First Approximation to QCD," *Phys. Rev. Lett.* **102** (2009) 081601, 0809.4899.

[128] G. F. de Teramond and S. J. Brodsky, "Light-Front Holography and Gauge/Gravity Duality: The Light Meson and Baryon Spectra," *Nucl. Phys. Proc. Suppl.* **199** (2010) 89–96, 0909.3900.

[129] S. J. Brodsky and G. F. de Teramond, "Light-Front Dynamics and AdS/QCD Correspondence: The Pion Form Factor in the Space- and Time-Like Regions," *Phys. Rev.* **D77** (2008) 056007, 0707.3859.

[130] S. J. Brodsky and G. F. de Teramond, "Light-Front Dynamics and AdS/QCD Correspondence: Gravitational Form Factors of Composite Hadrons," *Phys. Rev.* **D78** (2008) 025032, 0804.0452.

[131] S. J. Brodsky, G. de Teramond, and A. Deur, "AdS/QCD, Light-Front Holography, and the Nonperturbative Running Coupling," 1002.4660.

[132] G. F. de Teramond and S. J. Brodsky, "Light-Front Quantization Approach to the Gauge-Gravity Correspondence and Hadron Spectroscopy," 1001.5193.

[133] U. Gursoy, E. Kiritsis, and F. Nitti, "Exploring improved holographic theories for QCD: Part II," *JHEP* **0802** (2008) 019, arXiv:0707.1349.

[134] W. de Paula and T. Frederico, "Unifying Scalars and Light Mesons by Holographic QCD," 0908.4282.

[135] W. de Paula and T. Frederico, "Mesonic Spectrum from a Dynamical Gravity/Gauge model," *Nucl. Phys. Proc. Suppl.* **199** (2010) 113–118, 1004.1555.

[136] A. Vega and I. Schmidt, "Hadrons in AdS/QCD correspondence," *Phys. Rev.* **D79** (2009) 055003, 0811.4638.

[137] H. Forkel, "Hadrons as holograms," *PoS* **QCD-TNT09** (2009) 014, 0910.5955.

[138] I. Iatrakis, E. Kiritsis, and A. Paredes, "An AdS/QCD model from Sen's tachyon action," *Phys. Rev.* **D81** (2010) 115004, 1003.2377.

[139] U. Gursoy, E. Kiritsis, L. Mazzanti, and F. Nitti, "Deconfinement and Gluon Plasma Dynamics in Improved Holographic QCD," *Phys. Rev. Lett.* **101** (2008) 181601, 0804.0899.

[140] D.-f. Zeng, "Heavy quark potentials in some renormalization group revised AdS/QCD models," *Phys. Rev.* **D78** (2008) 126006, 0805.2733.

[141] U. Gursoy, E. Kiritsis, L. Mazzanti, and F. Nitti, "Holography and Thermodynamics of 5D Dilaton-gravity," *JHEP* **05** (2009) 033, 0812.0792.

[142] K. Skenderis and P. K. Townsend, "Gravitational stability and renormalization-group flow," *Phys. Lett.* **B468** (1999) 46–51, hep-th/9909070.

[143] S. He, M. Huang, and Q.-S. Yan, "Logarithmic correction in the deformed AdS_5 model to produce the heavy quark potential and QCD beta function," 1004.1880.

[144] S. He, M. Huang, and Q.-s. Yan, "Heavy quark potential and QCD beta function from a deformed AdS_5 model," 1007.0088.

[145] U. Gursoy, E. Kiritsis, L. Mazzanti, G. Michalogiorgakis, and F. Nitti, "Improved Holographic QCD," 1006.5461.

[146] C. Csaki and M. Reece, "Toward a systematic holographic QCD: A Braneless approach," *JHEP* **0705** (2007) 062, hep-ph/0608266.

[147] I. Kirsch and D. Vaman, "The D3 / D7 background and flavor dependence of Regge trajectories," *Phys.Rev.* **D72** (2005) 026007, hep-th/0505164.

[148] U. Gursoy, "Deconfinement and Thermodynamics in 5D Holographic Models of QCD," *Mod. Phys. Lett.* **A23** (2009) 3349–3365, 0904.2750.

[149] A. Falkowski and M. Perez-Victoria, "Holography, Pade Approximants and Deconstruction," *JHEP* **02** (2007) 086, hep-ph/0610326.

[150] A. A. Migdal, "Multicolor QCD as Dual Resonance Theory," *Ann. Phys.* **109** (1977) 365.

[151] C. Csaki, M. Reece, and J. Terning, "The AdS/QCD Correspondence: Still Undelivered," *JHEP* **05** (2009) 067, 0811.3001.

[152] O. Cata, "Towards understanding Regge trajectories in holographic QCD," *Phys. Rev.* **D75** (2007) 106004, hep-ph/0605251.

[153] S. S. Gubser, "Dilaton-driven confinement," hep-th/9902155.

[154] A. Kehagias and K. Sfetsos, "On running couplings in gauge theories from type-IIB supergravity," *Phys. Lett.* **B454** (1999) 270–276, hep-th/9902125.

[155] L. Girardello, M. Petrini, M. Porrati, and A. Zaffaroni, "Confinement and condensates without fine tuning in supergravity duals of gauge theories," *JHEP* **05** (1999) 026, hep-th/9903026.

[156] M. Porrati and A. Starinets, "RG fixed points in supergravity duals of 4-d field theory and asymptotically AdS spaces," *Phys. Lett.* **B454** (1999) 77–83, hep-th/9903085.

[157] Y. Kim, B.-H. Lee, C. Park, and S.-J. Sin, "The effect of gluon condensate on holographic heavy quark potential," *Phys. Rev.* **D80** (2009) 105016, 0808.1143.

[158] K. Ghoroku and M. Yahiro, "Chiral symmetry breaking driven by dilaton," *Phys. Lett.* **B604** (2004) 235–241, hep-th/0408040.

[159] D. Bak and H.-U. Yee, "Separation of spontaneous chiral symmetry breaking and confinement via AdS/CFT correspondence," *Phys. Rev.* **D71** (2005) 046003, hep-th/0412170.

[160] I. H. Brevik, K. Ghoroku, and A. Nakamura, "Meson mass and confinement force driven by dilaton," *Int. J. Mod. Phys.* **D15** (2006) 57–68, hep-th/0505057.

[161] Y. Seo, J. P. Shock, S.-J. Sin, and D. Zoakos, "Holographic Hadrons in a Confining Finite Density Medium," *JHEP* **03** (2010) 115, 0912.4013.

[162] N. R. Constable and R. C. Myers, "Exotic scalar states in the AdS/CFT correspondence," *JHEP* **11** (1999) 020, hep-th/9905081.

[163] R. Apreda, J. Erdmenger, and N. Evans, "Scalar effective potential for D7 brane probes which break chiral symmetry," *JHEP* **05** (2006) 011, hep-th/0509219.

[164] R. Apreda, J. Erdmenger, N. Evans, J. Grosse, and Z. Guralnik, "Instantons on D7 brane probes and AdS/CFT with flavour," *Fortsch. Phys.* **54** (2006) 266–274, hep-th/0601130.

[165] J. Erdmenger, N. Evans, and J. Grosse, "Heavy-light mesons from the AdS/CFT correspondence," *JHEP* **01** (2007) 098, hep-th/0605241.

[166] N. J. Evans and J. P. Shock, "Chiral dynamics from AdS space," *Phys. Rev.* **D70** (2004) 046002, hep-th/0403279.

[167] S. Nojiri and S. D. Odintsov, "Curvature dependence of running gauge coupling and confinement in AdS/CFT correspondence," *Phys. Rev.* **D61** (2000) 044014, hep-th/9905200.

[168] N. Evans, J. P. Shock, and T. Waterson, "D7 brane embeddings and chiral symmetry breaking," *JHEP* **03** (2005) 005, hep-th/0502091.

[169] M. Alishahiha, A. Brandhuber, and Y. Oz, "Branes at singularities in type 0 string theory," *JHEP* **05** (1999) 024, hep-th/9903186.

[170] G. Ferretti, J. Kalkkinen, and D. Martelli, "Non-critical type 0 string theories and their field theory duals," *Nucl. Phys.* **B555** (1999) 135–156, hep-th/9904013.

[171] K. Ghoroku, "Yang-Mills theory from non-critical string," *J. Phys.* **G26** (2000) 233–244, hep-th/9907143.

[172] L. Girardello, M. Petrini, M. Porrati, and A. Zaffaroni, "The supergravity dual of N = 1 super Yang-Mills theory," *Nucl. Phys.* **B569** (2000) 451–469, hep-th/9909047.

[173] C. Nunez, A. Paredes, and A. V. Ramallo, "Unquenched flavor in the gauge/gravity correspondence," 1002.1088.

[174] W. de Paula, T. Frederico, H. Forkel, and M. Beyer, "Dynamical AdS/QCD with area-law confinement and linear Regge trajectories," *Phys. Rev.* **D79** (2009) 075019, 0806.3830.

[175] Y.-L. Wu and Z.-F. Xie, "A Three-Flavor AdS/QCD Model with a Back-Reacted Geometry," *JHEP* **10** (2007) 009, 0705.2360.

[176] J. Schmude, "Comments on the distinction between color- and flavor- branes and new D3-D7 solutions with eight supercharges," 1007.1201.

[177] F. Benini, F. Canoura, S. Cremonesi, C. Nunez, and A. V. Ramallo, "Unquenched flavors in the Klebanov-Witten model," *JHEP* **02** (2007) 090, hep-th/0612118.

[178] F. Benini, "Backreacting flavors in the Klebanov-Witten model via D7- branes," *Fortsch. Phys.* **56** (2008) 936–942.

[179] F. Bigazzi, A. L. Cotrone, and A. Paredes, "Klebanov-Witten theory with massive dynamical flavors," *JHEP* **09** (2008) 048, 0807.0298.

[180] F. Bigazzi *et al.*, "D3-D7 Quark-Gluon Plasmas," *JHEP* **11** (2009) 117, 0909.2865.

[181] F. Bigazzi, A. L. Cotrone, A. Paredes, and A. V. Ramallo, "Screening effects on meson masses from holography," *JHEP* **05** (2009) 034, 0903.4747.

[182] B. A. Burrington, V. S. Kaplunovsky, and J. Sonnenschein, "Localized Backreacted Flavor Branes in Holographic QCD," *JHEP* **02** (2008) 001, 0708.1234.

[183] J. Gaillard and J. Schmude, "On the geometry of string duals with backreacting flavors," *JHEP* **01** (2009) 079, 0811.3646.

[184] F. Canoura, P. Merlatti, and A. V. Ramallo, "The supergravity dual of 3d supersymmetric gauge theories with unquenched flavors," *JHEP* **05** (2008) 011, 0803.1475.

[185] C. Sieg, "Holographic flavour in the N = 1 Polchinski-Strassler background," *JHEP* **08** (2007) 031, 0704.3544.

[186] R. Apreda, J. Erdmenger, D. Lust, and C. Sieg, "Adding flavour to the Polchinski-Strassler background," *JHEP* **01** (2007) 079, hep-th/0610276.

[187] A. Paredes, "On unquenched N = 2 holographic flavor," *JHEP* **12** (2006) 032, hep-th/0610270.

[188] T. Springer, C. Gale, S. Jeon, and S. H. Lee, "A shear spectral sum rule in a non-conformal gravity dual," 1006.4667.

[189] O. Andreev and V. I. Zakharov, "Gluon Condensate, Wilson Loops and Gauge/String Duality," *Phys. Rev.* **D76** (2007) 047705, hep-ph/0703010.

[190] D. K. Hong, M. Rho, H.-U. Yee, and P. Yi, "Dynamics of Baryons from String Theory and Vector Dominance," *JHEP* **09** (2007) 063, 0705.2632.

[191] L. Chang *et al.*, "Chemical Potential Dependence of Chiral Quark Condensate in Dyson-Schwinger Equation Approach of QCD," *Phys. Lett.* **B644** (2007) 315–321, hep-ph/0508094.

[192] J. Luecker, C. S. Fischer, and R. Williams, "Volume behaviour of quark condensate, pion mass and decay constant from Dyson-Schwinger equations," *Phys. Rev.* **D81** (2010) 094005, 0912.3686.

[193] D. E. Kharzeev, L. D. McLerran, and H. J. Warringa, "The effects of topological charge change in heavy ion collisions: 'Event by event P and CP violation'," *Nucl. Phys.* **A803** (2008) 227–253, 0711.0950.

[194] A. Karch and A. O'Bannon, "Metallic AdS/CFT," *JHEP* **09** (2007) 024, 0705.3870.

[195] G. Lifschytz and M. Lippert, "Anomalous conductivity in holographic QCD," *Phys. Rev.* **D80** (2009) 066005, 0904.4772.

[196] **STAR** Collaboration, S. A. Voloshin, "Experimental study of local strong parity violation in relativistic nuclear collisions," 0907.2213.

[197] P. V. Buividovich, M. N. Chernodub, E. V. Luschevskaya, and M. I. Polikarpov, "Numerical evidence of chiral magnetic effect in lattice gauge theory," 0907.0494.

[198] K. Fukushima, M. Ruggieri, and R. Gatto, "Chiral magnetic effect in the PNJL model," 1003.0047.

[199] T. Sakai and S. Sugimoto, "Low energy hadron physics in holographic QCD," *Prog. Theor. Phys.* **113** (2005) 843–882, 0412141.

[200] T. Sakai and S. Sugimoto, "More on a holographic dual of QCD," *Prog. Theor. Phys.* **114** (2005) 1083–1118, 0507073.

[201] V. A. Rubakov, "On chiral magnetic effect and holography," 1005.1888.

[202] M. A. Metlitski and A. R. Zhitnitsky, "Anomalous axion interactions and topological currents in dense matter," *Phys. Rev.* **D72** (2005) 045011, hep-ph/0505072.

[203] M. A. Shifman, "Anomalies and Low-Energy Theorems of Quantum Chromodynamics," *Phys. Rept.* **209** (1991) 341–378.

[204] H. Liu and A. A. Tseytlin, "D = 4 super Yang-Mills, D = 5 gauged supergravity, and D = 4 conformal supergravity," *Nucl. Phys.* **B533** (1998) 88–108, hep-th/9804083.

[205] H. Liu and A. A. Tseytlin, "D3-brane D-instanton configuration and N = 4 super YM theory in constant self-dual background," *Nucl. Phys.* **B553** (1999) 231–249, hep-th/9903091.

[206] G. Policastro, D. T. Son, and A. O. Starinets, "From AdS/CFT correspondence to hydrodynamics," *JHEP* **09** (2002) 043, hep-th/0205052.

[207] G. Policastro, D. T. Son, and A. O. Starinets, "The shear viscosity of strongly coupled N = 4 supersymmetric Yang-Mills plasma," *Phys. Rev. Lett.* **87** (2001) 081601, hep-th/0104066.

[208] D. T. Son and A. O. Starinets, "Minkowski-space correlators in AdS/CFT correspondence: Recipe and applications," *JHEP* **09** (2002) 042, hep-th/0205051.

[209] G. Policastro, D. T. Son, and A. O. Starinets, "From AdS/CFT correspondence to hydrodynamics. II: Sound waves," *JHEP* **12** (2002) 054, hep-th/0210220.

[210] L. D. Landau and E. M. Lifshitz, "Textbook On Theoretical Physics. Vol. 5: Statistical Physics,". Moscow, 1986, 484 pp.

[211] A. L. Kataev, N. V. Krasnikov, and A. A. Pivovarov, "Two Loop Calculations for the Propagators of Gluonic Currents," *Nucl. Phys.* **B198** (1982) 508–518, hep-ph/9612326.

[212] J. Erdmenger, N. Evans, I. Kirsch, and E. Threlfall, "Mesons in Gauge/Gravity Duals - A Review," *Eur. Phys. J.* **A35** (2008) 81–133, 0711.4467.

[213] K. Dusling *et al.*, "Quarkonium transport in thermal AdS/CFT," *JHEP* **10** (2008) 098, 0808.0957.

[214] K. Ghoroku, T. Sakaguchi, N. Uekusa, and M. Yahiro, "Flavor quark at high temperature from a holographic model," *Phys. Rev.* **D71** (2005) 106002, hep-th/0502088.

[215] D. N. Kabat, K.-M. Lee, and E. J. Weinberg, "QCD vacuum structure in strong magnetic fields," *Phys. Rev.* **D66** (2002) 014004, hep-ph/0204120.

[216] B. L. Ioffe and A. V. Smilga, "Nucleon Magnetic Moments and Magnetic Properties of Vacuum in QCD," *Nucl. Phys.* **B232** (1984) 109.

[217] P. Cea and L. Cosmai, "Probing the QCD vacuum using external fields," hep-lat/0602016.

[218] E. Shintani *et al.*, "Neutron electric dipole moment with external electric field method in lattice QCD," *Phys. Rev.* **D75** (2007) 034507, hep-lat/0611032.

[219] S. I. Kruglov, "The QCD string with quarks in external electromagnetic fields," *Phys. Lett.* **B390** (1997) 283–286.

[220] V. P. Gusynin, V. A. Miransky, and I. A. Shovkovy, "Catalysis of dynamical flavor symmetry breaking by a magnetic field in (2+1)-dimensions," *Phys. Rev. Lett.* **73** (1994) 3499–3502, hep-ph/9405262.

[221] V. P. Gusynin, V. A. Miransky, and I. A. Shovkovy, "Dimensional reduction and dynamical chiral symmetry breaking by a magnetic field in (3+1)-dimensions," *Phys. Lett.* **B349** (1995) 477–483, hep-ph/9412257.

[222] S. Schramm, B. Müller, and A. J. Schramm, "Quark - anti-quark condensates in strong magnetic fields," *Mod. Phys. Lett.* **A7** (1992) 973–982.

[223] I. A. Shushpanov and A. V. Smilga, "Chiral perturbation theory with lattice regularization," *Phys. Rev.* **D59** (1999) 054013, hep-ph/9807237.

[224] N. O. Agasian and I. A. Shushpanov, "Quark and gluon condensates in a magnetic field," *JETP Lett.* **70** (1999) 717–724.

[225] S. P. Klevansky and R. H. Lemmer, "Chiral Symmetry Restoration in the Nambu-Jona-Lasinio Model with a Constant Electromagnetic Field," *Phys. Rev.* **D39** (1989) 3478–3489.

[226] B. L. Ioffe, "Condensates in quantum chromodynamics," *Phys. Atom. Nucl.* **66** (2003) 30–43, `hep-ph/0207191`.

[227] V. G. Filev, C. V. Johnson, R. C. Rashkov, and K. S. Viswanathan, "Flavoured large N gauge theory in an external magnetic field," *JHEP* **10** (2007) 019, `hep-th/0701001`.

[228] T. Albash, V. G. Filev, C. V. Johnson, and A. Kundu, "Finite Temperature Large N Gauge Theory with Quarks in an External Magnetic Field," *JHEP* **07** (2008) 080, `0709.1547`.

[229] T. Albash, V. G. Filev, C. V. Johnson, and A. Kundu, "Quarks in an External Electric Field in Finite Temperature Large N Gauge Theory," *JHEP* **08** (2008) 092, `0709.1554`.

[230] J. Erdmenger, R. Meyer, and J. P. Shock, "AdS/CFT with Flavour in Electric and Magnetic Kalb-Ramond Fields," *JHEP* **12** (2007) 091, `0709.1551`.

[231] M. C. Johnson and M. Larfors, "An obstacle to populating the string theory landscape," *Phys. Rev.* **D78** (2008) 123513, `0809.2604`.

[232] O. Bergman, G. Lifschytz, and M. Lippert, "Response of Holographic QCD to Electric and Magnetic Fields," *JHEP* **05** (2008) 007, `0802.3720`.

[233] K.-Y. Kim, S.-J. Sin, and I. Zahed, "Dense and Hot Holographic QCD: Finite Baryonic E Field," *JHEP* **07** (2008) 096, `0803.0318`.

[234] J. Distler and F. Zamora, "Chiral symmetry breaking in the AdS/CFT correspondence," *JHEP* **05** (2000) 005, `hep-th/9911040`.

[235] I. R. Klebanov and A. A. Tseytlin, "Gravity Duals of Supersymmetric SU(N) x SU(N+M) Gauge Theories," *Nucl. Phys.* **B578** (2000) 123–138, `hep-th/0002159`.

[236] T. Sakai and J. Sonnenschein, "Probing flavored mesons of confining gauge theories by supergravity," *JHEP* **09** (2003) 047, `hep-th/0305049`.

[237] S. Kuperstein and J. Sonnenschein, "A New Holographic Model of Chiral Symmetry Breaking," *JHEP* **09** (2008) 012, `0807.2897`.

[238] J. Babington, J. Erdmenger, N. J. Evans, Z. Guralnik, and I. Kirsch, "A gravity dual of chiral symmetry breaking," *Fortsch. Phys.* **52** (2004) 578–582, hep-th/0312263.

[239] N. Evans, A. Gebauer, K.-Y. Kim, and M. Magou, "Holographic Description of the Phase Diagram of a Chiral Symmetry Breaking Gauge Theory," *JHEP* **03** (2010) 132, 1002.1885.

[240] J. I. Kapusta, T. M. Kelley, and T. Gherghetta, "Chiral Symmetry Breaking in a Soft-Wall Model of AdS/QCD," *Int. J. Mod. Phys.* **A25** (2010) 453–463, 0908.0725.

[241] K. Ghoroku, M. Ishihara, and T. Taminato, "Holographic Confining Gauge theory and Response to Electric Field," *Phys. Rev.* **D81** (2010) 026001, 0909.5522.

[242] M. Edalati, R. G. Leigh, and N. N. Hoang, "Transversely-intersecting D-branes at finite temperature and chiral phase transition," *JHEP* **05** (2009) 035, 0803.1277.

[243] N. Evans and E. Threlfall, "Quark Mass in the Sakai-Sugimoto Model of Chiral Symmetry Breaking," 0706.3285.

[244] M. Edalati and J. F. Vazquez-Poritz, "Chiral Condensates in Finite Density Holographic NJL Model from String Worldsheets," 0906.5336.

[245] A. Cherman, T. D. Cohen, and E. S. Werbos, "The chiral condensate in holographic models of QCD," *Phys. Rev.* **C79** (2009) 045203, 0804.1096.

[246] A. Vainshtein, "Perturbative and nonperturbative renormalization of anomalous quark triangles," *Phys. Lett.* **B569** (2003) 187–193, hep-ph/0212231.

[247] I. I. Balitsky, A. V. Kolesnichenko, and A. V. Yung, "On Vector Dominance in Sum Rules for Electromagnetic Hadron Characteristics. (In Russian)," *Sov. J. Nucl. Phys.* **41** (1985) 178.

[248] J. Rohrwild, "Determination of the magnetic susceptibility of the quark condensate using radiative heavy meson decays," *JHEP* **09** (2007) 073, 0708.1405.

[249] P. V. Buividovich, M. N. Chernodub, E. V. Luschevskaya, and M. I. Polikarpov, "Chiral magnetization of non-Abelian vacuum: a lattice study," 0906.0488.

[250] N. N. Bogolyubov and D. V. Shirkov, "Introduction to the Theory of Quantized Fields," *Intersci. Monogr. Phys. Astron.* **3** (1959) 1–720.

[251] S. V. Mikhailov and A. V. Radyushkin, "Quark Condensate Nonlocality and Pion Wave Function in QCD: General Formalism," *Sov. J. Nucl. Phys.* **49** (1989) 494.

[252] W. Dittrich and H. Gies, "Flavor condensate and vacuum (in)-stability in QED(2+1)," *Phys. Lett.* **B392** (1997) 182–188, `hep-th/9609197`.

[253] A. Gorsky and A. Krikun, "Magnetic susceptibility of the quark condensate via holography," `0902.1832`.

[254] J. Olamit *et al.*, "Loop bifurcation and magnetization rotation in exchange-biased Ni/FeF2," *Phys. Rev. B* **72** (2005) 012408.

[255] N. Bagraev, L. Vlasenko, and R. Zhitnikov, "Inversion of Nuclear Magnetization of Compensated Silicon in Interband Absorption of Light in Weak Magnetic Fields," *JETP Letters* **25** (1977) 207–210.

[256] M. Murakami, M. Morita, and N. Koyama, "Magnetization of a $YBa_2Cu_3O_7$ Crystal Prepared by the Quench and Melt Growth Process," *Japanese Journal of Applied Physics* **28** (1989) L1125–L1127.

[257] L. Li *et al.*, "Strongly Nonlinear Magnetization above T_c in $Bi_2Sr_2CaCu_2O_{8+\delta}$," *Europhys. Lett.* **72** (2005) 451457.

[258] M. N. Chernodub, "Superconductivity of QCD vacuum in strong magnetic field," `1008.1055`.

[259] B. C. Barrois, "Superconducting Quark Matter," *Nucl. Phys.* **B129** (1977) 390.

[260] D. Bailin and A. Love, "Superfluid Quark Matter," *J. Phys.* **A12** (1979) L283.

[261] D. Bailin and A. Love, "Superconductivity In Quark Matter," *Nucl. Phys.* **B205** (1982) 119.

[262] K. G. Wilson, "Confinement of Quarks," *Phys. Rev.* **D10** (1974) 2445–2459.

[263] A. Athenodorou, B. Bringoltz, and M. Teper, "The closed string spectrum of SU(N) gauge theories in 2+1 dimensions," *Phys. Lett.* **B656** (2007) 132–140, `0709.0693`.

[264] J. K. Erickson, G. W. Semenoff, and K. Zarembo, "Wilson loops in N = 4 supersymmetric Yang-Mills theory," *Nucl. Phys.* **B582** (2000) 155–175, `hep-th/0003055`.

[265] R. Alkofer, C. S. Fischer, M. Q. Huber, F. J. Llanes-Estrada, and K. Schwenzer, "Confinement and Green functions in Landau-gauge QCD," *PoS* **CONFINEMENT8** (2008) 019, 0812.2896.

[266] M. Q. Huber, R. Alkofer, C. S. Fischer, and K. Schwenzer, "The infrared behavior of Landau gauge Yang-Mills theory in d=2, 3 and 4 dimensions," *Phys. Lett.* **B659** (2008) 434–440, 0705.3809.

[267] C. S. Fischer, A. Maas, and J. M. Pawlowski, "On the infrared behavior of Landau gauge Yang-Mills theory," *Annals Phys.* **324** (2009) 2408–2437, 0810.1987.

[268] J. M. Pawlowski, D. F. Litim, S. Nedelko, and L. von Smekal, "Infrared behaviour and fixed points in Landau gauge QCD," *Phys. Rev. Lett.* **93** (2004) 152002, hep-th/0312324.

[269] C. D. Roberts and A. G. Williams, "Dyson-Schwinger equations and their application to hadronic physics," *Prog. Part. Nucl. Phys.* **33** (1994) 477–575, hep-ph/9403224.

[270] C. D. Roberts and S. M. Schmidt, "Dyson-Schwinger equations: Density, temperature and continuum strong QCD," *Prog. Part. Nucl. Phys.* **45** (2000) S1–S103, nucl-th/0005064.

[271] P. Maris and C. D. Roberts, "Dyson-Schwinger equations: A tool for hadron physics," *Int. J. Mod. Phys.* **E12** (2003) 297–365, nucl-th/0301049.

[272] A. Holl, C. D. Roberts, and S. V. Wright, "Hadron physics and Dyson-Schwinger equations," nucl-th/0601071.

[273] R. Alkofer, M. Q. Huber, and K. Schwenzer, "Infrared Behavior of Three-Point Functions in Landau Gauge Yang-Mills Theory," *Eur. Phys. J.* **C62** (2009) 761–781, 0812.4045.

[274] R. Alkofer, C. S. Fischer, F. J. Llanes-Estrada, and K. Schwenzer, "The quark-gluon vertex in Landau gauge QCD: Its role in dynamical chiral symmetry breaking and quark confinement," *Annals Phys.* **324** (2009) 106–172, 0804.3042.

[275] R. Alkofer, C. S. Fischer, F. J. Llanes-Estrada, and K. Schwenzer, "Dynamically induced scalar quark confinement: A link between chiral symmetry breaking and confinement," *POS* **LAT2007** (2007) 286, 0710.1154.

[276] R. Alkofer, C. S. Fischer, F. J. Llanes-Estrada, and K. Schwenzer, "What the Infrared Behaviour of QCD Vertex Functions in Landau gauge can tell us about Confinement," *Int. J. Mod. Phys.* **E16** (2007) 2720–2732, 0705.4402.

[277] C. S. Fischer and J. M. Pawlowski, "Uniqueness of infrared asymptotics in Landau gauge Yang- Mills theory," *Phys. Rev.* **D75** (2007) 025012, hep-th/0609009.

[278] C. S. Fischer and J. M. Pawlowski, "Uniqueness of infrared asymptotics in Landau gauge Yang- Mills theory II," *Phys. Rev.* **D80** (2009) 025023, 0903.2193.

[279] R. Alkofer, C. S. Fischer, and F. J. Llanes-Estrada, "Vertex functions and infrared fixed point in Landau gauge SU(N) Yang-Mills theory," *Phys. Lett.* **B611** (2005) 279–288, hep-th/0412330.

[280] Y. M. Makeenko, "Introduction to gauge theory," *Surveys High Energ. Phys.* **10** (1997) 1–117.

[281] R. A. Brandt, F. Neri, and M.-a. Sato, "Renormalization of Loop Functions for All Loops," *Phys. Rev.* **D24** (1981) 879.

[282] G. P. Lepage and P. B. Mackenzie, "On the viability of lattice perturbation theory," *Phys. Rev.* **D48** (1993) 2250–2264, hep-lat/9209022.

[283] C. S. Fischer, R. Alkofer, and H. Reinhardt, "The elusiveness of infrared critical exponents in Landau gauge Yang-Mills theories," *Phys. Rev.* **D65** (2002) 094008, hep-ph/0202195.

[284] C. S. Fischer and R. Alkofer, "Infrared exponents and running coupling of SU(N) Yang- Mills theories," *Phys. Lett.* **B536** (2002) 177–184, hep-ph/0202202.

[285] J. C. R. Bloch, "Two-loop improved truncation of the ghost-gluon Dyson-Schwinger equations: Multiplicatively renormalizable propagators and nonperturbative running coupling," *Few Body Syst.* **33** (2003) 111–152, hep-ph/0303125.

[286] L. von Smekal, R. Alkofer, and A. Hauck, "The infrared behavior of gluon and ghost propagators in Landau gauge QCD," *Phys. Rev. Lett.* **79** (1997) 3591–3594, hep-ph/9705242.

[287] L. von Smekal, A. Hauck, and R. Alkofer, "A solution to coupled Dyson-Schwinger equations for gluons and ghosts in Landau gauge," *Ann. Phys.* **267** (1998) 1, hep-ph/9707327.

[288] C. Lerche and L. von Smekal, "On the infrared exponent for gluon and ghost propagation in Landau gauge QCD," *Phys. Rev.* **D65** (2002) 125006, hep-ph/0202194.

[289] D. Zwanziger, "Non-perturbative Landau gauge and infrared critical exponents in QCD," *Phys. Rev.* **D65** (2002) 094039, hep-th/0109224.

[290] N. Brown and M. R. Pennington, "Studies of Confinement: How Quarks and Gluons Propagate," *Phys. Rev.* **D38** (1988) 2266.

[291] **Particle Data Group** Collaboration, C. Amsler *et al.*, "Review of particle physics," *Phys. Lett.* **B667** (2008) 1.

[292] P. Y. Boyko, F. V. Gubarev, and S. M. Morozov, "On the structure of QCD confining string," *PoS* **LAT2007** (2007) 307, 0712.0656.

[293] S. Necco, "The static quark potential and scaling behavior of SU(3) lattice Yang-Mills theory," hep-lat/0306005.

[294] **TXL** Collaboration, G. S. Bali *et al.*, "Static potentials and glueball masses from QCD simulations with Wilson sea quarks," *Phys. Rev.* **D62** (2000) 054503, hep-lat/0003012.

[295] A. Laschka, N. Kaiser, and W. Weise, "The heavy quark-antiquark potential from lattice and perturbative QCD," *PoS* **CONFINEMENT8** (2008) 168, 0901.2260.

[296] J. M. Maldacena, "Wilson loops in large N field theories," *Phys. Rev. Lett.* **80** (1998) 4859–4862, hep-th/9803002.

[297] S.-J. Rey and J.-T. Yee, "Macroscopic strings as heavy quarks in large N gauge theory and anti-de Sitter supergravity," *Eur. Phys. J.* **C22** (2001) 379–394, hep-th/9803001.

[298] A. Brandhuber, N. Itzhaki, J. Sonnenschein, and S. Yankielowicz, "Wilson loops, confinement, and phase transitions in large N gauge theories from supergravity," *JHEP* **06** (1998) 001, hep-th/9803263.

[299] G. B. West, "Confinement, the Wilson Loop and the Gluon Propagator," *Phys. Lett.* **B115** (1982) 468.

[300] T. Kugo and I. Ojima, "Local Covariant Operator Formalism of Nonabelian Gauge Theories and Quark Confinement Problem," *Prog. Theor. Phys. Suppl.* **66** (1979) 1.

[301] D. Zwanziger, "Vanishing of zero momentum lattice gluon propagator and color confinement," *Nucl. Phys.* **B364** (1991) 127–161.

[302] J. Braun, H. Gies, and J. M. Pawlowski, "Quark Confinement from Color Confinement," *Phys. Lett.* **B684** (2010) 262–267, 0708.2413.

[303] A. Cucchieri, A. Maas, and T. Mendes, "Three-point vertices in Landau-gauge Yang-Mills theory," *Phys. Rev.* **D77** (2008) 094510, 0803.1798.

[304] A. Sternbeck, L. von Smekal, D. B. Leinweber, and A. G. Williams, "Comparing SU(2) to SU(3) gluodynamics on large lattices," *PoS* **LAT2007** (2007) 340, 0710.1982.

[305] A. Di Giacomo, E. Meggiolaro, Y. A. Simonov, and A. I. Veselov, "Dynamics of quark-gluon plasma from field correlators," *Phys. Atom. Nucl.* **70** (2007) 908–924, hep-ph/0512125.

[306] A. V. Zayakin and J. Rafelski, "Nonlocal Gluon Condensate from the Dyson–Schwinger Equations," 0812.3616.

[307] C. S. Fischer, "Non-perturbative propagators, running coupling and dynamical mass generation in ghost - antighost symmetric gauges in QCD," hep-ph/0304233.

[308] S. V. Mikhailov and A. V. Radyushkin, "Nonlocal Condensates and QCD Sum Rules For Pion Wave Function," *JETP Lett.* **43** (1986) 712.

[309] S. V. Mikhailov and A. V. Radyushkin, "The Pion wave function and QCD sum rules with nonlocal condensates," *Phys. Rev.* **D45** (1992) 1754–1759.

[310] A. E. Dorokhov, S. V. Esaibegian, and S. V. Mikhailov, "Virtualities of quarks and gluons in QCD vacuum and nonlocal condensates within single instanton approximation," *Phys. Rev.* **D56** (1997) 4062–4068, hep-ph/9702417.

[311] G. W. Semenoff and K. Zarembo, "Wilson loops in SYM theory: From weak to strong coupling," *Nucl. Phys. Proc. Suppl.* **108** (2002) 106–112, hep-th/0202156.

[312] L. A. Trevisan, A. E. Dorokhov, and L. Tomio, "Path dependence of the quark nonlocal condensate within the instanton model," *Braz. J. Phys.* **34** (2004) 865–868, hep-ph/0405293.

[313] V. L. Chernyak and A. R. Zhitnitsky, "Asymptotic Behavior of Exclusive Processes in QCD," *Phys. Rept.* **112** (1984) 173.

[314] E. V. Shuryak, "The Role of Instantons in Quantum Chromodynamics. 1. Physical Vacuum," *Nucl. Phys.* **B203** (1982) 93.

[315] M. V. Polyakov and C. Weiss, "Mixed quark-gluon condensate from instantons," *Phys. Lett.* **B387** (1996) 841–847, hep-ph/9607244.

[316] W.-Y. P. Hwang, "Nonlocal condensates in QCD," hep-ph/9702232.

[317] Z.-G. Wang, S.-L. Wan, and K.-L. Wang, "Nonlocal quark vacuum condensate," *Phys. Lett.* **B498** (2001) 195–198.

[318] L.-J. Zhou and W.-X. Ma, "Structure of nonlocal vacuum condensate of quarks," *Chin. Phys. Lett.* **20** (2003) 2137–2139.

[319] L.-J. Zhou and W.-X. Ma, "Quark virtuality and QCD vacuum condensates," *Chin. Phys. Lett.* **21** (2004) 1471–1474.

[320] L.-J. Zhou, S.-M. Qin, Q. Wu, and W.-X. Ma, "Virtualities of quark and gluon in QCD vacuum," *Sci. China* **G51** (2008) 1439–1447.

[321] L.-J. Zhou, L. S. Kisslinger, and W.-x. Ma, "Nonzero Mean Squared Momentum of Quarks in the Non- Perturbative QCD Vacuum," 0904.3558.

[322] A. V. Zayakin and J. Rafelski, "The Confinement Property in SU(3) Gauge Theory," *Phys. Rev.* **D80** (2009) 034024, 0905.2317.

[323] R. Williams, C. S. Fischer, and M. R. Pennington, "anti-q q condensate for light quarks beyond the chiral limit," *Phys. Lett.* **B645** (2007) 167–172, hep-ph/0612061.

[324] R. Williams, C. S. Fischer, and M. R. Pennington, "Extracting the anti-q q condensate for light quarks beyond the chiral limit in models of QCD," 0704.2296.

[325] E. V. Shuryak, "Instantons In QCD. 3. Quark Propagators And Mesons Containing Heavy Quark," *Nucl. Phys.* **B328** (1989) 85.

[326] A. V. Pimikov, A. P. Bakulev, and N. G. Stefanis, "Nonlocal condensates and pion form factor," 0909.4624.

[327] G. V. Dunne, "Heisenberg-Euler effective Lagrangians: Basics and extensions," hep-th/0406216.

[328] J. Gasser and H. Leutwyler, "Chiral Perturbation Theory: Expansions in the Mass of the Strange Quark," *Nucl. Phys.* **B250** (1985) 465.

[329] Z. Bern, L. J. Dixon, and V. A. Smirnov, "Iteration of planar amplitudes in maximally supersymmetric Yang-Mills theory at three loops and beyond," *Phys. Rev.* **D72** (2005) 085001, `hep-th/0505205`.

[330] N. I. Usyukina and A. I. Davydychev, "Exact results for three and four point ladder diagrams with an arbitrary number of rungs," *Phys. Lett.* **B305** (1993) 136–143.

[331] M. E. Carrington, R. Kobes, and E. Petitgirard, "Cancellation of ladder graphs in an effective expansion," *Phys. Rev.* **D57** (1998) 2631–2634, `hep-ph/9708412`.

[332] A. P. Buchvostov and L. N. Lipatov, "High Orders of the Perturbation Theory in Scalar Electrodynamics," *Phys. Lett.* **B70** (1977) 48–50.

[333] Höhne, Stephan, *An Effective D-Brane Action in Quantized Anti de Sitter Space and The Local Renormalization Group of* $\mathcal{N} = 1$ *Supersymmetric Gauge Theories.* PhD Dissertation, LMU, Munich, 2008.

[334] J. Rafelski, "Electromagnetic fields in the QCD vacuum," `hep-ph/9806389`.

[335] H. T. Elze, B. Müller, and J. Rafelski, "Interfering QCD/QED vacuum polarization," `hep-ph/9811372`.

[336] M. D'Elia, A. Di Giacomo, and E. Meggiolaro, "Gauge-invariant field-strength correlators in pure Yang- Mills and full QCD at finite temperature," *Phys. Rev.* **D67** (2003) 114504, `hep-lat/0205018`.

[337] V. A. Novikov, M. A. Shifman, A. I. Vainshtein, M. B. Voloshin, and V. I. Zakharov, "Use and Misuse of QCD Sum Rules, Factorization and Related Topics," *Nucl. Phys.* **B237** (1984) 525.

[338] P. V. Buividovich, M. N. Chernodub, E. V. Luschevskaya, and M. I. Polikarpov, "Lattice QCD in strong magnetic fields," `0909.1808`.

[339] K. Balasubramanian and J. McGreevy, "Gravity duals for non-relativistic CFTs," *Phys. Rev. Lett.* **101** (2008) 061601, `0804.4053`.

[340] D. T. Son, "Toward an AdS/cold atoms correspondence: a geometric realization of the Schroedinger symmetry," *Phys. Rev.* **D78** (2008) 046003, `0804.3972`.

[341] S. A. Hartnoll, "Lectures on holographic methods for condensed matter physics," *Class. Quant. Grav.* **26** (2009) 224002, 0903.3246.

[342] C. P. Herzog, "Lectures on Holographic Superfluidity and Superconductivity," *J. Phys.* **A42** (2009) 343001, 0904.1975.

[343] G. T. Horowitz, "Introduction to Holographic Superconductors," 1002.1722.

[344] D. M. Broun, "What lies beneath the dome?," *Nat Phys* **4** (2008), no. 3, 170–172.

[345] T. Faulkner, H. Liu, J. McGreevy, and D. Vegh, "Emergent quantum criticality, Fermi surfaces, and AdS2," 0907.2694.

[346] M. Cubrovic, J. Zaanen, and K. Schalm, "String Theory, Quantum Phase Transitions and the Emergent Fermi-Liquid," *Science* **325** (2009) 439–444, 0904.1993.

[347] F. Benini, C. P. Herzog, and A. Yarom, "Holographic Fermi arcs and a d-wave gap," 1006.0731.

[348] D. Vegh, "Fermi arcs from holography," 1007.0246.

List of Publications by A.V.Zayakin

1. Johanna Erdmenger, A. Gorsky, P.N. Kopnin, A. Krikun, A.V. Zayakin. "Low-Energy Theorems from Holography," ITEP-TH-32-10, MPP-2010-167, arXiv:1101.1586. Accepted to JHEP.

2. A. Gorsky, P. N. Kopnin and A. V. Zayakin, "On the Chiral Magnetic Effect in Soft-Wall AdS/QCD," Phys. Rev. D, **83**, 014023 [arXiv:1003.2293 [hep-ph]].

3. A. V. Zayakin, V. Khandramai and J. Rafelski, "Quark Condensate and Effective Action from Dyson–Schwinger Equations," arXiv:0912.1753 [hep-ph].

4. P. Koroteev and A. V. Zayakin, "Wilson Loops in Gravity Duals of Lifshitz-like Theories," arXiv:0909.2551 [hep-th].

5. A. V. Zayakin and J. Rafelski, "Nonlocal Gluon Condensate from the Dyson–Schwinger Equations," arXiv:0812.3616 [hep-ph], ITEP-TH-51-08.

6. A. Gorsky, A. Monin and A. V. Zayakin, "Correlator of Wilson and t'Hooft Loops at Strong Coupling in $\mathcal{N} = 4$ SYM Theory," Phys. Lett. B **679** (2009) 529 [arXiv:0904.3665 [hep-th]].

7. A.V. Zayakin. QCD Vacuum Properties in a Magnetic Field from AdS/CFT: Chiral Condensate and Goldstone Mass. ITEP-TH-34-08, Jul 2008. 12pp. Published in JHEP 0807:116,2008. e-Print: arXiv:0807.2917 [hep-th].

8. A.K. Monin, A.V. Zayakin. Semiclassical Treatment of Induced Schwinger Processes at Finite Temperature. JETP Lett.87:709-714,2008. e-Print: arXiv:0803.1022 [hep-ph].

9. A.V. Zayakin. Euler-Heisenberg-Schwinger Lagrangian for nonadiabatically varying fields. 2007. 7pp. Phys.Part.Nucl.Lett.4:232-238,2007.

10. A.K. Monin, A.V. Zayakin. Nonperturbative decay of a monopole: The Semiclassical preexponential factor. ITEP-TH-47-06, Nov 2006. 16pp. Phys.Rev.D75:065029,2007. e-Print: hep-th/0611038.

11. A.K. Monin, A.V. Zayakin. Monopole Decay in a Variable External Field. ITEP-TH-18-06, May 2006. 15pp. JETP Lett.84:5-10,2006. e-Print: hep-ph/0605079.

12. D.V. Shirkov, A.V. Zayakin. Analytic perturbation theory for practitioners and upsilon decay. Dec 2005. 12pp. Phys.Atom.Nucl.70: 775-783,2007. e-Print: hep-ph/0512325.

13. A. V. Andreev, A. V. Zayakin. Moscow University Bulletin, 2004, No. 6, p. 29-33. "Dual" Perturbation Theory in Laser Physics Problems.

Curriculum Vitae

Andrey Zayakin

LMU-Physik, LS Habs, Am Coulombwall 1, 85748,
Garching bei München, Germany

Phone: +49 89 289 14062, Mobile:+49 152 038 50530, Fax: +49 89 289 14072

E-Mail: Andrey.Zayakin@physik.uni-muenchen.de

General Information

Date of birth:	23 Feb. 1981	Marital status:	Single
Place of birth:	Yakutsk / Russia	Citizenship:	Russian

Employment

01/2008 - 09/2010	Wissentschaftlicher Angestellter (Researcher), Ludwig Maximillians University, Munich, Lehrstuhl Prof. Dr. Dietrich Habs (Chair of Nuclear Physics), Am Coulombwall 1, 85748, Garching bei München, Germany
07/2007 - 12/2007	DAAD Scholarship holder, Freie Universität Berlin, Group of Prof. Kleinert
05/2005 - present	Junior Researcher, Institute for Theoretical and Experimental Physics, Moscow, Russia (since 01/2008 on leave of absence), group of Prof. Morozov
09/2005 - 12/2005	DAAD Scholarship holder, Freie Universität Berlin, Group of Prof. Kleinert
08/2005 - 12/2005	Junior Researcher, Joint Institute for Nuclear Research, Dubna, Russia
04/2004 - 08/2005	Engineer, Joint-Stock Co. "Tupolev Construction Bureau", Moscow, Russia, group of Prof. Baklanov

Education

01/2008 - 09/2010	PhD studies, thesis title: "Properties of the Vacuum in Models for QCD: Holography vs. Resummed Field Theory. A Comparative Study", supervised by Priv.-Doz. Dr. Johanna Erdmenger and Prof. Dr. Dietrich Habs, Ludwig Maximilians University , Munich,
01/2004	Diploma thesis defended *summa cum laude*, title: "Response of a Quantum System to an External Field in the Framework of the 'Harmonic Perturbation Theory' ", supervised by Prof. A.V. Andreev, Moscow State, University Qualification "Specialist in Physics" assigned (equivalent of Master Degree)
09/1998 - 01/2004	Undergraduate studies in physics, Moscow State University, Moscow, Russia
09/1988 - 06/1998	Elementary and High School Education, Graduated *summa cum laude*, Gymnasium 26, Yakutsk, Russia